Optimum community energy storage for end user applications

David Parra Mendoza, MSci (hons)

Thesis submitted to the University of Nottingham
for the degree of Doctor of Philosophy

March 2014

Abstract

The UK government determined that 30% of the total electricity and 15% of the total energy should be generated from renewable sources by 2020 according to the Low Carbon Transition Plan. However, most renewable energy technologies are intermittent because they depend on weather conditions and they do not offer matching capability. Energy storage is attracting intensive attention as a technology which converts renewable energy technologies into a dispatchable product which meets variable demand loads. There is increasing interest for energy storage located very close to consumers which is able to augment the amount of local renewable generation consumed on site, provides demand side flexibility and helps to decarbonise the heating sector.

This thesis optimises community energy storage (CES) for end user applications including battery, hydrogen and thermal storage performing PV energy time-shift, load shifting and the combination of them. The optimisation method obtains the economic benefits of CES by quantifying the levelised cost, levelised value and internal rate of return. The method follows a community approach and the optimum CES system was calculated as a function of the size of the community, from a single home to a 100-home community. A complimentary methodology was developed including three reference years (2012, 2020 and zero carbon year) to show the evolution of the economic benefits during the low carbon transition. Additionally, a sensitivity analysis including the key parameters which affect the performance and the economic benefits was developed. The community approach reduced the levelised cost down to 0.30 £/kWh and 0.14 £/kWh for PV energy time shift and load shifting respectively when projected to the year 2020. These values meant a cost reduction by 37% and 55% regarding a single home. A cost of the storage medium of 275 £/kWh for Li-ion batteries (equivalent to a 10% subsidy over the assumed cost, 310 £/kWh) is the break-even point for Li-ion batteries by 2020 for an electricity price equal to 16.3 p/kWh (R^2=0.6).

Secondly, this thesis presents a new community hydrogen storage system integrated in a low carbon community and the experimental results when performing PV energy time-shift, load shifting and the combination of them. Long term ES was demonstrated when the community storage hydrogen system performed load shifting and the capacity factor of the electrolyser increased by 116% when PV energy time-shift was performed in addition to load shifting. This system was designed in collaboration with industrial partners and the key findings obtained during the construction and testing phases are shared.

List of Publications

- David Parra, Mark Gillott and Gavin S. Walker **Optimum community energy storage system for PV energy time-shift**, *Submitted to Applied Energy*
- David Parra, Mark Gillott and Gavin S. Walker **The role of hydrogen in achieving the decarbonization targets for the UK domestic sector**, *International Journal of Hydrogen Energy*
- David Parra, Gavin S. Walker and Mark Gillott, **Modeling of PV generation, battery and hydrogen storage to investigate the benefits of energy storage for single dwelling**, *Sustainable cities and society*
- David Parra, Mark Gillott and Gavin S. Walker and Amir Fazeli **Energy Storage From PV In a Grid Connected House: Battery And Hydrogen Simulations**, *Sustainable Energy Technologies Conference. Istanbul (Turkey). September 2011*
- Amir Fazeli, Mark Gillott, Mark Johnson, Mark Sumner and David Parra **Incorporating Seasonal Variation of Occupancy in an Electricity Demand Model for Dynamic Demand Management Simulations**, *Sustainable Energy Technologies Conference. Istanbul (Turkey). September 2011*

Acknowledgments

I would like to firstly thank to my supervisors, Prof. Mark Gillott and Prof. Gavin Walker for his support, guidance and precise feedback during this PhD.

Secondly I would like to thank the European Regional Development and E.ON for funding this study. Further thanks go to Melanie Watts for managing the funding and Dr Stuart Norman for his interesting feedback in my modelling work. I also wish to acknowledge the collaboration of ITM Power and McPhy Energy during the design and construction of the community hydrogen system and especially the support of Graeme Robinson and Regis Berlioz.

I would like to show my gratitude to the technicians which help with the design, construction and testing of a community hydrogen storage: Waseem Mohamed, Chris Varley, Rory Screaton, David Oliver, Jonathan Moss, Leigh Birkin and William Boardman. Many thanks for their excellent work and friendship. I much appreciate the kind suggestions of some colleagues from the electrical departments including Sung Oe, Ian Moore, Saul Lopez, Richard Davies and Arthur Williams. I would also like to show my appreciation to all the members of the hydrogen group and the fellow students colleagues from the SRB building including Aneel Klaire, Xiaofeng Zheng, Lucy Liu, Isin Can, Bahar Durmaz, Jenny White, David Baley, Eldar Darwin, Nina Hornazabal and Michelle Tunzi.

Last, but not least a big, big thank to Linda for her enormous support and understanding during these years. Words cannot express my most sincere thanks for her encouragement. And to my mother, father, brother, sisters, nephews and grandmother for always being there whenever I need them and make everything possible.

Contents

Abstract i

List of Publications ii

Acknowledgments iii

List of Figures xi

List of Tables xix

List of Acronyms xxiii

Nomenclature xxiv

1 Introduction 1
- 1.1 World Energy outlook . . . 1
- 1.2 Technologies to reduce carbon dioxide emissions . . . 4
  - 1.2.1 Renewable energy technologies . . . 4
  - 1.2.2 Energy conversion efficiency improvement . . . 5
  - 1.2.3 Nuclear energy . . . 7
  - 1.2.4 Carbon capture and storage . . . 8
- 1.3 Renewable energy technologies variability . . . 9
- 1.4 Integration of renewable energy technologies into energy systems . . . 11
- 1.5 Motivation . . . 13
- 1.6 Aim . . . 15
- 1.7 Industrial collaboration . . . 15
- 1.8 Outline of Thesis . . . 16

2 Energy storage applications and technologies 19
- 2.1 Flexible generation . . . 19
- 2.2 Interconnection . . . 21
- 2.3 Demand side management . . . 22
- 2.4 Energy storage . . . 24
- 2.5 Energy storage applications . . . 27
  - 2.5.1 ES for the electricity generator . . . 27

2.5.2 Load shifting and peak shaving . . . 28
2.5.3 Energy Arbitrage . . . 29
2.5.4 Renewable energy integration . . . 29
2.5.5 Electrical system regulation . . . 30
2.5.6 Spinning reserves . . . 30
2.6 Energy storage technologies . . . 30
2.6.1 Power storage technologies . . . 32
2.6.2 Large scale energy storage technologies . . . 33
2.6.3 Modular energy storage technologies . . . 35
2.7 Previous ES modelling approaches in the literature . . . 41
2.8 Single home battery systems . . . 43
2.9 Summary . . . 44

3 End user applications 46
3.1 Smart customers . . . 46
3.2 The benefits of ES . . . 48
3.3 End user applications . . . 48
3.4 PV energy time shift . . . 50
3.5 Load shifting . . . 52
3.5.1 Economy 7 . . . 54
3.5.2 Four period Real-time pricing tariff based on the prices from the imbalance market . . . 54
3.6 Combination of applications: PV energy time-shift and load shifting 56
3.7 Power curtailment . . . 57
3.8 Heat decarbonisation . . . 58
3.9 Other service benefits . . . 58
3.10 The energy consumption level . . . 59
3.10.1 Demand data . . . 59
3.10.2 PV generation . . . 62
3.11 Low carbon heat generators . . . 63
3.11.1 Fuel cells . . . 64
3.11.2 Heat pumps . . . 66
3.12 Summary . . . 69

4 Energy storage technologies for end user applications 70
4.1 Energy storage requirements for the end-user applications . . . 70
4.2 ES technologies for end-user applications . . . 71
4.2.1 Battery technology . . . 71
4.2.2 Hydrogen technology . . . 72
4.2.3 Thermal storage . . . 72
4.3 Characteristics and requirements of ES models . . . 72
4.4 Modelling of ES technologies . . . 73

4.4.1 The performance submodel . . . 74
4.4.2 The durability submodel . . . 74
4.4.3 Economic submodel . . . 75
4.5 Performance submodels . . . 75
4.5.1 Battery technology . . . 75
4.5.2 PEM electrolyser performance submodel . . . 80
4.5.3 Hot water performance submodel . . . 81
4.6 Inverter modeling . . . 82
4.6.1 Battery inverter rating . . . 82
4.6.2 PEM electrolyser converter rating . . . 85
4.7 Durability submodels . . . 85
4.7.1 Lead acid and lithium-ion battery life submodels . . . 85
4.7.2 PEM electrolyser durability submodel . . . 88
4.7.3 Hot water tank and PV controller durability submodel . . . 88
4.8 CES performance parameters . . . 89
4.8.1 Battery technology performance parameters . . . 89
4.8.2 Hydrogen technology performance parameters . . . 90
4.8.3 Community performance parameters . . . 91
4.9 Economic submodel . . . 91
4.9.1 Levelised cost of energy storage . . . 91
4.9.2 Levelised value of energy storage . . . 93
4.9.3 The internal rate of return . . . 93
4.9.4 CES cost . . . 94
4.10 Summary . . . 97

5 A method for optimising CES **99**
5.1 A method for calculating the optimum CES system for end user applications . . . 100
5.1.1 Maximum CES requirements . . . 101
5.1.2 Performance and ageing . . . 102
5.1.3 Seasonal performance and ageing . . . 103
5.1.4 Economic assessment . . . 103
5.1.5 Optimum CES system . . . 103
5.2 PV energy time-shift . . . 104
5.3 Load shifting . . . 107
5.3.1 Load shifting with Economy 7 for battery technology . . . 108
5.3.2 Load shifting with the NETA tariff for battery technology . 108
5.3.3 Load shifting with the NETA tariff for H_2 technology . . . 112
5.4 Combination of applications . . . 113
5.4.1 Combination of PVts and LS with the NETA tariff for battery technology . . . 113
5.5 Reference years . . . 116

5.6 Reference scenarios . . . 117
5.6.1 Cross-application parameters . . . 118
5.6.2 PVts parameters . . . 118
5.6.3 LS parameters . . . 119
5.6.4 Energy storage technologies parameters . . . 120
5.7 Sensitivity analysis . . . 121
5.7.1 Energy storage technology sensitivity . . . 123
5.7.2 Demand and PV generation sensitivity . . . 123
5.7.3 Energy prices sensitivity . . . 124
5.7.4 PV generation curtailment sensitivity . . . 125
5.8 Community approach . . . 125
5.9 Summary . . . 127

6 Performance, economic benefits and optimum CES system for end user applications 129
6.1 Baseline scenario . . . 130
6.1.1 Performance results of battery systems in a single home in 2012 . . . 130
6.1.2 Performance results of hot water tanks in a single home in 2012 . . . 131
6.1.3 Economic results for ES systems in a single home in 2012 . . . 132
6.2 PV energy time shift: reference scenarios . . . 134
6.2.1 Performance results of PbA batteries performing PVts when projected to the year 2020 . . . 134
6.2.2 Performance results of Li-ion batteries performing PVts when projected to the year 2020 . . . 136
6.2.3 Performance results of H_2 systems performing PVts when projected to the year 2020 . . . 137
6.2.4 Performance results of PbA, Li-ion and H_2 technologies performing PVts when projected to a hypothetical zero carbon year . . . 139
6.2.5 Economic results of PbA, Li-ion and H_2 technologies performing PVts when projected to the year 2020 . . . 142
6.2.6 Economic results of PbA, Li-ion and H_2 technologies performing PVts when projected to a hypothetical zero carbon year . . . 145
6.3 PV energy time shift results: Sensitivity analysis . . . 147
6.3.1 Energy storage technology sensitivity . . . 147
6.3.2 Demand and PV sensitivity . . . 149
6.3.3 Energy prices sensitivity . . . 153
6.3.4 PV generation curtailment sensitivity . . . 154
6.3.5 Comparison of the reference case with a metering tariff . . . 156

6.4 Load shifting: reference scenarios . . . 157
6.4.1 Performance results of PbA batteries performing LS when projected to the year 2020 . . . 158
6.4.2 Performance results of Li-ion batteries performing LS when projected to the year 2020 . . . 160
6.4.3 Performance results of H_2 systems performing LS when projected to the year 2020 . . . 161
6.4.4 Performance results of PbA, Li-ion and H_2 technologies performing LS in the zero carbon year . . . 163
6.4.5 Economic results of PbA, Li-ion and H_2 technologies performing LS when projected to the year 2020 and a hypothetical zero carbon year . . . 164
6.5 Load shifting results: sensitivity analysis . . . 169
6.5.1 Energy storage technology sensitivity . . . 169
6.5.2 Demand sensitivity . . . 171
6.5.3 Energy prices sensitivity . . . 172
6.6 Combination of applications: PVts and load shifting . . . 173
6.7 Combination of applications: reference scenarios . . . 174
6.7.1 Performance results of PbA and Li-ion batteries performing PVts and LS when projected to the year 2020 . . . 174
6.7.2 Performance results of H_2 systems performing PVts and LS when projected to the year 2020 . . . 175
6.7.3 Economic results of PbA, Li-ion and H_2 technologies performing PVts and LS when projected to the year 2020 . . . 176
6.8 Summary and conclusions . . . 181

7 Design, construction, testing and evaluation of a community hydrogen storage system 185
7.1 Hydrogen technology for a community energy storage system . . . 185
7.2 The Creative Energy Homes . . . 186
7.2.1 Microgeneration at the Creative Energy Homes . . . 187
7.2.2 Demand at the Creative Energy Homes . . . 189
7.3 Community hydrogen storage system at The University of Nottingham . . . 190
7.3.1 Electrolyser system . . . 190
7.3.2 The hydrogen tank . . . 193
7.3.3 The PEMFC system . . . 196
7.4 H-CES system integration, building and safety . . . 201
7.5 Experimental results . . . 205
7.5.1 Results of the H-CES system performing PVts . . . 206
7.5.2 Metal hydride tank performance . . . 208
7.5.3 Results of the H-CES system performing LS . . . 210

7.5.4 Results of the H-CES system performing PVts and LS . . . 213
7.6 Practical considerations and learnings from the H-CES system . . . 216
7.7 Summary and conclusions . . . 217

8 Conclusions, outlook and future work 219
8.1 Contribution . . . 219
8.1.1 Review of the role of energy storage in new energy systems: end user applications . . . 220
8.1.2 An optimisation method for obtaining the optimum CES system . . . 221
8.1.3 Comprehensive CES methodology . . . 222
8.1.4 A CES system for a 7-home community . . . 223
8.2 Conclusions . . . 223
8.2.1 Conclusions from the CES modelling work . . . 223
8.2.2 Conclusions from the design, construction and testing of the CES using H_2 technology . . . 229
8.3 CES Outlook . . . 229
8.4 Future work . . . 231
8.4.1 Energy storage applications . . . 231
8.4.2 Energy storage technologies . . . 231
8.4.3 Method . . . 232
8.4.4 Methodology . . . 232
8.4.5 Community hydrogen storage system and Creative Energy Homes . . . 233

A Air source Heat Pump model 234
A.1 Evaporator . . . 234
A.2 Compressor . . . 235
A.3 Condenser . . . 235
A.4 Expansion valve . . . 235

B PbA and Li-ion literature review: EFC and cost 236
B.1 Maximum equivalent full cycles for battery technologies . . . 236
B.2 Battery system cost . . . 236

C Hydrogen literature review: durability and cost 238
C.1 Hydrogen durability . . . 238
C.2 Hydrogen cost . . . 238

D PEM Electrolyser model 241
D.1 Electrolysis and PEM electrolysers . . . 241
D.2 Polarisation voltage of PEM electrolysers . . . 242
D.2.1 Thermodynamic voltage . . . 243

D.2.2 Activation voltage . . . 243
D.2.3 Ohmic voltage . . . 245
D.2.4 Concentration voltage . . . 247
D.3 Performance parameters . . . 248
D.3.1 Current density . . . 248
D.3.2 Temperature . . . 248
D.3.3 Pressure . . . 249
D.3.4 Efficiency . . . 249

E Applications not considered in the analysis 251
E.1 Applications not considered in this work . . . 251
E.1.1 Peak shaving . . . 251
E.1.2 Decarbonisation of the transport sector . . . 252
E.1.3 Distributed energy storage applications . . . 253
E.1.4 Power to gas . . . 253

F Performance battery models in the literature 254
F.1 Performance lead-acid battery models in the literature . . . 254
F.2 Performance lithium-ion models used in the literature . . . 255

G CES discretizaton utilised by the optimization method 258

H Control of the PEMFC system 260

I Efficiency of the converter of the electrolyser 261

J CES system which optimizes different performance and economic parameter 263

K Algorithms developed for the CES optimisation 265
K.1 Algorithm for obtaining the maximum battery capacity for PVts and discretizes the capacity . . . 265
K.2 Algorithm for obtaining the optimum battery capacity for PVts . . . 267

List of Figures

1.1 World total primary energy supply in 1973 and 2011 depending on the fuel [1]. . 1
1.2 Global CO_2 emissions as a function of the year [2]. 2
1.3 Evolution of installed wind capacity including off-shore in the world from 2000 to 2010 showing the countries in which the market was more important [3]. 4
1.4 Global Energy Flows 2010 from World Energy Outlook 2012 [4]. 6
1.5 Aerial view of the new power plant that will be built in Somerset by EFC according to the design [5]. 7
1.6 CCS in the power and industry sector according to IEA projections assuming that CS contributes to one-sixth of CO_2 emissions reduction by 2050 [6]. 9
1.7 Scale of CES studied in this thesis ranging from a single home to the distribution level. 14
1.8 Approach followed in this thesis for investigating the optimum CES system. . . . 14
1.9 Structure of the thesis. 16

2.1 Generation mix by fuel type in the UK in the winter 2011/12 [7]. 20
2.2 Schematic representation of the Supergrid transport high volumes of renewable electricity to the European load centres using high DC voltage [8]. The Desertec project focuses on the use of solar-thermal power plants in South European and Middle Eastern and North African (MENA) regions. 21
2.3 Representation of a smart home with smart appliances, smart metering and communication with the network [9] 23
2.4 Potential benefits introduced by ES in different parts of the electricity value chain as [10]. 24
2.5 Different ES technologies as a function of the duration of the discharge [11]. . . . 25
2.6 Demand in the UK on the 30th November 2013 excluding Pumped storage hydroelectricity and interconnections according to the National Grid. 26
2.7 Daily demand (including the transmission losses, station transformer load, pumped storage demand and interconnection demand) and wind generation load factor (defined as the ratio of average output over the theoretical maximum output over a period of time) in the UK in the winter of 2011/12 [7]. 27
2.8 Thermal storage for a concentrated solar power plant. Excess heat collected in the solar field is sent to the heat exchanger and typically warms molten salts going from the cold tank to the hot tank. When needed, the heat from the hot tank can be returned to the heat transfer fluid and sent to the steam generator. [12]. . 29
2.9 Size and weight density ranges of different ES technologies as reported by the Electricity Storage Association [13]. 31
2.10 Schematic representation of an underground CAES plant [11]. 34
2.11 Schematic representation of a H_2 storage installation connected to a PV installation showing the three main components. 37

3.1 Different end user applications considered in the analysis. PVts, LS and the combination of them were optimised. Heat decarbonisation was investigated as a complimentary application to the previous ones, while power curtailment was integrated with PVts. 50
3.2 Daily and seasonal mismatch in a single house with a 3 kW_p array according to the demand data and PV model presented in the last part of this chapter. 51
3.3 Representation of load shifting performed by ES and its impact on the electricity imported by a community. 53
3.4 NETA prices from the imbalance market for every day of 2011. The daily market has been split into 48 half hour time periods. Four different periods have been distinguished for creating a real time tariff [14]. 54
3.5 Average value of the four electricity prices of the NETA tariff in 2020 and the zero carbon scenario. 56
3.6 Flowchart of the algorithm which converted hourly recorded electrical demand data into minute resolution data using a second set of electrical demand data recorded every minute. 60
3.7 Electrical and heat demand of a single home and 50 homes from the data set monitored at Milton Keynes after changing the temporal resolution to 1 minute. 61
3.8 Single diode model of a PV panel utilised in this work 62
3.9 Polarization curve of the PEMFC stack, electrical and heat efficiency of a natural gas fed PEMFC system as a function of the current density. The system is off for current densities less than 1600 A/m^2 due to the parasitic losses. 65
3.10 PEMFC rating according to the largest rectangle method when considering the electricity and heat demand loads. 65
3.11 Electricity, heat and total efficiency of the PEMFC system as a function of the size of the community in 2020. 67
3.12 Schematic representation of the HP with the different components modeled in this work as explained in the Appendix A. 68
3.13 COP as a function of the outdoor temperature when the water is generated at 40 °C and 60 °C including a cubic fitting. 68

4.1 Modelling of the ES technologies following a holistic approach which describes the performance, durability and the economic behaviour. 73
4.2 Schematic representation of the battery performance model utilised for PbA and Li-ion battery technologies. 75
4.3 PEM electrolyser polarization curve showing the Nernst, cathode, anode and ohmic voltages and the final electrolyser cell voltage. 80
4.4 Schematic representation of the bidirectional inverter connected to a battery system. Same configuration was used with H_2 technology when using an AC/DC converter instead of a bidirectional inverter. 82
4.5 Efficiency of the converters and inverters utilised in this work as a function of the load factor. 83
4.6 Levelised cost of ES for Li-ion battery when performing PV energy time-shift as a function of the size of the community for different inverter ratings. 84
4.7 Inverter rating (equal to half the maximum demand) as a function of the size of the community depending on the scenario. 84
4.8 Schematic representation of the balance between the *LVOES* and the *LCOES* which determines the value of the *IRR*. The *LVOES* is higher than the *LCOES* when the *IRR* is higher than the discount rate assumed in the economic analysis (10%) and vice versa. 92
4.9 Breakdown of the CES cost in four different costs as used in this study. 94

4.10 Cost of the inverter as a function of the rating as used in this work. 96
4.11 Holistic approach followed in this thesis for investigating CES. 97

5.1 Schematic representation of the five main steps which comprise the optimisation method presented and utilised in this work. 100
5.2 Schematic representation of the 10 CES sizes considered by the method to obtain the optimum CES system for any community. The larges CES size was equal to maximum ES requirements. The smallest CES size and the resolution of the CES discretization were a tenth of the maximum size. 101
5.3 Li-ion battery capacity as a percentage of the ES demand for different communities for (a) PVts and (b) LS with Economy 7 in 2020 and (c) PVts and (d) LS with Economy 7 in the zero carbon year. 102
5.4 Flow chart representing the algorithm which was utilised to obtain the maximum capacity of a battery system when performing PVts using 1 minute (loop variable k) data for every day (loop variable i) of the year. The flowchart sequence follows the number sequence in the boxes. The sum symbol represents the aggregation of results to obtain hourly values (from 1 minute data) or daily values (from hourly data). 104
5.5 Flow chart representing the algorithm which was utilised to obtain the performance of a battery system when performing PVts using 1 minute (loop variable k) data for every day (loop variable i) of the year. The flowchart sequence follows the number sequence in the boxes. The sum symbol represents the aggregation of results to obtain the daily values from hourly data. 105
5.6 Flow chart representing the algorithm which was utilised to obtain the maximum capacity of a battery system when performing LS with Economy 7 using 1 minute (loop variable k) data for every day (loop variable i) of the year. The flowchart sequence follows the number sequence in the boxes. The sum symbol represents the aggregation of results to obtain hourly values (from 1 minute data) or daily values (from hourly data). 106
5.7 Flow chart representing the algorithm which was utilised to obtain the performance of a battery system when performing LS with Economy 7 using 1 minute (loop variable k) data for every day (loop variable i) of the year. The flowchart sequence follows the number sequence in the boxes. The sum symbol represents the aggregation of results to obtain the daily values from hourly data. All the parameters which depended on the demand load forecast are represented in grey. 107
5.8 Flow chart representing the algorithm which was utilised to obtain the maximum capacity of a battery system when performing LS with the NETA tariff using 1 minute (loop variable k) data for every day (loop variable i) of the year. The flowchart sequence follows the number sequence in the boxes. The sum symbol represents the aggregation of results to obtain hourly values (from 1 minute data) or daily values (from hourly data). The index p represents the four periods of the NETA tariff. 109
5.9 Flow chart representing the algorithm which was utilised to obtain the performance of a battery system when performing LS with the NETA tariff using 1 minute (loop variable k) data for every day (loop variable i) of the year. The flowchart sequence follows the number sequence in the boxes. The sum symbol represents the aggregation of results to obtain daily values from hourly data. The index p represents the four periods of the NETA tariff. All the parameters which depended on the demand load forecast are represented in grey. 110

5.10 Flow chart representing the algorithm which was utilised to obtain the maximum electrolyser rating when performing LS with the NETA tariff using 1 minute (loop variable k) data for every day (loop variable i) of the year. The flowchart sequence follows the number sequence in the boxes. The sum symbol represents the aggregation of results to obtain hourly values (from 1 minute data) or daily values (from hourly data). The index p represents the four periods of the NETA tariff. 111
5.11 Flow chart representing the algorithm which was utilised to obtain the performance of a H_2 system when performing LS with the NETA tariff using 1 minute (loop variable k) data for every day (loop variable i) of the year. The flowchart sequence follows the number sequence in the boxes. The sum symbol represents the aggregation of results to obtain daily daily values from hourly data. The index p represents the four periods of the NETA tariff. All the parameters which depended on the demand load forecast are represented in grey. 112
5.12 Flow chart representing the algorithm which was utilised to obtain the maximum size of a battery system when performing PVts and LS with the NETA tariff using 1 minute (loop variable k) data for every day (loop variable i) of the year. The flowchart sequence follows the number sequence in the boxes. The sum symbol represents the aggregation of results to obtain hourly values (from 1 minute data) or daily values (from hourly data). The index p represents the four periods of the NETA tariff. 114
5.13 Flow chart representing the algorithm which was utilised to obtain the performance of a battery system when performing PVts and LS with the NETA tariff using 1 minute (loop variable k) data for every day (loop variable i) of the year. The flowchart sequence follows the number sequence in the boxes. The sum symbol represents the aggregation of results to obtain daily daily values from hourly data. The index p represents the four periods of the NETA tariff. 115
5.14 Schematic representation of the reference scenarios studied in this work. 117
5.15 Ten homes of which eight of them have a PV plant on the roof. This schematic was used to illustrate the self-select community approach together with Figure 5.16. 125
5.16 Evolution of the community PV percentage (yellow are in the pie charts) as a function of the size of the community in 2020 when the PV penetration in the UK was assumed to be 7.6%. 126

6.1 Performance results of PbA and Li-ion batteries performing PVts in 2012 as a function of the battery capacity: (a) equivalent full cycles, (b) round trip efficiency, (c) PV_{ES} and (d) D_{ES}. 131
6.2 Performance results of hot water tanks performing PVts in 2012 as a function of the tank capacity: (a) tank efficiency, (b) PV_{ES} and (c) D_{ES}. 132
6.3 (a) *LCOES*, (b) *IRR* and (c) *LVOES* optimised for PbA, Li-ion and water tank technologies using PVts in 2012. The capacity of the battery (kWh) and the water tank (l) which achieved the optimum values is shown in brackets. 133
6.4 Performance results of PbA batteries performing PVts in 2020 as a function of the size of the community and the battery capacity: (a) equivalent full cycles, (b) round trip efficiency, (c) PV_{ES} and (d) D_{ES}. The battery capacity is given as a percentage of the maximum ES demand. 135
6.5 Performance results of Li-ion batteries performing PVts in 2020 as a function of the size of the community and the battery capacity: (a) equivalent full cycles, (b) round trip efficiency, (c) PV_{ES} and (d) D_{ES}. The battery capacity is given as a percentage of the maximum ES demand. 137

6.6 Performance results of H_2 systems performing PVts in 2020 as a function of the size of the community and the electrolyser rating: (a) capacity factor, (b) electrolyser efficiency, (c) PV_{ES} and (d) H_{2ratio}. The electrolyser rating is given as a percentage of the maximum ES demand. 138
6.7 Performance results of PbA batteries performing PVts in the zero carbon year as a function of the size of the community and the battery capacity: (a) equivalent full cycles, (b) round trip efficiency, (c) PV_{ES} and (d) D_{ES}. The battery capacity is given as a percentage of the maximum ES demand. 139
6.8 Performance results of Li-ion batteries performing PVts in the zero carbon year as a function of the size of the community and the battery capacity: (a) equivalent full cycles, (b) round trip efficiency, (c) PV_{ES} and (d) D_{ES}. The battery capacity is given as a percentage of the maximum ES demand. 140
6.9 Performance results of H_2 systems performing PVts in the zero carbon year as a function of the size of the community and the electrolyser rating: (a) capacity factor, (b) electrolyser efficiency, (c) PV_{ES} and (d) H_{2ratio}. The electrolyser rating is given as a percentage of the maximum ES demand. 140
6.10 Required H_2 tank size for PVts (a) and LS (b) as a function of electrolyser rating and the size of the community in the zero carbon year. 141
6.11 (a) *LCOES*, (b) *IRR* and (c) *LVOES* optimised for PbA batteries, Li-ion batteries and H_2 systems performing PVts in 2020 as a function of the size of the community. 142
6.12 Optimum CES system which minimised the levelised cost, *LCOES*, associated with PVts as a function of the community size for (a) PbA and Li-ion batteries; (b) and H_2 systems in 2020. 143
6.13 (a) *LCOES*, (b) *IRR* and (c) *LVOES* optimised for PbA batteries, Li-ion batteries and H_2 systems performing PVts in the zero carbon year as a function of the size of the community. 145
6.14 Optimum CES system which minimised the levelised cost, *LCOES*, associated with PVts as a function of the community size for (a) PbA and Li-ion batteries; (b) and H_2 systems in the zero carbon year. 146
6.15 *LCOES* and *IRR* optimised for (a) PbA, (b) Li-ion and (c) H_2 technologies using PVts in 2020 depending on the cost and durability characteristics. 147
6.16 *LCOES* and *IRR* optimised for (a) PbA, (b) Li-ion and (c) H_2 technologies using PVts in the zero carbon year depending on the cost and durability characteristics. 149
6.17 Performance results of PbA batteries performing PVts in the zero carbon year as a function of the size of the community and the battery capacity when (a) the PV penetration was assumed to be 2.3% and (b) the HP penetration was assumed to be 0% in the UK. 149
6.18 *LCOES* and *IRR* optimised for (a) PbA, (b) Li-ion and (c) H_2 technologies using PVts in 2020 depending on the PV and HP penetration. 150
6.19 Optimum CES system which minimised the levelised cost, *LCOES*, associated with PVts as a function of the community size for (a) PbA, (a) Li-ion and (b) H_2 technologies depending on the PV and HP penetration in 2020. 151
6.20 *LVOES* and *IRR* optimised for (a) PbA, (b) Li-ion and (c) H_2 technologies using PVts in 2020 depending on the energy prices and the export bonus. 153
6.21 PV generation curtailment avoided and revenue associated with it for (a) PbA and (b) H_2 technologies performing PVts in 2020 as a function of the size of the community and the CES size. 154
6.22 *LVOES* and *IRR* optimised for (a) PbA, (b) Li-ion and (c) H_2 technologies using PVts in 2020 depending on if the curtailment obligation is applies. 155

6.23 *IRR* of the optimum Li-ion battery (41.6 kWh) performing PVts in a 10-home community in 2020 (community PV percentage of 76%) as a function of the storage medium cost (percentage variation over a reference cost of 1300 £/kWh i.e. 0% variation) for an electricity price of 16.3 p/kWh and 19 p/kWh; and as a function of the electricity price (percentage variation over a reference price of 16.3 p/kWh i.e. 0% variation) for a storage medium cost of 260 £/kWh and 780 £/kWh. . . 156
6.24 (a) *LCOES*, (b) *IRR* and (c) *LVOES* optimised for Li-ion batteries performing PVts depending on the tariff in 2020 as a function of the size of the community. 156
6.25 Performance results of PbA batteries performing LS with the NETA tariff in 2020 as a function of the size of the community and the battery capacity: (a) equivalent full cycles, (b) round trip efficiency and (c) D_{ES}. The battery capacity is given as a percentage of the maximum ES demand. 158
6.26 Performance results of PbA batteries performing LS with Economy 7 in 2020 as a function of the size of the community and the battery capacity: (a) equivalent full cycles, (b) round trip efficiency and (c) D_{ES}. The battery capacity is given as a percentage of the maximum ES demand. 159
6.27 Performance results of Li-ion batteries performing LS with the NETA tariff in 2020 as a function of the size of the community and the battery capacity: (a) equivalent full cycles, (b) round trip efficiency and (c) D_{ES}. The battery capacity is given as a percentage of the maximum ES demand. 160
6.28 Performance results of Li-ion batteries performing LS with the Economy 7 in 2020 as a function of the size of the community and the battery capacity: (a) equivalent full cycles, (b) round trip efficiency and (c) D_{ES}. The battery capacity is given as a percentage of the maximum ES demand. 161
6.29 Performance results of H_2 systems performing LS with the NETA tariff in 2020 as a function of the size of the community and the battery capacity: (a) capacity factor, (b) electrolyser efficiency and (c) $H2_{ratio}$. The electrolyser rating is given as a percentage of the maximum ES demand. 162
6.30 Optimum battery capacity which minimised the levelised cost, *LCOES*, associated with LS with Economy 7 and the NETA tariff as a function of the community size for PbA and Li-ion technologies in 2020 and the zero carbon year. 164
6.31 Optimum electrolyser which minimised the levelised cost, *LCOES*, associated with LS with Economy 7 and the NETA tariff as a function of the community size in 2020 and the zero carbon year. 166
6.32 (a) *LCOES*, (b) *IRR* and (c) *LVOES* optimised for PbA, Li-ion and H_2 technologies using LS in 2020 depending on the tariff. 166
6.33 (a) *LCOES*, (b) *IRR* and (c) *LVOES* optimised for PbA, Li-ion and H_2 technologies using LS in the zero carbon year depending on the tariff. 168
6.34 *LCOES* and *IRR* optimised for (a) PbA, (b) Li-ion and (c) H_2 technologies using LS with the NETA tariff in 2020 depending on the ES cost and durability characteristics. 170
6.35 Optimum CES system which minimised the levelised cost, *LCOES*, when performing LS as a function of the size of the community for the three technologies depending on the HP penetration in 2020. 170
6.36 *LCOES* and *IRR* optimised for (a) PbA and (b) Li-ion technologies as a function of the size of the community when performing LS with the NETA tariff depending on the HP penetration in 2020. 171
6.37 *LCOES* and *IRR* optimised for (a) PbA, (b) Li-ion and (c) H_2 technologies as a function of the size of the community when performing LS with the NETA tariff depending on the energy prices in 2020. 172

6.38 Performance results of PbA batteries performing PVts and LS with the NETA tariff in 2020 as a function of the size of the community and the battery capacity: (a) equivalent full cycles, (b) round trip efficiency, (c) PV_{ES} and (d) D_{ES}. The battery capacity is given as a percentage of the maximum ES demand. 174
6.39 Performance results of PbA batteries performing PVts and LS with Economy 7 in 2020 as a function of the size of the community and the battery capacity: (a) equivalent full cycles, (b) round trip efficiency, (c) PV_{ES} and (d) D_{ES}. The battery capacity is given as a percentage of the maximum ES demand. 175
6.40 Performance results of H_2 systems performing PVts and LS with the NETA tariff in 2020 as a function of the size of the community and the electrolyser rating: (a) capacity factor, (b) electrolyser efficiency, (c) PV_{ES} and (d) H_{2ratio}. The electrolyser rating is given as a percentage of the maximum ES demand. 176
6.41 Optimum PbA battery capacity which minimised the levelised cost, *LCOES*, associated with PVts, LS and both applications combined with the NETA tariff and Economy 7 as a function of the size of the community in 2020 and the zero carbon year. 177
6.42 Optimised (a) *LCOES*, (b) *IRR* and (c) *LVOES* as a function of the size of the community for PbA technology depending on the application developed when considering the NETA tariff in 2020. 178
6.43 (a) *LCOES*, (b) *IRR* and (c) *LVOES* optimised for PbA technology as a function of the size of the community depending on the application when considering Economy 7 in 2020. 179
6.44 (a) *LCOES*, (b) *IRR* and (c) *LVOES* optimised for Li-ion technology as a function of the size of the community depending on the application when considering the NETA tariff in 2020. 180
6.45 (a) *LCOES*, (b) *IRR* and (c) *LVOES* optimised for Li-ion technology as a function of the size of the community depending on the application when considering Economy 7 in 2020 181
6.46 (a) *LCOES*, (b) *IRR* and (c) *LVOES* optimised for H_2 technology as a function of the size of the community depending on the application when considering the NETA tariff in 2020. 182

7.1 Panoramic view of the Creative Energy Homes at the University on Nottingham. The H-CES system was installed for this community. 187
7.2 Schematic representation of the microgrid which is being created at the Creative Energy Homes community with a battery system, H_2 system and demand side management. 188
7.3 Electrical consumption and PV generation in one of the Creative Energy Homes, the Tarmac Code 6, in two different days. 190
7.4 PEM electrolyser at The University of Nottingham. The model is the 1.1 kW_e HBox-PV manufactured by ITM Power. 191
7.5 Magnesium metal hydride tank at The University of Nottingham. 195
7.6 Gas panel of the H_2 tank including its main components. 197
7.7 PEMFC system located at The University of Nottingham. 198
7.8 Voltage and power of the PEMFC stack as a function of the current generated based on the polarization curve of a single cell according to the manufacturer specification when considering the 20 cells. 199
7.9 Optimum temperature of the PEMFC stack as a function of the current generated according to the manufacturer specification. 200
7.10 Cabinet where all electrical and electronic equipment was located. 202

7.11 Schematic representation of the H-CES system with the main energy flows and fluids utilised by the electrolyser, H_2 tank and PEMFC systems. 203
7.12 H-CES system at the Creative Energy Homes community of The University of Nottingham. 205
7.13 H_2 flows and related power flows of the electrolyser and PEMFC systems when performing PVts in two different days in a 5-home community. (a) The day 1 and (b) the day 2 represent a day with low (7.1 kWh) and high (22.0) PV generation respectively. 206
7.14 Electrolyser and PEMFC systems efficiency when performing PVts in a 5-home community in two different days in a 5-home community. (a) The day 1 and (b) the day 2 represent a day with low (7.1 kWh) and high (22.0) PV generation respectively. 208
7.15 Temperatures of the H_2 tank when performing PVts according to the day 1 in the previous section. 209
7.16 Evolution of the pressures of the H_2 tank when performing PVts according to the day 1 in the previous section. 211
7.17 (a) H_2 flows and (b) related power flows of the H-CES system (electrolyser and PEMFC systems) in two consecutive days (29 September and 30 September) when performing LS with the NETA tariff. 212
7.18 Electrolyser and PEMFC systems efficiency in two consecutive days (29 September 2007 and 30 September 2011) when performing LS with the NETA tariff. 213
7.19 (a) H_2 flows and (b) related power flows of the electrolyser and PEMFC systems in a day when performing PVts and LS with the NETA tariff. 214
7.20 Electrolyser and PEMFC system heat and electricity efficiencies when performing PVts and load shifting with the NETA tariff. 215

D.1 Schematic representation of the PEM electrolysis with the different reactants, products, reaction sites and reactions [15]. 241

E.1 Illustrative schematic representation of the power line and wireless control connections between electric drive vehicles and the electric power grid for vehicle to grid applications [16]. 252

F.1 Equivalent electrical circuit of a Li-ion battery considering capacitors and coils conforming a RC network 256

G.1 PEM electrolyser rating as a percentage of the ES demand for different communities for (a) PVts and (b) LS with the NETA tariff in 2020, and (c) PVts and (d) LS with the NETA tariff in the zero carbon year. Ten electrolysers were tested for each community. 258
G.2 Battery capacity as a percentage of the ES demand for different communities in 2020 for PbA batteries performing (a) PVts and LS with the NETA tariff and (b) PVts and LS with Economy; and for Li-ion batteries performing (c) PVts and LS with the NETA tariff and (d) PVts and LS with Economy. 259
G.3 Battery capacity as a percentage of the ES demand for different communities in the zero carbon year for PbA batteries performing (a) PVts and LS with the NETA tariff and (b) PVts and LS with Economy; and for Li-ion batteries performing (c) PVts and LS with the NETA tariff and (d) PVts and LS with Economy. 259

I.1 Efficiency of the DC/DC converter of the electrolyser and input DC power test during a test. 262
I.2 Efficiency of the DC/DC converter of the electrolyser versus the input DC power. 262

J.1 PbA battery system which optimized different performance and economic parameters as a function of the size of the community when performing (a) PVts and (b) LS with Economy 7 in the zero carbon year. 263
J.2 Li-ion battery system which optimized different performance and economic parameters as a function of the size of the community when performing (a) PVts and (b) LS with Economy 7 in the zero carbon year. 264
J.3 Electrolyser which optimized different performance and economic parameters as a function of the size of the community when performing (a) PVts and (b) LS with the NETA tariff in the zero carbon year. 264

List of Tables

2.1 Qualitative comparison of PbA, NiCd, NiMH and Li-ion batteries. 36
2.2 Comparison of different H_2 storage system when supporting RE technologies in three different European projects. 39
2.3 Summary of the data reported in this chapter and comparison of different ES technologies including basic characteristics for stationary applications [11,17,17–19]. 41

3.1 Relationship among the ES drivers, applications and the economic (internalizable) benefit derived from the applications at the energy consumption level. 49
3.2 Electrical characteristics of the PV panel modelled in this work. 63

4.1 Comparison of the control levels implemented by the management system for PbA and Li-ion chemistries. 79
4.2 *EFC*, cycle dimensionless life parameter (Z) and calendar losses (monthly percentage of capacity reduction) depending on the battery technology and the reference year. 87
4.3 Water tank price as a function of the capacity utilised in this work. 95

5.1 Cross-application parameters and reference values utilised in 2012, 2020 and the zero carbon year 118
5.2 PVts parameters and reference values utilised in 2012, 2020 and the zero carbon year. 119
5.3 LS parameters and reference values utilised in 2020 and the zero carbon year . . 119
5.4 ES technologies parameters and reference values utilised in 2012, 2020 and the zero carbon year 120
5.5 Parameters included in the cost and durability sensitivities for battery technology for 2020 and the zero carbon year. 122
5.6 Parameters included in the cost and durability sensitivities for H_2 technology for 2020 and the zero carbon year. 123
5.7 Parameters included in the cost and durability sensitivities for battery and H_2 technologies for 2020 and the zero carbon year. 123
5.8 PV and HP penetration sensitivity and the respective value for 2020 and the zero carbon target. 124
5.9 Different energy prices and export bonus considered in the sensitivity analysis depending on the reference year. 124
5.10 Community PV and HP percentages based on the PV and HP penetration in the UK. PV penetration and HP penetration are based on estimations from DECC [20] 127

6.1 Performance parameters optimised for PbA, Li-ion and water tank technologies using PVts in 2012. The capacity of the battery (kWh) and the water tank (l) which achieved the optimum values is shown in brackets. 131

6.2 Economic parameters optimised for PbA, Li-ion and hot water tank technologies using PVts in 2012. The capacity of the battery (kWh) and the hot water tank (l) which achieved the optimum values is shown in brackets. If the hot water tank already exits, only a PV controller is installed to divert the surplus PV generation. 134
6.3 Performance parameters optimised for PbA batteries, Li-ion batteries and H_2 systems performing PVts in the zero carbon year. The size of the community and the capacity of the battery (kWh) or the rating of the electrolyser (kW) which achieved the optimum values is shown in brackets. 141
6.4 Economic parameters optimised for PbA batteries, Li-ion batteries and H_2 systems performing PVts in the zero carbon year. The size of the community and the capacity of the battery (kWh) or the rating of the electrolyser (kW) which achieved the optimum values is shown in brackets. 144
6.5 Performance parameters optimised for PbA, Li-ion and H_2 technologies using LS depending on the tariff in 2020 and the zero carbon year. The size of the community and the capacity of the battery (kWh) or the rating of the electrolyser (kW) which achieved the optimum values is shown in brackets. 163
6.6 Economic parameters optimised for PbA, Li-ion and H_2 technologies using LS with Economy 7 and the NETA tariff in 2020 and the zero carbon year. The size of the community and the capacity of the battery (kWh) or the rating of the electrolyser (kW) which achieved the optimum values is shown in brackets. . . . 169
6.7 Performance parameters optimised for PbA, Li-ion and H_2 technologies using PVts and LS in 2020 and the zero carbon year. The size of the community and the capacity of the battery (kWh) or the rating of the electrolyser (kW) which achieved the optimum values is shown in brackets. 177
6.8 Economic parameters optimised for PbA, Li-ion and H_2 technologies using PVts and LS in 2020 and the zero carbon year. The size of the community and the capacity of the battery (kWh) or the rating of the electrolyser (kW) which achieved the optimum values is shown in brackets. 183

7.1 PV arrays located at the Creative Energy Homes and their maximum power. . . 188
7.2 Different electrical demand loads with the electrical rating in one of the Creative Energy Homes, the Tarmac Code 6 189
7.3 Electrolyser performance parameters and values reported by the manufacturer. . 192
7.4 Deioniser water unit performance parameters and values reported by the manufacturer. 192
7.5 AC/DC converter performance parameters and values reported by the manufacturer 193
7.6 MgH_2 storage system specifications as reported by the manufacturer 197
7.7 DC/AC inverter technical characteristics as reported by the manufacturers. . . . 201
7.8 Parasitic loads and the nominal value as reported by the manufacturer. 202
7.9 Prices for the four periods in the two consecutive days (29 September 2007 and 30 September 2011) utilised to demonstrate the performance of the H-CES system when performing LS with the NETA tariff. 211
7.10 Performance parameters obtained by the H-CES system depending on the application. 215

B.1 Equivalent full cycles data for PbA and Li-ion batteries reported in the literature. 237
B.2 Cost of the storage medium data for PbA and Li-ion batteries reported in the literature. 237

C.1 Comparison between the targets set by the European Commission for 2010 and 2020 for FC technology. 239

D.1 Efficiency of different commercial electrolysers available in the market based on HHV of hydrogen. 250

List of Acronyms

- AC/DC: AC to DC
- BoP: balance of plant
- CAES: compressed air energy storage
- CES: community energy storage
- CHP: combined heat and power
- DC/AC: DC to AC
- DECC: department of energy and climate change (UK)
- DNO: distribution network operator
- DOE: Department of Energy (USA)
- DOD: depth of discharge
- FC: fuel cell
- ES: energy Storage
- H2: hydrogen
- H-CES: hydrogen community energy storage
- HP: heat pump
- HHV: high heating value
- IPCC: Intergovernmental Panel on Climate Change
- IRR: internal rate of return
- LCOES: levelised cost of energy storage
- LVOES: levelised value of energy storage
- LS: load-shifting:
- NETA: new electricity trading arrangements
- PCM: phase change material
- PEM: polymer electrolyte membrane
- PEMFC: polymer electrolyse r membrane fuel cell
- PV: photovoltaics
- PVts: PV energy time-shift
- RE: renewable energy
- SOC: state of charge
- SOFC: Solid oxide fuel cell

Nomenclature

- A_{Wt}= External area of a water tank (m^2)
- ADC= Ampere direct current (V)
- c_{H2O}= Specific heat of water (kg ·K)
- C= Effective battery capacity (kWh)
- C_{Ah}= Effective battery capacity (Ah)
- C_{factor}= Capacity factor of an electrolyser
- C_{nom}= Nominal battery capacity (kWh)
- CF= Cash flow (£)
- $Cost_{sm}$= Total storage medium cost (£)
- $cost_{sm}$= Storage medium cost (£/kWh)
- $D_{\%ES}$= Proportion of the total demand of a community met by a CES system
- E_{char}= Seasonal CES charge (kWh/year)
- E_{Ct}= Seasonal renewable energy which is not curtailed due to energy storage (kWh/year)
- E_d= Seasonal demand of a community (kWh/year)
- E_{dis}= Seasonal discharge of a battery system (kWh/year)
- E_{dise}= Seasonal electrical discharge of a hydrogen storage system (kWh/year)
- E_{dish}= Seasonal heat discharge of a hydrogen storage system (kWh/year)
- E_{nele}= Nernst voltage of the electrolyser (V)
- E_{PV}= Seasonal PV generation (kWh/year)
- E_{PVCES}= Seasonal PV energy supplied to a CES system (kWh/year)
- EF= Seasonal energy flow (kWh/year)
- EFC= Equivalent full cycles (cycle)
- H_{year}= Electrolyser operational hours in a year (h)
- $H2$= Hydrogen.
- H_{2ratio}= Proportion of hydrogen consumed by a FC system generated by a local electrolyser.
- I_{bat}= Battery current (A)
- IRR= Internal rate of return (£/kWh)
- K= Constant that represents the limit capacity when the discharge current tends to zero
- kW_e= Electrical Kilowatt generated by a H_2 system

- kW_h= Thermal Kilowatt generated by a H_2 system
- kWh_e= Electrical Kilowatt hour generated by a H_2 system
- m= Capacity of a water tank (kg)
- m_{ele}= Seasonal hydrogen generated by an electrolyser (kg/year)
- m_{H2}= Hydrogen mass stored in the tank (kg/year)
- m_{PEMFC}= Seasonal hydrogen consumed by a PEMFC system (kg/year)
- $LCOES$= Levelised cost of energy storage (£/kWh)
- $Life$= Operational years of a CES system (year)
- $LVOES$= Levelised value of energy storage (£/kWh)
- P_{ex}= Price of the electricity export i. e. export bonus (£/kWh)
- P_i= Price of the electricity import (£/kWh)
- P_{iv}= Price of the electricity import at the valley period (£/kWh)
- P_{ip}= Price of the electricity import at the peak period (£/kWh)
- P_h= Heat price (£/kWh)
- $PV_{\%ES}$= Proportion of the community PV generation supplied to the CES system
- Q= Battery charge delivered or supplied at time of interested (A·h)
- Q_{in}= Heat supplied to hot water tank (W)
- Q_{out}= Heat supplied by the hot water tank (W)
- R_{bat}= Battery resistance (Ω)
- Rev_{PVts}= Revenue from PV energy time shift (£)
- Rev_{LS}= Revenue from load shifting (£)
- Rev_{Ct}= Revenue from preventing renewable power curtailment (£)
- $Size_l$= Limit storage size for cost reduction (kWh for battery and kW for electrolyser).
- $Size$= Storage size for cost reduction (kWh for battery and kW for electrolyser).
- U_{Wt}= Heat loss coefficient (W/(m^2· K))
- T_{bat}= Battery temperature (K)
- T_{ele}= Electrolyser temperature (K)
- T_{Wt}= Hot water tank temperature (K)
- T_{Wtmax}= Maximum hot water tank temperature (K)
- T_{Wtmin}= Minimum hot water tank temperature (K)
- T_{room}= Room temperature (K)
- $Tank_{size}$= Hydrogen tank size (kg)

- $TLCC$= Total levelised cost (£)
- $V_{eleacta}$= Activation voltage in the anode of an electrolyser cell (V)
- $V_{eleactc}$= Activation voltage in the cathode of an electrolyser cell (V)
- V_{bat}= Battery voltage (V)
- V_{batc}= Battery voltage during the charge (V)
- V_{batd}= Battery voltage during the discharge (V)
- VDC= Volt direct current (V)
- V_{elecon}= Concentration voltage of the electrolyser (V)
- V_o= Open circuit voltage (V)
- V_{eleohm}= Ohmic voltage of the electrolyser (V)
- W_e= Electrical Watt (W)
- W_h= Thermal Watt (W)
- η= Round trip efficiency of a battery system
- η_{ele}= Efficiency of an electrolyser
- η_e= Electrical round trip efficiency of a hydrogen storage system
- η_h= Heat round trip efficiency of a hydrogen storage system
- Z= Linear durability coefficient of battery technology.

Chapter 1

Introduction

1.1 World Energy outlook

Renewable energy (RE) technologies are a key alternative to reduce carbon dioxide (CO_2) emissions. However, they do not offer the same level of dispatchability as fossil generators do. Energy storage (ES) is a flexible option to increase the penetration and value of RE technologies. Community energy storage (CES) refers to small scale and broadly distributed ES at customer sites for managing the RE generation by plants owned by customers and their demand.

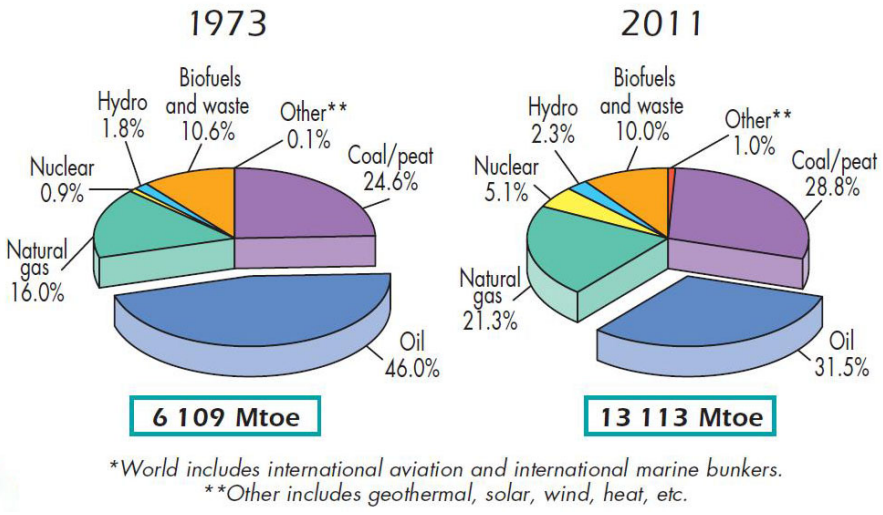

Figure 1.1: World total primary energy supply in 1973 and 2011 depending on the fuel [1].

The world total primary energy supply was 6109 Mtoe in 1973, which increased to 13113 Mtoe by 2011 [1]. In 2011, most of the energy generated came from fossil fuels such as oil (31.5%), coal/peat (28.8 %), natural gas (21.3%) and nuclear (5.1 %). RE technologies together with energy generated from waste contributed the remaining 13.3% of primary energy generation as shown in Figure 1.1. Of the 6109 Mtoe and 13133 Mtoe of energy generated in 1973 and 2011, only 4671 Mtoe and

8918 Mtoe were actually consumed in 1973 and 2011 respectively. The difference in energy production and consumption was due to losses in conversion processes such as generation, transport and consumption. The related global emissions were equal to 15611 Mt of CO_2 and 30273 Mt of CO_2 in 1973 and 2010 (the last data available) respectively, showing a total increase of 94% as calculated by the International Energy Agency (IEA) [2]. The increase in CO_2 emissions was more marked between 2005 and 2010 and only there was a deceleration in 2009 due to the global economic crises as shown in Figure 1.2. Similarly, emission reductions happened in previous economic crisis such as the oil crisis in the mid-1970s and the early 1980s recession.

There are several reasons why the level of CO_2 emissions together with the energy consumption figures are not sustainable. Although there is remarkable uncertainty in when fossil fuels will become scarce, they are finite resources and will be eventually exhausted. New resources for oil and gas will run out before carbon reserves according to current assessments [21]. Another aspect related to the finite nature of fossil fuels is that cost of extraction will increase as reserves become scarce and this is already impacting the current prices.

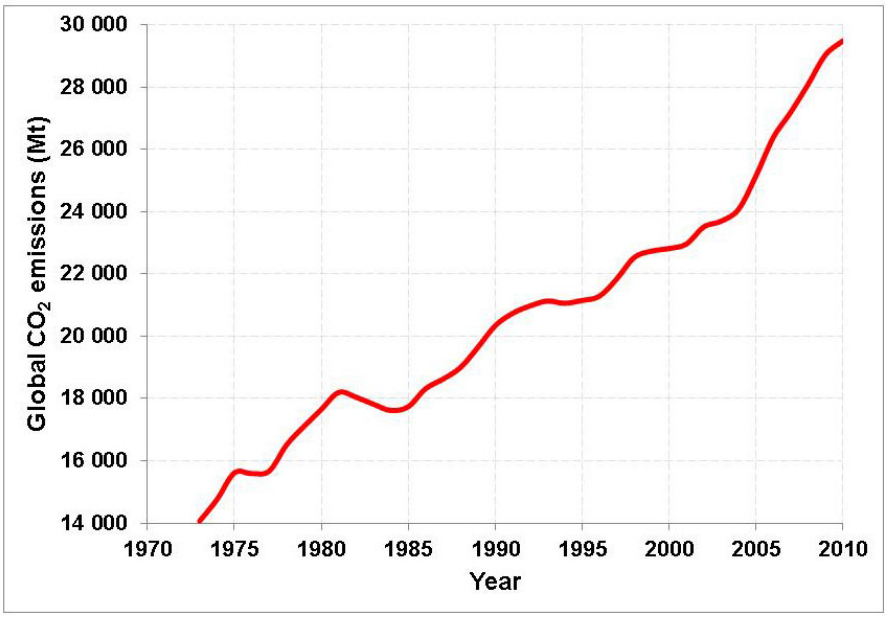

Figure 1.2: Global CO_2 emissions as a function of the year [2].

Secondly, energy security is a key concern for most countries, especially those which lack their own natural reserves. This is increasing the geopolitical tension between countries which own fossil fuel reserves and those which do not. The problem has become more complex when countries use energy security as a political or defense strategy. Energy is necessary for the development of any country and the treatment of energy as a political resource can negatively impact even

more on those countries which are poorer.

Finally, 87.7% of the total energy is generated from fossil fuels which generate CO_2 and other gases which are liberated to the atmosphere according to Figure 1.2. This is affecting the natural carbon cycle and as a result the CO_2 concentration in the atmosphere increased to 379 ppmv considering that the value was around 290 ppmv in the pre-industrial area [2]. At the same time, the earth's surface temperature is rising and an increase of 0.89 °C was measured between 1901 and 2012. The last decade was the warmest on records according to the last IPCC report published in 2013 [22]. This is a consequence of the greenhouse effect of gases produced by human activities, mainly due to the use of fossil fuels. There is debate about whether anthropogenic increase of the temperature is related to different natural disasters but there is clear evidence between CO_2 concentration and temperature increase.

The Kyoto Protocol was adopted in 1997 to set binding emission reduction targets for different countries. As part of the Protocol, industrialized or Annex I countries legally agreed to reduce their GHG emissions between 2008-2012 to 5.2% below those in 1990 [16]. There are 192 parties to the Protocol (191 States and one regional economic integration organisation, which is the EU). United States (USA) is not a party to the Protocol, even tough it is the country which pollutes most. However, emissions in Europe were reduced only by 3.1% by 2012 (USA emissions increased by 24.0% by 2012) [72]. RE generation increased from 763.6 Mtoe to 1744.0 Mtoe from 1973 to 2011 but this did not avoid the failure in meeting the above targets. In fact, the absolute increase of 980.4 Mtoe only meant a percentage increase of 0.8% when considering the total energy generation presented in Figure 2.1. In contrast, the percentage of energy generated from fossil fuels reduced from 87.5% to 86.7% but the absolute value increased from 5345.4 Mtoe to 11386.3 Mtoe between 1973 and 2011.

Negotiations regarding a second commitment period of Kyoto took place in Doha, Qatar, on 8 December 2012, where parties adopted the "Doha Amendment to the Kyoto Protocol". The amendment includes a new commitment for Annex I Parties to the Kyoto agreement to reduce their GHG emissions by at least 18% below 1990 levels in a second commitment period that would comprise the eight-year period from 2013 to 2020 [94].The main focus of Doha negotiations were on the real implementation of the agreement and the creation of institutional mechanism to address loss and damage in developing countries that are particularly vulnerable to the adverse effects of climate change. It is important to note that the Doha Amendment has not yet entered into force and even if it does, it will not be legally binding for those countries that are not party to the Kyoto Protocol, such as USA, Canada, Japan and Russia.

1.2 Technologies to reduce carbon dioxide emissions

Fossil fuels are the main fuel utilised to generate the energy necessary to meet the world's energy demand as seen in Figure 1.1. This fact will not change in the short and mid term but there are some alternatives to reduce the related GHG emissions. There are different technologies which will contribute to tackle the emissions and security of energy supply problems.

1.2.1 Renewable energy technologies

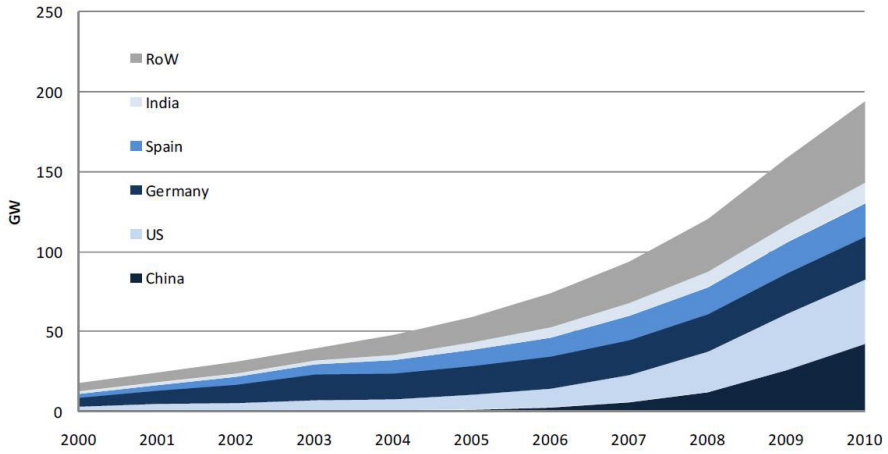

Figure 1.3: Evolution of installed wind capacity including off-shore in the world from 2000 to 2010 showing the countries in which the market was more important [3].

RE technologies are those which make use of sustainable resources available in nature. The main source of RE is the sun, which supplies on average 8000 times more energy than the currently world primary energy consumption [21]. The energy from the sun is already used to generate heat when using solar thermal collectors for domestic hot water (DHW) and to a lesser extent for space heating. Solar energy and natural light solutions are also integrated in passive designs to reduce space heating and lighting needs. Electricity generated by PV panels and concentrated solar power are two reliable options to generate power. The case of PV energy is discussed deeper in Sections 3.3 and 3.10.2.

Additionally, the energy from the sun is also responsible for other RE technologies such as wind energy (due to the different temperatures in the atmosphere),

hydropower (due to water evaporation) and biomass and biofuels (due to photosynthesis) [3]. Although tidal energy is more related to the orbital characteristics of the moon around the earth, it is also affected by the orbit of the earth around the sun. Finally, geothermal energy makes use of the thermal energy stored internally in the earth's core.

RE technologies are diverse and flexible in terms of the energy vector generated by them and there are different technological options for electricity (hydro energy, solar PV, concentrated solar power, wind energy, tidal and biomass), heat (solar thermal energy, biomass and geothermal), biofuels and even H_2 (directly from solar energy using photocalytic water splitting, from biomass using gasification and other chemical process and using electrolysis run by renewable electricity). However, RE technologies which generate electricity are more mature and the electricity is easily transported using the current network. This helped promote the use of RE technologies in the power sector more than in the heat and transport sectors. For example, RE technologies accounted for 19.3% of the global electricity generated in 2009 while biofuels only accounted for 2% of the total transport needs in 2009 [23]. Renewable electricity, heat and biofuels grew 17.8%, 5.9% and 26.0% respectively from 2005 to 2009. Among RE technologies which generate electricity, hydro energy is the most important in terms of annual generation equal to 3252 TWh in 2009 (16.2% global electricity production), wind energy has the largest installed capacity just below 200 GW in 2009 as shown in Figure 1.4 and solar PV is the technology which grew faster in the last decade, specifically with a compound average growth rate of 50.2% between 2000 and 2009 [23]. The cumulative capacity was 1.5 GWp and 40 GWp in 2000 and 2010 respectively [3]. Additionally, continuous progress has reduced the system cost dramatically (according to the International Energy Agency (IEA), the costs of PV exhibits a learning rate of 19.3% being defined as the reduction of cost for every doubling of capacity) and it has increased the efficiency steadily (according to the Franhoufer ISE the average efficiency of commercial wafer-based silicon modules have increased from about 12% to 15% in the last decade [24])

1.2.2 Energy conversion efficiency improvement

Efficiency can refer to a better use of current energy generation and a reduction of the final demand requirements. According to the data presented in Section 1.1, the global efficiency of the energy sector, defined as the ratio between final consumption and primary energy supply, was 0.77 and 0.68 in 1973 and 2011 respectively. Considering that 8918 Mtoe were consumed in 2011, it would have been possible either to reduce this consumption or at least use less than 13133 Mtoe to meet this demand requirement.

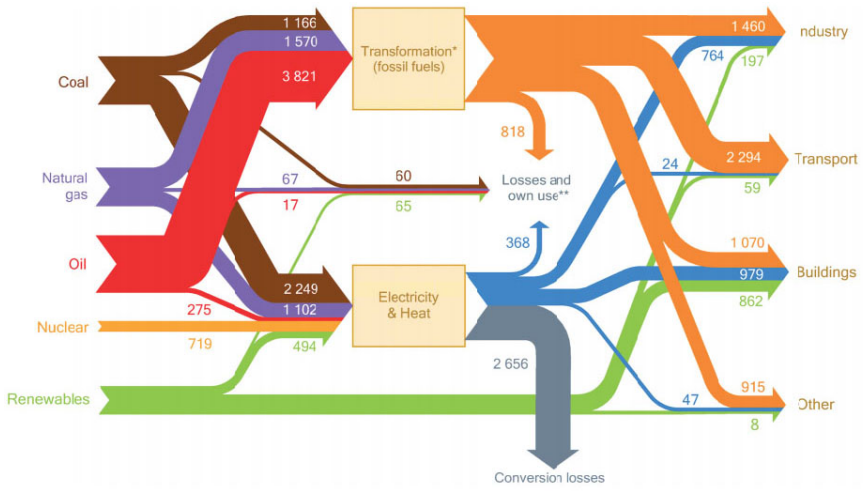

Figure 1.4: Global Energy Flows 2010 from World Energy Outlook 2012 [4].

The increase of the efficiency is a key factor to reduce the GHG emissions and efficiency maximization can be implemented in all sections of the energy value chain such as generation, transmission and demand. In terms of generation, the use of more efficient thermodynamic cycles and heat recovery such as combined cycle gas turbines and combined heat and power (CHP) plants are able to increase the efficiency of the primary energy use up to 60% and 80% respectively [21]. Condensing gas boilers and heat pumps (HP) offer seasonal efficiency and coefficient of performance (COP) equal to 85% [25] and higher than 2 respectively [26]. For the transport sector, FC systems seem to be a promising technology to increase the efficiency of electric drive vehicles up to 42% considering considering the drive train [27]. Batteries are another alternative for the transport sector, achieving even higher efficiency up to 60% considering the drive train [28]. But the efficiency of internal combustion engines (ICE) has also increased with improvements up to 10% (30%) in the case of gasoline and up to 3.5% (35%) for diesel between 2002 and 2010 [29, 30].

There is also potential for efficiency improvement in both electricity and heat distribution. In the UK, 2% of the total electricity transported is lost in the national grid, being this was equivalent to 6.9 TWh in 2009 [31]. Similarly, heat losses in heat exchangers and distribution pipes can mean up to 10% of the total heat generation. Finally, new technologies are helping to improve the efficiency of final loads in industries, commercial buildings and homes. Some examples are the use of control techniques to use energy only when required and efficient light bulbs and appliances, which can reduce the energy consumption by 75% [20].

In the UK, energy use in the domestic sector accounts for 30% of the total energy consumption and it has risen by 23% over the last 35 years [32], a trend

comparable to that of many other countries. In fact, the domestic sector is attracting a lot of attention because buildings account for 27.1% of final global energy consumption (40% including the commercial sector) [33]. The decarbonisation of the heating demand is one of the challenges to arise because heating and DHW demand account for around 75% of the energy consumption in buildings [34]. Two strategies for decreasing the energy consumption in the domestic sector are the reduction of the demand requirements by introducing improvements such as insulation, reduction of the stand-by consumption of appliances, low energy appliances and lighting (passive measures), and the penetration of small scale RE technologies and other types of efficient distributed generation technologies (active measures).

1.2.3 Nuclear energy

Figure 1.5: Aerial view of the new power plant that will be built in Somerset by EFC according to the design [5].

Controversy has always been related to nuclear energy but the reality is that it is a technological option which has become more important in the total energy share as seen in Figure 1.1. In 1973 nuclear energy generated only 0.9% of the global energy, this percentage rose to 5.1% in 2011. Nuclear energy is advertised as a carbon-free technology for those who support its uptake. Nuclear energy uses uranium and this fuel does not generated CO_2, however there are three aspects which make nuclear energy not a completely renewable and sustainable technological option:

- Uranium reserves are also finite and expected to last for around 100 years [35], occurring the same with other radiative elements such as thorium and plutonium.

- The construction of nuclear reactor plants demand large amounts of materials, capital costs and time.
- Accidents like the one that happened in Fukoshima in 2011 increase the social opposition to this technology.
- At the end of their useful life and after removal from the reactor core, the fuel elements are highly radioactive. Although residues can be chemically reprocessed to be reused as a thermal reactor fuel, there are great concerns related to the high radioactivity of the residues and public rejection.

According to electric utility EDF, which is the main industrial partner of the new nuclear plant which is going to be built in the UK (Somerset), Hinckley point C technology will be used which is safer and more efficient than previous nuclear technology [36]. Figure 1.5 shows an aerial view of the projected nuclear plant. EDF claims the carbon footprint of a nuclear power station, defined as the average level of GHG emissions it is responsible for over its lifetime (from construction to decommissioning), is about 16 g/(kWh·year) of equivalent CO_2. Uranium extraction accounts for 40% of emissions from nuclear power; decommissioning is responsible for 35%, and less than 1% comes from operation [37]. EDF has significant experience in the nuclear sector because it manages 59% of the total nuclear power in France, where nuclear energy is proportionally more important (75% [38]). The British government declared this technology as a clean technology and put it in the same context as RE technologies and carbon capture and storage (CCS) in its low carbon transition plan [34].

1.2.4 Carbon capture and storage

Still at the research and demonstration phases, CS is a technology in which many countries have great expectations to cut CO_2 emissions. For example, the UK government launched a competition in 2007 to build one of the first commercial CS demonstrative plants. Also, a CCS office was opened in 2011 by the UK government where the objective is having a cost competitive industry by 2020 [34]. In fact, CS is one if the key technologies used by the UK government in its available pathways analysis and pathways calculator for the decarbonisation pathway [20].

According to the IEA, CCS is a cost competitive technology to cut CO_2 emissions when incentives are in place to support carbon capture. According to their estimations, with a cost of 50 \$/t CO_2, 5.1 Gigatonnes (Gt) per year of CO_2 would be captured and stored by 2050, which is 14% of the total needed for global temperature stabilisation [39]. This idea was reinforced by the fact that fossil fuels usage will not vary in the mid-term. The IEA concluded that the key technological challenge to overcome is the integration of the three main processes involved

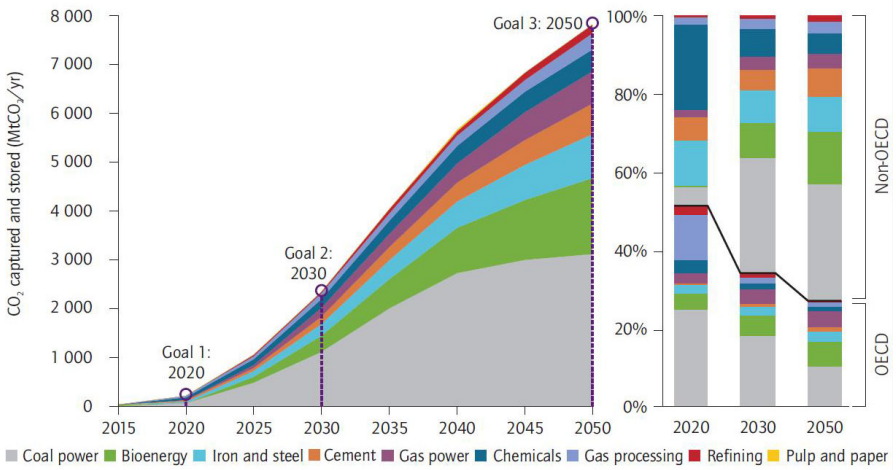

Figure 1.6: CCS in the power and industry sector according to IEA projections assuming that CS contributes to one-sixth of CO_2 emissions reduction by 2050 [6].

(capture, transport and storage) at large scale, since these individual components are well understood independently [6]. CCS is not only envisaged for the energy sector but also for big industries such as cement and other chemical industries as schematically represented in Figure 1.6. The collaboration of different stakeholders such as governments and utility companies is a key factor for the up-take of this industry [6]. The IEA stated that fighting climate change could cost 70% more without CCS. Around two thirds of the total CCS costs rely on the sequestration of CO_2 and there is great potential for research development in this field [20].

The IEA aim is having 30 operating CCS projects by 2020 across a range of processes and industrial sectors. The European Union is keen to provide financial support to 12 of those demonstrations project. Four of these demonstration projects will take place in the UK where the government legislated to have CCS in new coal plants by 2025 [20].

1.3 Renewable energy technologies variability

RE technologies together with increased system efficiency are two key options to make world economies sustainable and clean without environmental concerns and other issues related to fossil fuels, such as its increasing cost, uncertainty of supply and the expected depletion of reserves. The Directive 2009/28/CE (Union, 2009) suggested the use of RE technologies and it established binding objectives (20% of gross end energy consumption to be supplied by RE technologies in 2020 and 10% in transport). All new construction buildings must be zero energy buildings by 2020. The UK government also set this objective of achieving net zero carbon dwellings by 2016 [34]. However, the penetration of RE technologies and other distributed generation will challenge the current energy system based on cent-

ralised power generation far from consumer points. The flexibility necessary for the continuous balance of demand and generation is given by thermal generation plants (gas, coal and diesel) which offer ramping capability. Most RE technologies are intermittent because they depend on weather conditions and they do not offer matching capability. All RE technologies outlined in Section 1.2.1 offer a temporal pattern which is directly related to the natural resource they are based on:

- Mean wind energy changes from one season to another (seasonal variations); there are variations due to meteorological phenomenon such as anticyclone and low pressure areas in consecutive weeks; on a daily basis (daily variations), wind blows faster at night; and even turbulence modifies the instantaneous speed profile second by second.

- The solar resource reaching the earth surface varies depending on the season specially far from the equator; as it happened wind energy, anticyclone and low pressure areas modify the presence of clouds on the sky; every day of the year there is a clear pattern due to the day and night cycle; and the movement of the clouds changes the radiance in a matter of minutes.

- Hydro generation does not vary in short time scales like wind and solar energy. It is basically affected by the flow of the rivers which is related to the seasons (wet and dry) and the melt of the snow.

- The moon and the sun's gravitational field cause the natural rise and fall of coastal tidal waters. These forces create two tides every day of the year although the different relative position of the moon and to a lesser extent of the sun varies the size of the tides along the year.

- Biomass resource availability also varies with the season according to the growing time scales of the different crops.

Additionally, RE generation is affected by the geographical availability of the wind, irradiance and tidal resources which modifies the yield in different spatial scales. For example, the irradiance is always higher next to the equator; off-shore wind turbines generate more electricity than on-shore in the same country and tidal schemes are not commercially interesting in the Mediterranean sea. Finally, it is not completely possible to forecast the real output of any RE technology although yield uncertainty varies depending on the technology. In the case of PV generation, day-ahead forecast error can be up to 60% in areas like central Europe as calculated when comparing four different regions in Europe [40] but power availability from tidal schemes is highly predictable. Forecasting RE generation is very important for the integration of RE technologies in electrical markets which are based on scheduling according to the demand. The potential of ES to help RE technologies to behave as conventional plants is discussed in Section 3.1. There are several

technological options to improving the matching capability of RE technologies which are presented in Chapter 2.

1.4 Integration of renewable energy technologies into energy systems

The intrinsic variability and unpredictability of RE technologies together with their geographic dispersion is an important driver for the redesign of electrical power networks. Most RE technologies are converted into electricity and the current network is utilised to transport variable RE generation to the electrical demand loads. At the same time, the decarbonisation of the heating and transport sectors will be necessary to achieve the above targets because both sectors rely on fossil fuels and accounted for 21% and 15% of the total emissions in the UK in 2010 [41]. The use of flexible energy vectors such as hydrogen and electricity will be a key element in order to balance renewable generation and electricity, heating and transport demands.

The domestic sector is attracting a lot of attention because buildings account for 27.1% of final global energy consumption (40% including the commercial sector) [33] and heating and domestic hot water (DHW) demand account for around 75% of the energy consumption in buildings [34]. Low carbon heat generators such as biomass boilers, HPs as electrical heating with coefficient of performance (COP) higher than 2.5 as seen in this work (based on a steady-state model and assuming appropriate installation and control by the customer) and fuel cell (FC) systems running as CHP generators will replace conventional natural gas boilers in the coming years. CCS is capital intensive and therefore will be most cost effective if deployed as base-load generation [20].

Significantly increasing the input from RE sources (20% of energy consumption produced from renewable resources by 2020 in the European Union [42]) and the decarbonisation of the heat and transport sector requires extra flexibility to match supply and different demand loads continuously due to the modification of the generation and demand profiles. At the moment, this flexibility is given by fossil fuel generators which offer ramping capability. However, the worldwide agreement on the need to reduce greenhouse gas (GHG) emissions demands the alternative solutions. Energy storage (ES) has already been considered in the literature as the missing link for electrical power networks due to its potential to increase the robustness and reliability of energy systems, reduce the volatility in markets which govern the price structure, optimize the use of current and future assets and deliver RE generation to final loads when managing energy vectors [10].

ES is not the only technology available to guarantee the continuous balance between supply and demand. Others technologies are demand side management, interconnection between different countries (or keeping the same status quo by using flexible fossil generators). However, ES could be a game changer due to its intrinsic flexibility. ES can play the role of a load or a generator, can provide short-term or long-term flexibility, can be located at the distribution or generation levels and in scales which range from kWh to MWh.

Any decarbonised grid should integrate RE technologies, heating and transport technologies at the energy consumption level in order to reduce the carbon dioxide emissions of the domestic sector (and those related to heat supply in particular), engage with the public, empower customers to meet decarbonisation targets and create business models based on low carbon technologies [20]. The modularity of some RE technologies like solar PV is shifting part of the generation from large power parts to next to the consumption loads. This migratory path of generators is converting communities in generation plants and the existence of new loads is altering demand profiles. Simultaneously, customers aim to generate their own electricity and use it at home.

The way ES may be utilised within energy systems is being reviewed at the moment in response to the changing requirements and opportunities derived from the migratory path of RE generators and the use of different energy vectors. Community energy storage (CES) is coming to the spotlight as a technology which:

1. Supports the further penetration of RE technologies at the energy consumption level while keeping the grid stable at the edge.

2. Helps customers to use their own RE generation by shifting surplus generation to meet the demand load later as argued in Section 3.4).

3. Enables utility companies to create new business models which satisfy customers' preferences including cost-effective energy prices and green energy.

4. Introduces service benefits such as voltage support and grid stability which are very valuable for distribution network operators (DNOs) [43].

5. Plays a role in different markets (aggregations of benefits) and obtain related economic revenues including PV energy time-shift and demand load shifting as explained in Section 5.4.

Germany and Australia are the two countries in which conditions are ripe enough for the development of a market for battery storage in conjunction with domestic PV energy. In Germany, the take off of domestic ES was driven by the massive deployment of PV generation in the recent years (36.5 GWp of PV power

installed by May 2014) and a subsidy for domestic battery systems launched in 2013. This subsidy equates up to 30% of the battery capital cost if PV self-consumption is demonstrated to be 60% or higher [44]. In the case of Australia, the uptake is also related to the recent boost of PV plants installations (3.2 GWp in February 2014) considering it is the continent which has the highest average solar radiation, 2111 kWh/($m^2 \cdot year$), but also the sharply increase of households electricity prices (72% on average in the last 10 years). The average price of the electricity in Australia was 0.28 A$/kWh in 2013 [45].

1.5 Motivation

There in an increased interest for ES located very close to consumers which is able to augment local RE technologies (and convert them into a dispatchable product), help to decarbonise the heat and provide demand side flexibility [43]. Community energy storage (CES) was suggested by American Electric Power who is installing smaller and broadly distributed ES systems at customer sites, their Ohio GridSMART Demonstration project [46]. However, there are several technical and economic questions which should be answered before the full deployment of these systems. These questions include:

- What is the real cost, value and profitability of CES associated with end user applications?
- What is the impact of the size of the community on the performance and the economic benefit of CES?
- How are these parameters affected by the performance and the size of the CES system?
- What is the optimum CES system considering the technology and size?
- How does the aggregation of ES applications affect the business case?

Such a holistic approach which focuses on CES for end user applications has not been reported in the literature. Previous attention was on a specific ES technologies and/or applications as detailed in Section **??**. In particular, there has been an special emphasis on ES systems for single homes or alternatively on distributed ES located at the substation level. Therefore, there is a research gap studying the impact of the size of the community and the CES size on the performance and business case. The literature tends to report on the technological performance of ES without considering any cost analysis or on the economic benefit based on basic performance assumptions.

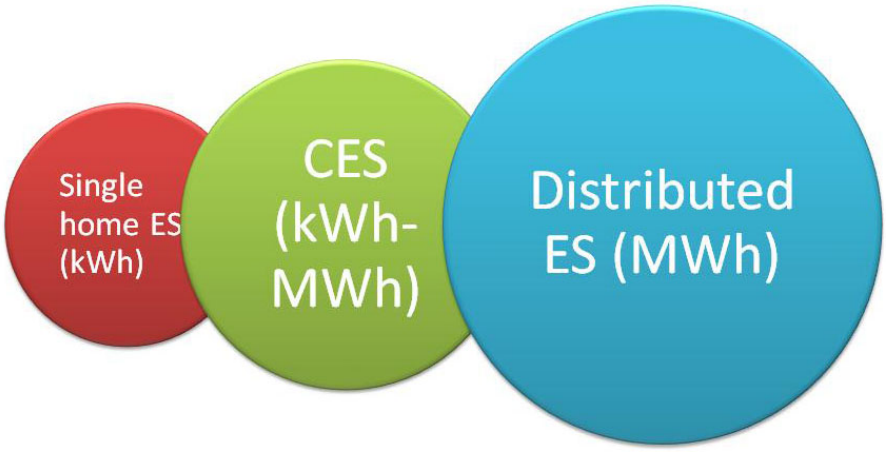

Figure 1.7: Scale of CES studied in this thesis ranging from a single home to the distribution level.

Finally, combining modeling and experimental work adds value to the research by using the experimental research to validate those from simulation as represented in Figure 1.8. Addressing CES in the field and include all product stages from concept design to testing and appraisal is key for expanding the knowledge on practical aspects such as the integration of different subsystems and installation of a CES system into a community. This is valuable information for utility companies and customers interested in installing and running CES systems.

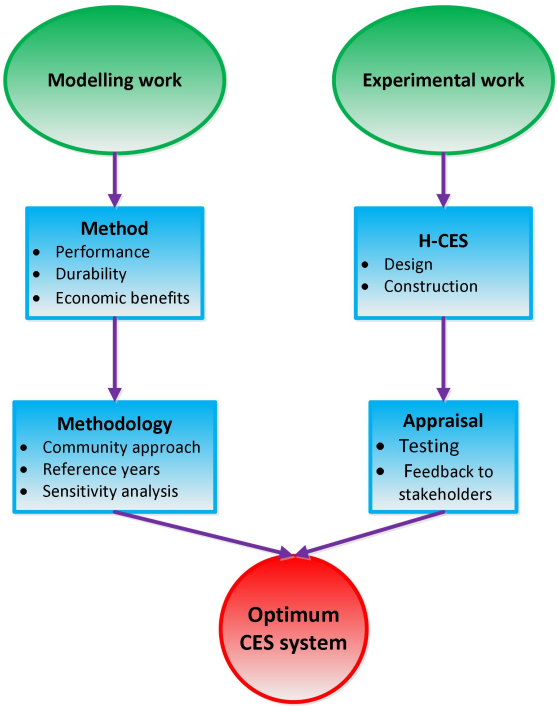

Figure 1.8: Approach followed in this thesis for investigating the optimum CES system.

1.6 Aim

The aim of the work presented in this thesis was to identify the optimum CES system for different end user applications by evaluating the performance and economic benefits. It makes use of a new method and methodology using simulation modeling to obtain the optimum CES system, as a function of the size of the community. The project also designed, built and tested a CES system using H_2 technology in a seven home community. Key research objectives were:

1. Optimise CES for different end user applications as a function of size of the community.
2. Investigate the effect of different technological and economic parameters on the performance and business case.
3. Determine the potential impact of the UK's decarbonisation roadmap in the performance and economic benefits of CES.
4. Design and build a CES system using H_2 technology (H-CES) for a seven home community.
5. Test the performance of the H-CES system when performing end user applications and validate the modelling results.

1.7 Industrial collaboration

This work was in collaboration with different industrial partners. The simulation modelling work was made in collaboration with E.ON as part of a Community Battery Project undertaken at the University of Nottingham and part funded by E.ON. This project investigated the potential benefits of a community battery (through theoretical and simulation studies) to provide an initial demonstration of "second use" 24 kWh Li-ion battery operating within the Creative Energy Homes at the University of Nottingham, undertaking a battery energy management algorithm which performs community energy optimization functions. From E.ON perspective, the interest was in understanding the optimum size of battery for a particular size of energy community and how this may be influenced by future changes in the UK energy energy system.

The H-CES system for the Creative Energy Homes was made in collaboration with two manufacturers: ITM Power which manufactured the polymer electrolyte membrane (PEM) electrolyser and McPhy Energy which supplied a solid state hydrogen store based on magnesium (Mg) technology (a Ballard Power systems' polymer electrolyte membrane fuel cell (PEMFC) stack was also used in the system). For these manufacturers, the interest was to take part in integrating a

H-CES system into a micro grid which manages the demand and the generation of a smart energy community.

1.8 Outline of Thesis

This thesis is grouped into eight chapters. These nine chapters can be structured in three different parts as schematically represented in Figure 1.9. After the introduction given in Chapter 1, Part I comprises Chapter 2 which reviews ES in the energy arena and different ES applications and technologies respectively. Part II focuses on end user applications (Chapter 3) and technologies which are suitable for them (Chapter 4). Part III searches for the optimum CES using two different strategies: a novel method and methodology (Chapter 5) which is implemented using simulation modelling (Chapter 6)and the design and construction of a H-CES system in a seven home community (Chapter 7).

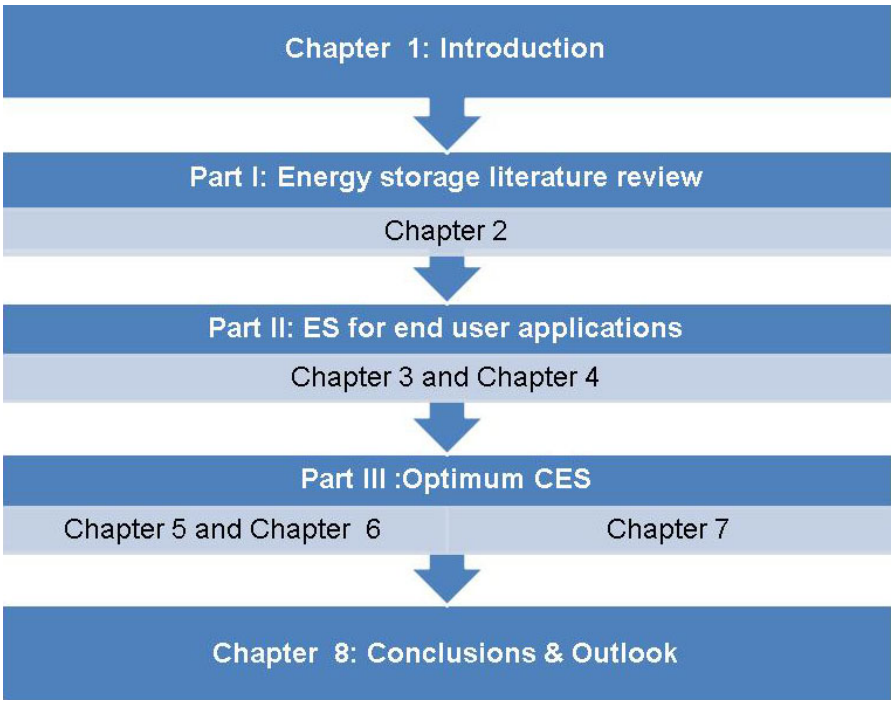

Figure 1.9: Structure of the thesis.

Chapter 2 reviews the role of ES in the current energy arena and provides a comprehensive review of ES state of art. RE technologies do not offer the same level of dispatchability as traditional fossil generators do and therefore flexibility should be provided by alternative technologies such as interconnection, demand side management and/or ES. Interconnection and demand side management are firstly introduced, and then main ES applications are related with the different ES

technologies available in the market. Opposite to power applications, attention is paid to energy applications, ES technologies being classified according to this criteria. The last part of this chapter discusses previous ES models utilised in the literature and previous approaches to assess the economic benefits of ES.

Chapter 3 selects the applications which are the main focus of this work: end user applications. Firstly, the strategic benefits derived from the performance of end user applications are reported. Then, PV energy time-shift (PVts), load shifting (LS), heat decarbonisation, power curtailment and the combination of them are defined. These applications are investigated with the modelling and experimental work of this thesis. This is followed by the modeling of the energy consumption level including different technologies and loads which are managed by CES. The community demand data used in this work, the PV array model and the models of HPs and FC systems are introduced.

Chapter 4 selects the ES technologies which are suitable for playing the role of CES when performing the end-user applications chosen in Chapter 3. Battery by means of lead-acid (PbA), lithium-ion (Li-ion), H_2 storage and water tanks were selected as key technologies. The chapter also introduces a holistic approach for modelling these ES technologies including the performance, durability and economy of CES. Then, the performance and durability submodels utilised for the different ES technologies are presented, the same economy submodel being used for all of them.

Chapter 5 introduces the method developed for obtaining the optimum CES system when performing end user applications as a function of the size of the community. Firstly, the method is presented and the algorithms which apply the method depending on the ES technology and applications are explained. The methodology includes three reference years (2012, 2020 and hypothetical zero carbon target) to assess the impact of the changes on PV penetration, HP penetration and demand, among others, in the performance and economic benefits of CES. A sensitivity analysis is designed in order to tackle the uncertainty in CES performance and economic benefits during the decarbonisation pathway. Data from the UK is utilised for these three reference years.

Chapter 6 identifies the optimum CES system as a function of the size of the community for different end user applications when analysing modelling results obtained from the application of the method. The performance and the economic benefits of different ES technologies are compared for a given end user application and how different applications impact on the performance, cost, value and profitability of a given ES technology is quantified. Additionally, the benefits introduced by the community approach are discussed when comparing results on

different community sizes.

Chapter 7 describes the H-CES system designed, built and tested for the Creative Energy Homes at the University of Nottingham. Learnings gained from the integration of the different subsystems are explained and potential improvements suggested. The second part of this chapter presents and discusses the experimental results obtained from the H-CES system when performing PVts, LS and the combination of them. The efficiency and capacity factor of the electrolyser and the PEMFC system were quantified depending on the application together with the description of the performance of the solid state hydrogen storage.

Chapter 8 concludes this thesis by analysing the method and methodology utilised in this study and drawing out the main conclusions derived from the application of both of them to the different communities. It also discusses the benefits and drawbacks of the H-CES system and concludes with some interesting areas which arise out of this work and should be recognized as further research.

Chapter 2

Energy storage applications and technologies

This chapter begins with an introduction of different technological options for facilitating the integration of variable and unscheduled RE generation such as flexible generators, interconnection, demand side management and ES. Among all of them, ES offers great flexibility due to the range of technologies available which provide versatility in terms of energy density, power density, discharge duration and scale of deployment, among others.

A review of different ES applications is performed including those to support the penetration and performance of RE technologies, manage different demand loads, assure the proper network capacity management, reliability and performance. Next, ES technologies which are suitable for different applications depending on their main characteristics are presented. The last part of this chapter discusses different ES technologies models used in the literature and previous approaches to analyse the economic benefits and the cost of ES.

This literature review was accomplished in order to select what ES applications are relevant for end users and what technologies are suitable for them. The selected applications which are the focus of this work are explained in more detailed in Chapter 3 including the current economic drivers to perform them. Additionally, a critical review of the ES technologies selected to perform end user applications and the ES modelling approach is presented in Chapter 4.

2.1 Flexible generation

There are different requirements of the electrical markets which call for flexible generation to meet variable demand such as the peaks in the demand load, frequency regulation and spinning reserves. Currently, around 98% of the demand is met by dispatchable generation in the electricity market ahead of time [20]

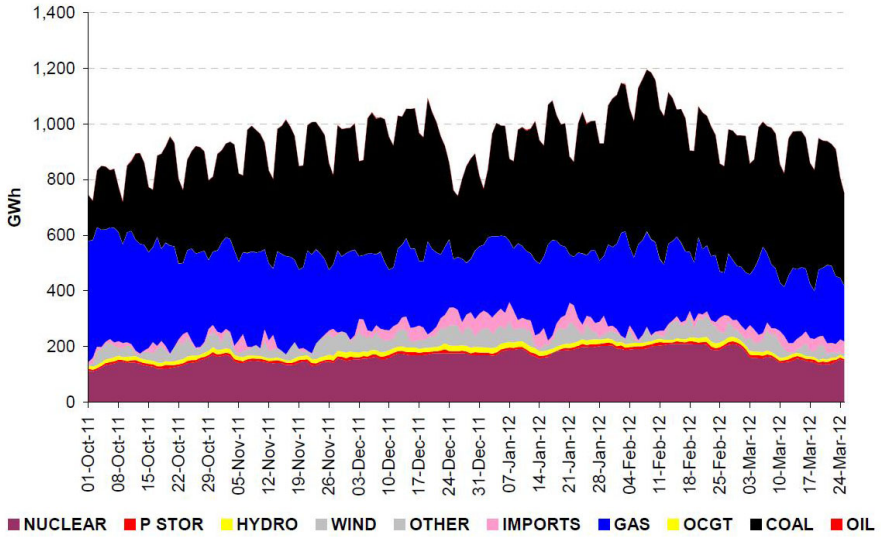

Figure 2.1: Generation mix by fuel type in the UK in the winter 2011/12 [7].

and according to this figure, most flexibility is provided from the generation side using dispatchable generators. As seen in Figure 2.1, nuclear power plants are allocated first because they are relatively inflexible. More efficient gas and steam power plants are next in merit because the have low operational cost and therefore attract high load factors (base load plants or high merit plants). Alternatively, plants with high operating costs including open cycle gas turbines and diesel generators only run during peak demand and generate a small share of the total electricity. Finally, renewable electricity generation has a considerable impact on market prices due very low marginal cost and/or obligation schemes [47].

Likewise, frequency response and generation reserve are provided by generators equipped with appropriate governing systems that control their outputs to counteract the frequency fluctuations that arise from relatively modest changes in demand or generation [48]. Coal fired power plants together with pumped storage hydroelectricity schemes are two of the preferred options for frequency response. Finally, power systems increase their robustness by using open cycle gas turbines and reciprocating combustion engines for tertiary reserves which are on standby in case of any generation failure and can be connected quickly [21].

The current energy system does not lack flexibility from the generation side but, as reported above, most of the flexible generators are not high merit and consequently they are carbon intense. Advances in nuclear technology suggest that new nuclear reactors may offer at least some degree of flexibility for weekly load variations but there is much uncertainty related to the potential of CCS for generation flexibility [20]. Therefore, the way in which electricity markets operated should be reviewed in order to keep the supply/demand matching while reducing

CO_2 emissions. Also, if the approach to counterbalance the penetration of RE technologies and other distributed energy technologies is increasing the reserve capacity, the system efficiency reduces and the assets are misused (typically, only 50% of the generation assets and the network are utilised [49]).

2.2 Interconnection

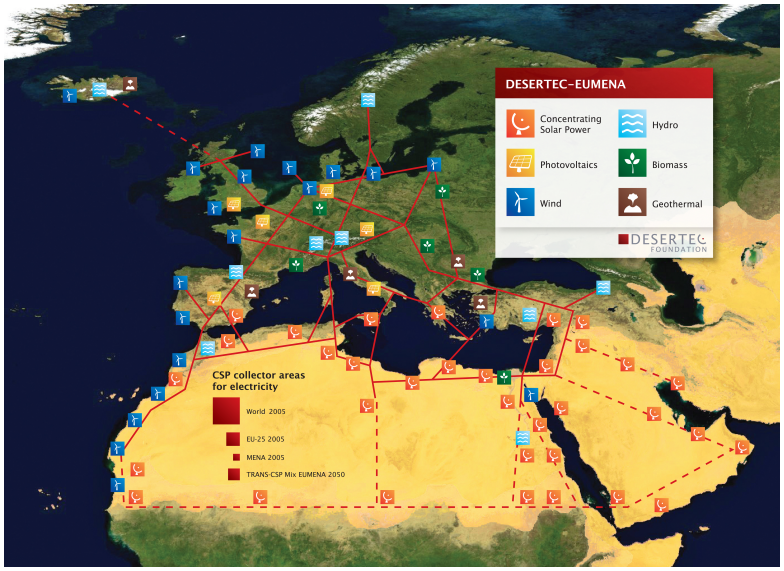

Figure 2.2: Schematic representation of the Supergrid transport high volumes of renewable electricity to the European load centres using high DC voltage [8]. The Desertec project focuses on the use of solar-thermal power plants in South European and Middle Eastern and North African (MENA) regions.

Interconnection is a robust alternative for varying regional flows in short-term temporal scales (minutes or even seconds) and helping to integrate variable RE generation by exporting it where simultaneous demand is occurring. The UK is taking part in the construction of a 1 GW connection with the Netherlands and there is potential to construct new lines with other countries such as Norway and France. According to the UK Government in 2010, capacity could grow between 200-500% during the next 15 years [20]. The interconnection of networks allows the transmission of electricity and gas between markets usually organised on a national basis.

The European Union is a good example of this technological option when considering the Priority Interconnection Plan created in 2007 [50]. The European Union stated that interconnected networks are vital to the development of healthy competition and constitute a prerequisite to the successful development of an internal European energy market. It also prevents the risk of short supply by di-

versifying sources, for example for electricity by facilitating the development of a "green network" based on RE technologies. The reality is that national networks were designed and developed following national interests and they are separated by natural barriers such as seas and mountains. However, interconnection among the different national grids can increase the reliability, efficiency, competitiveness and secure of supply as argued by the European Commission [51].

There currently are seven interconnections among different European regions. Additionally, there are intercontinental interconnections such as the Iberian peninsula with Morocco and the Baltic countries with Russia. There are also gas interconnections between Baltic countries and Russia, Central eastern Europe and Russia, and Mediterranean countries and north Africa, among others. The Supergrid was envisaged to make use of the different RE technologies which are located far from the European main demand load centres as shown in Figure 2.2. According to this mega project which would incorporate high voltage DC links, solar energy in the Sahara and south of Europe, off-shore wind energy on the seas around northern Europe and hydro energy in central Europe and Nordic countries would meet most European demand load throughout the year [52]. However, Siemens and Bosh already left the Desertec Project due to the uncertainty on the economic feasibility of the project and the geopolitical tensions in the north of Africa.

2.3 Demand side management

Demand side management with deferrable loads could be utilised to make the demand play a role in the matching of variable generation and demand, voltage stabilisation and frequency control [53]. If flexible generation and interconnection are large scale technological options for enhancing the flexibility, then demand side management can be utilised to match variable generation and demand locally. However, demand side management can be implemented regionally and nationally when the standardization necessary for the communication technology infrastructure and data protocols are delivered [54]. Previously, balancing demand and generation has been achieved by controlling the supply and short-term demand has been assumed inelastic. In fact, there was no incentive or available technology for changing customer demand profiles on the short-term. In addition to regulated incentives, tariffs are one of the main economic drivers to stimulate the participation of industrial, commercial and domestic customers in demand side management [55].

Electric drive vehicles and HPs can also play a role as flexible demand loads in the coming years and research is looking at the best ways of integrating the transport and heat sectors into the smart grid. By achieving this, demand side

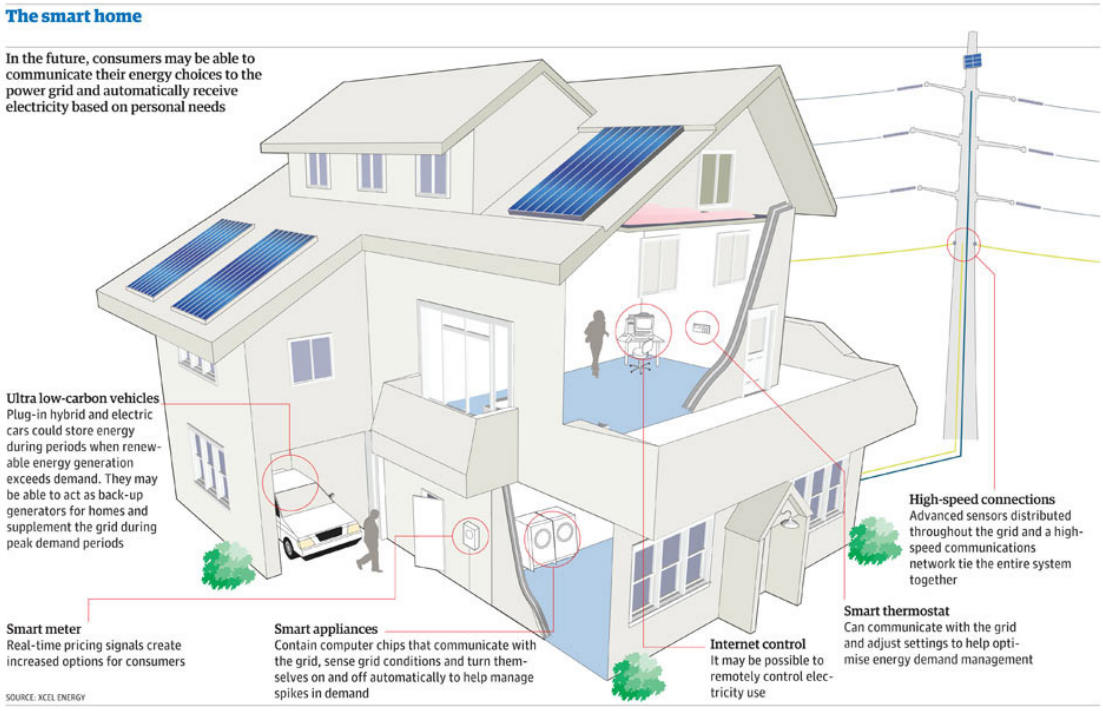

Figure 2.3: Representation of a smart home with smart appliances, smart metering and communication with the network [9]

management techniques would allow higher penetration of RE technologies, enhance the reliability of the grid and decarbonising the transport and heating sector at the same time. Car charging and electric heat can provide large quantities of short-term flexibility ranging from a few minutes to several hours [20].

Among demand side management advantages, it has been argued that it has the potential of providing flexibility at lower cost than ES [21]. However, its impact is limited by the amount and type of demand loads which can be deferred (up to 30% of the demand [20]) and customer preferences should always be considered. There is also a debate about whether demand side management should be introduced using a compulsory roll-out in which a regulator sets the rules of installation, communication and market or a deregulated model in which the installation is left to free initiative or market agents [55]. The UK government set the ambitious objective for every house to have a smart meter by 2020 to increase the information which people have about their energy use and engage them with demand side management alternatives [34]. Figure 2.3 shows a representation of a future smart house with demand side management tools.

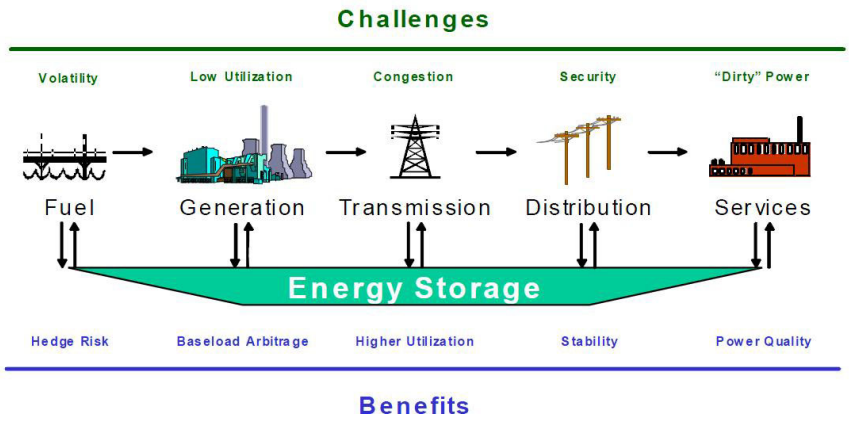

Figure 2.4: Potential benefits introduced by ES in different parts of the electricity value chain as [10].

2.4 Energy storage

ES is a technological option which can also increase the dispatchability of RE technologies and its value [56]. ES is an enabling technology which can develop multiple applications but as concluded by different reports [10, 11, 19] , the lack of understanding of the role of ES in the future energy system is currently an obstacle limiting its uptake. Alternative technologies such as flexible generation or interconnection can reduce the future value of storage up to 25% but not displace its role. However, demand side management in the form of electrified space and water heating in residential and commercial sectors, electrified transport sector and smart appliances in the household sector could reduce the market size for storage by more than 50% when providing energy arbitrage, reserve and frequency regulation services [49]. This conclusion for the UK was based on not cost attribution for demand side management based on the mandatory deployment of smart metering infrastructure mandated by the British Government.

ES is already utilised in the UK with 1.7 GW (equivalent to 10 GWh) of pumped storage hydroelectricity, hot water tanks in 19.3 million dwellings in 2006, electrical storage heaters in around 1.55 million flats which run with Economy 7 [57]. Likewise, the storage of fossil fuels has been successfully used for the power, transport and heating sectors, specifically 47 TWh of natural gas and 30 TWh of coal [57].

There are several technologies available for electricity and heat storage. Electricity is stored as another type of energy such as mechanical, chemical or thermal. Some of these technologies, such as lead-acid (PbA) batteries for small scale standalone RE applications and pumped storage hydroelectricity for bulk storage have been successfully utilised in the last few decades. However, most ES technologies

still are under research and development. There are many pilot ES installations worldwide which are providing real-world data related to technical performance and economic feasibility beyond the research and manufacturing testing environment [43]. The opinion in favour of ES is growing at the same time that the penetration of RE technologies does. In this sense, the Energy Storage Council and The Electricity Advisory Committee of USA published two reports in which the potential benefits of ES in different parts of the energy value chain were explained as schematically explained in Figure 2.4 [10, 58]. The European Union considered ES as a research priority for the integration of RE technologies [59]. In the UK, the Department of Energy and Climate Change also suggested that scenarios with great penetration of RE technologies require a very significant increase in ES capacity, demand shifting and interconnection in their 2050 pathway analysis [20].

The penetration of RE technologies is the main driver for the deployment of ES at different sections of the energy value chain. The increasing presence of RE technologies in the energy mix requires RE technologies to take part in ancillary services such as frequency control, voltage control and power quality [60]. Weather conditions already affect both daily and seasonal demand profiles. However, as RE technologies become more important, the influence of weather conditions on the generation sector will increase but ES can reduce this dependency. ES strategically allocated at different points of the energy value chain can help to assure reliability and quality of the supply. ES can also island a portion of the grid and reduce the negative impact of a power cut [43].

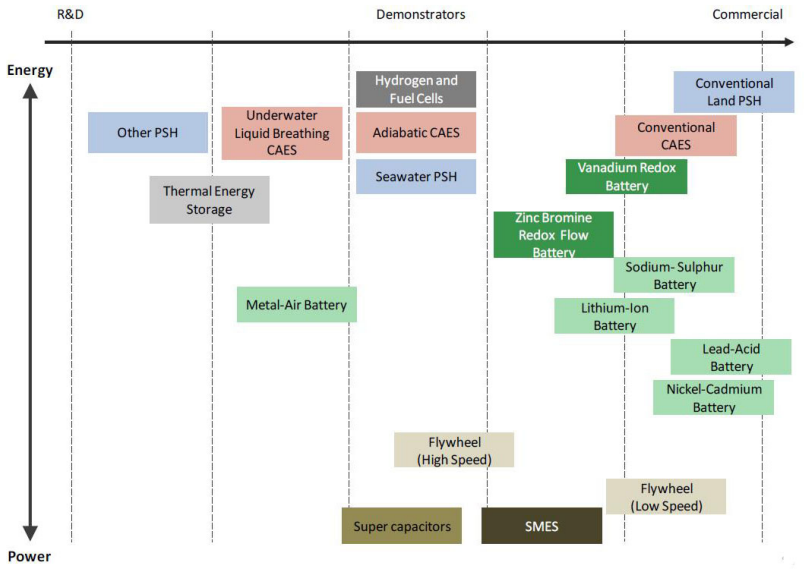

Figure 2.5: Different ES technologies as a function of the duration of the discharge [11].

Most ES installed worldwide correspond to bulk storage (pumped storage hy-

droelectricity) located at the generation level within the grid to improve the load factor of power plants which supply the base demand load and also contribute to frequency regulation. The Llyn Stwlan plant in Wales with a power rating of 90 MW and capacity of 360 MWh is a good example in the UK [61]. However, ES is a residual asset at the moment in all electricity systems and pumped storage hydroelectricity accounts for only 140 GW worldwide (840 GWh approximately assuming a 6 h discharge), compressed air energy storage (CAES) being the next technology with a mere 0.5 GW (3 GWh approximately approximately assuming a 6 h discharge) in 2012 [11]. In contrast, natural gas reserves of 33647 GWh in the UK (4% of the annual demand) while 193734 GWh in Germany (20% of the annual demand) are used to buffer any weather impact on the demand or technical lack of supply [62]. In the case of the electrical systems, electricity generation must be equal to the demand continuously. As a consequence, the distribution networks are sized to meet the maximum load which only occurs several hours per year. Figure 2.6 shows the demand profile in Great Britain on the 30th November 2013. The incorporation of new electrical loads (HPs and electric drive vehicles) will require a upgrade to the distribution lines but the size of the new cables and related equipment will be expensive to install and difficult to justify. This is the reason why some countries such as Japan and Germany plan to install a energy storage capacity (GW) equal to 15% and 10% of the total installed generation capacity, respectively, in the coming years [43].

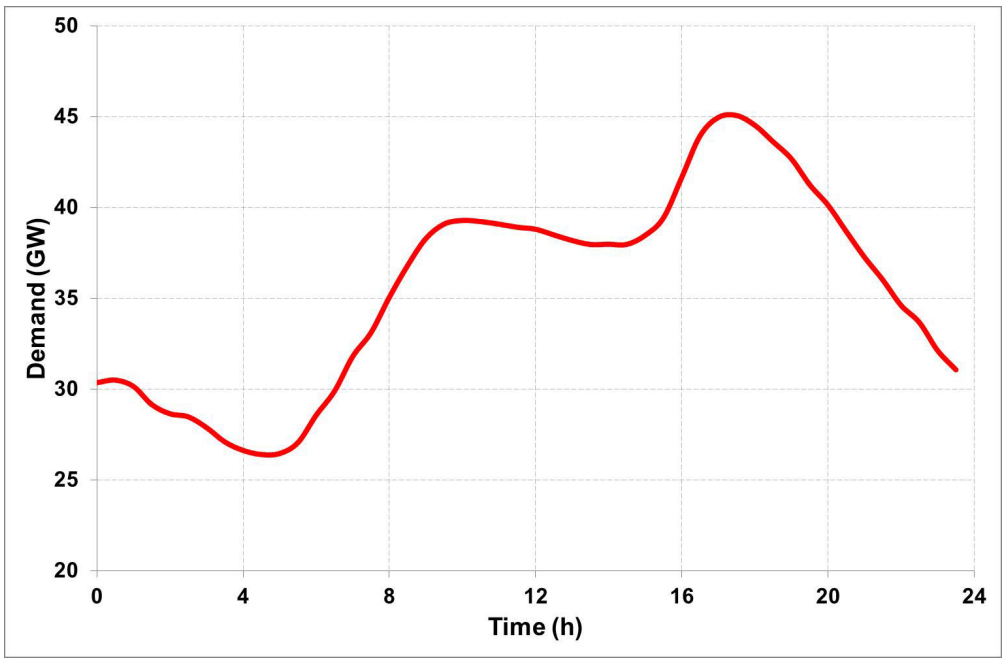

Figure 2.6: Demand in the UK on the 30th November 2013 excluding Pumped storage hydroelectricity and interconnections according to the National Grid.

2.5 Energy storage applications

H. Ibrahim et al. compared ES technologies depending on different characteristics such as efficiency, cost and energy density [17]. Among different type of classifications for ES, power applications versus energy applications as shown in Figure 2.5 is key for understanding different type of stationary applications. This classification is related to the time scale of the discharge necessary for the application. Power applications are characterised by high power discharges which last for a short period of time ranging from seconds to minutes. Alternatively, energy applications are characterized by discharge which last several hours. Finally, long term storage is defined as the use of discharges during different days, weeks or even seasons.

2.5.1 ES for the electricity generator

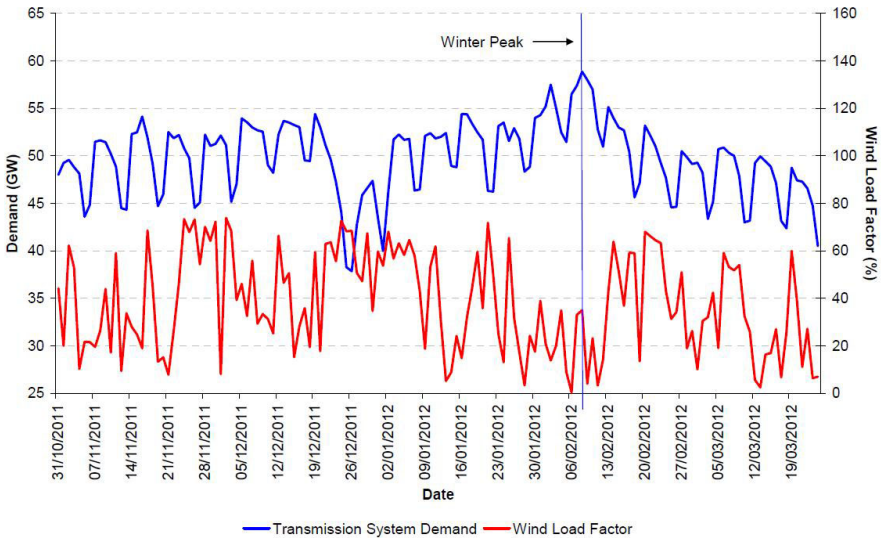

Figure 2.7: Daily demand (including the transmission losses, station transformer load, pumped storage demand and interconnection demand) and wind generation load factor (defined as the ratio of average output over the theoretical maximum output over a period of time) in the UK in the winter of 2011/12 [7].

From an electricity generation perspective, ES can help to improve the competitiveness, capacity factor and management of different power and heat plants. From a market point of view, ES can be used to maximize the revenues associated with generation by selling energy when it is most profitable for the generator. Depending on the time structure of the market, ES technologies which perform cycles of several hours (typically half a day) are necessary for this purpose. Additionally, the scale of the generator fixes which ES technologies are suitable for this application, pumped storage hydroelectricity being the most suitable option so far [60].

Likewise, ES can help to reduce the impact of weather conditions on the output of RE generators. Figure 2.7 compares the wind generation load factor with the UK demand load profile in consecutive winter days as reported by National Grid [7]. As demonstrated in this figure, the peaks in the wind load factor (which depends on the wind speed across the UK) do not always coincide with the demand peaks (affected by weather conditions, day of the week and hour of the day, among others) and ES can be utilised to better match them. Therefore, ES is necessary to increase the penetration of wind energy as explained in Section 1.3. Wind energy peaks and troughs can be up to 30 times higher and lower than the daily average production and anticyclone weather can last for several weeks [63]. Any country like the UK which wants to rely more on wind energy could use a combination of short and fast ramping storage with long term energy storage to become less vulnerable to the weather patterns.

2.5.2 Load shifting and peak shaving

LS consists of levelling-out the demand (grid import) by charging ES systems at valley periods and meet the demand load which occurs at periods in which the price of the electricity is higher. Peak shaving strictly means to meet the maximum peak demand load. From a generation point of view, demand load-levelling is achieved by using big scale technologies such as pumped storage hydroelectricity and CAES. At the distribution level, battery storage could be utilised, typically at the sub-station level or even closer to the consumption points as studied in this work.

ES can also be used to meet the maximum peaks in the demand. The maximum peaks are met by power plants that are switched on for short periods of time operating at higher cost as seen in Figure 2.1 for the UK. An alternative solution would be to use more efficient power plants, store the energy generated by them and use it for the peak periods. There are several ES technologies available for this application depending on the magnitude of the peak and its duration.

From a customer perspective, electricity bills are typically broken down into a part which is proportional to the subscribed power and another related to the consumed energy. The subscribed power becomes monetary more important in the case of industrial customers which use high intensive electrical demand loads. However, they usually pay for a maximum value which is not often used. ES can be used to smooth the real demand load and even reduce the subscribed power, especially when the value of the maximum demand load and when it occurs can be forecasted [60]. In the domestic sector, ES can reduce the typical peak during the afternoons and/or evenings by performing LS.

By increasing the efficiency and improving the performance of current electricity assets, ES balances the electricity system and can help to postpone the use of new generation units and transmission lines. The generation, transport and distribution systems were designed to meet the maximum peak demand load using the traditional network approach as seen in Figure 2.1. There are several factors which suggest that this approach is not the most efficient. For instance, daily demand is very variable and the maximum value is only required during several hours per year. On top of that, maximum power required increases more rapidly than maximum daily energy demand [64]. ES acting as a variable demand can modify the profile seen by the generator, optimise the transmission and distribution systems and defer upgrades.

2.5.3 Energy Arbitrage

Energy arbitrage is conceptually similar to LS but differs on the scale of the application, the price structure and stakeholders which are involved. Energy arbitrage consists of purchasing electricity in the wholesale market when it is cheap (high generation and/or low demand) and sell it to the distributors or final customers to create an economic benefit. ES is a tool which can help to reduce the risk of electricity price and volume derived from the retailer activity. Energy arbitrage is typically accomplished by bulked ES technology such as pumped storage hydroelectricity and CAES which help to reduce the cost of the cycles [56].

2.5.4 Renewable energy integration

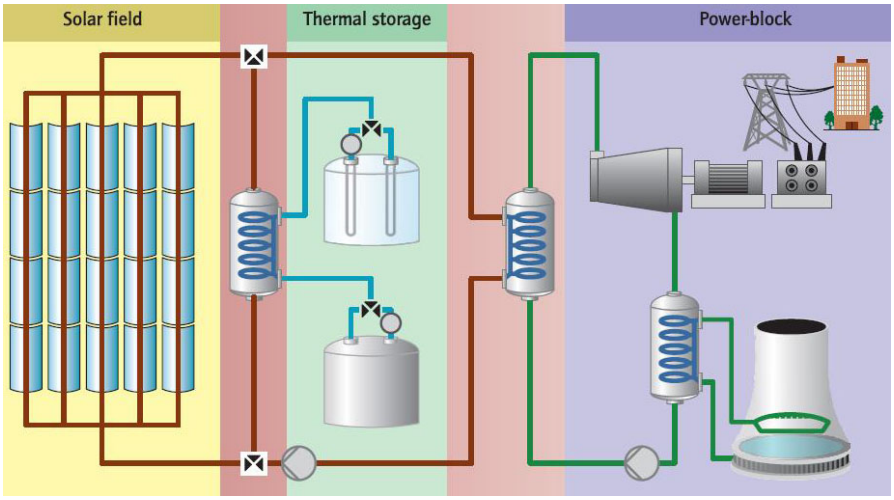

Figure 2.8: Thermal storage for a concentrated solar power plant. Excess heat collected in the solar field is sent to the heat exchanger and typically warms molten salts going from the cold tank to the hot tank. When needed, the heat from the hot tank can be returned to the heat transfer fluid and sent to the steam generator. [12].

ES can facilitate the integration of RE technologies according to different strategies [56]. As discussed in Section 2.5.1 , ES transforms intermittent (and unscheduled) RE profiles into a high-value dispatchable energy product (good citizen within the grid). From a network perspective, ES can support the participation of RE technologies in different electricity markets (regulation markets) and allow them to behave as conventional power plants performing frequency regulation and network restoration. The curtailment of RE generation on weak distribution networks or in periods of low demand can also be avoided by ES [65]. Molten salt ES systems are already helping concentrated solar power plants generate electricity at night, to be explained further in Figure 2.8. ES can also be help RE plants to meet the local demand of communities as investigated in this work.

2.5.5 Electrical system regulation

ES can help to keep the national grid frequency in acceptable boundaries by meeting short-term demand fluctuations. In fact, ES can play two opposite roles: demand load or energy source. Currently, grid frequency response is developed by generators able to increase and decrease their output on the minute scale. ES can replace traditional generators running at partial load for adjusting the frequency in the different markets developed for this purpose. Likewise, ES can be used in the voltage regulation market and support voltage regulation and even other types of power quality requirements. For this range of applications, ES technologies with great cycling capacity and power density such as supercapacitors and flywheels are required. Another ancillary service which can be developed by ES is the restoration of the network after a total or partial failure. For this purpose, large scale ES systems can contribute (as power plants do) following every country specific protocol [60].

2.5.6 Spinning reserves

Similarly to the electrical system regulation, ES can be used instead of or in combination with traditional generators to respond to unexpected failures in the electricity system. Similarly, it consists of using existing efficient generators at optimum load and then store energy generated for this market. Again, flywheels and supercapacitors in addition to batteries with good dynamic response like Li-ion technology are candidates to supply the necessary additional capacity.

2.6 Energy storage technologies

Most important factors which should be considered to select any ES technology for any of the applications introduced above are: energy capacity, power rating, depth of discharge (DOD), discharge time, round trip efficiency, durability, cost, self-

discharge, environmental impact, energy and power densities [17]. ES technologies have been compared as a function of these parameters using comparison graphs as the one shown in Figure 2.9 for the size and weight density for different ES technologies. The ideal ES technology should meet [66]:

- long cycle life
- high specific energy (Wh/kg) and high energy density (Wh/m^3)
- high energy efficiency
- able to operate at a wide range of environmental conditions
- reliable in operation
- maintenance-free
- made of readily available and inexpensive materials that are environmentally friendly
- efficient reclamation of materials at end of service-life

Next, ES technologies are individually presented and the main characteristics regarding the criterion outlined above are emphasized.

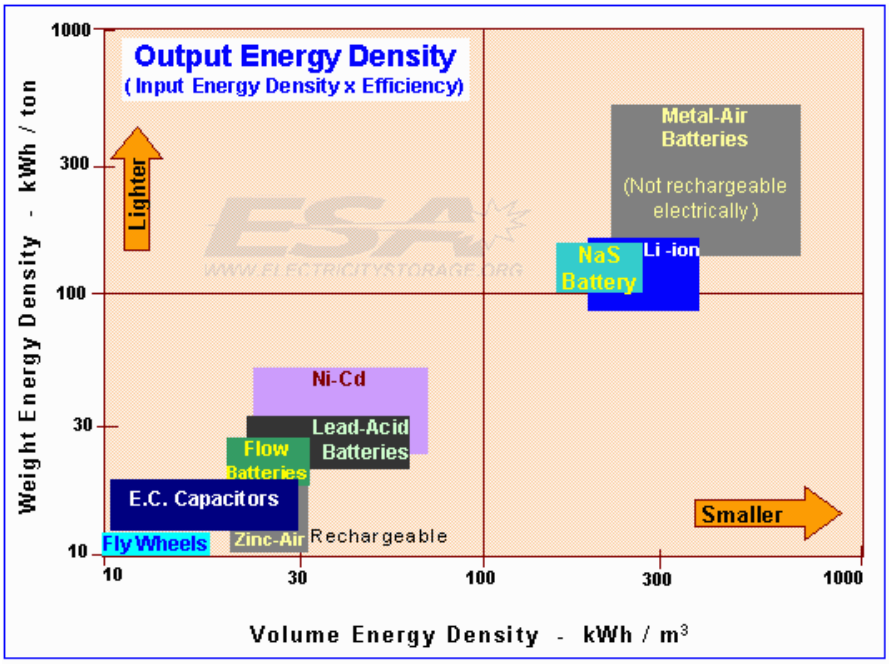

Figure 2.9: Size and weight density ranges of different ES technologies as reported by the Electricity Storage Association [13].

2.6.1 Power storage technologies

Flywheels

Electricity can be stored by converting it to kinetic energy using flywheels coupled with a motor generator in a vacuum atmosphere to reduce friction. Flywheels are high power storage devices with a high cycling capacity (10000-100000 cycles) and efficiency higher than 90% [11]. Other advantages are that they can be manufactured following a modular design (the power rating typically ranges between 1-20 MW while the energy capacity varies between 5-10 kWh), with little maintenance and absence of harmful raw materials.

Flywheels were previously used for propulsion applications such as engines and large road vehicles as a short energy storage system which smooths the power load during deceleration (charge) and acceleration (discharge). According to the material utilised for the wheel, high and low speed flywheels are defined using high strength, low-density composite material such as carbon-fiber/epoxy or Kevlar/epoxy and metallic alloys respectively [67]. The maximum energy which can be stored depends on the tensile strength of the raw material of the flywheel. Cost varies massively depending on the material ranging between 160-16000 £/kWh [19]. Flywheels are suitable for applications in which energy must be discharged in short periods (1 minute typically). They have been used to prevent fast fluctuations in the power output of wind and PV farms and for frequency regulation [68]. Some manufacturers of flywheels are Beacon Power and Powerthru^{TM}.

Supercapacitors

Energy is stored by creating an electric field between two electrodes. Due to the absence of electrochemical reactions, supercapacitors have good cycling capacity. This technology still has high cost (90-440 £/kW and 8700-17000 £/kWh [11]) and it is characterised by low energy density (5-15 Wh/kg) but high power density (800-2000 W/kg) [17]. Supercapacitors usually have long-life, high round-trip efficiency (>95 %) but they suffer from considerable self-discharge. As a consequence, they are more suitable for short-term ES.

Supercapacitors are suitable for power quality, frequency control, voltage control in electrical systems even in points close to consumers (the dynamic response of supercapacitors being superior to flywheels). At the moment, supercapacitors are currently utilised in the portable electronics, automotive industries, aviation and military industries. Maxwell Technologies (USA) is one of the main manufacturers for solutions for RE technologies support at the moment.

Superconducting Magnetic Energy Storage

Superconducting magnetic energy storage (SMES) uses a magnetic field created by the flow of DC current in a coil of cryogenically cooled superconducting material to store energy [10]. A SMES system includes a superconducting coil, a power conditioning system, a cryogenic refrigerator, and a cryostat/vacuum vessel to keep the coil at the low temperature required to maintain the coil in a superconducting state. SMES are highly efficient at storing electricity (greater than 95%) and can provide both real and reactive power for grid applications.

Power is available almost instantaneously and very high power output can be provided for a brief period of time. Due the construction requirements, this technology has high operating costs and it is therefore best suited to provide continuous deep discharges. Grid stability in distribution system and power quality at manufacturing facilities requiring ultra-clean power would be possible applications. SMES is commercially available with manufacturers such as Bruker EST and SuperPower and companies like ABB showing interest in pilot projects. The still very high initial cost (>200 £/kW [11]) limits the development of this technology.

2.6.2 Large scale energy storage technologies

Pumped storage hydroelectricity

Pumped storage hydroelectricity consists of using hydroelectric energy for storage purposes. Whenever demand is low (valley time), water is pumped to an upper level where water is stored. Then, it is used to activate a hydraulic turbine in periods with increased demand. This is a well-proved technology which has been used for high power (more than 200 MW) and high energy (several GWh) applications by energy producers such energy arbitrage and frequency regulation. By 2012, it accounted for 99% of the global ES capacity [11].

The round-trip efficiency ranges from 65% to 80% depending on the technology, and the lifetime of the plant can be higher than 40 years. The main disadvantage of this mature technology is the necessity of specific geographical locations. As a consequence, most potential locations are already being used. Pumped storage hydroelectricity storage remains the most cost effective technology for bulked energy storage and as a consequence, it has been utilised when comparing ES with other alternative solutions such as flexible generation and interconnection [69, 70]

Compressed air energy storage

CAES is another technology suitable for large scale power and energy storage. It is conceptually similar to pumped storage hydroelectricity and the basic difference

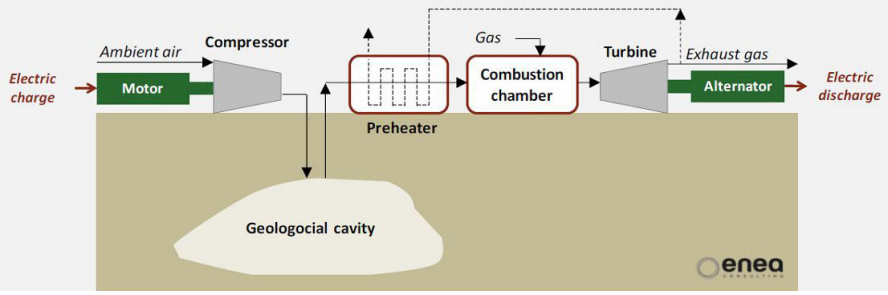

Figure 2.10: Schematic representation of an underground CAES plant [11].

lies in the type of substance used to store energy (compressed air instead of water). In this case, off-peak electricity is used to compress air (typically between 40-70 bar), which is then stored in large caverns suitable for keeping pressurised gas. Then, the compress air is released through a turbine to generate electricity as shown in Figure 2.10. This technology has been proven in a few installations worldwide [71] and it can be used as a middle-term, or even long-term energy storage with round trip efficiencies close to 70%.

Similarly to pumped storage hydroelectricity, the main disadvantages are the requirement for specific natural caverns which have a geographically limited availability and the high capital required [72]. Depending on the location and technology utilised, initial cost varies between 10-160 £/kWh and 260-1000 £/kW [11, 19].

Lifetimes of more than 30 years are achieved by CAES plants. Two real examples of large scale CAES can be found in Germany (the plant in Hunfort with a power rating of 290 MW built in 1978) and USA (the plant in McIntosh with a power rating of 110 MW built in 1991). CAES has been also suggested for small scale installations by using high pressure cylinders up to 300 bars [17]. The need for high pressure drops the efficiency down to 50%.

Flow batteries

This is a technology which receives several names in the literature such as Flow batteries, Redox batteries, regenerative fuel cells or redox fuel cell batteries due to its hybrid nature between battery and FC. The storage principle is based on the electrochemical reaction between two electrolyte tanks separated by an ion-exchange membrane. Typically bromine salt solutions are used as electrolytes (ZnBr and NaBr). The two electrolytes are pumped separately from the two tanks to two different electrodes where oxidation and reduction reactions take place. An ion-exchange membrane separates the two electrodes and it allows ions to move in one direction only.

The energy system scale depends primarily on the size of the electrolytic tanks (as in the case of H_2 storage) while the power output is determined by the size of the electrochemical cell stack [18]. Round trip efficiencies range between 75% and 85% and self discharge is not relevant [64]. This technology is expected to achieve energy and power capacities similar to CAES (MW and MWh) and it is also a promising technology for demand load levelling applications (MWh) but CAES cost is lower at this moment. Published cost of flow batteries ranges between 100-650 £/kWh and 400-1600 £/kW [19].

One of the first flow batteries was installed for demand load levelling in the UK by Innogy plc (12 MW and 120 MWh). Other companies working with real pilot demonstrations worldwide are Reflow Limited (Australia) and Prudent Energy (USA). According to them, some advantages are that flow batteries can run over the whole state of charge (SOC) range without impacting on the round trip efficiency and life of the system (in comparison with traditional batteries). This fact together with the unlimited cycling capacity is promising to reduce the cost of performing any application. Among potential disadvantages, effort is being done to increase the power and energy densities.

2.6.3 Modular energy storage technologies

Battery technology

There are many batteries technologies available in the market ranging from the traditional and well-proven PbA technology to the emerging lithium-ion (Li-ion) technology. Basically, batteries are chemical energy storage devices consisting of two electrodes separated by an electrolyte. Electrochemical reactions transform chemical energy into discharging currents and vice versa. Generally speaking, batteries have high energy density (up to 150 Wh/kg for Li-ion [17]) but low power density (up to 100 W/kg [64]) in comparison with supercapacitors (always higher than 1 kW/kg [64]). They have been traditionally considered ES systems (instead of power storage systems) because of limited life when operated with short and continuous cycles. Power and energy ratings are not separated in a battery.

PbA batteries are the standard technology because they have been used in the automotive and PV industry for a long time. The main reasons are the low cost, relatively easy maintenance and low self-discharge. On the other hand, some disadvantages are limited cycle life (especially at deep and continuous cycling), poor performance at extreme temperatures and unfriendly lead-acid content which makes these batteries very heavy. Among nickel-cadmium (NiCd), nickel-metal (NiMH) and Li-ion chemistries, the last one is the most promising technology and it is capturing the attention of vehicle and power industries. At this moment, Li-ion

Table 2.1: Qualitative comparison of PbA, NiCd, NiMH and Li-ion batteries.

Battery	Advantages	Disadvantages
PbA	Low self-discharge; easy maintenance; low cost	Limited DOD and cycle life; low energy density; Lead content
NiCd	Good cycle life and performance; low maintenance	severe self-discharge, toxic heavy material; low energy density
NiMH	Good voltage characteristic; no toxic materials; great energy density	Severe self-discharge
Li-ion	high efficiency and energy density	high cost and suffer at deep-discharge

batteries are intensively used in electronic equipment such as laptops and mobile phones because they have the highest energy efficiency (>90% when considering DC electricity) and the highest energy density as shown in Figure 2.9. The main downside is the still high initial cost as reported in Appendix B.2. Nevertheless, active research and increasing demand will help to introduce Li-ion batteries in both vehicle and stationary applications.

Table 2.1 compares the main chemistries used with small scale RE installations [73]. Previously, PbA was the best candidate for small RE autonomous systems because it offered a good compromise between cost and performance [17]. However, Li-ion offers a better performance and therefore PbA may be substituted when the cost of Li-ion reduces sufficiently as investigated in Chapter 6.

Finally, high-temperature battery technologies such as sodium sulfur battery (NaS) and Zebra battery have been used in several demonstrations projects to support RE technologies, peak demand load management at substation level and smart grid implementation. Japan is the best example for the successful deployment of NaS at the substation level with several examples [74]. Despite high efficiency (80%) and great power density, the high temperature makes the thermal management complex to develop and control. As a consequence, these technologies have only been used in the MW/MWh scale [43]. An example of a 1 MW NaS battery manufactured by NGK is being utilised by SSE in the island of Shetland (Scotland) funded by the UK Government [75]. This NaS battery matches RE generation and demand in the island and meets the peak demand load.

Hydrogen technology

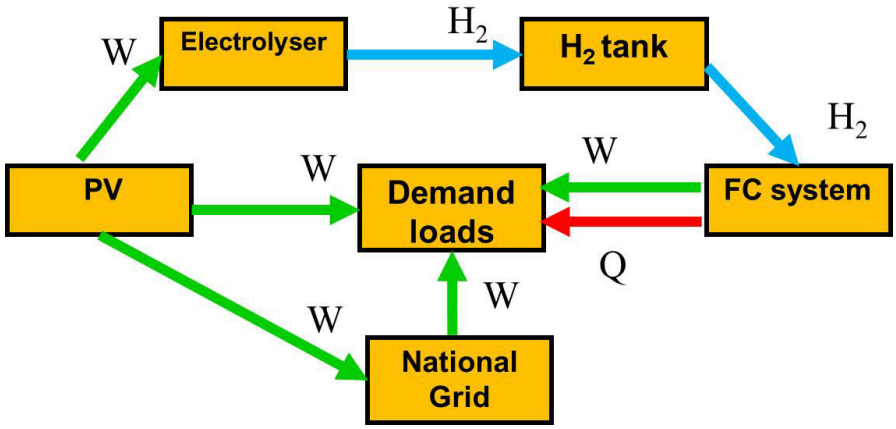

Figure 2.11: Schematic representation of a H_2 storage installation connected to a PV installation showing the three main components.

H_2 is typically utilised for mid-term and long-term ES because it does not suffer from self-discharge and the energy rating is decoupled from the power rating [76]. Thirdly, it does not offer same level of cycling capability and dynamic response of other technologies such as supercapacitors, flywheels and Li-ion batteries. H_2 ES systems comprise three basic elements: electrolyser, H_2 tank and FC system as schematically represented in Figure 2.11.

The electrolysis process consists of using direct current to electrochemically split water into its constituents, namely hydrogen and oxygen [77]. Different electrolytes have been used to generate H_2. First electrolysers used an acid electrolyte but most commercial electrolysers use low-temperature technologies, either alkaline electrolyte or polymer electrolyte membrane (PEM). Alkaline is the most mature technology (see Table 2.2) because it does not require expensive platinum-based catalyst which is used in PEM electrolysers. However, PEM technology is currently the centre of attention because it has several advantages such as ecological cleanliness, higher power density and easier maintenance [78].

Regarding the H_2 tank, pressurised gas has been used widely as seen in Table 2.2 and it is the standard technology. High pressures are used to increase the energy density of the tank and composite materials are used instead of metals to increase the volumetric energy density. As a result, H_2 can be stored at 700 bar yielding densities of 4.5 wt% and 2.5×10^2 kg/l. Increasing the pressure even more is not interesting because of the amount of energy required by the compressor [79]. Another alternative is liquid H_2, but the cost of H_2 liquefaction is relatively high, requiring around 30% of the LHV of the stored H_2. Moreover, very low temperatures and boil-off issues mean liquefied H_2 is not a suitable technology for portable

applications.

Compressed and liquid storage H_2 do not offer the potential to meet the gravimetric and volumetric targets for on-board transport applications published by different bodies such as the DOE [79]. This is the driver for research on metal hydrides. Chemically bound H_2 in metal hydrides is a promising technology for applications in which there is weight or a space constraint. In this technology, H_2 is released from the metal hydride by increasing the temperature or reducing the pressure. A qualitative measurement of how easy is to store H_2 as metal hydride is given by the temperature at which H_2 uptake starts at 1 bar. In the case of magnesium, with a storage capacity of 7.6 wt%, this temperature is 280 °C. MgH_2 is a promising technology because it has the highest energy density equal to 9 MJ/kg of all reversible hydrides. The main disadvantage of MgH_2 is that a relatively large amount of heat should be managed at high temperature (typically between 300 °C and 500 °C) to operate the tank [80]. Current cost of the technology is still high for further application (around 4350 £/kg in 2010 [81]).

Lastly, H_2 must be transformed back to electricity and heat using FC systems. FC systems produce electricity directly from chemical energy, so they are more efficient than internal combustion engines without including moving parts and harmful emissions. There are different types of FC technologies such as phosphoric acid fuel cell (PAFC), polymer electrolyte membrane fuel cell (PEMFC), alkaline fuel cell (AFC), molten carbonate fuel cell (MCFC) and solid-oxide fuel cell (SOFC). The basic differences rely on the temperature regimes, materials, fuel tolerance and performance characteristics. For example, PEMFC systems typically use NAFION® for the membranes which operates at low temperature and offers high power density. PEMFC systems are a really promising technology for the vehicle sector. According to S. Barret [82], FC electric drive vehicles will be an important actor to achieve the 2050 decarbonisation targets due to several advantages such as refuelling time, driving range, well to wheel efficiency and demand side management possibilities.

H_2 is an encouraging ES technology because it is suitable for different project scales ranging from very small applications (W) to SOFC generation plants (MW). Important challenges are the high cost of the technology and the need to further improvement the durability (affected severely by the start-stop cycling [83]). A comprehensive literature review of H_2 cost and durability is included in Appendix C. Additionally, the required ancillary equipment increases the complexity, especially of small scale systems. H_2 offers larger energy densities than batteries and faster charging.

Three comprehensive demonstration projects were developed in Europe to test

Table 2.2: Comparison of different H_2 storage system when supporting RE technologies in three different European projects.

	HARI	**RE2H2**	**UTSIRA**
RE technologies	Wind (50 kW), PV (13 kW), hydro (3 kW)	Wind (225 kW)	Wind (300 kW)
Alkaline electrolyser	36 kW	55 KW	50 kW
H_2 tank	2856 Nm^3(137 bar)	500 Nm^3 (25 bar)	2400 Nm^3 (200 bar)
PEMFC	7 kW	30 kW	10 kW
Other		Reverse osmosis (30 kW)	H_2 engine (55 kW)
Integration	600 DC bus	48 DC bus bar	AC micro grid

the ability of H_2 to support RE technologies. Table 2.2 compares different technologies utilised in each project. These projects focused on different stages such as design, installation, simulation, operation and maintenance. Experimental research, modelling and simulation were used in different phases. All the projects share some elements in common. Firstly, they were stand-alone applications for supporting RE technologies. Also, alkaline and PEM technologies were chosen for the electrolyser and FC system respectively. Additionally, H_2 was stored as a pressurised gas at high pressure requiring a compressor (as indicated in Table 2.2).

Due to the flexibility of H_2 storage and the three different subsystems required (electrolyser, tank and FC system), there are many different manufacturers involved in H_2 technology. For example, the CES system presented in Chapter 7 was made in collaboration with two of the most dynamic manufacturers at the moment. ITM Power is an electrolyser manufacturer and PEMFC developer which is focusing on the use of large scale PEM electrolysers for grid stability, power to gas and H_2 refuelling for the transport industry. McPhy Energy manufactures metal hydrides tanks using Mg technology. Its main customers are industrial companies which use H_2 in their industrial processes and want to control their H_2 supply. Additionally, they provide H_2 storage solutions (as the one presented in Chapter 7) and after acquiring the Italian manufacturer Piel at the beginning of 2013, they also offer hybrid systems (electrolyser and tank). Finally, Ballard Power Systems supplied the PEMFC stack, this company being a manufacturer of PEMFC systems with a focus on the transport industry.

Thermal storage

Thermal storage depends on the heat mechanism used to store the heat: sensible or latent heat. Among sensible heat storage technologies, water tanks which store hot water at temperature typically lower than 100 °C have been widely used in the domestic sector supporting solar thermal installations, natural gas boilers and electrical heating. Rocks and concrete have also been used due to their cost effectiveness. For higher temperatures, sensible thermal storage by means of molten salts has been successfully applied into concentrated solar power plants to counteract the daily cycles of solar energy [84]. Typical mixtures are based on sodium nitrate, potassium nitrate and calcium nitrate and work at temperatures higher than 300 °C.

Phase change material (PCM) is a latent heat technology which is currently being introduced in the domestic sector. PCMs can be easily integrated in the building structure without taking up any extra space to increase the thermal mass. Some PCMs with great potential for low temperature applications are water/ice, salt hydrates, certain polymers paraffins and zeolites [85]. Current prices varies between 2.2-6.5 £/kg depending on the technology [86]. PCM cost depends on the material and the energy density. Paraffin wax is more expensive than salt hydrates, but is more commonly used due to its stability. Normal energy density ranges from 0.01-0.06 kWh/kg. The objective is reducing the cost down to 50 £/kWh [87]. PCMs are also interesting for industrial applications when integrated with other energy systems such as HPs, FC systems and other ES systems. A PCM is utilised to manage the heat required by the metal hydride tank presented in Chapter 7.

Alternatively, there is a strong opinion in favour of shifting surplus renewable electricity into heat because this approach:

- reduces the problem related to the variability and uncertainty of RE technologies.
- decarbonises the heating sector which is one of the most important objectives to reduce carbon emissions.
- is more cost effective than electrical storage and widely available.

In all future scenarios considered by the UK Government, electric heating becomes more important due to the penetration of HPs [20]. Water tanks by means of immersion heaters and domestic storage heaters (heated brick-type) have been used in the UK to transform electricity into heat. The latter were typically introduced in flats around 20 years ago and they account for 7% of the heating systems in the UK [88].

Table 2.3: Summary of the data reported in this chapter and comparison of different ES technologies including basic characteristics for stationary applications [11, 17, 17–19].

Technology	Scale (MW)	Discharge time	Initial cost (£/kWh)	Efficiency (%)[a]
Flywheels	0.5-20	minutes	160-16000	80-90
Supercapacitors	0.01-5	ms to minutes	8700-17600	90-95
SMES	0.1-10	ms to s	>10000	90-95
Pumped storage	100-1000	hr	3-70	70-80
CAES	10-300	hr	10-160	50-80
Flow batteries	0.05-10	s to hr	100-600	65-85
Batteries	0.001-10	minutes to hr	130-1300	60-88
Hydrogen	0.001-50	hr to days	10-500	25-50
Thermal storage	10-500	min to days	20-100	60-95

[a] Round trip efficiency

Similarly, electrical heaters and/or HPs can run using RE generation and the heat generated can be stored in any of the thermal technologies discussed above. There are currently several companies selling immersion heaters integrated with domestic solar PV applications such as ImmerSun® and Coolpower in the UK. Likewise, research is looking into the use of district heating schemes or the use of water tanks in single homes for this purpose [89, 90]. There are some pilot projects which have implemented this demand flexibility to match stochastic RE generation such as in the City of Summerside in the Canadian province of Prince Edward Island, with a 12 MW wind farm and electrical storage heaters and DHW tanks [91], The Smart Region Project in the island of Pellworm and EcoIsland project in Scotland [92]. EDF is already working on this technological possibility to manage the peak demand load in France and they argued that there are 11 million individual water tanks which potentially account for 20 TWh a year of electricity storage when coupled with HPs or immersion heaters [93].

2.7 Previous ES modelling approaches in the literature

Different ES technology models have been developed and utilised in the literature with different levels of detail and comprehensiveness depending on the research purpose and the level of accuracy pursued. Previous work can be classified as studies which considered only technical aspects, only economic aspects or both of them.

An example of the first category is the study of the voltage stabilization and power management of an ES system in distribution grids [94]. An electrical model approach was followed and the ES system was modeled as a combination of a load and generator. The impact of ES in distribution grids with high penetration of PV power was quantified using perfect ES properties [95]. It was concluded that

using a storage of 1 kWh per 1 kWp PV may reduce the PV induced over-voltage up to 100%. At the single home scale, the integration of ES and demand side management was studied using constant ES properties in a different work [96]. The technical aspects of others ES models utilised in the literature are discussed in Chapter 4 for the technologies which are compared in this thesis.

A technology-agnostic approach has been widely used in previous work which focused more on the economic benefits and/or cost of ES. For example, the different economic benefits and the potential market of the whole range of ES applications (17 in total) have been assessed using market data from the USA [56]. According to this comprehensive report, load shifting, RE capacity firming, load following (frequency control) and demand charge management (peak shaving) are the four applications which greater economical potential with 79,30,29 and 19 million dollars respectively. Whether distributed ES can economically foster the integration of RE technologies and other distributed technologies by providing demand flexibility was investigated in another study [97]. The revenue obtained by distributed ES when performing arbitrage was maximised using a linear optimisation model. The ES technology model included the capacity, power rating, round trip efficiency and durability following an agnostic approach and assuming constant values. It was concluded that distributed ES can reduce he electricity cost of a standard household up to 17%. Additionally, the impact of the uncertainty related to the forecast of the electricity prices and the demand load was evaluated. It was established that the less accurate forecast techniques only deviated the economic benefit by 15% (from results obtained from perfect foresight). Finally, the aggregation of distributed ES system was able to reduce the cost of electricity by 24.8% from a market perspective. A similar approach was also followed for the assessment of the future value of ES across the energy value chain in the UK including large scale and distributed ES [49]. According to the conclusions, ES (bulked and distributed) for more than 6 hours does not add value significantly because the marginal value of ES reduced sharply to less than 5 £/(kWh·year). Efficiency affects the value of ES modestly, specially for low ES penetration levels e.g. high initial ES cost. This conclusion is valid as long as the installed ES capacity is low and the potential for arbitrage i.e saving renewable curtailment remains high. When the efficiency increased from 50% to 90%, the value increased less than 20%. It was argued that efficiency has a secondary role for applications related to savings in capital expenditures across the network, saving in operating costs and RE integration.

In a different study, wind energy time-shift and the connection of wind generators on weak areas of the distribution network was studied using a methodology to calculate the annual revenue and cost of different ES technologies assuming constant round trip efficiency [65]. Alternatively, engineering-economic models for

NaS, Li-ion, flywheel and supercapacitor technologies were developed to calculate the cost associated with power applications, specifically frequency regulation, base load wind integration, load-following wind integration and peak shaving [98]. A cost sensitivity analyses in which the impact of main ES parameters such as cost, efficiency and lifetime on the annual cost of performing these applications was included. It was concluded that the capital cost together with the power/energy ratio were the two most important factors which affected the cost of performing power applications. While the approach was comprehensive and it considered most factors which affect the value of ES such as round trip efficiency and life of the project, these parameters were assumed constant based on the literature.

Eleven different ES technologies were compared when performing LS, frequency regulation and quality power improvement with wind farms [99]. CAES reduced the cost of performing LS to 0.329 million dollars (considering a power capacity of 3 MW and a 5 h discharge) and the cost of performing frequency regulation to 0.994 million dollars (based on a 10 MW power capacity and a 15 min discharge) while flywheels reduced the cost of improving the power quality with a total cost of 0.994 million dollars (when discharging 10 MW for 30 s). S. Nykamp et. al analysed the break-even point for battery technology supporting PV in power distribution grids as a function of the efficiency and durability including operational and capital expenditures [100]. This study concluded that the break-even points range between 90 and 440 £/kWh depending on the lifetime of the storage asset.

According to this literature review, previous studies which focused on the economic benefits of ES used a technology-agnostic approach and/or constant values of key ES parameters such as round trip efficiency and life. Additionally, the cost and the benefits of ES were ignored in those studies in which the technological performance was the main focus.

2.8 Single home battery systems

The implementation of battery technology at single homes has been identified as one of the key potential ES business opportunities taking place in the next 10 years. The German residential battery storage subsidy of 30% of the initial investment has already been a success and 4000 new batteries were installed based on it by May 2014 after the first year [101]. As a consequence, previous research has analysed the power flows and seasonal energy flows [76] and identified the optimum power flows of battery systems [102, 103]. The voltage characteristics of different battery technologies available in the market were compared using simulation modelling and experimental research [73]. Using only the chemistry cost, the research concluded that Li-ion technology offers the most stable voltage plateau and this technology will be the most cost competitive when the capital cost of

Li-ion batteries comes down to four times higher that for PbA batteries.

However, most work has focused on calculating the optimum battery system for single homes according to different RE generation and demand profiles. The same optimization method based on discrete time-series was utilised in all the cases [96, 104–106]. The optimum battery capacity was defined as the one which maximize the ratio between the self-consumption (kWh) and the battery capacity (kWh) and only Braun et al. took the optimization decision based on the *IRR* [105]. Another study concluded that batteries become quickly attractive, even without government subsides, with an electricity price annual growth rate of 4% [107]. Only two of the works did not assume constant battery round trip efficiency [76, 105].

Interestingly, an analysis of the environmental impact of PbA batteries (including their manufacture) in addition to an economic analysis, found that a battery system for home would cost around £1000 pa. [108]. The environmental impact analysis considered the manufacture (GHG emissions, fossil fuel depletion and metal depletion) and the operation. It was concluded that the environmental impact of a PbA battery has an equivalent impact in terms of equivalent CO_2 as driving 4362 km in a new petrol vehicle.

2.9 Summary

After the introduction of other technological options for improving the dispatchability of RE technologies, ES characteristics were highlighted by describing different ES applications and technologies in this chapter. Most applications focus on supporting RE technologies and the role they play in different electricity markets that provide versatility to the energy system. The fact that ES can play the role of a demand load and a generator convert it into a very flexible asset.

ES flexibility was also emphasized by the range of different technologies which are currently available on the market. A comprehensive literature review was made including the current state of the art, cost, durability and manufacturers. Some technologies like pumped storage hydroelectricity and CAES are the most suitable for large scale ES. Pumped storage hydroelectricity is the most mature technology and has been successfully implemented in many countries for optimising the production of electricity but the lack of new available sites limits further deployment. CAES together with flow batteries and H_2 are others alternatives for the MWh scale. Power energy storage is provided by different technologies such as supercapacitors, flywheels and even Li-ion batteries. The higher cost of SMES limits its application. Power storage is suitable for the distribution lines (close

to customers) where electricity supply quality makes a difference. There are also a range of technologies which are suitable for small scale and distributed applications (kWh-MWh) such as batteries, H_2 and thermal storage which demand is increasing due to the penetration of RE technologies next to consumption points, the penetration of HPs, FC systems, electric drive vehicles and the development of the smart grid strategies.

Regarding ES models utilised in previous research, those studies which focused on the economic benefits of ES used a technology-agnostic approach and/or constant values of key ES parameters such as round trip efficiency and life. These studies mainly focused on single home battery systems, distributed ES or ES to support generation plants, CES not being included in their analyses. Additionally, the cost and the benefits of ES were ignored in those studies in which the technological performance was the main focus.

ES has the potential of introducing several benefits on different sections of the energy value chain and increase the flexibility of energy systems when integrating RE technologies and new demand loads. All technologies are available at the moment and they have been already proven for different applications satisfactorily. There are two main gaps to overcome for the wider use of ES in energy systems. The still high initial cost of many of the ES technologies and the lack of understanding about what benefits ES bring and what stakeholder (or stakeholders) is the beneficiary. Regarding the initial cost, only technologies which are sustainable when produced in mass can effectively play a role in a sustainable future. There are four key aspects which need to be addressed for the deployment of ES in the energy sector:

- The performance of ES technologies depending on the application and the ES capacity.
- The cost of ES technologies depending on the application or applications they perform (£/kWh). This levelised cost can be compared with alternative technologies depending on the application.
- The value (£/kWh) and profitability added by different applications
- The interaction between different applications i.e. how adding another application impacts on the performance and economic benefits.

The rest of this thesis introduces an optimisation method which addresses these four research priorities for end user applications. Chapters 3 and 4 use this ES review as a starting point to delimit the applications which are relevant for end users and the technologies which are suitable for them respectively.

Chapter 3

End user applications

Among all ES applications introduced in Chapter 2, only some of them meet the end users' requirements by increasing the value of their RE plant and/or managing their demand. This chapter focuses on applications which help customers to manage their own RE generation and demand and describes the related technical characteristics. Attention was paid to the relation between the applications and the economic and strategic benefits derived from them. Firstly, customer applications were analysed independently and the possible integration of several of them by a CES system when performing two different applications at the same time is discussed. The final part of this chapter models the PV generation, heat generation and demand managed in the customer applications considered in this work. Specifically, models for the PV generators, domestic demand loads and low carbon heat generators are presented together with the required input data. The output of these models are the input data for the method and methodology presented in Chapter 5.

3.1 Smart customers

The role that end users play in the energy system has changed over the last 20 years and it is being reviewed at the moment. An end user refers to a customer who consumes and potentially generates energy (electricity and heat) at home. Commercial and industrial companies are not considered in the analysis. The increasing cost of energy firstly in the seventies and especially in recent years has made customers pay more attention to RE technologies together with other measures to reduce their bills. Among others, the refurbishment of their homes with the introduction of more insulation, more efficient appliances and new controls for them.

Governments have also responded to the increasing cost of energy and legislation has been introduced to support more efficient technology and improve the insulation level in the domestic sector [34,109]. However, the development of more

efficient and cost-competitive micro RE technologies such as solar PV and solar thermal has been the key driver to change the role that customers play in the energy arena. Customers requirements and interests are evolving as the grid does and customers require new services but also they want to play a more active role by:

- Reducing their energy bills or at least keeping them at similar levels.
- Generate and manage their own energy.
- Reduce their carbon footprint.
- Securing their energy supply.
- Monitoring and managing their own demand to take decisions in real-time.

Although these new requirements may be seen as challenging for generators, utility companies and governments, they can also be seen as potential opportunities. Some of the potential benefits are being explored in different pilot projects. For example, The SmartRegion Pellworm project is lead by E.ON in collaboration with other industrial and research partners, which manages a decentralised hybrid ES system comprising a vanadium redox flow battery, a Li-ion battery and HPs. This hybrid system uses RE generated in the island and provides a stable and cost-efficient electricity supply based on RE technologies. Specifically, the renewable generation, 21 GWh per year, is three times larger than the demand. The objective is minimised the dependency on the connection to the mainland's grid via two 20-kilovolt-undersea cables [110].

While ES is not the only technology available to meet customer requirements and as discussed in Chapter 2 there are alternative solutions for integrating intermittent RE, ES has the potential to meet all customer requirements outlined above. In fact, when a CES system supports local RE technology, is also connected to the grid and incorporates an in-built monitoring system, it is able to reduce customers' energy bills, reduce carbon emissions, help customers maximize the benefit afforded from variable tariffs and secure the supply. CES has the potential of enabling:

- Utility companies to create new business models to integrate customers' needs while allowing the optimum performance of a smart grid.
- Governments to reduce the carbon footprint of the country and reduce energy imports.
- End users to satisfy their expectations in the new energy arena.
- DNOs to manage their assets efficiently.

3.2 The benefits of ES

By legislating for CES, governments would support technology which helps integrating RE technologies next to the demand load centres. CES can contribute to reduce the intermittency of local RE power supply to the grid and helps to meet peak demand [43]. The multiple benefits associated with the deployment of distributed ES were classified by A. Nourai et al. in three different categories: strategic, service and market benefits [111]. The key aspect for the creation of an ES business case is the consideration of applications with internalizable benefits (those that can be received by a given stakeholder in the form of revenue or reduced cost) for one or more stakeholders [56, 65, 111]. While the related economic revenue of applications which offer ancillary services such as energy arbitrage and frequency regulation is determined by the way in which electricity markets work in terms of generation schedule, reserve, frequency control and ensuring its reliability [21], the revenue related to other ES applications such as RE technology integration and LS is not so straightforward because markets are rapidly developing. Likewise, the economic impact of societal benefits such as CO_2 reduction and engagement of zero carbon customers is even more complicated to estimate [56, 111].

As it is suggested in the latest German Renewable Energy Act [112], RE plants should be able to operate as traditional power plants and ES can help to achieve this target. Related to this, different market models and environmental initiatives can be developed. An example of this is the use of CES to maximize the self-consumption of PV generation and reduce the CO_2 generated by the domestic sector. Additionally, when a CES system incorporates a management system and monitors different energy flows, energy balances can be visualized by the end users contributing positively to reduce energy consumption by increasing the awareness of the balance between the local RE generation and demand. Customers can also profit from having their own energy back-up for any outage and some degree of independence (energy *autarky*) [106]. Table 3.1 shows the relationship between new drivers for the implementation of CES, the related applications and how they could be internalized. This work focuses on ES applications with internalizable benefits in order to investigate the optimum CES system. In the next section, applications which help to manage the local RE generation and demand are discussed.

3.3 End user applications

End user/utility customer applications are those which satisfy end user needs by managing their local RE generation and demand. This terminology was utilised by a report prepared from Sandia Laboratories to the DOE Energy Storage Systems Program [56]. In this work, a similar approach was utilised and end user/utility customer applications which offer internalizable benefits are the focus in order to

Table 3.1: Relationship among the ES drivers, applications and the economic (internalizable) benefit derived from the applications at the energy consumption level.

ES driver	ES application	Internalizable Benefits
PV generation	PVts	Self-consumption bonus
Network optimization	LS (tariffs)	Bill reduction
Peak demand load reduction	Peak-shaving	Bill savings/cost deferral
Grid stability	Avoiding RE curtailment	Electricity not curtailed
Renewable heat	Heat decarbonisation	Renewable heat incentive

explore the economic benefit. The stakeholder who internalizes the benefits can be the final customer, a utility company or an energy service company depending on who owns the CES system. In shake of the simplicity, end user/utility customer applications are referred as end user applications in this work.

Among the different applications presented in Chapter 2, two of them were investigated in depth and the optimum CES system was obtained for them: RE time-shift and LS. The reasons for choosing these applications were that they are energy applications instead of power applications and that domestic RE generation and demand are covered by them. By considering energy applications, this work investigated applications that occur on a daily basis instead of power applications e.g. voltage control and power quality which are more related to punctual events or problems derived with the network performance [60]. Additionally, customers are charged mainly by their energy use. By dealing with RE generation and local demand, RE time-shift (which manages the local RE) and load shifting (which manages the demand) cover the customer requirements outlined in the Section 3.1. Other applications such as the avoidance of PV curtailment and heat decarbonisation were investigated but as complimentary applications, with no dedicated optimization algorithms. This implies that the optimum CES system was not obtained for these applications.

REts was investigated for only PV energy, as this is the most widespread power technology in the built environment due to its modularity, very low maintenance and quiet performance [113]. The PV penetration in the UK was 1.7 GWp with 1.3 GW_p (77%) due to installations with a capacity less than 4 kW_p in September 2013 [114]. In the UK and other countries such as Germany and Spain, the main reason for the PV success was the legislation of feed-in tariffs by different governments. The reason why CES linked to wind generators was not considered in this work is the yield of micro-wind turbines in the built environment is not very attractive due to obstacles reducing wind speed and increasing turbulence. According to a report prepared by the Energy Saving Trust, micro wind turbines

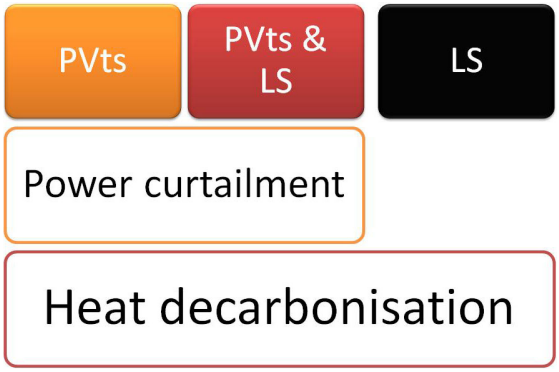

Figure 3.1: Different end user applications considered in the analysis. PVts, LS and the combination of them were optimised. Heat decarbonisation was investigated as a complimentary application to the previous ones, while power curtailment was integrated with PVts.

are only suitable for locations in which the average wind speed is higher than 5 m/s, typically located in remote rural areas [115]. Moreover, wind generators are noisy and this means that they cannot be easily integrated in urban and semi-urban areas [116]. However, large wind farms (onshore and offshore) will provide most RE generation in the UK by 2020 [34] and it will be one of the drivers for performing LS and the use of related tariffs according to the wind energy patterns described in Section 1.3 [65, 117]. Figure 3.1 shows the hierarchical relationship of the applications considered in this work that build from top to bottom.

3.4 PV energy time shift

CES can support the penetration and the use of PV generation according to different control strategies. The application of the different control strategies depend on the size of the PV plant and if its main purpose is meeting the local demand or exporting to the grid. Some ES strategies considered for PV generation in the literature include constant output power control or capacity firming, fluctuations reduction control and other strategies which aim at optimizing the ES performance or durability [56, 118]. For example, the call for tenders of the French government stated that new power PV plants with an installed capacity greater than 250 kW_p were encouraged to integrate ES in order to guarantee a grid daily power injection with a trapezoidal shape in French islands. The injection profile should be known one day before by the grid operator and the final profile should not vary more than $\pm 2.5\%$ in order to be paid [119].

PVts consists of storing surplus PV energy and using it on-site later to meet the local demand. PV generation mismatch to the domestic daily and seasonally demand loads are shown in Figure 3.2. PVts allows end users (or utility com-

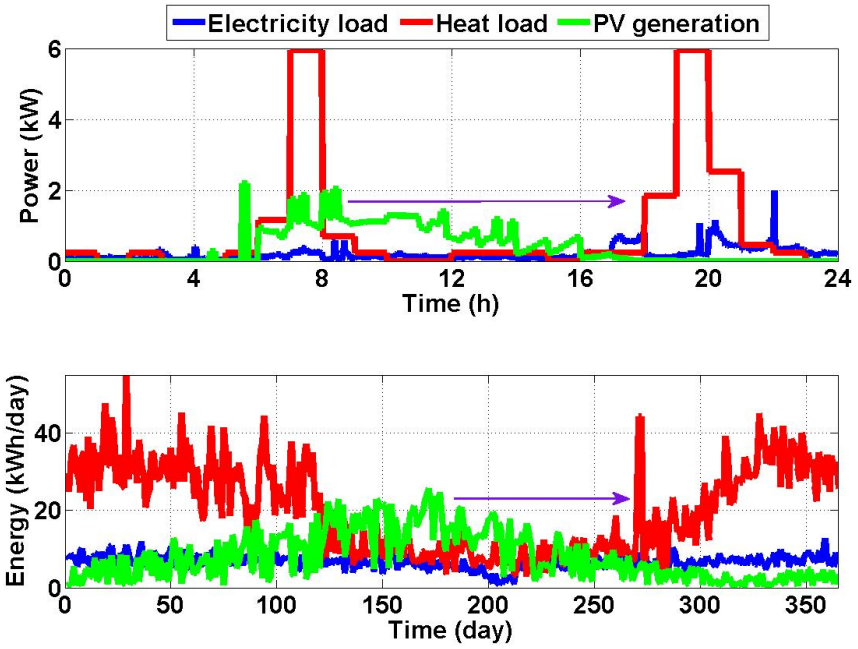

Figure 3.2: Daily and seasonal mismatch in a single house with a 3 kW_p array according to the demand data and PV model presented in the last part of this chapter.

panies) to manage their own PV electricity, reduce their energy bills and secure their energy supply. From a DNO perspective, PVts can contribute to reduce the maximum peak demand load and defer or avoid distribution capital investment, mitigate possible voltage problems, reduce the losses (and the related power regulation needs) and increase the reliability of the distribution system [95]. This is the reason why governments of different countries such as Germany, Spain and the UK (among many others) are promoting the use of local PV generation on-site instead of exporting electricity to the grid at the moment.

Self-consumption was explicitly promoted in Germany by the creation of a self-consumption bonus in 2009 which gave incentives to PV owners who use the PV power generated on-site, as opposed to exporting it into the grid [105]. The addition of the self-consumption bonus (0.2501 €/kWh) plus the price of the electricity for the customer (0.1945 €/kWh being the average in Germany) was higher than the export tariff (0.4301 €/kWh). The self-consumption bonus was eliminated in the latest German Renewable Energy Act published in 2012 [112]. However, using PV generation to meet the local demand is interesting at the moment because the price of the electricity is higher than the export tariff in Germany and in the UK. In the UK (from March 2012), all electricity generated by PV installations with a peak power rating lower than 4 kW_p is paid 0.218 £/kWh, reducing to 0.168 £/kWh for installations between 4 and 10 kW_p [76]. The export tariff is equal to 0.031 £/kWh, which is significantly lower than the cost of the electricity

(around 0.13 £/kWh) (Ltd, 2012). As a result, the use of PV energy on-site is valued (August 2012) at 0.348 £/kWh or 0.298 £/kWh reducing to 0.249 £/kWh or 0.199 £/kWh when exporting to the grid for installations with a peak power rating higher than 4 kW_p [120]. From a CES system perspective, whenever there is surplus PV generation, electricity is stored and used later when demand is larger than generation.

The economic benefit derived of performing PVts, Rev_{PVts} (£), was obtained using Equation 3.2 for battery technology. The round trip efficiency, η, is obtained from the ratio between the electricity discharge, E_{dis} (kWh), and the charge, E_{char} (kWh), as shown in Equations 3.1 and 3.2. From an economic point of view, PVts only makes sense for battery technology when η is higher than the ratio between the export bonus, P_{ex} (£/kWh), and the price of the electricity, P_i (£/kWh), ($\eta > P_{ex}/P_i$) as demonstrated by Equation 3.2.

H_2 storage generates electricity, E_{dise} (kWh), and heat, E_{dish} (kWh), simultaneously when using a FC system running as CHP generator as explained in Section 3.11.1. Therefore, the heat round trip efficiency, η_h, plays a role in addition to the electrical round trip efficiency, η_e, according to Equations 3.3 and 3.4. The price of the heat denoted as P_h (£/kWh) was obtained when dividing the price of the natural gas by the typical efficiency of a condensing gas boiler, 0.85 [25]. The heat generation is multiplied by the ratio $P_h/P_i < 1$ due to the fact that electricity is worth more than heat and therefore the PVts condition became $\eta_e + \eta_h \times (P_h/P_i) > P_{ex}/P_i$. Equation 3.2 is a simplification of Equation 3.4 when considering that all the energy stored is transformed into electricity only.

$$Rev_{PVts} = E_{dis} \times P_i - E_{char} \times P_{ex} \tag{3.1}$$

$$Rev_{PVts} = E_{char} \times P_i \times \left(\eta - \frac{P_{ex}}{P_i}\right) \tag{3.2}$$

$$Rev_{PVts} = E_{dise} \times P_i + E_{dish} \times P_h - E_{char} \times P_{ex} \tag{3.3}$$

$$Rev_{PVts} = E_{char} \times P_e \times \left(\eta_e + \eta_h \times \frac{P_h}{P_i} - \frac{P_{ex}}{P_i}\right) \tag{3.4}$$

3.5 Load shifting

A CES system can shift the electricity imported by a home or community without changing the customer habits and this is the key advantage over demand-side management tools as represented in Figure 3.3. LS with ES is related to tariffs which make a difference in the electricity price depending on time of day. There

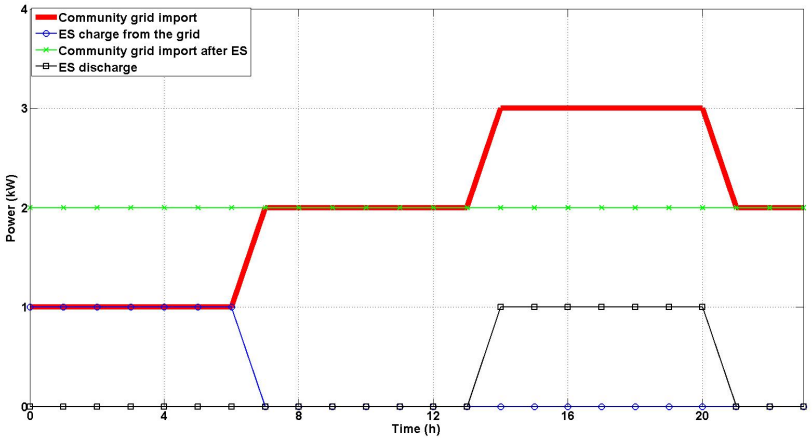

Figure 3.3: Representation of load shifting performed by ES and its impact on the electricity imported by a community.

are different types of tariffs, Time-of-use tariffs or Real-time pricing tariffs being the most common options [55]. In terms of the CES management, it consists of charging the CES system whenever the price of electricity is low at the valley period, P_{iv} (£/kWh), and using the energy stored when the price of the utilities electricity, P_{ip} (£/kWh), and heat, P_h (£/kWh), is higher (peak period). The revenue obtained from LS, Rev_{LS} (£), is calculated using Equations 3.6 and 3.8 derived from Equations 3.5 and 3.7 for battery and H_2 storage respectively.

$$Rev_{LS} = E_{dis} \times P_{ip} - E_{char} \times P_{iv} \tag{3.5}$$

$$Rev_{LS} = E_{char} \times P_{ip} \times \left(\eta - \frac{P_{iv}}{P_{ip}}\right) \tag{3.6}$$

$$Rev_{LS} = E_{dise} \times P_i + E_{dish} \times P_h - E_{char} \times P_{iv} \tag{3.7}$$

$$Rev_{LS} = E_{char} \times P_{ip} \times \left(\eta_e + \eta_h \times \frac{P_h}{P_{ip}} - \frac{P_{iv}}{P_{ip}}\right) \tag{3.8}$$

For battery technology, LS is only possible when the round trip efficiency is higher than the ratio between the valley and the peak prices ($\eta_e > P_{iv}/P_{ip}$). The LS condition also includes the heat price, P_h (£/kWh), and the heat round trip efficiency, η_h, for H_2 technology ($\eta_e + \eta_h \times (P_{iv}/P_h) > P_{iv}/P_{ip}$) as it happened with PVts. Similarly to PVts, Equation 3.6 is a simplification of Equation 3.8.

In this work, two different tariffs were investigated: a Time-of-use tariff and a Real-time pricing tariff. The two tariffs selected in this work are Economy 7 and a 4 period tariff derived from the prices of the imbalance market in the UK, described in more detail below.

3.5.1 Economy 7

Economy 7 is a 2-period Time-of-use tariff which should be considered as a reference because it has been used in the UK in homes with electrical space heating for the last 40 years to promote the smoothing of the daily peak by using more cost-effective based load generation. The two prices are constant through the year and the consumer knows them beforehand. This tariff defines two different periods: day (peak) and night (valley). Although there are several versions of Economy 7 depending on the electricity supplier, the Economy 7 tariff assumed in this work is supplied for a total of 7 hours between midnight and 7 am (local time). The day and night electricity prices were taken from a real tariff in 2012: 0.1347 £/kWh and 0.0632 £/kWh including VAT respectively.

3.5.2 Four period Real-time pricing tariff based on the prices from the imbalance market

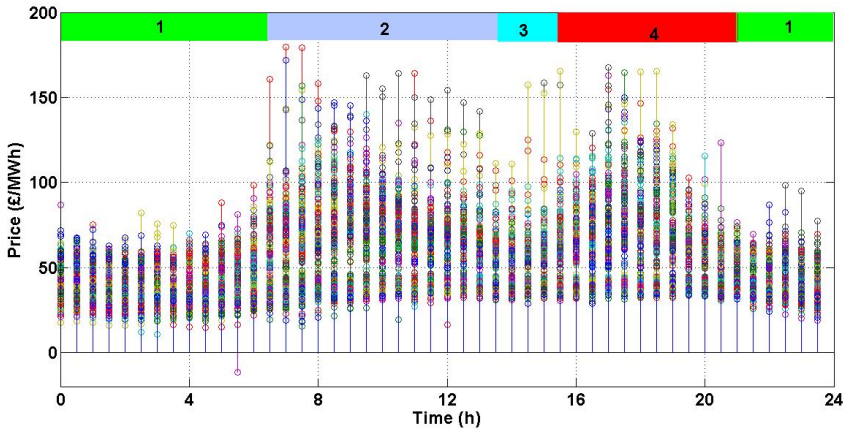

Figure 3.4: NETA prices from the imbalance market for every day of 2011. The daily market has been split into 48 half hour time periods. Four different periods have been distinguished for creating a real time tariff [14].

As an example of a future consumer tariff, a real-time pricing tariff based on the electricity prices of the New Electricity Trading Arrangements (NETA) in the UK in 2011 is suggested. NETA is a daily market in which generators and suppliers sell and buy electricity respectively by notifying their position for each half-hour (48 prices per day) according to the generation and demand for the day ahead. The price is obtained from the equilibrium between generators and suppliers in the market. Figure 3.4 shows the half hourly prices from the market for every day of 2011. The minimum and maximum half hourly prices in 2011 were equal to -11.6 £/MWh and 179.7 £/MWh respectively, the average being equal to 46.6 £/MWh. According to pattern followed by the prices shown in Figure 3.4, four fixed periods were selected for every day of the year and the four prices of the tariff

per day, $\bar{p}$, were calculated using the half hourly prices from the NETA market, p_i, using a weighted arithmetic mean with respect to the amount of electricity which was traded per period, E_i, as represented in Equation 3.9. The four periods were defined as:

$$\bar{p} = \frac{E_1 \times p_1 + E_2 \times p_2 + \cdots + E_n \times p_n}{E_1 + E_2 + \cdots + E_n} \tag{3.9}$$

1. Period 1: between 21:30 and midnight and between midnight and 06:30 hours. The average of the weighted price for the period 1 is 40.6 £/MWh (0.0406 £/kWh).

2. Period 2: between 06:30 and 13:30 hours. The average of the weighted price for the period 2 is 53.0 £/MWh (0.053 £/kWh).

3. Period 3: between 13:30 and 15:30 hours. The average of the weighted price for the period 3 is 47.0 £/MWh (0.047 £/kWh).

4. Period 4: between 15:30 and 21:00 hours. The average of the weighted price for the period 4 is 50.4 £/MWh (0.0504 £/kWh).

The ES management system forecasts the community demand load which will be shifted when it receives the price signals from the market the day before. Then, it schedules the valley charging e.g. Day-Ahead Real-Time Pricing. In the rest of this work, this tariff is referred to as the NETA tariff.

For the 2020 and zero carbon scenarios, the NETA tariff prices were increased to consider customer prices because prices from the NETA market do not reflect the real selling price. Assuming a typical selling price of 0.13 £/kWh in 2012, the weighted price for the four periods was increased by the ratio between 0.13 £/kWh and the average price of the NETA tariff (0.048 £/kWh). Therefore, the ratio between the prices of the four periods in a day were always kept constant. The prices presented above for both tariffs were obtained from data available in 2011. In order to study different scenarios in different reference years (2020 and zero carbon), the prices of the NETA tariff were increased using the average trend of the last 7 and 25 years as shown in Table 5.3. These two set of data were used to consider all prices since records were found (70s) but giving more relevance to the data of the last seven years in order to forecast future energy prices. Figure 3.5 shows the average value of the four electricity prices of the NETA tariff in 2020 and the zero carbon scenario after increasing the prices regarding the weighed average values in 2011 while keeping the ratio between the prices constant.

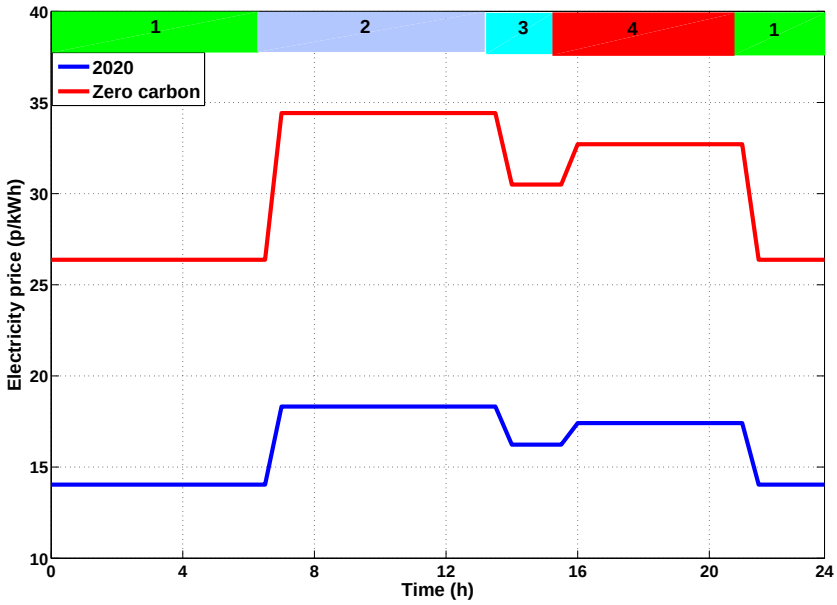

Figure 3.5: Average value of the four electricity prices of the NETA tariff in 2020 and the zero carbon scenario.

3.6 Combination of applications: PV energy time-shift and load shifting

It has been argued that the combination of different economic benefits derived from more than one application should be used to create a business case [11]. However, this potential benefit from the combination of applications has not translated into actual research investigating how to integrate different applications by an ES system, most studying the applications independently [65,98,121,122]. Alternatively, S. Sundararagavan et al. included the combination of LS, frequency regulation and power quality in their analysis, but they only studied the cost of performing these applications (not the profitability or value as defined in Section 4.9) and assumed some of the most important parameters of ES systems such as durability and efficiency are constant [99]. The cost of performing all applications combined was just 2.6% higher than the cost of performing the three of them individually for CAES, while a 38.1 % and 39.7 % higher for PbA and Li-ion batteries respectively. Wade et al. reported on simulation work prior to the deployment of a real ES system taking place on a 11 kV distribution network, investigating how a generic ES system responded to voltage control and power flow management. They argued that the corresponding economic benefit should be identified fore each application in order to prioritise the events which add more value and identifying where in the value chain and what stakeholder could take advantage of it [94].

Additionally, the comprehensive report prepared by Sandia for the DOE includes a specific section about the combination of applications, what they called storage Value Prepositions [56]. They also outlined the main reasons why the aggregation of benefits is not a common practice yet. Among the market failures, they argued that different benefits sometimes accrue different stakeholders which is why coordination is a key factor. Among the technical issues to be solved, the lack of engineering standards was highlighted.

The performing of PVts and LS together was investigated for the different ES technologies included in this work. PVts was combined with Economy 7 and the NETA tariff. Unlike ES systems which operation at the distribution level respond to different events on multiple networks but the occurrences of those events is given by the network state, CES considered in this work perform PVts and LS on a daily basis.

3.7 Power curtailment

Power curtailment is a straightforward solution for a local network which is not flexible enough to cope with high levels of RE export when the local demand is low. This happens in countries such as Germany, Spain and the UK in which the percentage of RE generation is high enough to be able to destabilize the network frequency or the local voltage in a period with low demand. For example, wind curtailment peaked in 2010 in Spain with 202.2 GWh (losses approximately €70 million) [123]. Power curtailment has been investigated on weak electricity grids and it was found that, long-term ES (charging capability longer that 1 day) is necessary to exclude curtailment but that daily storage (24 h) allowed 3 times more wind power injection than short-term energy storage (10 min) [65]. Germany was the first country to introduce curtailment capability as a new requirement for PV plants [112]. According to latest German Renewable Energy Act, all existing and new PV generators should be able to curtail the power output when it is higher than 70% of the peak capacity installed and any power which is curtailed is only paid at 95% of the FiT. In the case of a PV installation with ES, the maximum power injected to the grid should be lower than 60%. The PV owner must pay 50% of the cost of installing the curtailment equipment.

In the present work, PV power curtailment was considered in the sensitivity analysis for 2020 and the reference scenario for the zero carbon year as shown in Table 5.2. It was assumed that the PV power is curtailed when the electricity injected into the grid is higher than 70% of the rating of the plant. It was also assumed that any electricity which is curtailed is not paid the generation bonus, G_b(£/kWh). The electricity which is not curtailed but stored by a CES system can be used later to meet the demand load. Therefore, a revenue can be obtained from

avoiding RE curtailment, Rev_{Ct} (£), as shown in Equation 3.10 (for batteries). Different to PVts and LS, power curtailment was studied as a complimentary application to PVts and therefore was not independently optimised in this work.

$$Rev_{Ct} = E_{Ct} \times (G_b + \eta \times P_e) \tag{3.10}$$

3.8 Heat decarbonisation

Another illustrative ES application is the use of CES to support the decarbonisation of the heating sector. One of the key objectives of the UK and many other countries is the decarbonisation of the heating sector because heat accounts for over three quarters of the energy which is used in houses [34]. In the UK, the Renewable Heat Incentive was launched in 2012 and it promoted the use of low carbon heat generators [109]. However, this incentive is directly related to the heat generation system and does not include the CES system. However, CES can be an attractive option to meet the spacing heating and DHW demands using RE technologies. Heat decarbonisation is considered in this thesis as a societal benefit (it implies the reduction of the CO_2 emissions) but there is not a direct internalizable benefit related to the use of CES for this purpose at the moment.

The impact of meeting the heat demand on the CES performance, durability and economic benefits have not been assessed yet in the literature and this is one of the key considerations of this work. This research assessed the impact of the heat demand load on the CES size, performance, durability and economic benefits depending on the application (PVts, LS and the combination of them). Heat decarbonisation is accomplished when batteries connected to HPs or electrolysers connected to FCs (running as CHP generators) are charged with electricity from local PV generation and/or from a decarbonised grid. Models of HPs and FCs running as CHP generators are presented in Sections 3.11.2 and 3.11.1 at the end of this chapter.

3.9 Other service benefits

If the applications listed above can obtain service benefits which can be internalized due to the current possibility of obtaining economic revenue by customers or utility companies, there are other service benefits which associated revenue is difficult to quantify [56] but their calculation is out of the scope of this work. However, these service benefits should be considered by governments and other stakeholders in order to determine the level of support to CES [111]. Among them, transmissions and distribution (T&D) capital deferral, service reliability and voltage support can be considered the most important. The maximum peak

in the demand could be reduced (or at least it does not increase markedly), less PV generation is injected to the grid in weak areas and/or at periods when demand is not high by performing any or several of the applications discussed in this work. These positive effects can defer the upgrading of the current electrical lines and transformers or even make them not necessary (T&D capital deferral), voltage would keep close to the safety level in the area (voltage support) and less faults may occur (improved service reliability). Additionally, the improvement in the reliability of the community energy supply against any possible grid failure could be another factor to consider.

3.10 The energy consumption level

The ES applications discussed above manage the electricity demand, heat demand and the local PV generation of customers. Therefore, modelling these different parameters is necessary to investigate these applications. The second part of this chapter presents the models and experimental data selected to quantify the different domestic loads, the PV generation and the performance of low carbon heat generators. These models and related input data together with the ES technology models presented in Chapter 4 are necessary to apply the method presented in Chapter 5.

3.10.1 Demand data

A large domestic demand data set including electricity and heat demand data was required in order to evaluate the optimum CES system as a function of the community size for the different applications introduced above. The most suitable data set was the hourly electricity and natural gas consumption data recorded at the Milton Keynes residential community located at the north of London (UK) [124] for a year and a half between 1990 and 1991. 130 dwellings with different sizes and number of occupants were recorded but only the data related to 102 of these dwellings was usable due to problems with the monitoring system. As a consequence, 100 homes were used to probe the method which also matches the largest community size tested in the present work. These dwellings have a conventional design for the UK but the construction included energy efficiency features (primarily increased insulation in the roof, wall, and flooring and energy efficient boilers). The average heat and electricity demands of the 102 homes were equal to 12.5 and 3.2 MWh/year respectively. This consumption can be qualified as medium when compared with the consumption of an average house in the UK. According to Utley and Shorrock [32], the annual space heating and domestic hot water demand of the average household was 16.8 MWh in 2006 and the annual electricity consumption was 3.0 MWh. However, the total energy consumption due to space heating in the UK reduced from 30.5 Mtoe to 29.9 Mtoe (2%) from 2006

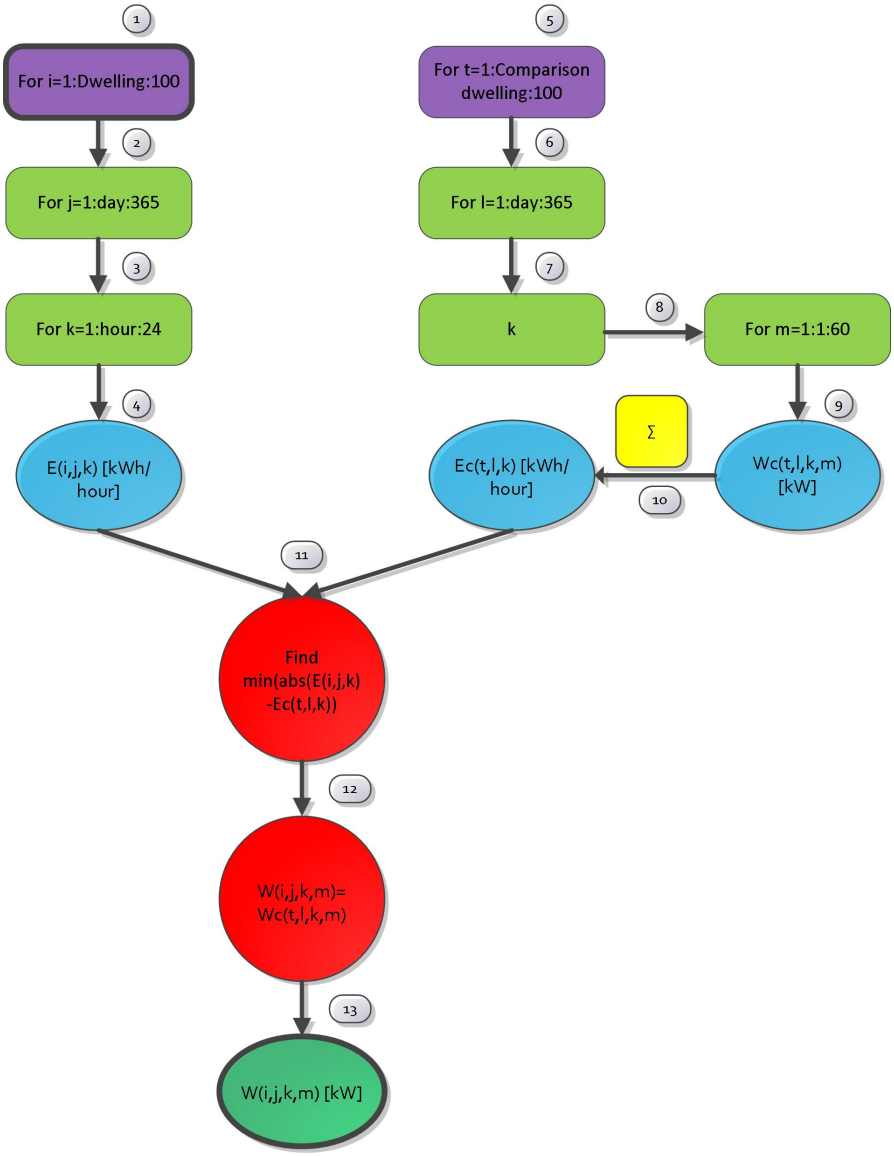

Figure 3.6: Flowchart of the algorithm which converted hourly recorded electrical demand data into minute resolution data using a second set of electrical demand data recorded every minute.

to 2008 due to improved insulation and heat generators (boilers) while electricity consumption (6.8 Mtoe) keeps almost constant. According to the standard assessment procedure (SAP) used by DECC, the dwellings range between 75-90 (the average SAP in the UK was 54 in 2010 [125]). Overall, it has been considered that the data recorded at Milton Keynes is representative of the current stock of houses.

Electricity hourly consumption was transformed into minute resolution data when comparing with another set of data from 57 houses while keeping the hourly energy consumption invariable. The "comparison" set of data was built when using a combination of real demand data from 7 homes and modeled demand data from 50 homes. The real demand data was selected from a total of 22 homes in the East Midlands, UK [126] and only the homes with similar characteristics

e.g. no electrical heating and no electrical shower were selected. In order to make the "comparison" set of data larger, modeling results from dwellings with similar characteristics were incorporated to the comparison set of data [127]. The reason why the "comparison" set of data was not directly incorporated in the final set of data was heat demand was not monitored or modeled.

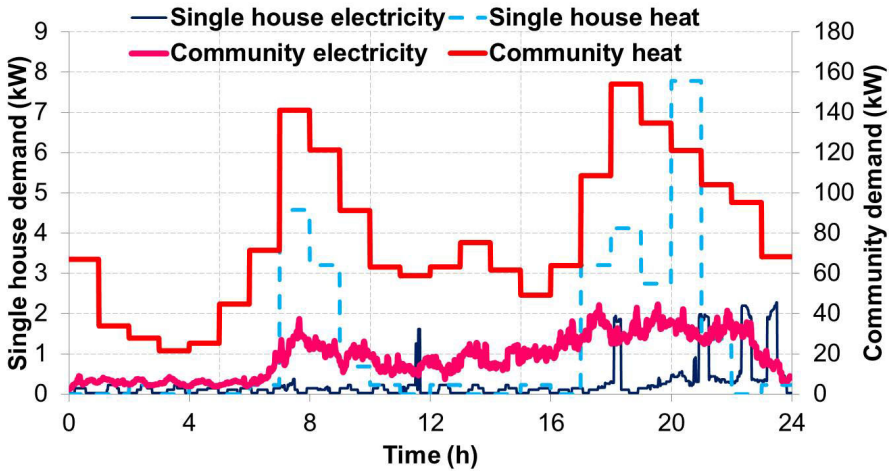

Figure 3.7: Electrical and heat demand of a single home and 50 homes from the data set monitored at Milton Keynes after changing the temporal resolution to 1 minute.

The algorithm utilised to transform the temporal resolution is explained in Figure 3.6. Any dwelling from the "final" set of data from Milton Keynes (i) is referred in the chart as "Dwelling". Any dwelling from the "comparison" set of data (t) was referred in the chart as "Comparison dwelling". Every "Dwelling" had an hourly (k) energy consumption E (kWh/h) for every day (j) of the year and the algorithm searches the minute (m) demand data W_c (kW) which represent the closest hourly (k) energy consumption E_c (kWh/h) from any "Comparison dwelling" at the same hour of any day of the year (l). In the case of the heat demand, it was assumed constant for every hour due to the fact that the dwellings monitored in Milton Keynes had water tanks to facilitate the performance of the natural gas boilers. The electrical and heat demand of a single home and the aggregation of the demands of 50 homes with a temporal resolution of 1 minute are represented in Figure 3.7.

In addition to the demand data, the irradiance, dry bulb temperature and other environmental variables were also recorded at a weather station located in the community. This environmental data were necessary to model the performance of the PV generators and the low carbon heat generators as shown below.

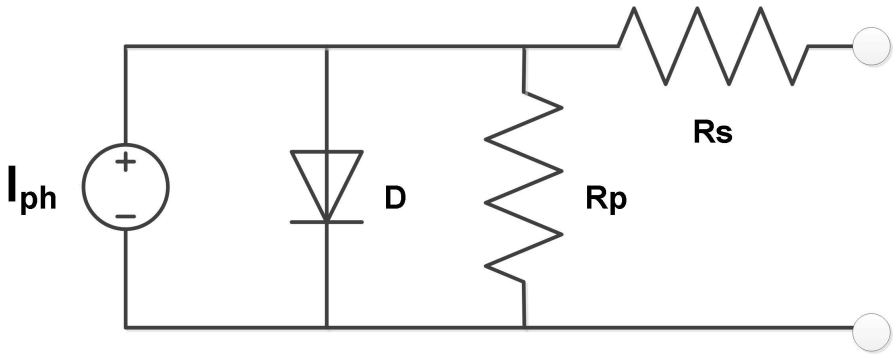

Figure 3.8: Single diode model of a PV panel utilised in this work

3.10.2 PV generation

The objective was to accurately calculate the performance of PV panels using technical data supplied by manufacturers of PV arrays and the environmental variables recorded at the Milton Keynes community. The model selected was developed by Villalva et al. [128] and it is based on a single diode model as represented in Figure 3.8. The model includes the temperature dependence through the nominal operation cell temperature (NOCT) [129]; losses due to current flow through different semiconductors and contacts are represented by a series resistance, Rs; and losses due to leakage current of solar cells are represented by a parallel resistance, Rp. A double diode model was not considered because accuracy would only be slightly improved despite it introduces a lot of complexity [113]. The current source is not ideal and it depends on the irradiance (W/m^2) and the PV panel temperature (K).

The irradiance and outdoor temperature are the necessary input data. A sky model presented by J.A. Duffie and W.A. Beckman which simulates the presence of clouds on the sky was used to calculate the tilted irradiance from horizontal irradiance measured with the pyranometer [130]. Finally, a maximum power point tracker system (MPPTS) was simulated to obtain the maximum power from the PV panel depending on the irradiance and temperature conditions.

PV array size and orientation

The domestic PV installations with a rating up to 4 kWp were 348360 in 2012 and added 996.7 MWp according to DECC [114]. This means that the average domestic PV installation was 3 kWp. This value was also concluded by a research report created by the UKERC in which it was explained that future domestic solar applications will average round 3 kWp based on arrays areas between 15-20 m^2. As a consequence, 3 kWp was selected as PV array size for the different PV scenarios studied. Regarding the orientation, different azimuth angles were incorporated to simulate different orientation possibilities in a real community. The azimuth

Table 3.2: Electrical characteristics of the PV panel modelled in this work.

PV panel parameters	Value
Maximum power (W)	235
Voltage at maximum power (V)	43
Current at maximum power (A)	5.48
Open circuit voltage voltage (V)	51.8
Module efficiency (%)	18.6
Temperature coefficient at open circuit voltage (V/K)	-0.130

angle γ varied between -50° and $+50^\circ$ according to 10° degree changes. These orientations were proportionally introduced in the communities. The electrical characteristics of the PV panel selected for this work at standard conditions are shown in Table 3.2. They are based on the PV panel HIT-N235SE10 manufactured by Sanyo which uses silicon monocrystalline technology [131].

3.11 Low carbon heat generators

In order to decarbonise the heating sector, low carbon heat generators are being introduced in the domestic sector. There are several technologies which can be used to meet the heat demand without using traditional fossil fuels (typically natural gas).

- CHP generators. In this work, FC systems working as CHP generators are considered.
- HP systems.
- Biomass boilers will be very interesting when there are biomass resources in the area. Biomass boilers are not discussed in this work due to the fact that their integration will be similar to previous gas boilers integration.
- Solar thermal energy has been successfully utilised for DHW application and new domestic and commercial buildings should integrate solar thermal installations in many countries such as Spain, Germany and the UK. A well designed installation can achieve solar factors of around 50% when using a thermal buffer in the form of water tank [132]. Solar energy is not discussed in this work because it is a well-established technology which already uses thermal storage (water tanks) to increase its load factor.

3.11.1 Fuel cells

CHP systems generate both electricity and heat on-site aiming at increasing the efficiency of fuel utilisation and they have been considered as a complementary energy system to RE technologies in a transition to a low carbon economy [133,134]. CHP systems have already been introduced for service buildings such as hospitals and airports where electricity demand is more constant and heating and cooling demands complement throughout the year [135] and in communities where the aggregation of demands increases the number of operational hours using a district heating network to supply heat.

FCs are electrochemical energy conversion devices with no moving parts, quiet operation and low emissions due to high efficiency which are used as CHP systems [27]. There are three main decisions to take when using a FC system for a domestic application: technology, operational strategy and size. Polymer electrolyte membrane (PEMFC) and Solid oxide fuel cells (SOFC) are the technologies which attract more attention in spite of being very different in terms of the range of operational temperatures, materials used in the manufacturing and performance. The basic difference is that a SOFC operates at high temperature (typically between 500 °C and 1000 °C) and it generates heat with higher exergetic content. A PEMFC system usually performs at a nominal temperature around 80 °C and it requires high purity hydrogen to avoid the poison of the electrocatalysts (e.g. platinum) [136]. When the PEMFC system has a reformer integrated, this is more complex and costly than in the case of a SOFC (SOFCs internally reforms the natural gas). On the other hand, PEMFCs have faster response time, including shorter start-up times. In this work. PEMFC was selected for the modelling work because a PEMFC stack was also utilised for the real community hydrogen storage system (H-CES) presented in Chapter 7. Additionally, PEMFC systems offer quicker response time (on the ms scale) and higher power densities (0.7 $W \cdot cm^{-2}$).

The 1D PEMFC theoretical model utilised in this work was previously presented by O'Haire et al. [27]. The approach suggested by Mench [137] was used to calculate the Nernst voltage of a PEMFC cell. This theoretical model was integrated with the balance of the plant (BoP) together with other practical aspects of FC systems using an approach presented in a previous work [138].

Figure 3.9 shows the electrical and heat efficiency for the PEMFC system as a function of the current density of the stack. The model took into account activation losses, ohmic losses and concentration losses at uniform temperature based on standard parameters for the technology [27]. At very low load, all the electricity generated is utilised by the parasitic losses and it has been considered that the PEMFC system only runs when the electricity generated is larger than

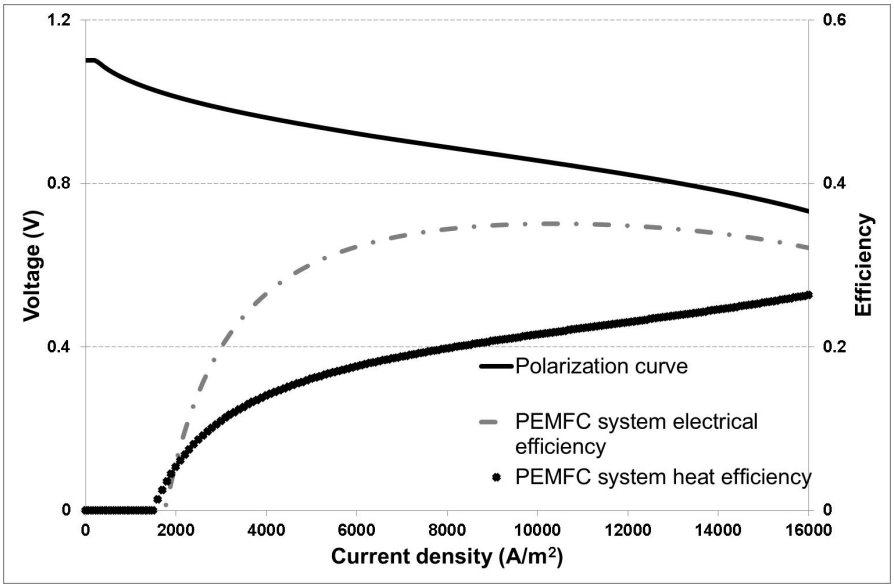

Figure 3.9: Polarization curve of the PEMFC stack, electrical and heat efficiency of a natural gas fed PEMFC system as a function of the current density. The system is off for current densities less than 1600 A/m^2 due to the parasitic losses.

the BoP´s electrical consumption. This corresponds to a current density higher than 1600 A/m^2. Once the electricity generation is higher than the parasitic load, the PEMFC system is able to supply both electricity and heat. According to the Figure 3.9, the electrical efficiency is higher when the PEMFC runs at a intermediate load. The electrical and heat efficiency impacts on the results obtained by H_2 technology, especially for LS as discussed in Chapter 6.

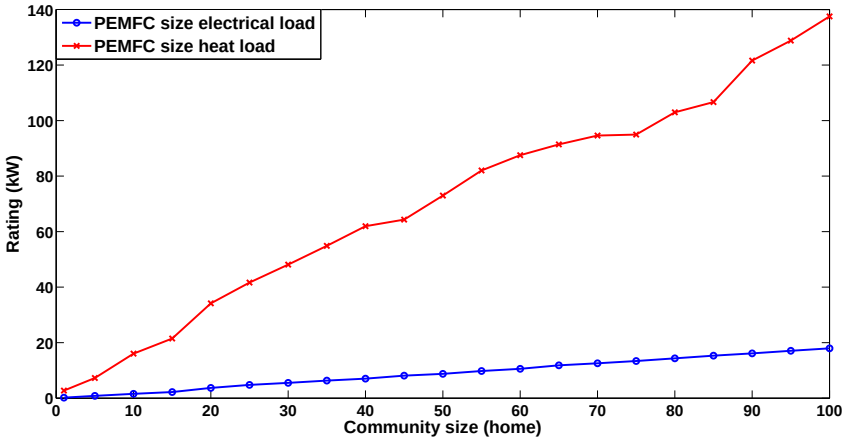

Figure 3.10: PEMFC rating according to the largest rectangle method when considering the electricity and heat demand loads.

Having selected the technology, the next step consisted of selecting the size of the PEMFC system for any community and the performance strategy. The largest rectangle method is given by the PEMFC system which maximizes the energy de-

livered throughout the year (the sides of the rectangle are the PEMFC rating and the number of operational hours) [139]. The novelty in this case was that instead of using the heat load to obtain the size of the PEMFC system, the community electrical load was utilised. This decision reduced the size of the PEMFC systems for any community and reduced the electricity export to the grid [138]. The comparison between the results from the largest rectangle method considering the heat and the electrical demand loads are shown in Figure 3.10. Regarding the strategy, the PEMFC systems followed the thermal load. The objective was to increase the number of operational hours [138]. The rating of the PEMFC system was proportional to the size of the community as seen in Figure 3.10. The heat demand load has a stronger seasonal pattern than the electrical load but the PEMFC systems were rated to run close to full load continuously for any community.

Figure 3.11 shows the electrical, heat and total efficiency of the PEMFC systems as a function of the size of the community. The total efficiency was lower than that obtained for a SOFC system in a previous work [76] because a PEMFC system generates more heat due to lower electrical efficiency and the fraction of heat which is supplied to the heat demand load was reduced by the efficiency of the heat exchanger for the thermal application (equal to 0.7 [27]). The total efficiency was kept constant with the size of the community but the electrical efficiency was higher for the 5 and 10 communities.

The different load factor of the PEMFC systems also affected the H_2 requirements for the communities. This was clearer in the transition between the single home and the 5-home community due to the randomness of the heat demand load in the single home. Specifically, the annual H_2 consumption of the PEMFC system in the single home, 5-home and 10-home communities was 60 kg, 661 kg and 1201 kg.

3.11.2 Heat pumps

HP technology is already available in the market and HPs are being used as alternative to natural gas boilers for decarbonising the heating sector using electricity as energy vector. HP technology is modular and very suitable for single homes, specifically those with thermal requirements which can be classified as low or medium [140]. HPs can harness electricity generated by RE technologies but one of the main environmental problems derived from their use is the high CO_2 potential of the refrigerants used in the thermodynamic cycle. In fact, their global warming potential can be up to 3500 times greater than CO_2 on a 25-year horizon [141].

A HP transports heat from a low temperature heat source to the indoor environment (high temperature) by using a compressor which increases the pressure of

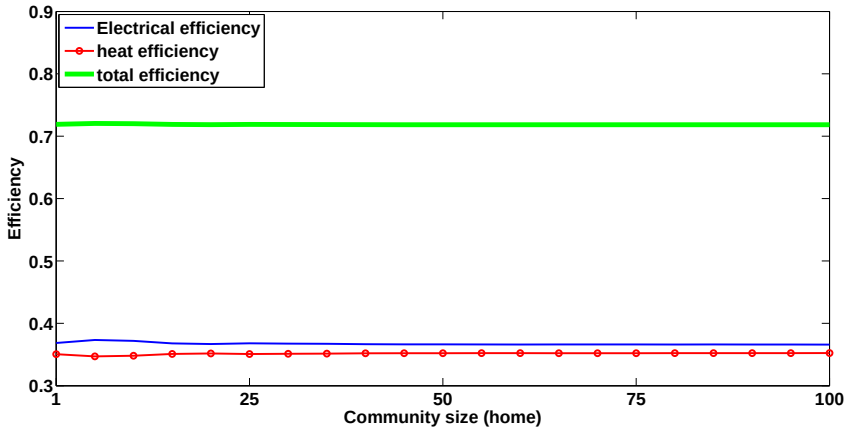

Figure 3.11: Electricity, heat and total efficiency of the PEMFC system as a function of the size of the community in 2020.

a refrigerant. An evaporator is used to extract the heat from the low temperature heat source and a condenser is used to supply the heat into the space to heat up. An expansion valve closes the refrigeration cycle and supplies liquid refrigerant to the evaporator. Depending on the temperature of the heat and cold sources, different refrigerants are used such as R-134A, R-718 (water), R-22 and R-407. For this work, the R-134A refrigerant is selected because it evaporates and condenses at temperature suitable for domestic applications.

Depending on the fluids used to transport the heat between the low heat source and the final application, there are different HP systems: water to water, water to air; air to water and air to air. Air-source HPs are widely used due to easier installation in spite of lower coefficient of performance (COP) when the outdoor temperature is very low (less than 0 °C). Ground-source HPs use the ground which has a more constant temperature through the year (ranging from 7 °C-15 °C [142]) to increase the COP. The type of fluid used to distribute the heat inside the building is usually air or water. Air is used when the HP warms a small dwelling or a single a room. For this work, air-source HPs which use water to distribute heat were simulated because this is commonly utilised for individual dwellings when considering its modularity, ease of installation and limited space requirements.

In order to quantify the performance of a HP, modelling the main components which integrate the system shown in Figure 3.12 was necessary. The model utilised in this work is detailed in the Appendix A. The COP as a function of the outdoor temperature when the water is generated at 40 °C and 60 °C is represented in Figure 3.13. The COP is proportional to the outdoor temperature since the difference between the evaporator and condenser pressure reduces. For the same reason, the COP increases when the heat supplied is generated at lower temper-

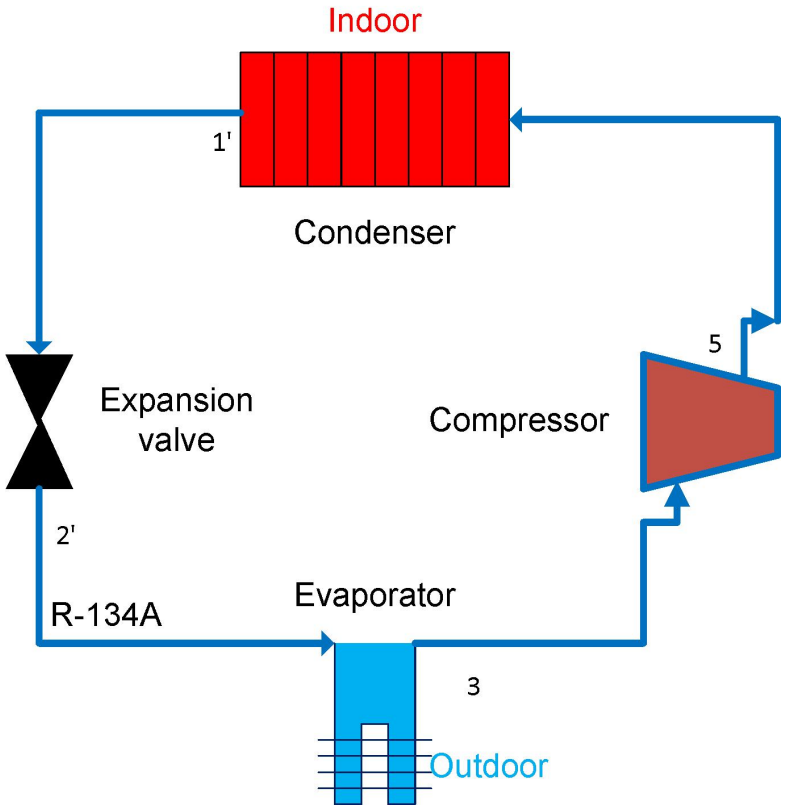

Figure 3.12: Schematic representation of the HP with the different components modeled in this work as explained in the Appendix A.

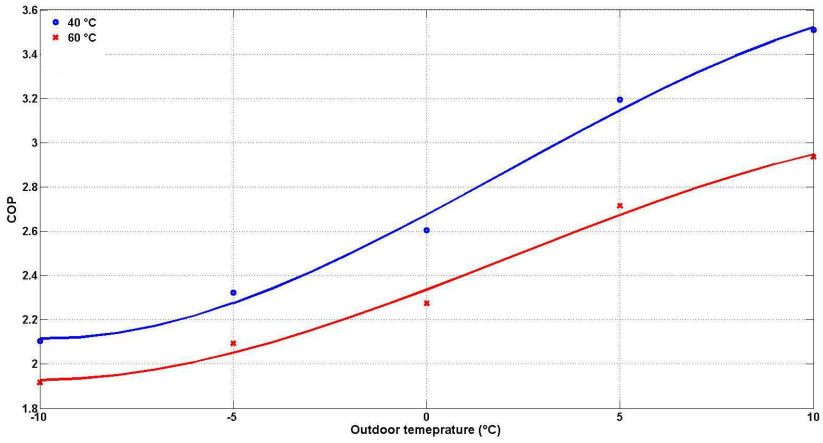

Figure 3.13: COP as a function of the outdoor temperature when the water is generated at 40 °C and 60 °C including a cubic fitting.

ature. The values obtained by this steady-state model are based on appropriate HP installation as well as appropriate control by the end users. Results in Figure 3.13 are in agreement with those reported by the most wide-ranging monitoring exercise of domestic HP installations performed by the Energy Saving Trust [140]. According to this comprehensive report, the mid-range COP for air-source HPs

was between 2.3 and 2.5, while efficient, proper installed and well used air-source HPs achieved seasonal COP up to 3.3. However, the HP model presented in the Appendix A does not consider operational aspects including high temperature generation to combat Legionnaires and transients for preventing frost formation on the evaporation coil [143]. Regarding the size of the HPs, the heat rating is given by the maximum heat demand load for any home considering in the community (comprising space heating and DHW demand as explained in Section 3.10.1).

3.12 Summary

This chapter delimited the ES applications which are the focus of this study. CES introduces different types of benefits with are relevant for different stakeholders such as end users, utility companies, DNOs and governments. While economic benefits are key for the developing of a business case, strategic and service benefits should also be considered in the analysis although calculate the monetary value of them is not straightforward. Indeed, "smart" customers aim to play a more active role in the energy system and CES has the potential of being a game changer for them.

PVts and LS were identified as key applications because they are energy applications which manage the end users' RE generation and demand on a daily basis. According to this, the current economic incentive for performing PVts in the UK was assessed. PVts makes sense due to the fact that importing electricity is worth more than exporting electricity. In the case of LS, two different tariffs were defined in terms of number of periods and price structure: Economy 7 and a four period tariff derived from the prices of the imbalance market. Additionally, heat decarbonisation and the avoidance of power curtailment complemented the range of applications which are included in the analysis as complimentary applications.

In order to simulate the different end user applications, this research uses demand monitored in a real 100-home community in the UK. Additionally, PV panel, PEMFC system and HP models were developed. These models use the environmental variables monitored at the community as input data and are utilised to simulate the different scenarios explained in Chapter 5.

The consideration of several applications by the same CES system including the optimum management of the PV generation and the demand of end users has been considered a key factor for the deployment of CES in the coming yeas. Additionally, the potential strategic benefits derived from the performance of CES systems and the impact in the role of customers in the energy area should also be considered in the analysis.

Chapter 4

Energy storage technologies for end user applications

Among all the ES technologies introduced in Chapter 2, only some of them are suitable for CES to meet the technical requirements of end user applications presented in Chapter 3 and play the role of CES. The current chapter will present the ES technologies selected for performing PVts, LS and the combination of them according their discharge and scale characteristics. Battery by means of PbA and Li-ion, H_2 storage and water tanks were modeled for performing these applications.

A comprehensive modeling approach using robust models to fully understand the performance and the economic benefits of CES is presented in this chapter. The models are comprised of a performance, durability and economic submodels. Although the performance and durability submodels depend on the specific characteristics of each technology, the same rationale was used for all the technologies considered. This is one of the strengths of this work and helped to compare different ES technologies and extract conclusions from their performance and economic benefits in Chapter 6.

4.1 Energy storage requirements for the end-user applications

End user applications are energy applications (instead of power applications) because of the duration of the discharge. In the case of LS, the discharge could be as long as the length of the peak period (17 h for Economy 7) and it lasts for several hours depending on the available charge for PVts. These discharge requirements rules out ES technologies such as flywheels and supercapacitors which offer maximum discharges of several minutes. Secondly, pumped storage hydroelectricity and CAES usually have power ratings (100 MW-1 GW) too large for community applications and the ability to store energy is linked to certain geographical loca-

tions.

Thirdly, technologies for end-user applications should be modular to be integrated in communities of different sizes ranging from a single home to hundreds of homes (up to 11/0.4 kV substations which range between 150-500 houses). Only battery, H_2 and thermal storage offer this modularity with systems which can range from the kW to MW scale and are suitable technologies for PV management and demand management.

4.2 ES technologies for end-user applications

4.2.1 Battery technology

Two different batteries technologies are compared: PbA and Li-ion batteries. PbA was selected because it is the standard battery used in different applications such as off-grid RE installations. The main reason for this widespread use is the capital cost of the storage medium a seventh that of Li-ion batteries in 2009 [144]. Other advantages are low self-discharge current and relatively easy maintenance. Finally, PbA batteries are highly recyclable and this fact can be very attractive for demonstrating the complete sustainability of the storage technology. However, PbA batteries have limited cycle life, especially in environments with extreme temperatures and they are made of environmentally unfriendly lead [108]. There is also interest in utilising PbA technology for CES due to the fact that efficiency and durability keep on increasing while maintenance requirements and capital cost reduce. Advanced PbA batteries can achieve round trip efficiencies up to 85-90% [145] but still have low energy density up to 35 Wh/kg [64]. PbA technology has been already investigated for end-user applications, typically at singe homes [76,102,104,104] along with companies offering PbA products such as Solon and Hitachi.

As reviewed in Section 2.6.3, Li-ion batteries are characterized by high round trip efficiency (up to 93% DC efficiency) [99] and high energy density up to 150 Wh/kg [17]. This chemistry is already used in the portable industry for laptops and mobile phones. Its high discharge rating (up to three times the nominal capacity, 3×C, according data reviewed from Hitachi) makes it attractive for electric drive vehicles. The reduction of cost expected by manufacturers [105] and the exploration of new business models (like the use of second-hand batteries from the vehicle industry in stationary applications) is the reason why Li-ion technology has been investigated for end user applications by different authors [103, 105, 118] and companies such as Hitachi and Saft have already put into practice the first field trials to better understand the performance and durability of Li-ion batteries depending on the application [105].

4.2.2 Hydrogen technology

Regarding the H_2 generation, PEM technology was selected for the experimental and modelling work. PEM technology was already introduced for FC systems in Section 3.11.1. In addition to the advantages outlined in Section 2.6.3, PEM electrolysers are able to generate pressurized H_2, therefore a H_2 compressor is not necessary, resulting in higher efficiency. Using PEM technology for the modeling and experimental work allowed the comparison between simulation and experimental results as discussed in Chapters 6 and 7.

In the case of the H_2 tank, the modelling approach was technological agnostic. Only the H_2 storage requirements resulted from the balance between the H_2 generation by PEM electrolysers and H_2 consumption by PEMFC systems were identified. In other words, the storage tank capacity is a dependent variable of the balance between the PEM electrolyser H_2 generation and the PEMFC system's consumption. A solid state H_2 tank selected for the experimental installation is introduced in Chapter 7.

4.2.3 Thermal storage

Among the different technological options for thermal storage discussed in Chapter 2, a hot water tank in a single home has been considered in this work. The main reason for this is that there are 19.3 million hot water tanks in the UK (2006) [32]. Most of them were deployed in the 1970s before the development of "combi" natural gas boilers (which do not need the support of a water tank to provide instantaneous DHW). Therefore, only a totally distributed thermal storage scenario is considered in this work by studying the performance of a water tank in a single home.

4.3 Characteristics and requirements of ES models

As reviewed in Section 2.7, one of the key gaps for fully understand the economic benefits of CES (and ES in general) is the lack of models which describe the performance and ageing of ES technologies together with the economic benefits derived from ES applications. In order to fully understand the performance and economic benefits of CES, ES models should fulfill the following:

- Be comprehensive enough to describe key ES parameters including round trip efficiency and effective capacity under partial loads [144].
- Simulation step should be equal to one minute in order to reflect how changes in RE generation and demand affect the CES performance. A shorter sim-

ulation step was not considered because capturing the dynamics of CES systems and their transient response was not the objective.

- Being holistic and describe the performance, durability and economic benefits of CES.
- Being conceptually simple to allow the comparison between different technologies and perform parallel sensitivity analysis by modifying the same or equivalent parameters.
- Being representative of ES technologies and not specific to one manufacturer of ES.
- Not being too computationally heavy to run different ES scenarios.

4.4 Modelling of ES technologies

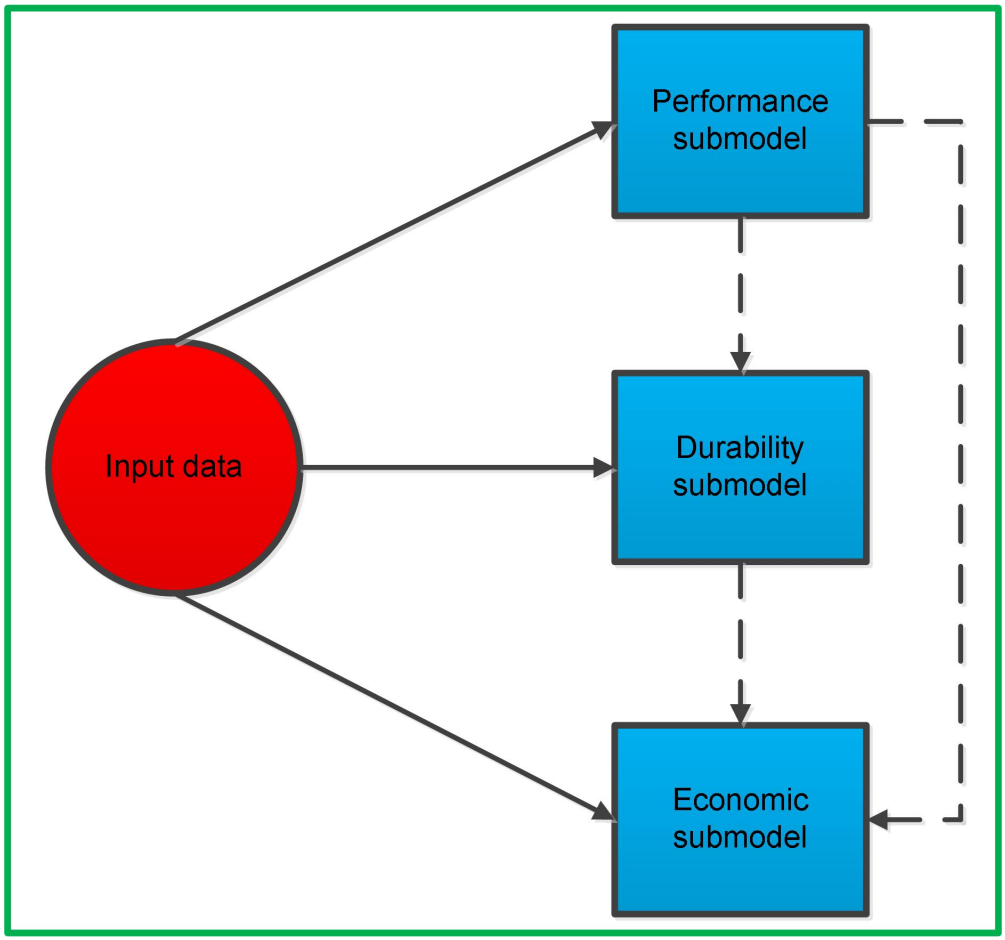

Figure 4.1: Modelling of the ES technologies following a holistic approach which describes the performance, durability and the economic behaviour.

The four technologies discussed in this work have been modelled following the same rationale. This can be considered one of the key aspects of this work because these technologies use different chemical and physical principles as seen in Section 4.5. The holistic approach considered in this work is schematically represented in Figure 4.1.

Although not always mentioned in the literature, PbA, Li-ion and H_2 are families of ES technologies within which similar materials, chemical and physical principles to store energy are shared. For instance, there are several types of PbA batteries which use the same electrochemistry principles but are different in terms materials used to form plate grids, separators, containers and battery construction [18]. Similarly, there are many Li-ion electro-chemistries depending on the anode, cathode and electrolyte materials. In the case of H_2 storage, there are different types of PEM membranes. The models used in this work focused on those specific technologies which have been developed for being integrated with RE technologies and the input data parameters were based on average performance values.

Finally, the environmental impact of different ES technologies was not considered in this work. Regarding the in-use impacts, this work assumes that electricity managed by the CES comes from local PV plants or has an important share of RE generation when imported from the grid (which make prices of electricity more variable) in the 2020 and zero carbon scenarios. Additionally, the manufacturing impacts are already assumed in the initial cost. In fact, ES technologies which are expensive typically use raw materials which are difficult to extract and/or process and this impacts on the cost.

4.4.1 The performance submodel

The performance submodel describes the technological behaviour of the technology for any given size and obtains the round trip efficiency together with other parameters derived from the application developed such us the equivalent full cycles (EFC) and discharge (kWh). A mathematical model which describes the charge and discharge principles was selected for each technology. Together with the physics and chemistry principles, the input data necessary for the performance submodels include the maximum charge and discharge ratings and the depth of discharge (DOD) or effective capacity.

4.4.2 The durability submodel

The durability of a CES system is quantified depending on the technology. Key factors which affect the degradation are the depth of discharge and discharge rate, and start-ups and operation hours for batteries and PEM electrolysers respectively.

4.4.3 Economic submodel

The same economic submodel was applied with each technology. It assesses the cost, profitability and value of CES when performing the applications considered in this work. The economic submodel obtains three financial parameters which are interesting for different stakeholders such as customers, utility companies, governments and manufacturers. Specifically, the internal rate of return, *IRR*, the levelised cost of energy storage, *LCOES*, and the levelised value of energy storage, *LVOES*, were used to assess the economic performance of the four technologies. In addition to the performance results, the main input data are the initial cost of the CES system, the durability of the project, the energy prices and governments incentives in the form of feed-in tariffs.

Results obtained from the different submodels depends on the ES application, the PV generation, the demand and the CES size. The available input data for the performance submodels were less diverse than the input data necessary for the durability and economic submodels. This is related to the level of uncertainty associated with the durability and cost of ES technologies as seen in Appendices B and C.

4.5 Performance submodels

In this section, the submodels selected for each technology in this work are presented after reviewing different performance models available in the literature.

4.5.1 Battery technology

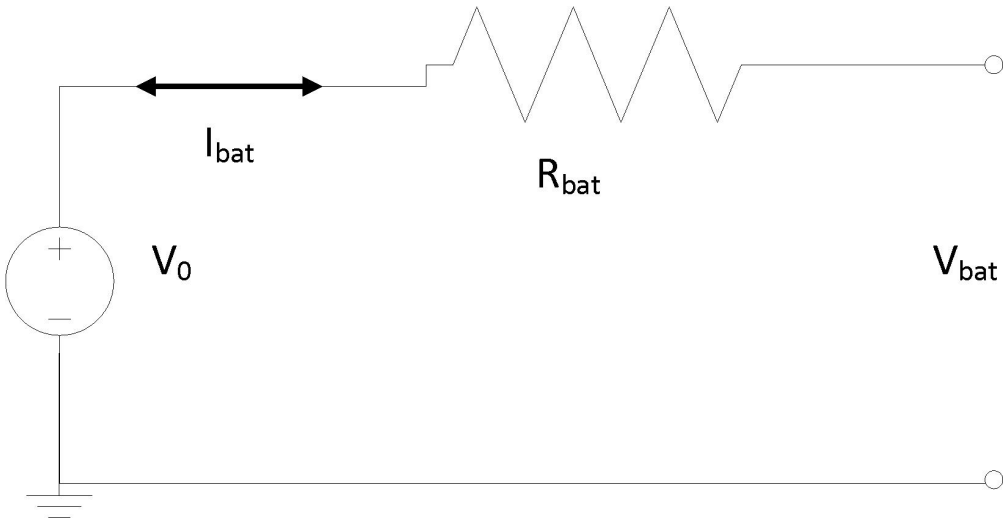

Figure 4.2: Schematic representation of the battery performance model utilised for PbA and Li-ion battery technologies.

There are three main types of performance models which have been used in the literature for battery technology: mathematical models (more simple but inaccurate), electrical circuits which are more intuitive and easy to use and electrochemical models which are more comprehensive but complex to integrate in simulations [146]. For end user applications, the second option has been more widely adopted, using a voltage source in series with a resistance to model the battery voltage and considering how the state of charge (SOC) affects these electrical parameters. A literature review of PbA and Li-ion performance models is included in Appendix F.

An equivalent electrical circuit was also utilised in this work for both PbA and Li-ion batteries as represented in Figure 4.2. The resistor is used to model the losses derived from the charge and discharge processes and therefore increases and reduces the voltage at the battery terminal respectively. The SOC is the key parameter which affects the battery voltage. The SOC is a dimensionless parameter utilized to quantify the amount of energy stored by a battery related to the maximum capacity $SOC=1-Q/C$, Q being the real charge, and C the battery capacity. The SOC is calculated using the charging and discharging currents and the battery capacity. The SOC was the independent variable used to obtain several dependent variables: voltage V_b , round trip efficiency η, etc. Equation 4.1 represents the voltage of the battery V_{bat} as a function of the charging (positive) and discharging (negative) current I_{bat}, the internal resistance R_{bat} and the equilibrium voltage V_0.

$$V_{bat} = V_0 + R_{bat} \times I_{bat} \tag{4.1}$$

PbA performance submodel

The PbA performance model selected for this work is derived from the experimental work carried out by J. B. Copetti et al. [147]. They tested different types of PbA batteries manufactured for PV applications in different performance conditions according to variable PV generation. Using the Shepherd model (Equation F.1) as a starting point, the voltage for a single PbA cell was modelled as a function of the SOC. The Shepherd model was expanded by using experimental results which were normalised as a function of the effective capacity C. Then, mathematical equations which represent the charge and discharge voltages, V_{batc} and V_{batd} respectively, as a function of the SOC, the battery current, and temperature, ΔT_{bat}, were derived. ΔT_{bat} is the difference between the battery temperature and a reference temperature equal to 25 °C.

Different values were used depending on the charge and discharge cycle as shown in Equations 4.2 and 4.3 respectively. The model considered the variation

of the internal resistance and the capacity with the SOC, with I_{bat} and the temperature. The temperature was assumed to be constant in this work (the thermal approach is explained in Section 4.5.1). C_{Ah} is the effective battery capacity in Ampere-hour, K represents the variation of the real capacity with the current and it was defined as a function of the nominal capacity and I_{bat} [147].

$$V_{batc} = (2+0.16\times\frac{Q}{C_{Ah}})-\frac{I_{bat}}{C_{Ah}}\times\left(\frac{6}{1+(I_{bat})^{0.6}}+\frac{0.48}{(1-\frac{Q}{K})^{1.5}}+0.036\right)\times(1-0.025\times\Delta T_{bat}) \tag{4.2}$$

$$V_{batd} = (2.085-0.12\times\frac{Q}{C_{Ah}})-\frac{I_{bat}}{C_{Ah}}\times\left(\frac{4}{1+(I_{bat})^{1/3}}+\frac{0.27}{(1-\frac{Q}{K})^{1}.5}+0.02\right)\times(1-0.007\times\Delta T_{bat}) \tag{4.3}$$

Li-ion performance submodel

A similar approach to the one followed with PbA was used for Li-ion batteries. The model selected represents the battery as a voltage source (open-circuit voltage) with a series impedance which represents the main losses and is based on the work developed by O. Tremblay et al. [148]. This model is available in the library SimPowerSystems of Simulink [149]. Some assumptions of the model are:

- The internal resistance was assumed constant during the charge and discharge cycles.
- The voltage changed according to the community size as explained with PbA technology.
- The parameters of the model were deduced from discharge characteristics and assumed to be the same for charging.
- Temperature was assumed constant.
- The self-discharge of the battery was not taken into account.

Previous battery performance submodels for end user applications

The Li-ion model utilised in this work simplifies the dynamic response of the battery with regard other models found in the literature as detailed in Section F.2. This modelling assumption was based on two different factors. Firstly, Li-ion models in which the transient behaviour is considered were used with power applications. However, battery systems were sized according to the daily energy requirements (although the power requirements were also included as explained in Section 4.6.1) for any application in this work. As a result, the ratio between the discharge rating and the capacity of different battery systems was conservative

(the minimum equal to 3 kW/7.2 kWh for a Li-ion battery performing in the single home) and this reduced the impact of several dynamic effects such as temperature and fast cycling [146].

Secondly, those models which describe the transient behaviour were designed and simulated for short periods of time. Demonstrating the accuracy of different models or simply validate them when performing power applications was the objective. Some of the applications of these models were continuous, pulse and periodic four-step discharges over a three hour period [146]; charge and discharge cycles over three hours in addition to transient response test using pulse simulations [150]; test and validation of the model at different temperature and charge and discharge rates [151].

The level of detail of the PbA and Li-ion models utilised in this work is more exhaustive than those utilised in the literature for end user applications. Previous studies which focus on PV energy time-shift also simplified the battery models by using constant round trip efficiency [96, 102–104]. Only Braun et al. used a comprehensive model of a Li-ion battery for a single home provided by the battery manufacturer, Saft, in a collaboration project [105].

Temperature considerations

The operational temperature of a battery affects the performance but its effect have been further discussed in the case of Li-ion technology. The temperature mainly affects the open-circuit voltage and the SOC [150]. In addition to these two parameters, how temperature affects the capacity fading of a battery was considered in a different research work [151].

M. Chen et al. investigated the temperature and self-discharge of Li-ion batteries [146]. It was concluded that these effects can be neglected in low power applications and the derived model did not consider any temperature effect. Same approach was also utilised for investigating Li-ion technology for PV integration [118].

In this work, temperature effects were neglected for both battery technologies assuming a constant temperature equal to 25 °C when considering battery systems were sized for energy applications. As explained in Section 4.5.1, any battery system integrates a management system which controls the temperature of the battery. Secondly, the capacity of the battery reduces but the efficiency of the battery increases if the temperature is higher than the optimum. Therefore, these results partially counteract each other [152].

Table 4.1: Comparison of the control levels implemented by the management system for PbA and Li-ion chemistries.

Control Parameter (Unit)	**PbA**	**Li-ion**
Maximum charge rate (A)	0.2·C	3·C
Maximum discharge rate (A)	0.4·C	3·C
ΔSOC	0.5	0.6
Maximum SOC	0.9	0.8
Minimum SOC	0.4	0.2
Temperature (°C)	25	25

Self-discharge considerations

It has been broadly reported in the literature that self-discharge in periods in which the energy is stored internally by batteries is one of the disadvantages of this ES technology, especially for nickel based chemistries [17]. PbA tubular technology only suffers from 5-20% of self-discharge per month [144]. The self-discharge of PbA technology in a single home when performing PVts was investigated in modelling simulation work using manufacturer data [76]. Self-discharge only accounted for less than 0.5% of the annual charge due to the fact that the battery performed daily cycles and energy was not stored for more than two hours typically. Therefore, self-discharging effects are not considered for PbA and Li-ion technologies in this work.

Energy storage management system for battery technology

The management system is responsible for managing the performance of the battery by limiting the maximum charge and discharge ratings, the depth of discharge, *DOD*, and controlling the temperature. The voltage of the battery should be continuously monitored to set the optimum commands. There is a maximum voltage which is used as upper threshold for battery charging and on the other hand, there is a low battery threshold which prevents aggressive discharging. Table 4.1 summarizes the values assumed in this work for PbA and Li-ion technology.

It has been suggested by manufacturers and discussed in the literature that charging PbA batteries is less efficient than subtracting the charge [104]. Therefore, the maximum charge rating is usually limited more than the maximum discharge rating and this approach was followed in this work. Specifically, the maximum charge and discharge rates were C/5 and C/2.5 in agreement with technical data from the manufacturer Hitachi. This manufacturer was also contacted for the maximum charge and discharge ratings for Li-ion technology according to the values indicated on Table 4.1. The SOC range was fixed by the own PbA perform-

ance submodel and it agreed with the data supplied by the manufacturer Solom. Likewise, to enable the deployment of the Li-ion batteries over 20 years, the active SOC range was constantly limited to 60% of the capacity [105]. The maximum and minimum SOC for Li-ion technology was based on technical data from Saft. The management system prevents high voltages and deep *DOD* and the degradation is slowed to ensure that any replacement of the battery within its expected operation time is not necessary.

4.5.2 PEM electrolyser performance submodel

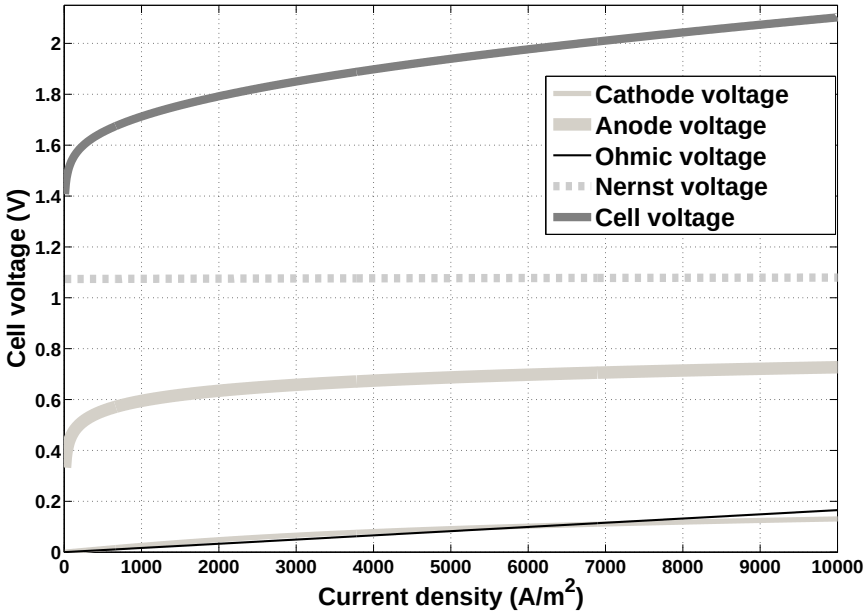

Figure 4.3: PEM electrolyser polarization curve showing the Nernst, cathode, anode and ohmic voltages and the final electrolyser cell voltage.

The PEM electrolyser model took into account activation losses, ohmic losses and temperature variation in the PEM electrolyser cells [153–155] and uniform temperature was assumed. Equation 4.4 shows the voltage of a single electrolyser cell, V_{ele}, considering the Nernst voltage, E_{elen}, the activation voltage in the cathode, $V_{eleactc}$, the activation voltage in the anode, $V_{eleacta}$, ohmic loss, V_{eleohm}, and concentration loss, V_{elecon}. Figure 4.3 shows the polarization curve of the electrolyser. The literature review performed and the details of the PEM electrolyser model are detailed in the Appendix D.

$$V_{ele} = E_{elen} + V_{eleactc} + V_{eleacta} + V_{eleohm} + V_{elecon} \tag{4.4}$$

For any electrolyser rating, the consumption required by the auxiliary equipment or BoP was considered constant and equal to 10% of the nominal electrolyser rating based on the standard state of art. This means that the electrolyser

needs more electricity than a tenth of its rating to start generating H_2. This parameter together with modelling parameters were checked with the PEM electrolyser manufacturer ITM Power which collaborated with the experimental installation presented in Chapter 7. The theoretical PEM electrolyser model work was presented and used in two previous works [76, 138].

4.5.3 Hot water performance submodel

This model is based on the thermodynamic behaviour of a hot water tank when considering uniform temperature (perfect mixed) across the tank. The water tank was defined by the following parameters:

- Tank capacity m_{Wt} (kg)
- External area of the tank A_{Wt} (m^2)
- Heat loss coefficient U_{Wt} ($W/m^2\dot{K}$)
- Control of the tank: maximum temperature, T_{Wtmax} (K), and minimum temperature, T_{Wtmin} (K). The minimum temperature is given by the application.

The amount of water stored by the tank, m_{Wt} (kg), is the optimization variable and therefore it will be varied as explained in Section 5.1. The external area of the tank depends on the volume of the tank which is a function of the capacity. Real water tank data was selected for this variable. Finally, the heat loss coefficient was taken from a well insulated tank integrated in a solar heating and cooling installation and it was equal to 0.548 $W/(m^2 \cdot K)$ [141].

Hot water tank storage in a single home was used for the baseline scenario due to its current use in the UK. It will be connected with a PV array of a single home to supply DHW using electricity. As a consequence, the temperature of the tank, T_{Wt} (K), was controlled between 40 °C and 60 °C. Equation 4.5 shows the equation which governs the performance of the tank. Q_{in} (W) and Q_{out} (W) refer to the inlet heat flow generated by the electricity from the PV array and the outlet heat flows to the DHW demand load respectively. Finally, c_{H2O} (4180 J/(kg·K)), refers to the specific heat of the water and, T_{room}, is the temperature of the room where the tank is based. In shake of the simplicity, it has been considered a constant temperature equal to 15 °C.

$$\Delta T_{Wt} = \frac{(Q_{in} - Q_{out})}{m_{H2O} \times c} - \frac{U_{Wt} \times A_{Wt} \times (T_{Wt} - T_{room})}{m_{H2O} \times c_{H2O}} \tag{4.5}$$

Additionally, a PV controller system should be installed in order to divert any surplus PV generation into the immersion heater placed in the tank. There currently are several products in the market which integrate the control and the electrical connections such as the ImmerSun® , EMMA® and the Optimmersion®. In

shake of the simplicity, the thermodynamic behaviour of the water tank depending on the PV supply was only considered in the analysis.

4.6 Inverter modeling

ES systems need electronic components to deliver and absorb the electricity that they manage. Assuring the quality of the electricity supplied meets the networks standards is really important and this is achieved by the use of power converters and inverters. Battery and H_2 technologies are based on electrochemical reactions using DC electricity. LS requires an AC/DC converter for charging the CES system and a DC/AC inverter for the discharge. Same configuration was suggested in this work for PVts because CES systems were linked to several PV installations in the community. This configuration is schematically represented in Figure 4.4. A bidirectional inverter performs the DC/AC and the AC/DC conversion for the charge and discharge respectively for battery technology. The electrolyser only requires an AC/DC converter due to the fact that the inverter is integrated in the PEMFC system [138].

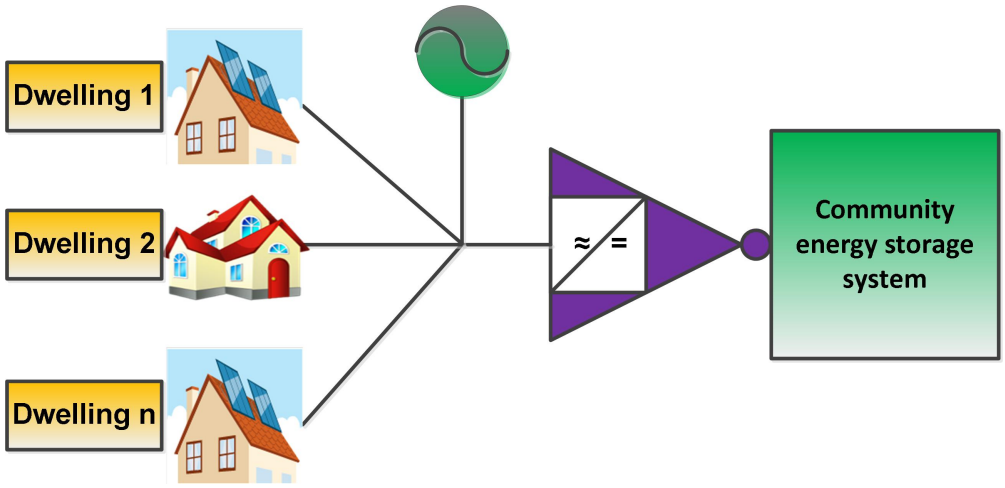

Figure 4.4: Schematic representation of the bidirectional inverter connected to a battery system. Same configuration was used with H_2 technology when using an AC/DC converter instead of a bidirectional inverter.

4.6.1 Battery inverter rating

The rating of the inverter is a key parameter for understanding the performance results as discussed in Chapter 6. The objective of any CES system is not meeting the maximum peak demand load of the community. On the contrary, smoothing the maximum peak load should be accomplished. Additionally, the inverter efficiency depends on the load factor as shown in Figure 4.5 [103]. According to this figure, the inverter efficiency sharply falls when the load factor is less than 20%.

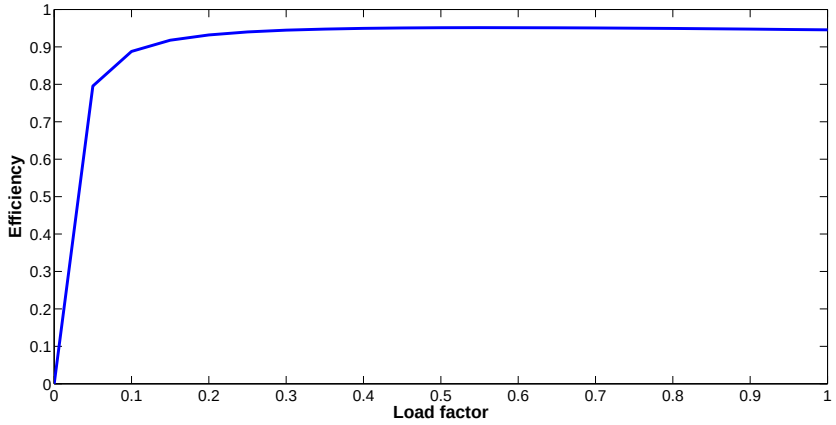

Figure 4.5: Efficiency of the converters and inverters utilised in this work as a function of the load factor.

As it can be seen in Figure 3.7, the ratio between the minimum and the maximum demand load is sometimes lower than 0.2, especially for smaller communities due to the random nature of the different demand loads.

The inverter rating fixes how much power is absorbed (and discharged) by the battery but also affects its round trip efficiency. The optimum inverter rating is a trade-off among the battery charge/discharge capability, round trip efficiency and capital cost. The *LCOES* defined in Equation 4.14 is a parameter which accounts for these three variables. In order to select the inverter rating for any battery system, three different ratings were compared: equal to the maximum demand load (22.6 kW for the 10 home community), equal to half the maximum demand load (11.3 kW for the 10 home community) and a rating which makes sure the load factor of the inverter is higher than 20% with percentile equal to 95% (5.2 kW for the 10 home community). Figure 4.6 shows the *LCOES* as a function of the size of the community for these three inverter ratings. Finally, an inverter rating equal to half the maximum load was selected because it obtained *LCOES* values on the range of the lower rating but the impact of the CES system in the community is much larger i.e. the larger inverter rating allows the CES system to shift more generation or demand depending on the application. However, using an inverter rating higher than 50% of the maximum demand load reduces the efficiency due to the random nature of the demand (according to Figure 4.5) and increases the cost (as seen in Figure 4.6). Finally, Figure 4.7 shows the inverter rating as a function of the size of the community for different scenarios defined in Chapter 5 and analysed in Chapter 6.

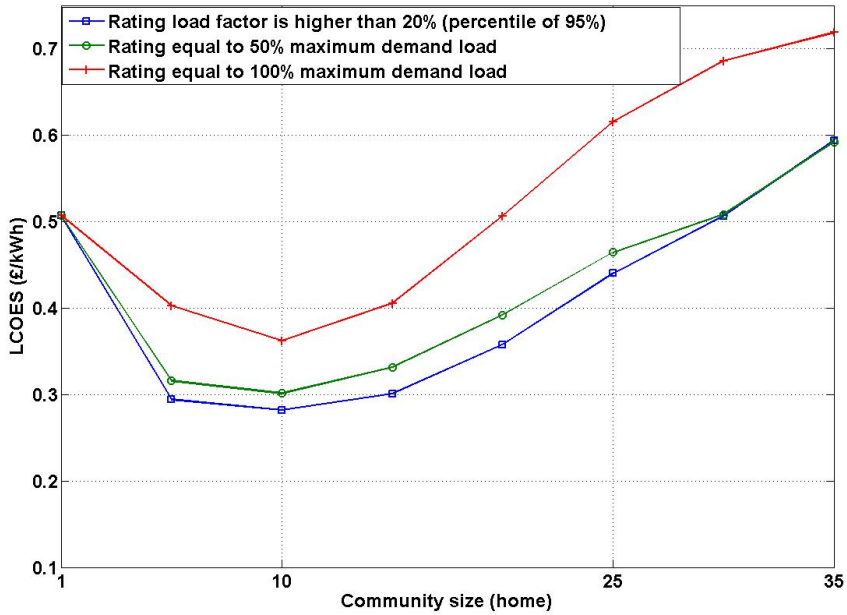

Figure 4.6: Levelised cost of ES for Li-ion battery when performing PV energy time-shift as a function of the size of the community for different inverter ratings.

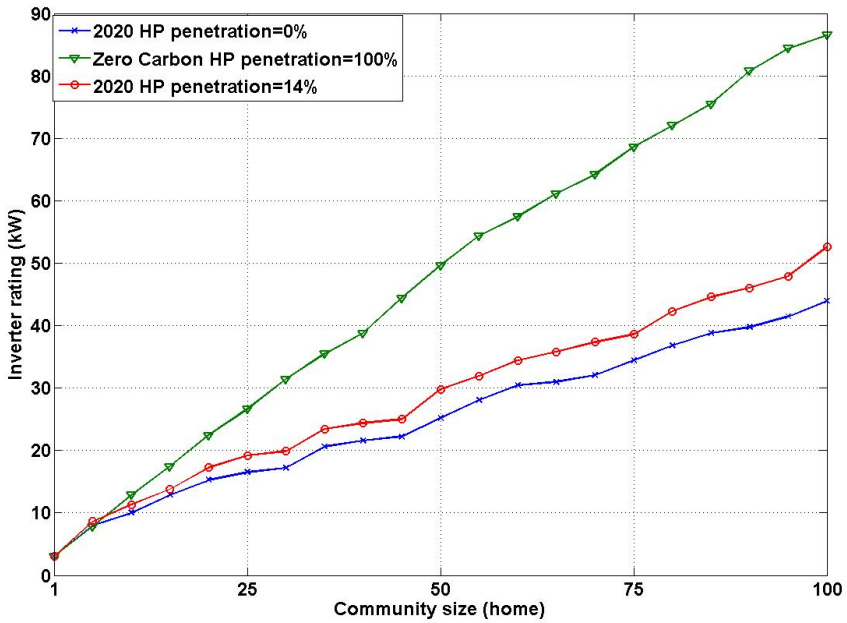

Figure 4.7: Inverter rating (equal to half the maximum demand) as a function of the size of the community depending on the scenario.

4.6.2 PEM electrolyser converter rating

An electrolyser uses an AC/DC converter to generate H_2. From a technical and economic point of view, the rating of the converter is equal to the rating of the electrolyser stack in all electrolysers including the one in the H-CES at the University of Nottingham [156]. The electrolyser converter was also characterized by the same efficiency curve represented in Figure 4.5. Likewise, Figure 4.4 also applies for H_2 storage when considering an AC/DC converter instead of a bidirectional inverter.

4.7 Durability submodels

The durability of the CES system is limited by several performance and environmental factors for any ES technology. Therefore, quantifying the durability depending on the performance is necessary in order to assess the CES economic benefits. Wear factors are those which deteriorate the performance characteristics such as the effective battery capacity and round trip efficiency. Wear factors also end up reducing the durability of the ES system.

4.7.1 Lead acid and lithium-ion battery life submodels

Battery durability submodels for PbA and Li-ion are discussed in the same section because same principles apply and the same submodel was used for both technologies. Cherif et al. determined that the battery capacity is the factor which is most affected by the life conditions [157]. Another parameter which is affected by the battery wear is the resistance of the battery. This was considered by Braun et al. who used a formula to relate the internal resistance with the state of health (SOH) of the battery for Li-ion technology using confidential parameters from Saft [105]. The SOH is defined as the fraction of allowable performance degradation remaining before the end of the life, (when the SOH has been reduce to zero). It was assumed that a fresh Li-ion battery offers an efficiency of 97.4% (when discharging with a current of C/2 A and the SOC varied from 0.8 to 0.2 at a room temperature equal to 25 °C). They argued that the resistance and the losses as a result doubled by the end of the life (efficiency equal to 94.1%). Due to the limited impact of the internal resistance, its variation was not considered in this study. Therefore, the battery wear was represented by the capacity reduction for PbA and Li-ion batteries in this work.

Calendar losses

A battery deteriorates as a result of the number of cycles, the DOD, the temperature and the environment where it is operating. Typically, these factors are grouped in the literature as calendar losses (when the battery does not operate)

and cycles losses (when it does) [151]. The battery temperature plays an important role in the calendar losses and the effect has been modeled using an Arrhenius formula for Li-ion technology [151]. This approach was utilised in this work for Li-ion technology.

Calendar losses have not been considered for PbA technology in the literature because cycle losses are more important. However, the durability of PbA batteries continues improving and according to technical data supplied by Solom, new PbA batteries can last up to 20 years. It was argued that the traditional floating mode operation together with new battery management strategies reduce the impact of the *DOD*. As a consequence of the reduction of the impact of the cycle losses, calendar losses become relatively more important. This is the reason why calendar losses for PbA battery were also considered in this work. However, modeling the calendar losses as a function of the environmental parameters and the chemistry was out of the scope of this work. A linear relationship between the capacity loss with the maximum battery life (years) was chosen. This means that even if a battery is not used, the battery capacity reduces and the battery would have to be finally disposed when reaching a specified minimum capacity.

Regarding the temperature effect, it was assumed this parameter is controlled by the management system minimizing its effect. This assumption was also considered in a previous work about battery life prediction models based on experimental results [152]. This decision reduced the computational heaviness of the final models.

Cycle losses

Regarding the cycle losses, the number of cycles and the *DOD* were considered by the wear model. A dimensionless parameter, Z, which quantifies the loss of capacity per *EFC* which is discharged was utilised. The model was suggested by Riffoneau et al. when they investigated the optimum algorithm for battery scheduling for PVts [103]. Z is a linear life coefficient characteristic of any battery technology. For any discharge, the reduction of the capacity, ΔC, was assumed linear to ΔSOC (and the initial capacity, C_{nom}) within the SOC range given in Table 4.1 as shown in Equation 4.6.

$$\Delta C = Z \times C_{nom} \times \Delta SOC \tag{4.6}$$

Battery end of life

The state of health, (SOH), of the battery has been suggested in several works to measure the continuous loss of capacity of the battery (in parallelism with the

Table 4.2: *EFC*, cycle dimensionless life parameter (Z) and calendar losses (monthly percentage of capacity reduction) depending on the battery technology and the reference year.

	Parameter	2012	2020	Zero carbon
	EFC	1000	1250	1500
PbA	$\boldsymbol{Z}$	$3{\cdot}10^{-4}$	$2{\cdot}10^{-4}$	$1{\cdot}10^{-4}$
	Calendar losses (%/month)	0.17	0.15	0.12
	EFC	2400	3000	3600
Li-ion	$\boldsymbol{Z}$	$2.4{\cdot}10^{-4}$	$1.25{\cdot}10^{-4}$	$0.83{\cdot}10^{-4}$
	Calendar losses (%/month)	0.10	0.09	0.08

SOC)) [103, 105]. Although there are different criteria, the capacity fade (or capacity reduction due to the performance) is also used to estimate the end of the life.

Typically, a percentage of the initial capacity is used for assessing the end of the life, 80% being used before [105]. This value is usually chosen because the manufacturers do not guaranty the battery performance under this value. This is not a physical constraint as batteries still operate under 80% of their nominal capacity, but the performance and behaviour under this limit is not well characterized. Taking into account that batteries still work when the capacity is lower than 80% of the initial capacity, a battery reduction of 70% was considered to estimate the durability of the battery in this work.

A literature review was performed in order to quantify the maximum *EFC* that PbA and Li-ion batteries can achieve as shown in Appendix B. According to data collected, 1000 EFC and 2400 EFC were selected as representative of the current state for PbA and Li-ion technologies when considering ΔSOC of 0.5 and 0.6 respectively in 2012 [158]. Additionally, the data presented in Table B.1 were used to quantify the improvement on the cycle capability of both battery technologies for 2020 and the zero carbon year as discussed in Section 5.4. The data used in this thesis is presented in Table 4.2. This table shows the *EFC* selected for each technology as a function of the reference year and the equivalent dimensionless parameter Z used by the durability model. It also shows the calendar losses (capacity reduction) when the battery is not used.

The *EFC* shown in Table 4.2 refer to the discharge would be performed for any battery system throughout the whole life if only cycle losses play a role (battery continuously cycling). However, the battery is not always cycling and calendar losses also impact the performance reducing the durability. As a consequence, the real *EFC* performed by the batteries are lower than the maximum *EFC* used as

input data.

4.7.2 PEM electrolyser durability submodel

Durability data is not available for PEM electrolysers and therefore data of PEMFC systems were utilised when considering that materials and principles utilised in both technologies are similar. The degradation of FC systems and electrolysers responds to electrochemical processes (oxidation and reduction, transportation of cations and electricity conduction) as explained in Appendix D. These processes are affected by the factors such as the pressure balance between the cathode and the anode, temperature and quality of the deionised water.

The PEMFC stack utilised in the H-CES system presented in Chapter 7 was manufactured by Ballard and it is able to perform up to 1650 cycles. A review of current FC technology for small scale residential applications concluded that the average life of PEMFC systems and SOFC systems is 4 years and 3 years respectively [134].

The electrolyser degradation increases the voltage necessary to perform the electrolysis reducing the electrolyser efficiency over its lifetime. Degradation also increases the heat generated during the process. It was found that the voltage increase is greater in the first 2000 hours of operation ranging between 20 and 50 μV/h and then reduces to less than 3 μV/h [156]. In a different experimental research, the degradation rate of a PEM electrolyser was constant and equal to 1.5 μV/h [159].

In this work, the wear model of the PEM electrolyser comprises a degradation rate (V/cell) per start-up and a degradation rate as a function of the number of operational hours. The durability model of the electrolyser was based on the targets published by different organisation and research councils. A literature review was performed for this purpose and values are presented in Appendix C. According to this literature review, 20000 h, 40000 h and 60000 h were selected as maximum operation hours for the electrolyser in 2012, 2020 and the zero carbon year respectively.

4.7.3 Hot water tank and PV controller durability submodel

Two manufacturers of hot water tanks were contacted for assessing the life of a water tank: Mcdonald Engineers and Grant. According to them, hot water tanks can last 20 years or more when properly maintained (a typical product guarantee is for 5 years). In this work, 20 years were selected as replacement of the tank.

Regarding the PV controller, the company ImmerSUN® was contacted. In this case, the PV controller is called ImmerSUN® and it is guaranteed for three years. In terms of life expectancy, the components used in the unit are similar to the components found in inverters and other electronic devices, all of which the manufacturers publish a life expectancy of between 15 and 20 years. The company therefore considers that the ImmerSUN® should match the life expectancy of these electronic devices. In this work, 20 years were also considered for the PV controller.

4.8 CES performance parameters

The parameters which were used to quantify the performance of CES systems are presented below. These parameters depend on the application and the technology as quantified in Chapter 6.

4.8.1 Battery technology performance parameters

Equivalent full cycles

The *EFC* are the number of full discharges (ΔSOC=1) that a battery system performs throughout its life. In reality, the management system prevents the battery to be fully charged or discharged on a cycle. However, the *EFC* is widely utilised to quantify how well the asset (the battery) in the battery industry. The calculation is given by the equation 4.7 in which the life, *Life* (year), is the number of years the battery system is operational according to the durability model presented in Section 4.7.1, E_{dis} (kWh/year) is the annual discharge during those years and C_{nom} is the initial battery capacity.

$$EFC = \frac{E_{dis} \times Life}{C_{nom}} \tag{4.7}$$

Round trip efficiency

The round trip efficiency η is defined as the ratio between the annual electricity discharged by the battery system, E_{dis} (kWh/year), and the annual electricity charged into the battery system, E_{char} (kWh/year), taking into account the efficiency of the electronics (converter and inverters) as modeled in Section 4.6. Therefore, the seasonal value of the round trip efficiency is shown in Chapter 6 according to Equation 4.8:

$$\eta = \frac{E_{dis}}{E_{char}} \tag{4.8}$$

4.8.2 Hydrogen technology performance parameters

For H_2 technology, the capacity factor, the electrolyser efficiency, the H_2 ratio and the tank size were selected as key performance parameters.

Capacity factor

The capacity factor, C_{factor}, is a parameter which is used to quantify how much an asset performs throughout the year. It is typically used with RE technologies because the operational hours depend on the location. It is defined as the ratio of the operational hours per year, H_{year} (h), divided by the number of hours in a year (86400 h) as shown in the Equation 4.9:

$$C_{factor} = \frac{H_{year}}{86400} \tag{4.9}$$

Electrolyser efficiency

The electrolyser efficiency, η_{ele}, was obtained using the Equation 4.8 and it considers the losses of the stack and the BoP when generating H_2 throughout the year. The seasonal electrolyser efficiency was obtained by using Equation 4.8 when considering that the annual discharge, E_{dis} (kWh/year), is the annual electrolyser yield.

Hydrogen ratio

The H_2 ratio, H_{2ratio}, is the ratio between the annual hydrogen yield of the electrolyser, m_{ele} (kg/year), and the annual H_2 mass consumed by the PEMFC system, m_{PEMFC} (kg/year), as shown in Equation 4.11:

$$H_{2ratio} = \frac{m_{ele}}{m_{PEMFC}} \tag{4.10}$$

Tank size

The size of the H_2 storage tank, T_{size} (kg), is a dependent variable, the electrolyser rating (kW) and the PEMFC system rating (kW) being independent variables in this work. The H_2 mass stored in the tank depends on the balance between the electrolyser generation and the consumption from the PEMFC system and the H_2 mass in the tank was obtained according to this balance. The tank size was obtained from the maximum storage requirement i.e. the moment of the year in which the amount of H_2 stored is larger. The maximization is shown in Equation 4.11 in which m_{H2} (kg) refers to the H_2 mass in the tank for any minute of the year.

$$T_{size}(kg) = max(m_{H2}) \tag{4.11}$$

4.8.3 Community performance parameters

Two parameters were defined in order to quantify the impact of a CES system in the community in relation to the community PV generation and the demand: the PV ratio and the demand ratio.

PV generation supplied to the CES system

The PV_{ES} is the fraction of the total PV generation, E_{PV}(kWh/year), which is supplied to the CES system, E_{PVES} (kWh/year), as shown in Equation 4.12.

$$PV_{ES} = \frac{E_{PVES}}{E_{PV}} \tag{4.12}$$

Demand load met by the CES system

The D_{ES} is the fraction of the demand met by a CES system as shown in Equation 4.13. E_{dis} (kWh/year) is the total annual energy discharge for the CES system and E_d (kWh/year) is the annual energy demand for the community.

$$D_{ES} = \frac{E_{dis}}{E_d} \tag{4.13}$$

Depending on the scenarios, the annual demand and the discharge include different types of domestic demand loads. For example, if HPs are considered in the analysis, the demand considers the community global electrical consumption which is the addition of the electrical demand load and the electrical consumption of the HPs.

4.9 Economic submodel

The economic submodel assesses the economic performance of CES when performing one or more applications. It obtains three different economic parameters which can be used to evaluate the attractiveness of CES: the levelised cost of energy storage, the levelised value of energy storage and the internal rate of return. The calculation of three complementary economic parameters is another interest point of this work in comparison with other works in the literature which only calculated the internal rate of return [105] or the net present value [56].

4.9.1 Levelised cost of energy storage

The levelised cost of energy (£/kWh) is a parameter which has been widely used to compare the total cost associated with the electricity generation of different generation technologies throughout the life [160]. In this work, the same concept was utilised to evaluate the cost of ES. The levelised cost of energy storage, ($LCOES$) (£/kWh), compares the cost associated with the development of an application

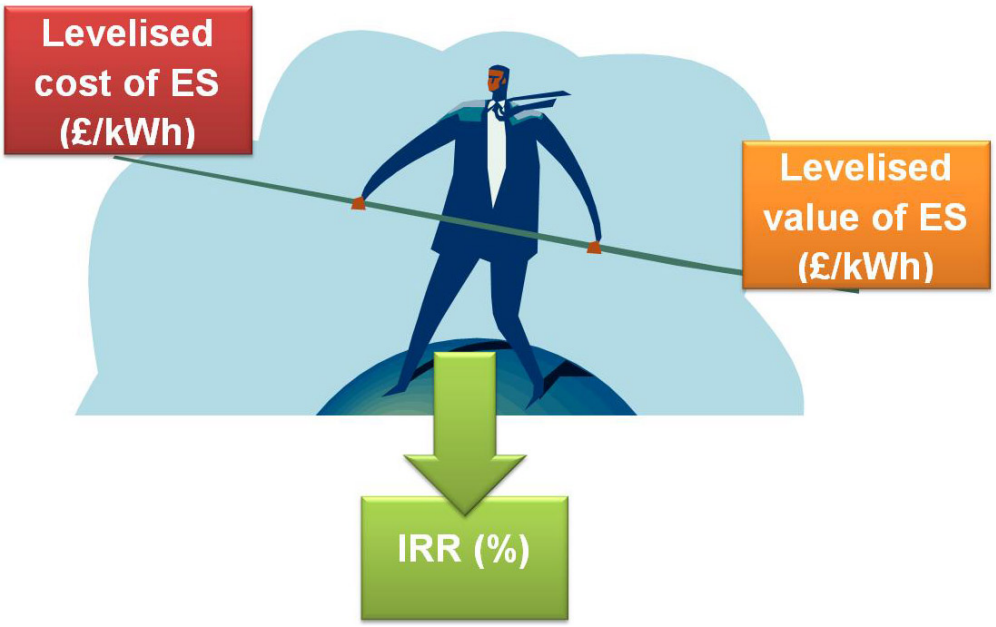

Figure 4.8: Schematic representation of the balance between the *LVOES* and the *LCOES* which determines the value of the *IRR*. The *LVOES* is higher than the *LCOES* when the *IRR* is higher than the discount rate assumed in the economic analysis (10%) and vice versa.

throughout the life of the system. It is calculated as shown in Equation 4.14. *TLCC* (£) refers to the total levelised cost (initial cost and maintenance cost) throughout the life of the project considering the value of money with time. *EF* (kWh) refers to the energy flow related the performance of an ES application by the CES system. A discount rate, r, equal to 0.1 was utilised after discussing this value with one of the sponsors of this project (E.ON), this value also being used in previous ES evaluations [56, 99]. The discount rate is the rate used to calculate the present value of cash flows in the valuation of a project and includes the time value of money, the risk associated with the project and the inflation.

$$LCOES = \frac{TLCC}{\sum_{k=0}^{n} \frac{EF}{(1+r)^k}} \tag{4.14}$$

The *LCOES* was used with the different applications discussed in this thesis. When applied to PVts, this parameter quantifies the cost of meeting the demand load by using surplus PV energy stored from the PV arrays (£/kWh). Likewise, it quantifies the cost of meeting the demand load by using energy stored from the grid for LS. The cost associated with the charge can be obtained when multiplying the *LCOES* calculated here by the round trip efficiency. Therefore, the *LCOES* is an economic parameter which is related to the applications performed by CES systems. In the case of H_2, two different *LCOES* were calculated according to the electricity and heat generation.

4.9.2 Levelised value of energy storage

The levelised value of energy storage, *LVOES* (£/kWh), quantifies the CES value considering the revenue throughout the life. The value is quantified when considering the future cash flows (CF_0, CF_1,..., CF_n) and the time value of money.

The *LVOES* states the money obtained per unit of discharge (kWh) when performing one or several applications 4.15. Every application has a *LVOES* associated with it. When any CES system performs several applications, an aggregated *LVOES* was calculated. This means that the aggregated *LVOES* of a CES system performing two applications weighs up the different revenues and energy flows associated with them. For example, a CES system performing PVts can increase its value when avoiding power curtailment. In the case of H_2, the *LVOES* was calculated according to energy content of H_2 using its high heating value (HHV).

$$LVOES = \frac{\sum_{k=1}^{n} \frac{CF}{(1+r)^k}}{\sum_{k=0}^{n} \frac{EF}{(1+r)^k}} \tag{4.15}$$

4.9.3 The internal rate of return

The *IRR* of an investment that has a series of future cash flows (CF_0, CF_1,..., CF_n) is the rate that sets the net present value of the cash flows to zero as defined in Equation 4.16 [160]. The *IRR* is a measurement of the profitability of an investment and it allows the comparison of different project alternatives. The *IRR* can be used by any investor or stakeholder to evaluate the attractiveness of CES when performing end user applications and compare it with other energy (or financial) investments according to the discount rate selected (10%). The *IRR* is directly associated with the CES system and not with the application but the *IRR* of a CES system changes when it performs different applications.

$$0 = NPV = \sum_{k=0}^{n} \frac{CF_i}{(1+IRR)^k} \tag{4.16}$$

The *IRR* is higher than the interest rate selected (10%) when the *LVOES* is higher than the *LCOES* and vice versa. Figure 4.8 schematically represents the balance between the *LVOES* and the *LCOES* to determine the *IRR*.

The economic model used the results obtained by the performance and durability submodels as input data together with the CES investment cost. The next section details how the cost of a CES system was obtained.

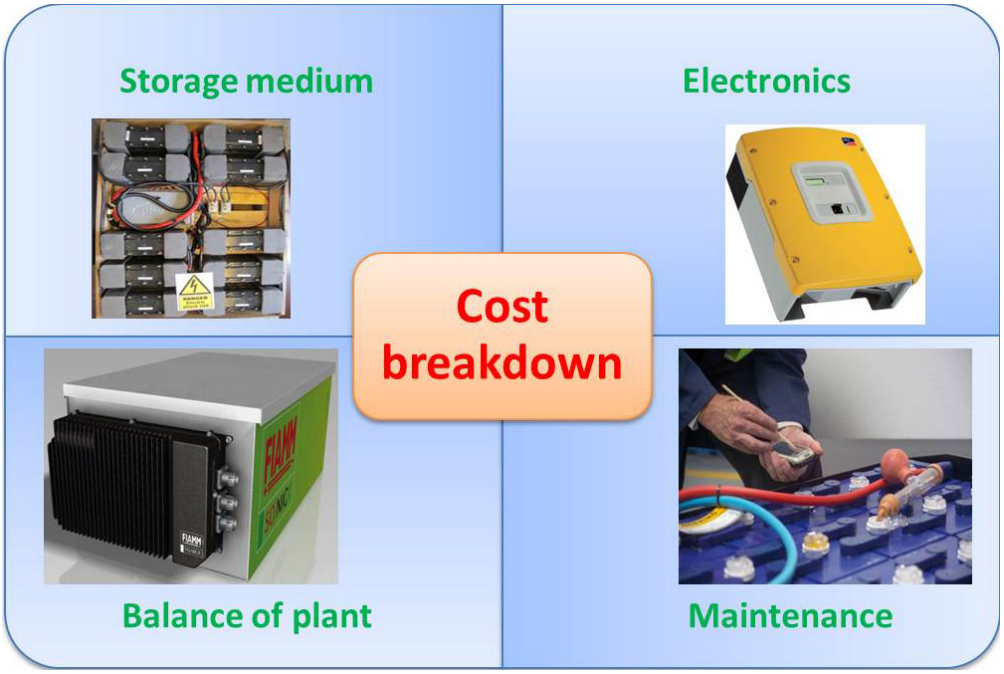

Figure 4.9: Breakdown of the CES cost in four different costs as used in this study.

4.9.4 CES cost

The investment cost is one of the key input data to assess the economic benefits for CES. Together with the different annualized revenues (cash flows) obtained from the performance of one or several applications, the total cost determines the *IRR* and the *LCOES*. The CES cost is the addition of four different costs [99] as represented in Figure 4.9: the cost of the storage medium, the electronics cost, the BoP cost and the maintenance cost. The consideration of the total cost of CES systems made economic results more accurate, opposed to other works which only reflect the chemistry cost [73].

Storage medium cost

The storage medium refers to the materials which are utilised to store the energy for battery technology or to generate H_2 and store it in the case of H_2 storage. The relative cost of the storage medium, $cost_{sm}$, refers to the battery cells stack (£/kWh) for battery technology, electrolyser cell stack (£/kW) and the H_2 tank (£/kg) for H_2 technology. For battery and H_2 technology, the relative cost of the storage medium values selected for the different reference years are presented in Section 5.6.4 based on the literature review presented in Appendixes B and C respectively. Many different currencies were used in the literature but int his work the cost is expressed in £/kWh, £/kW and £/kg for battery technology, the H_2 electrolyser and H_2 tank respectively.

An approximation to the reduction of the cost with the size was utilised by

Table 4.3: Water tank price as a function of the capacity utilised in this work.

Capacity (l)	100	200	300	400	500	600	700	800	900	1000
Price (£)	670	1230	1540	1800	2640	3230	3540	3860	4470	5090

means of a power relationship in order to reflect the fact that the absolute cost of the storage medium, $Cost_{sm}$ (£), is not linear with the size. The absolute cost of the storage medium was assumed to be linear with the capacity up to a limit storage capacity, C_l (kWh or kW for a battery and electrolyser). For any storage capacity larger than C_l, the cost of the storage medium, was obtained from Equation 4.17 in which 0.7 is the power factor selected to demonstrate the manufacturing economy of scale [161]. C_l was assumed to be 100 kWh battery technology and 10 kW for an electrolyser [162].

$$Cost_{sm} = ((\frac{Size}{Size_l})^{0.7}) \times Size_l \times cost_{sm} \tag{4.17}$$

In the case of a hot water tank, the two companies contacted for the durability (Mcdonald Engineers and Grant) also supplied initial cost data shown in Table 4.3. Specifically, the cost of cooper unvented cylinders was supplied as a function of the amount of the capacity. These cost data is not representative of the majority of hot water tanks previously installed in the UK which are made of cooper and vented and much cheaper as a consequence. Two different situations will be investigated for the single home scenario: the house already has a water tank or it is necessary to buy a water tank.

The cost of the storage medium is the most important of the four different costs which comprises the CES total cost (around 60% in the case of PbA batteries and higher for Li-ion batteries). From a financial point of view, it has been assumed that this cost is paid at the beginning of the project in accordance with previous studies [56, 99, 105].

Electronics cost

This is the cost of the electronic and electrical components which facilitate the integration of the CES system into the electrical network as discussed in Section 4.6. The cost of the battery inverter and the electrolyser converter was modelled using real data from the manufacturer SMA Solar Technology AG. Figure 4.10 represents the cost of the inverter for this manufacturer. Any inverter with a rating higher than the range showed in Figure 4.10 was obtained using linear interpolation.

Regarding the PV controller which diverts surplus PV generation into the hot water tank, it has been assumed that the cost is equal to £500 based on the current cost of a product in the market, the ImmerSUN®. The electronics cost represents the second most important part of the CES investment (around 30% in the case of PbA batteries and lower for Li-ion batteries). The relative cost of the electronics (£/kW) kept constant with the size in shake of the simplicity. From a financial point of view, it has been assumed that this cost is paid at the beginning of the project [56, 99, 105].

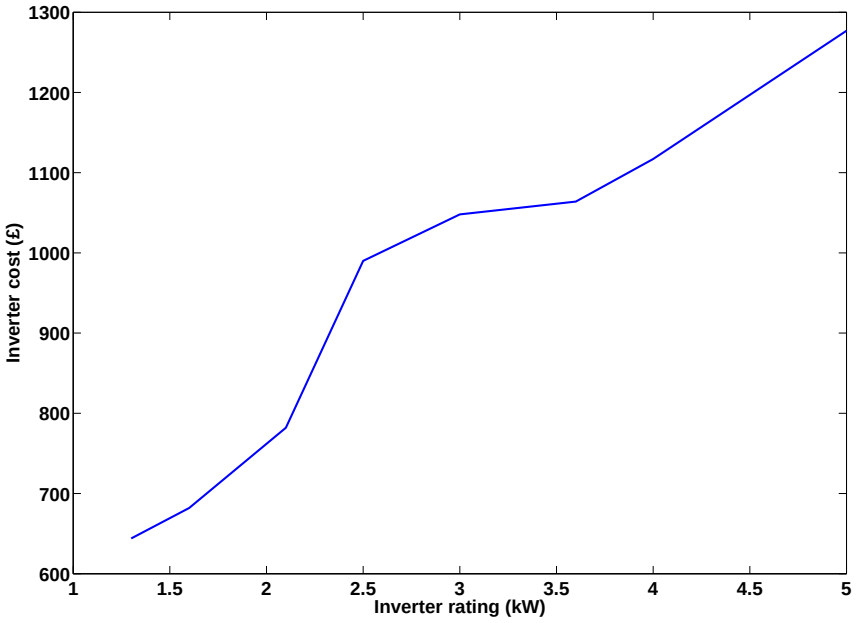

Figure 4.10: Cost of the inverter as a function of the rating as used in this work.

Cost of the balance of plant

In addition to the electronics, a CES system incorporates a management system which controls its performance in addition to other elements such as frame, case, thermal system and monitoring system which guarantee the safe and optimum performance. All these different elements have a cost which was incorporated into a more comprehensive BoP cost. The source for the BoP was the work performed by the DOE in which the BoP was assumed to be 100 $/kW [163]. From a financial point of view, it has been assumed that this cost is also paid at the beginning of the project [56, 99, 105].

Maintenance cost

After some conversations with several manufactures [162], it was suggested that their products only require small checks which are executed on a yearly basis in

terms of schedule maintenance. According to them, these operations only mean the checking of some key parameters like the open circuit voltage for battery technology and the stack voltage for the electrolyser. This is performed either by the manufacturer or a contracted service company on a year basis. Due to the simpleness of the tasks, the maintenance cost was assumed to be applied at the beginning of the project and cover all annual checks performed during the life of the project. The maintenance cost was assumed to be 10 \$/kW [99]. From a financial point of view, it was assumed that this cost is paid at the beginning of the project [56, 99, 105].

4.10 Summary

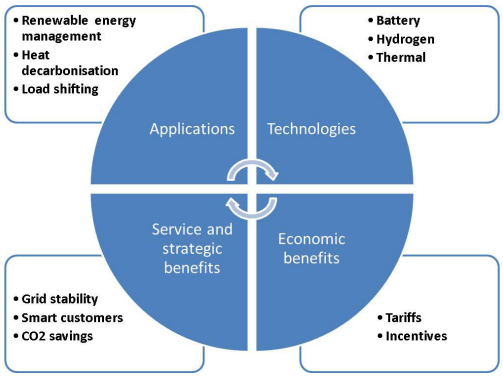

Figure 4.11: Holistic approach followed in this thesis for investigating CES.

Suitable ES technologies for the end user applications were selected in this chapter among those discussed in Chapter 2 according to their suitability to discharge for several hours (for energy applications) and modular size ranging from the kWh to the MWh scale. Specifically, battery technology considering PbA and Li-ion chemistries, H_2 technology (considering PEM electrolysers) and hot water tanks for single homes are the focus of this study. Thermal storage by means of hot water tanks in single homes was the choice due to the current penetration of this technology in the UK with 19.3m dwellings with a water tank in 2006.

In order to obtain accurate values of the cost, value and profitability of CES, a holistic approach using comprehensive models which take into account the performance, durability and cost of different ES technologies were detailed. This holistic approach was based on the same model structure for all the technologies.

After the presentation of the general characteristics of the ES model, specific details about the performance, durability and cost were given depending on the technology. A unique economic submodel was shared by the different technologies. The accuracy of the results obtained by any model strongly depend on the quality

of the input data. As a consequence, a comprehensive literature review was made to select the best data available for the cost and durability of different technologies. These input data are considered for the definition of the reference scenarios and the sensitivity analysis presented in Chapter 5. Chapters 3 and 4 have presented the holistic approach followed in this thesis to investigate CES as schematically represented in Figure 4.11.

Chapter 5

A method for optimising CES

This chapter describes the method and methodology developed to obtain the optimum CES system for end user applications as a function of the size of the community. The optimization method firstly obtains the key performance parameters such as the round trip efficiency and the *EFC* for battery technology and electrolyser efficiency and the capacity ratio for H_2 technology depending on the ES application. Based on these parameters, the cost ($LCOES$), the value ($LVOES$) and the profitability (IRR) are quantified for the ES applications introduced in Chapter 3 and the technologies presented in Chapter 4.

This chapter has the following structure. Firstly, the method followed in this work including the key steps to implement it are presented. Secondly, the algorithms developed to apply the method are explained depending on the application and technology. These algorithms made use of the ES technology models presented in Chapter 4.

Next, the different scenarios which were studied to understand the impact of the UK's decarbonisation roadmap in the optimum CES system are introduced. These scenarios were based on three reference years (2012, 2020 and a hypothetical zero carbon scenario) and made use of the community generation and demand models presented in the second part of Chapter 3. Finally, the parameters which have the greatest impact on the CES performance and economic benefits were identified and a sensitivity analysis was developed in order to tackle the uncertainty associated with them. The sensitivity analysis included the technology cost, technology durability, PV penetration, export bonus and utility prices.

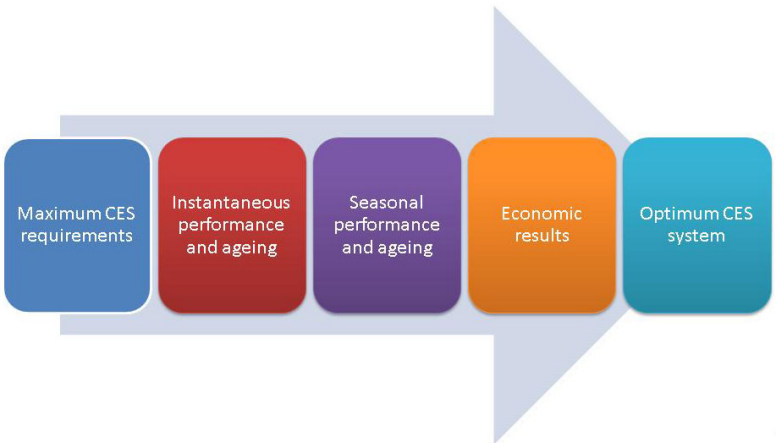

Figure 5.1: Schematic representation of the five main steps which comprise the optimisation method presented and utilised in this work.

5.1 A method for calculating the optimum CES system for end user applications

In order to investigate the optimum CES system for end user applications as a function of the size of the community, a new method was developed to evaluate the cost ($LCOES$), the value ($LVOES$) and the profitability (IRR) of CES systems. The method first obtained the technological performance such as round trip efficiency, EFC and annual discharge of CES systems. The optimum CES system was then calculated as a function of the community size for different key ES performance and economic parameters. This method included five main steps as schematically represented in Figure 5.1. The method developed to investigate the optimum CES system presented in this thesis is novel and adds value to the ES literature because:

- It obtained the CES system which optimized both performance and economic parameters which play a role on the business case. Key parameters which are interesting for different stakeholders such as round trip efficiency, cost, value and profitability were considered.
- Instead of focusing on a single home, it used a community approach to investigate the benefits of the aggregation of demands, PV generation and heat generation on the performance, economic benefits and sizing.
- It focused on different end user applications. The method was tested with PVts, LS and the combination of them.
- It is robust enough to compare four different ES technologies which are suitable for end user applications by using the comprehensive ES models presented in Chapter 4.

- Key parameters such as the round trip efficiency and durability were not assumed constant but calculated according to the application and the CES system.
- A sensitivity analysis was integrated including key ES parameters to tackle the uncertainty of the CES performance and businesses case in the decarbonisation pathway.

5.1.1 Maximum CES requirements

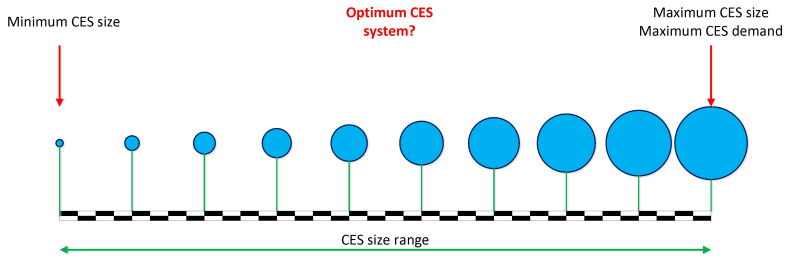

Figure 5.2: Schematic representation of the 10 CES sizes considered by the method to obtain the optimum CES system for any community. The larges CES size was equal to maximum ES requirements. The smallest CES size and the resolution of the CES discretization were a tenth of the maximum size.

The maximum CES size was calculated considering the day of the year in which the ES requirements were the largest depending on the application. Specifically, PV generation and the domestic demand were compared every day in order to quantify the maximum surplus PV generation for PVts. Likewise, the demand which occurred at peak time was quantified on a daily basis in order to determine the maximum peak demand. This was accomplished with two tariffs, Economy 7 and the NETA tariff, introduced in Section 3.5 to quantify the maximum peak demand load requirements. The maximum CES size was obtained to limit the range of sizes which were tested to determine the optimum size.

Once the maximum size was determined, the method searched for the optimum CES system. The optimum CES system was searched between the maximum and the minimum size, the minimum being defined as the tenth part of the maximum. This value was selected because the daily ES requirements were larger than the minimum size for more than 95% of the days. Next, the method varied the CES size between the minimum and the maximum using a size discretization equal to the minimum size. This means that for any scenario, the method tested 10 different sizes (10 nodes). A representation of the CES size discretization in this work is shown in Figure 5.2. As a consequence, all parameters discussed in this work were calculated for ten different CES sizes ranging from the minimum size to the maximum size. This discretization was selected because it offered a size resolution high

enough to show the evolution of the parameters (without markedly steep changes) and it proved the optimum CES system with a reasonable computational time (which could be managed during this study). This was specified after several trials performed with different size steps. Figure 5.3 shows the maximum, minimum and the other eight Li-ion battery capacities tested for each community to determine the optimum battery system depending on the application and the reference year. The results of the application of the first step of the method for H_2 and the combination of applications are presented in Appendix G. The computational time necessary for obtaining the optimum CES system for all the applications, technologies, scenarios and community sizes included in this work was larger than three months and this time was a resource which was managed and optimized during this study.

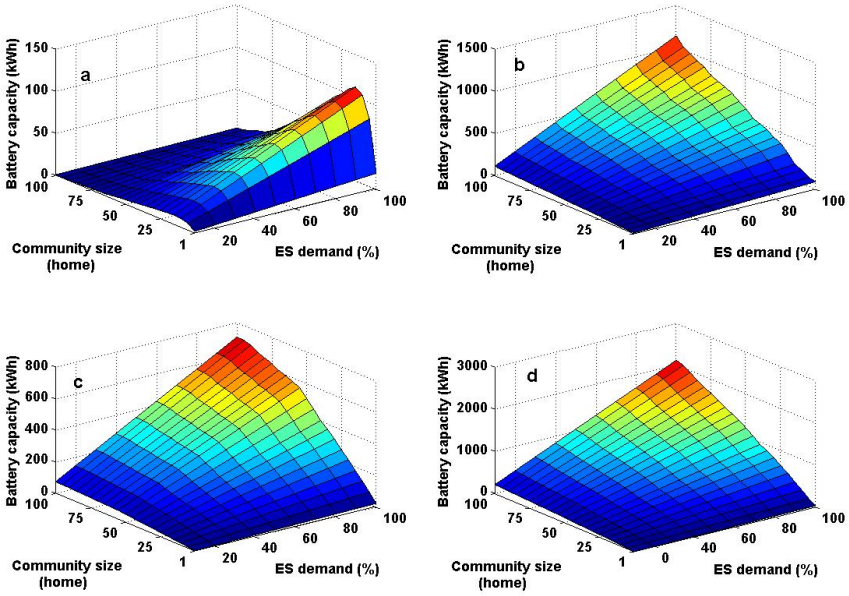

Figure 5.3: Li-ion battery capacity as a percentage of the ES demand for different communities for (a) PVts and (b) LS with Economy 7 in 2020 and (c) PVts and (d) LS with Economy 7 in the zero carbon year.

5.1.2 Performance and ageing

This step of the method also made use of the PV generation and demand load for PVts, and the demand and tariff structure for LS. In this second step, the method tested the 10 CES capacities when performing an end user application for any community using the performance and the durability submodels presented in Sections 4.5 and 4.7 respectively. All the power flows related to the performance such as charge, discharge and the round trip efficiency were calculated throughout

the year using a 1-minute temporal resolution. At the same time, the durability submodels were used to calculate the ageing based on the operation (or no operation) of the CES system.

5.1.3 Seasonal performance and ageing

Subsequently, the power flows were converted into daily and seasonal (annual) energy flows when aggregating the results. The simulation period was set to a whole year from the 1^{st} of January to the 31^{st} of December in order to obtain detailed seasonal results.

5.1.4 Economic assessment

Finally, the annual ageing of the CES system is used to determine the life of the CES system. Then, the economic submodel obtained the *LCOES*, the *LVOES* and the *IRR* for any community presented in Section 4.9 based on the annual energy flows and the life of the CES system. The CES initial investment according to the structure represented in Figure 4.9 was included at this step.

5.1.5 Optimum CES system

Once the method has been applied to all the different community sizes, the optimum performance and economic parameters were obtained together with the CES system which achieved them. This information can be utilized by the different stakeholders and decision makers to select the ES technology and size for any community. The method obtains the CES system which optimizes any performance and economic parameter defined in Sections 4.8 and 4.9 respectively. The CES systems which minimised the *LCOES* are shown in Chapter 6. The CES systems which optimised different performance and economic parameters depending on the technology and the application are shown in Appendix J.

The method presented in Figure 5.1 was utilised for PVts, LS and the combination of them. The different characteristics of battery technology (short-term and/or mid-term ES) and H_2 storage (mid-term and/or long-term ES) and the different philosophy behind PVts and LS made that the first step (calculation of the maximum size) and the second step (calculation of the power flows) of the method depended on the application and technology. These differences will be schematically presented in the next part of this chapter by different flowcharts which show the core ideas for obtaining the maximum CES requirements and the performance (with a 1 minute temporal resolution) for determining the optimum CES system.

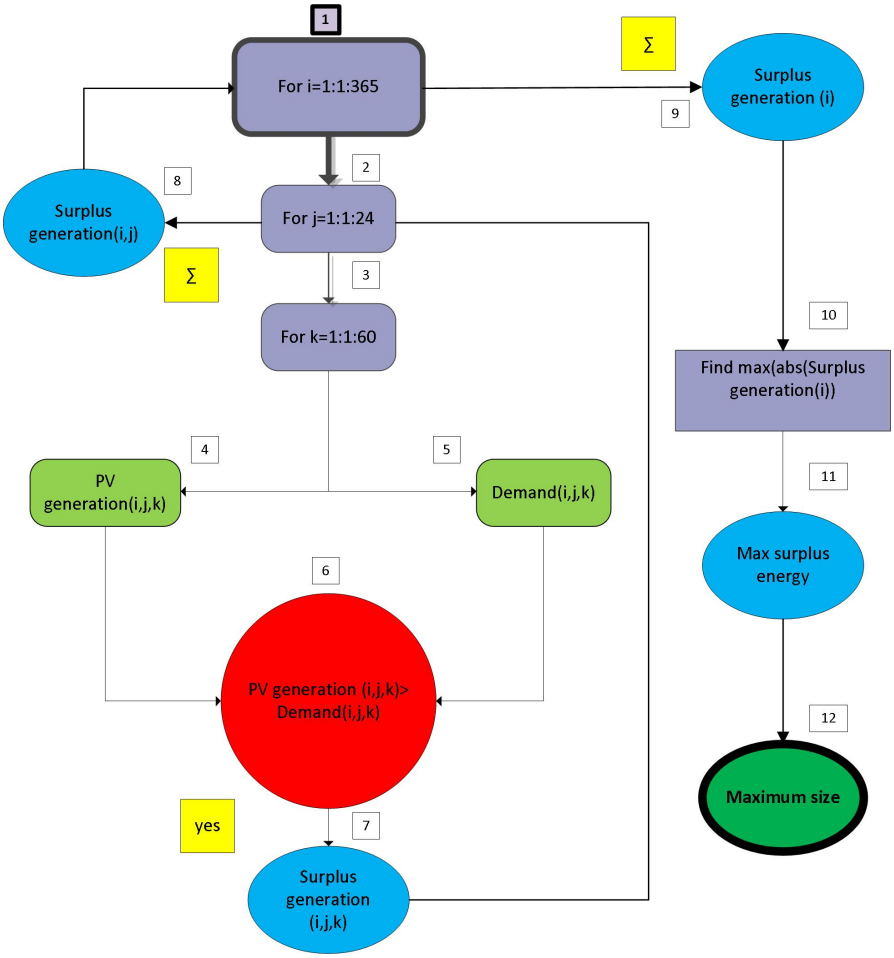

Figure 5.4: Flow chart representing the algorithm which was utilised to obtain the maximum capacity of a battery system when performing PVts using 1 minute (loop variable k) data for every day (loop variable i) of the year. The flowchart sequence follows the number sequence in the boxes. The sum symbol represents the aggregation of results to obtain hourly values (from 1 minute data) or daily values (from hourly data).

5.2 PV energy time-shift

Battery systems should not store electricity for the day after on a daily basis. The fact that the rating power of the battery (kW) is directly proportional to the capacity (kWh) does not make the investment attractive for long term ES (more than 1 day). This approach was followed in this work and the largest battery system was defined by the maximum daily PV surplus electricity (kWh) when considering the balance between the PV generation and the demand throughout the year.

The flowchart represented in Figure 5.4 gives the algorithm used to determine the maximum ES capacity. This algorithm compared the PV generation with the demand every minute of every day throughout the year. The index i refers to any day of the year; the index j refers to any hour of a day; and the index k to

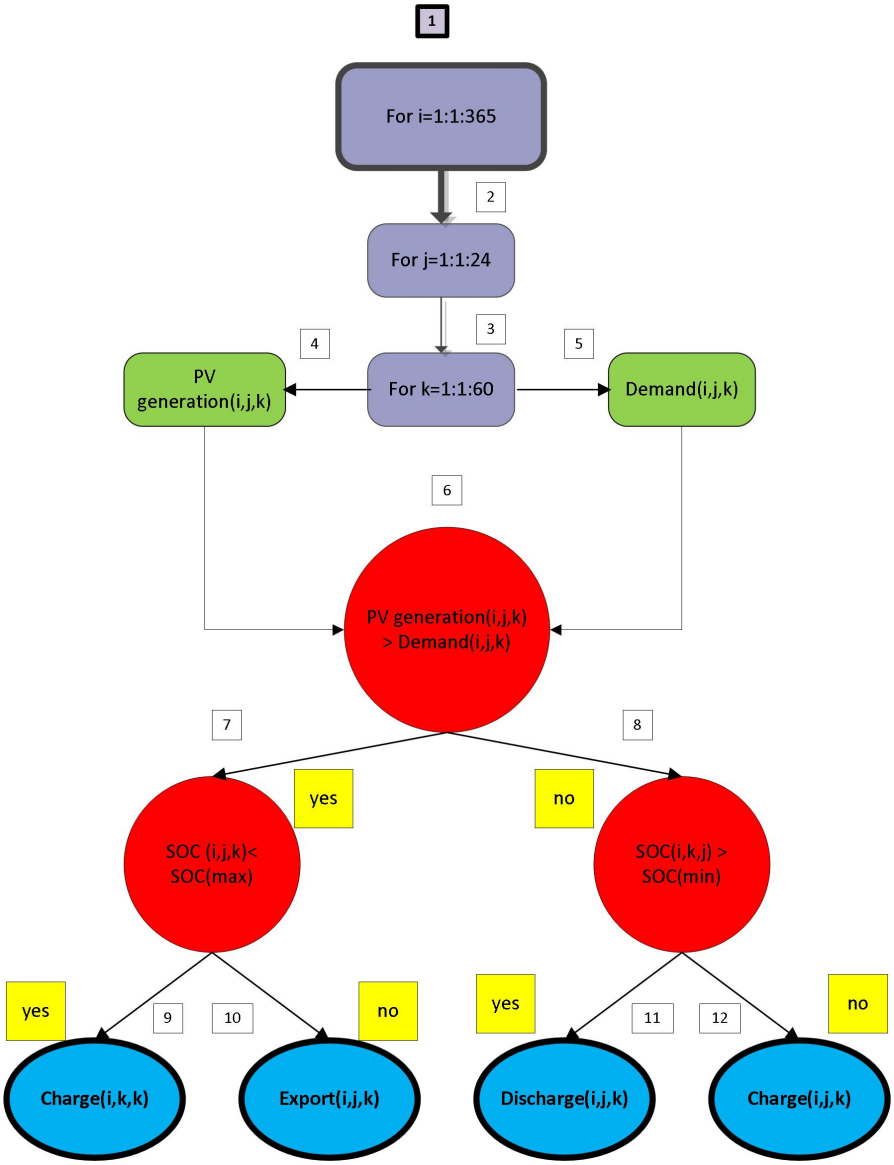

Figure 5.5: Flow chart representing the algorithm which was utilised to obtain the performance of a battery system when performing PVts using 1 minute (loop variable k) data for every day (loop variable i) of the year. The flowchart sequence follows the number sequence in the boxes. The sum symbol represents the aggregation of results to obtain the daily values from hourly data.

any minute of an hour. This algorithm obtained the surplus PV energy with a temporal resolution of 1 minute. Then, the surplus PV energy was aggregated over the 24 hours of a day to obtain the daily surplus energy. The largest battery capacity (kWh) was equal to the maximum surplus daily energy when considering all the days of the year (kWh/day). In the case of H_2 storage, the only difference was that the algorithm obtained the maximum surplus power (kW) which fixes the maximum electrolyser rating instead of aggregating the power flows. The maximum size of the tank (kg) resulted from the balance between the H_2 generation from the electrolyser and the H_2 consumption from the PEMFC system as

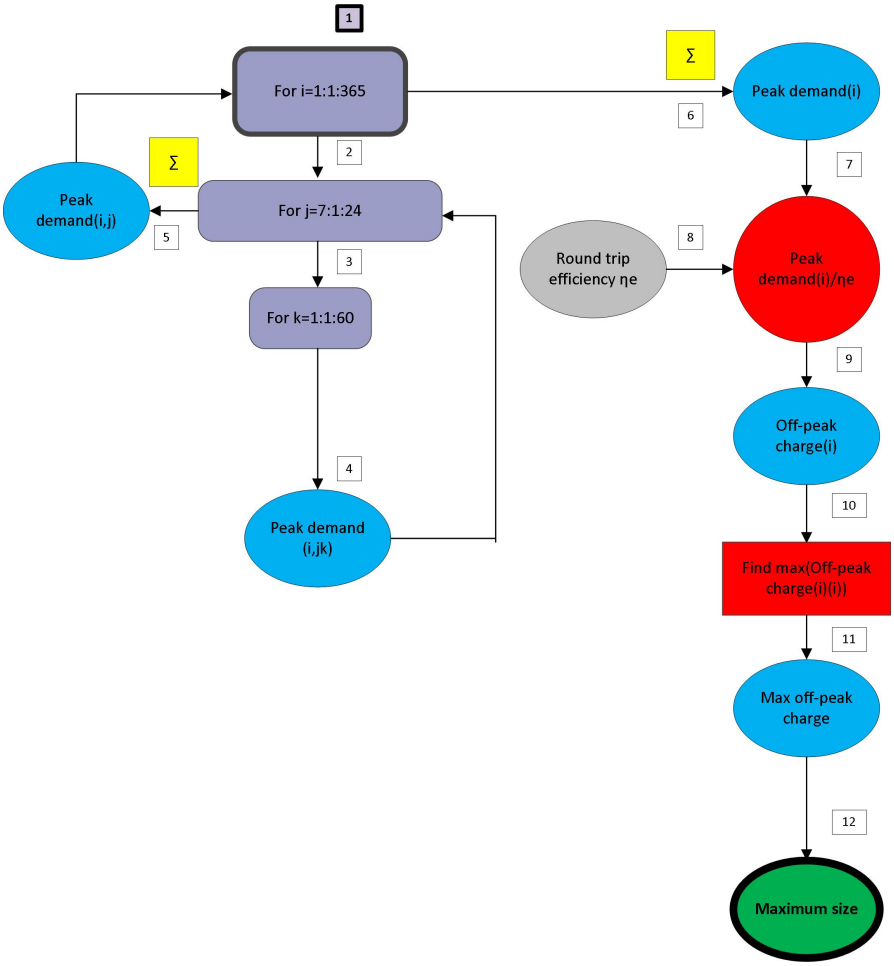

Figure 5.6: Flow chart representing the algorithm which was utilised to obtain the maximum capacity of a battery system when performing LS with Economy 7 using 1 minute (loop variable k) data for every day (loop variable i) of the year. The flowchart sequence follows the number sequence in the boxes. The sum symbol represents the aggregation of results to obtain hourly values (from 1 minute data) or daily values (from hourly data).

explained in Section 4.8.2.

Figure 5.5 shows the algorithm which was used to determine the battery performance. The algorithm compared the PV generation (kW) and demand load (kW) to obtain the performance of the battery system. The management system limited the maximum charge rating, discharge rating and *DOD* as explained in Section 4.5.1. This algorithm also applied to H_2 storage when considering that the *SOC* is not limited by a maximum value for this technology. The code utilised to obtain the maximum battery capacity and the optimum battery capacity for PVts is presented in Appendix K. Other programs developed for the rest of applications and technologies discussed below are available with the CD-ROM enclosed with this thesis.

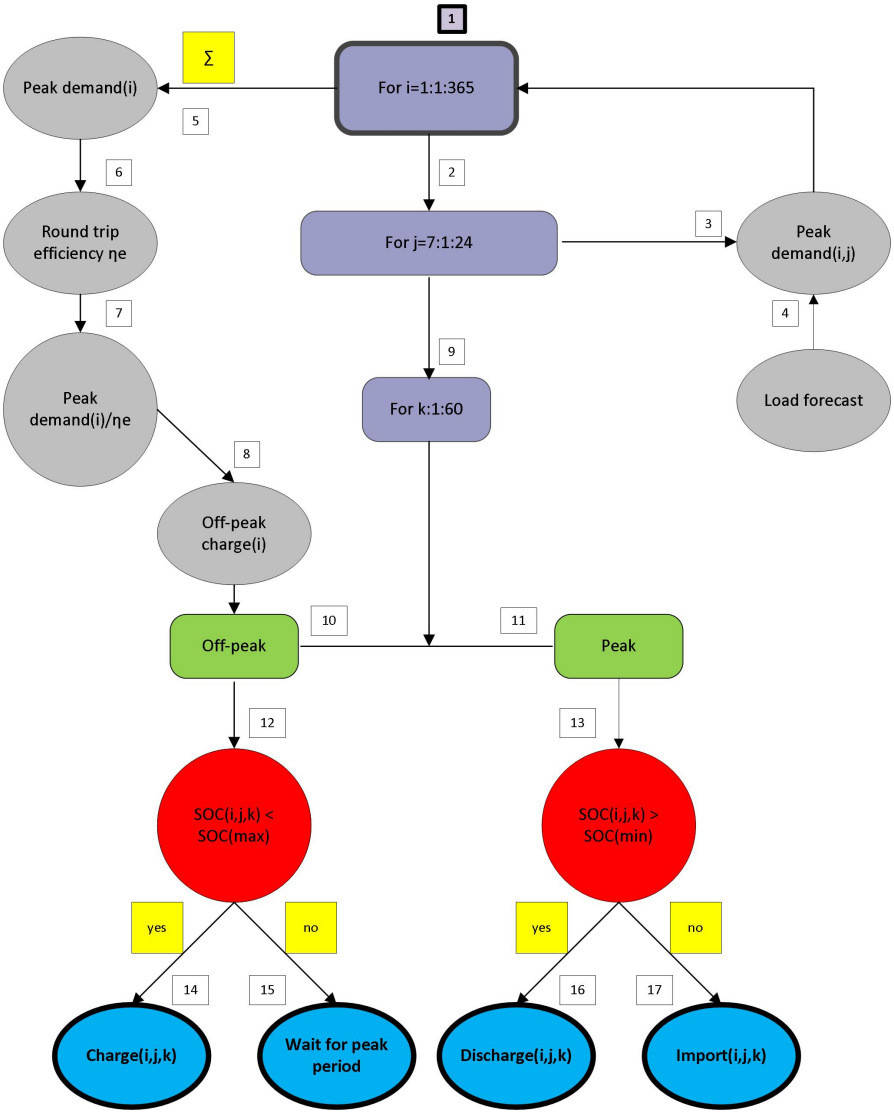

Figure 5.7: Flow chart representing the algorithm which was utilised to obtain the performance of a battery system when performing LS with Economy 7 using 1 minute (loop variable k) data for every day (loop variable i) of the year. The flowchart sequence follows the number sequence in the boxes. The sum symbol represents the aggregation of results to obtain the daily values from hourly data. All the parameters which depended on the demand load forecast are represented in grey.

5.3 Load shifting

The rationale behind the decision of performing LS relies on the comparison between the round trip efficiency of the CES system and the ratio between the energy prices at the valley and peak periods as discussed in Section 3.5. The algorithms used to obtain the maximum and the optimum size depend on the tariff, specifically on the number of periods of the tariff. As a consequence, two different algorithms were developed for Economy 7 and the NETA tariff using the same rationale.

5.3.1 Load shifting with Economy 7 for battery technology

Figure 5.6 shows the algorithm which was used to determine the maximum size of battery systems when performing Economy 7. As explained in Section 3.5.1, the peak period occurs between 7 am and midnight on a daily basis. The main input data of the algorithm were the demand load of the community with a temporal resolution of 1 minute and the estimated round trip efficiency of the battery. The algorithm selected the day of the year with the largest demand load at peak time. Then, the largest battery system was obtained when dividing the largest peak demand by the battery round trip efficiency. The round-trip efficiency of any battery system performing LS was obtained after using a trial and error method.

The same logic followed to obtain the maximum size was used to determine the performance of a battery system when performing Economy 7. If the charging or discharging decision for PVts was made when comparing the PV generation and the demand, this decision only depended on the round-trip efficiency of the battery for LS according to Equation 3.6. The management system controlled the performance of the battery as discussed in the previous section with PVts.

As Figure 5.7 shows, forecasting the demand load which occurred at the peak time was necessary on a daily basis. The result of the forecast was divided by the battery round trip efficiency to obtain the required charge of the battery during the valley period for every day. The demand load forecasting was performed with a time resolution of 1 h.

5.3.2 Load shifting with the NETA tariff for battery technology

In addition to the number of periods, the basic difference between Economy 7 and the NETA tariff is the fact that Economy 7 is a time-of-use tariff in which the prices are known previously and they are the same for every day of the year while the NETA tariff is a real-time pricing tariff in which the prices vary each day. These two aspects were considered by the algorithm in Figure 5.8.

It was assumed that the four prices per day of the NETA tariff were known one day ahead as discussed in Section 3.5.2. For every day, the algorithm searched for the minimum price which defined the off-peak period. Subsequently, the algorithm obtained the ratio between the minimum price and the subsequent prices every day. Then, it compared these ratios with the round trip efficiency of the battery. If the round trip efficiency of the battery was higher than the price ratio, a peak period was defined. LS with battery systems was only possible when the minimum

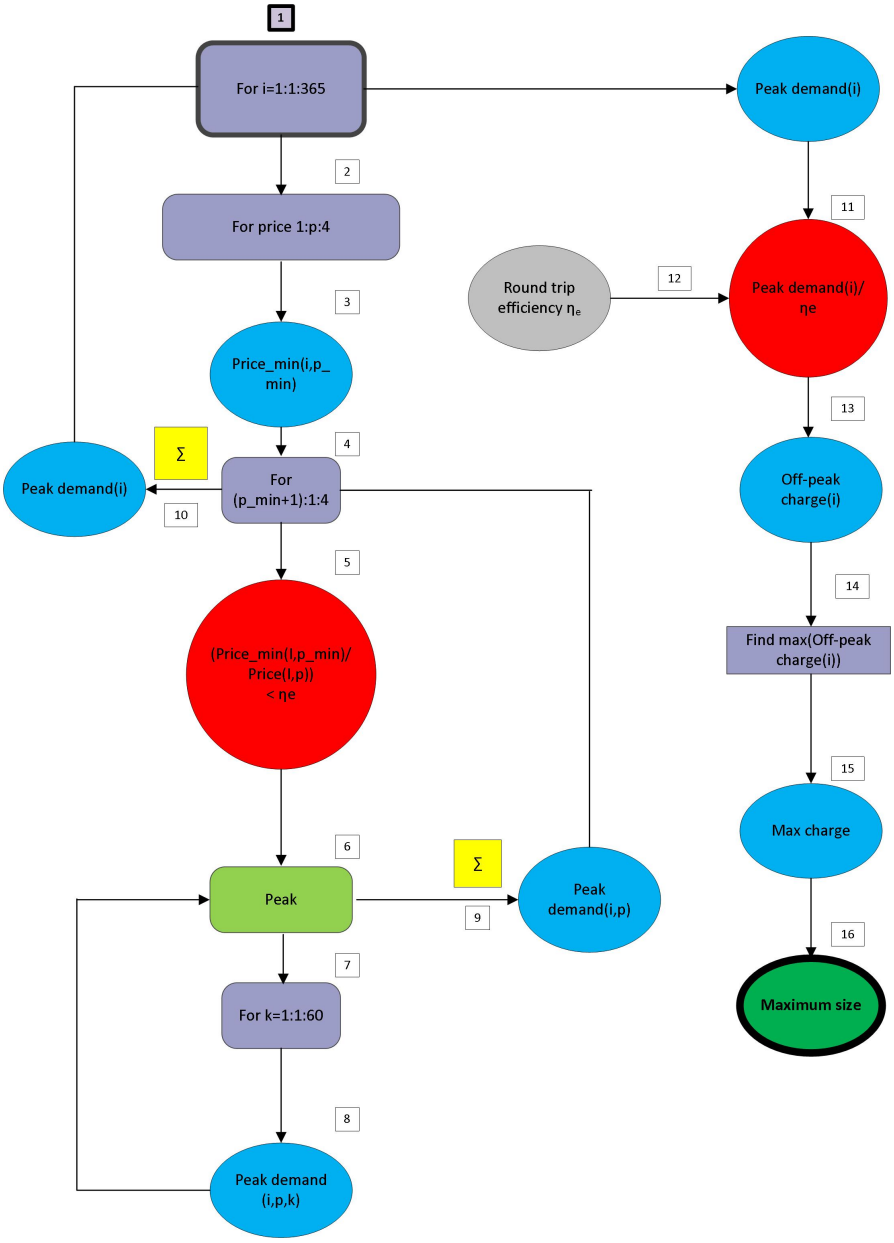

Figure 5.8: Flow chart representing the algorithm which was utilised to obtain the maximum capacity of a battery system when performing LS with the NETA tariff using 1 minute (loop variable k) data for every day (loop variable i) of the year. The flowchart sequence follows the number sequence in the boxes. The sum symbol represents the aggregation of results to obtain hourly values (from 1 minute data) or daily values (from hourly data). The index p represents the four periods of the NETA tariff.

price did not occur at the four period of the NETA tariff defined in Section 3.5.2. As it occurred with Economy 7, the largest battery capacity resulted from the day in which the electricity prices and the domestic demand load determined the maximum peak demand to be shifted. This is schematically represented in Figure 5.8.

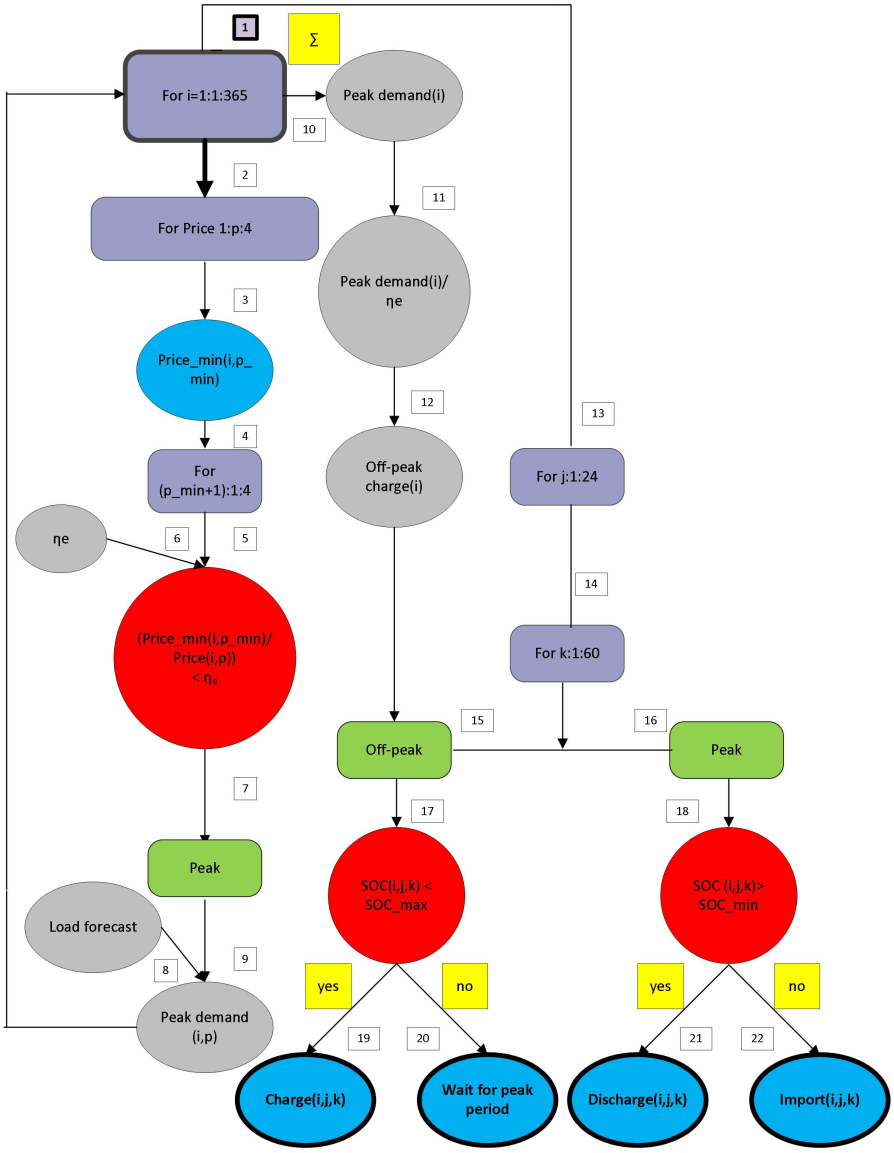

Figure 5.9: Flow chart representing the algorithm which was utilised to obtain the performance of a battery system when performing LS with the NETA tariff using 1 minute (loop variable k) data for every day (loop variable i) of the year. The flowchart sequence follows the number sequence in the boxes. The sum symbol represents the aggregation of results to obtain daily values from hourly data. The index p represents the four periods of the NETA tariff. All the parameters which depended on the demand load forecast are represented in grey.

Figure 5.9 shows the algorithm which was used to calculate the performance of a battery system when performing LS with the NETA tariff. The rationale was the same as shown in Figure 5.8 for obtaining the maximum size. Firstly, the algorithm determined the period in which the price of the electricity was the lowest for the day after and how much the battery system should be charged according to the forecast of the demand load and the round trip efficiency. Secondly, the battery system was charged and discharged depending on the type of period (off-peak or peak).

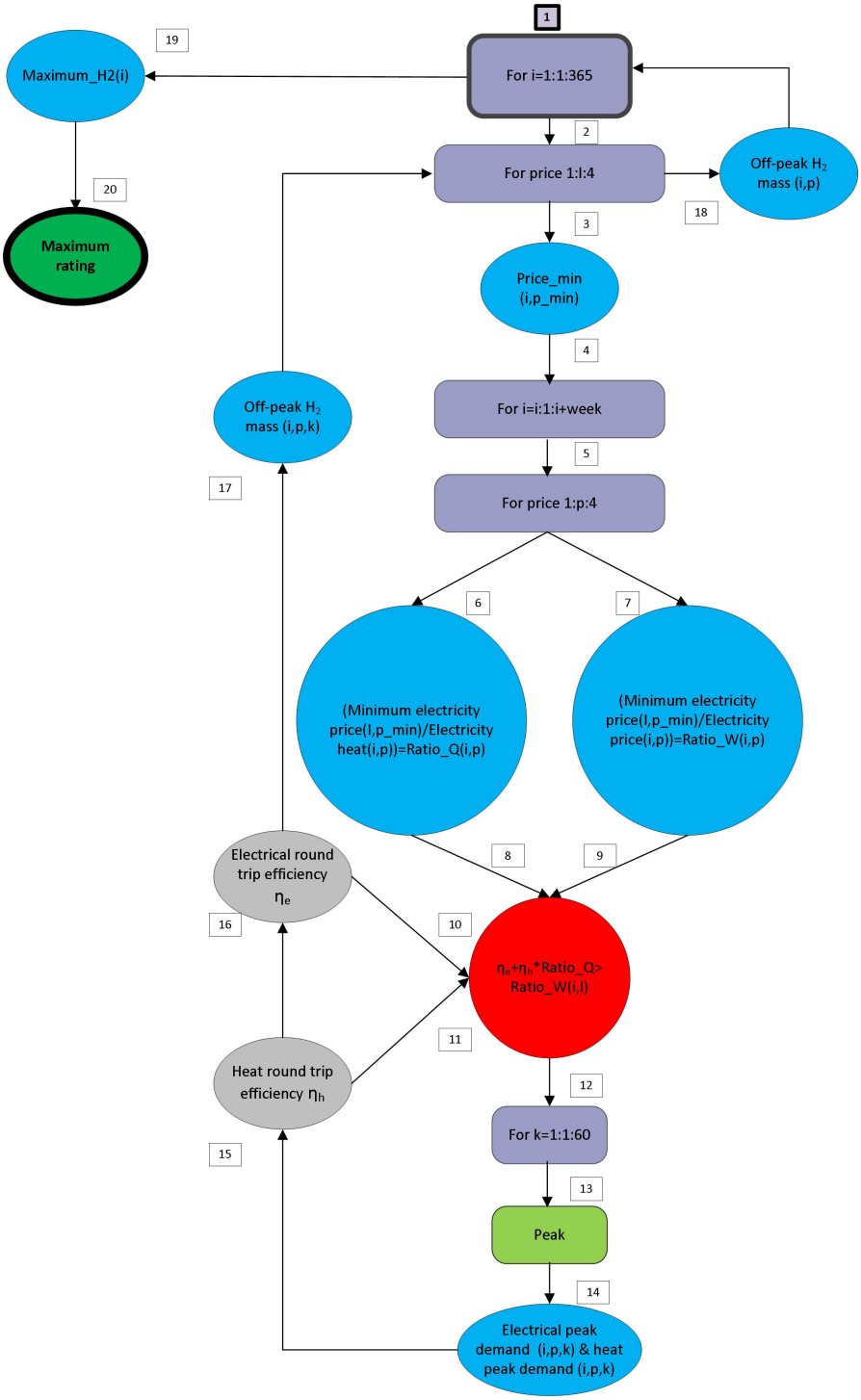

Figure 5.10: Flow chart representing the algorithm which was utilised to obtain the maximum electrolyser rating when performing LS with the NETA tariff using 1 minute (loop variable k) data for every day (loop variable i) of the year. The flowchart sequence follows the number sequence in the boxes. The sum symbol represents the aggregation of results to obtain hourly values (from 1 minute data) or daily values (from hourly data). The index p represents the four periods of the NETA tariff.

5.3.3 Load shifting with the NETA tariff for H_2 technology

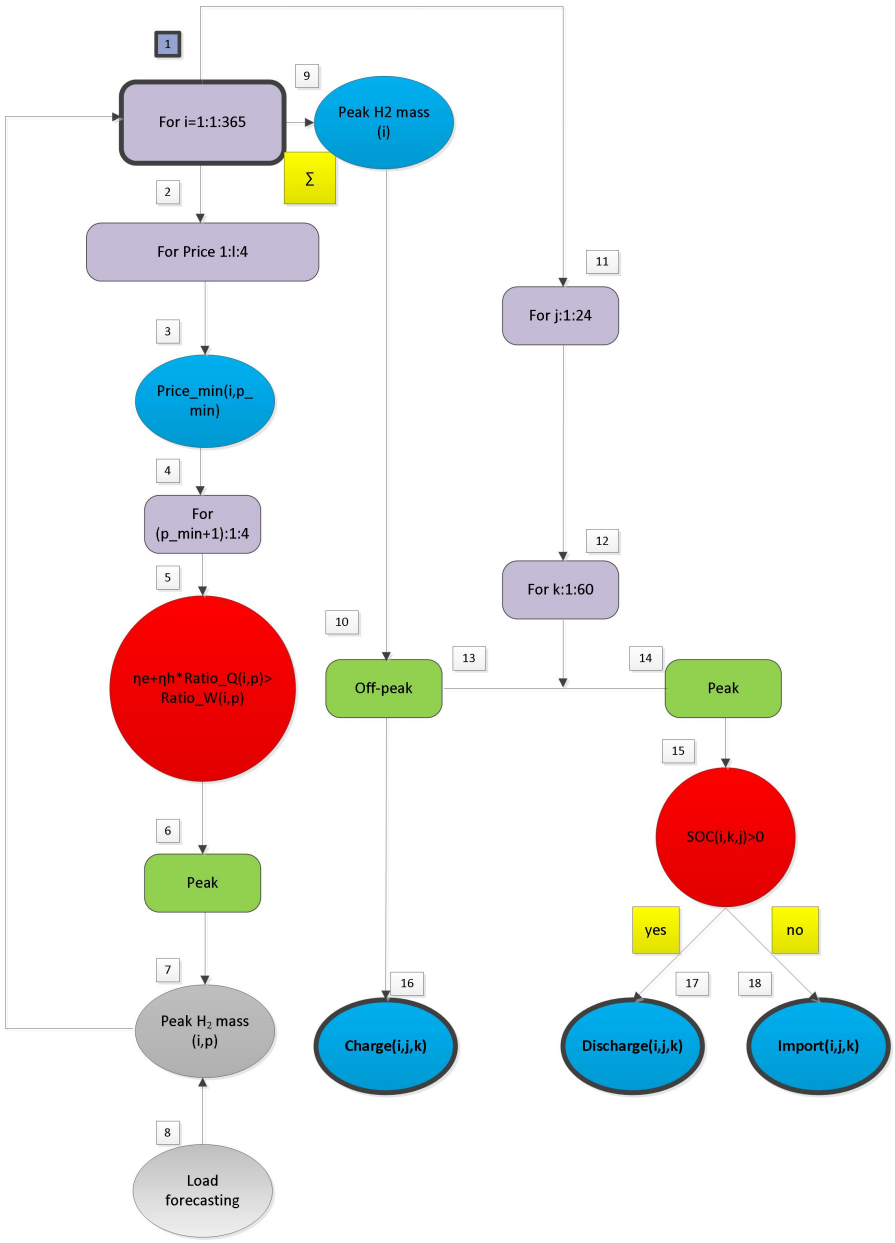

Figure 5.11: Flow chart representing the algorithm which was utilised to obtain the performance of a H_2 system when performing LS with the NETA tariff using 1 minute (loop variable k) data for every day (loop variable i) of the year. The flowchart sequence follows the number sequence in the boxes. The sum symbol represents the aggregation of results to obtain daily daily values from hourly data. The index p represents the four periods of the NETA tariff. All the parameters which depended on the demand load forecast are represented in grey.

As demonstrated by Equation 3.8, LS with H_2 should be accomplished when the condition $\eta_e + \eta_h \times (P_{iv}/P_h) > P_{iv}/P_{ip})$ is met. The mid and long term ES capacity of H_2 storage suggested that an electrolyser should run at full load whenever electricity price is low (according to the LS condition expressed above) as H_2 can be stored for several days or even weeks until the price of the electricity is high.

As a consequence, the maximum rating of the electrolyser performing LS is not fixed by any technical constraint (as it happened with battery technology).

The maximum electrolyser rating was defined by the electrolyser which was able to generate the H_2 consumed by the PEMFC system during the week in which LS was more attractive. This condition is schematically represented in Figure 5.10 from the step 4. Finally, Figure 5.11 shows the algorithm which was used to obtain the performance of a H_2 system. This algorithm is very similar to the one used for battery technology shown in Figure 5.9. The two basic differences are that H_2 mass should be forecasted (using the electrical demand load, heat demand load and prices) instead of forecasting the electrical demand load and the *SOC* does not limit the H_2 charge.

5.4 Combination of applications

This section describes the algorithms used to determine the optimum CES system when performing PVts and LS at the same time. For the two tariffs discussed in this work, the algorithms which obtained the maximum size and the performance for the combination of applications were based on the algorithms shown in the previous section for LS. This is the reason why only the main modifications or extra considerations will be addressed here. Battery technology when performing PVts and LS with the NETA tariff will be used to illustrate the combination of applications. In addition to the forecasting of the demand load, the combination of PVts and LS required the forecast of the PV generation in order to integrate both applications.

5.4.1 Combination of PVts and LS with the NETA tariff for battery technology

As argued previously in Section 5.2, a battery system is suitable for daily cycling and therefore the charge from the PV arrays and the grid can overlap. The discussion on this issue is expanded in Section 6.7. As a result, integrating these applications by the same battery system requires a strategy which is executed using forecast.

The main difference between the algorithms which determined the maximum size for battery systems performing only LS and PVts and LS together was the calculation of the peak demand load which the battery should meet the day after. The peak demand was reduced by the amount of demand load directly met by the PV generation in the combination of applications. Additionally, the surplus PV energy available should charge the battery system and meet the peak demand

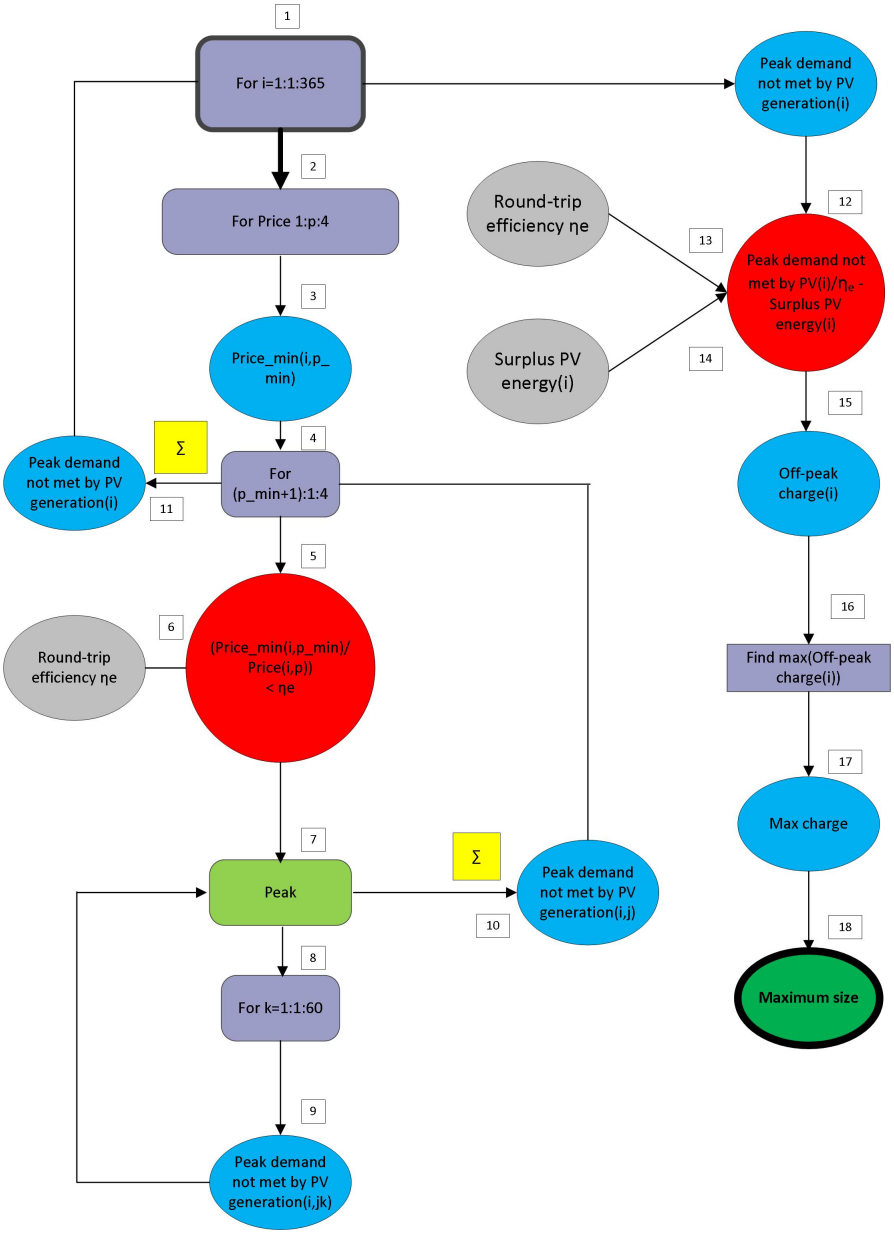

Figure 5.12: Flow chart representing the algorithm which was utilised to obtain the maximum size of a battery system when performing PVts and LS with the NETA tariff using 1 minute (loop variable k) data for every day (loop variable i) of the year. The flowchart sequence follows the number sequence in the boxes. The sum symbol represents the aggregation of results to obtain hourly values (from 1 minute data) or daily values (from hourly data). The index p represents the four periods of the NETA tariff.

load afterwards. Therefore, the maximum size and the optimum size algorithms employed the demand load, the PV generation and the round trip efficiency to calculate firstly the fraction of the demand load met by the PV generation and then, the surplus available PV energy which reduced the LS requirements. The fraction of the demand load directly met by the PV generation is then subtracted from the peak demand load calculated when only LS was performed (shown in Figures 5.8 and 5.9). This subtraction was made to quantify the peak demand

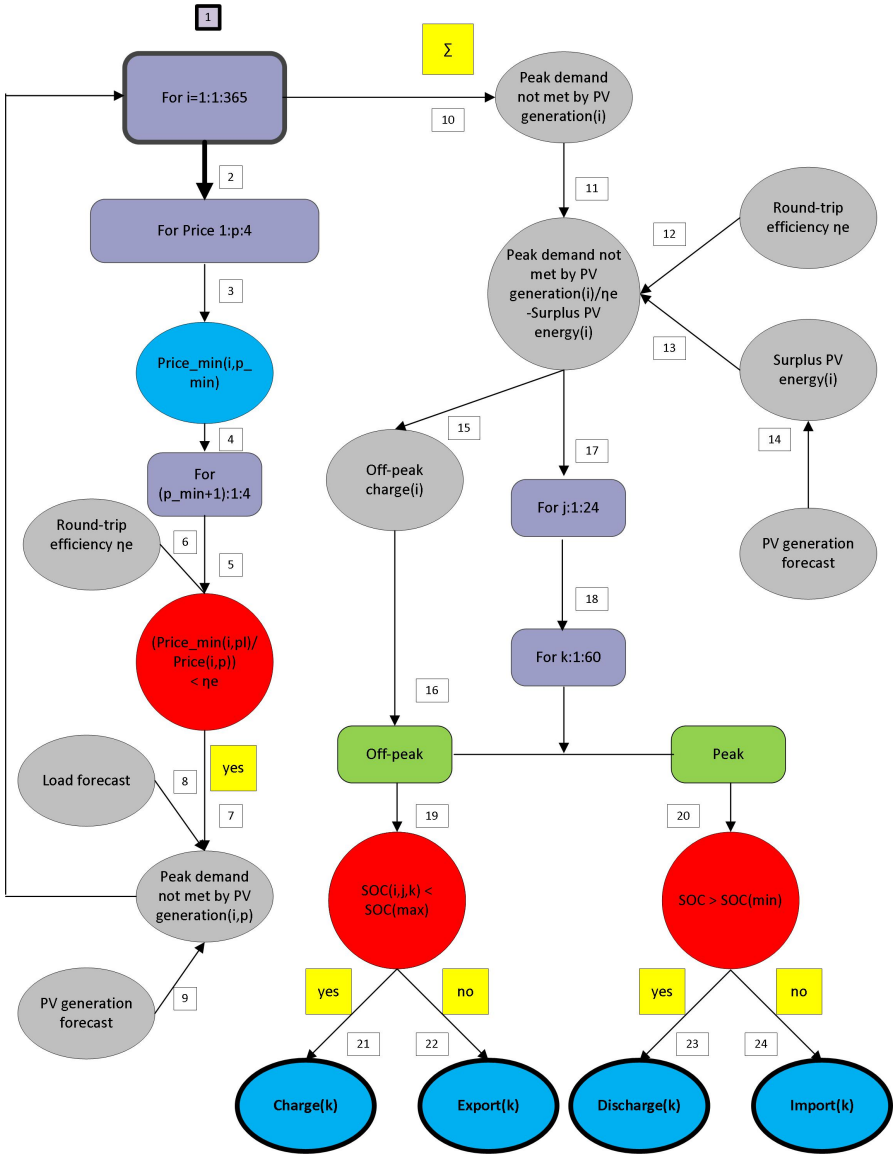

Figure 5.13: Flow chart representing the algorithm which was utilised to obtain the performance of a battery system when performing PVts and LS with the NETA tariff using 1 minute (loop variable k) data for every day (loop variable i) of the year. The flowchart sequence follows the number sequence in the boxes. The sum symbol represents the aggregation of results to obtain daily daily values from hourly data. The index p represents the four periods of the NETA tariff.

load which was not met by the PV generation. The maximum size algorithm used real data while the algorithm which determined the performance used forecast data as shown in Figures 5.12 and 5.13 respectively. Alternatively, the maximum electrolyser rating for the combination of applications was fixed by the maximum of the ratings utilised for PVts and LS independently.

Electricity charged from the PV plants was prioritized over electricity charged from the grid in this study because it is generated on-site by the end users' PV plants. The electricity charged from the PV arrays was only discharged at peak

times. Identifying the optimum management solution for the combination of applications was out of the scope of this work. Finally, perfect forecast of the demand load and the PV generation was used to determine how much electricity was necessary to charge from the grid, yet the valley charge calculation was also affected by the battery round trip efficiency as shown in Figure 5.12, this being a dynamic parameter. The optimization of the charging process from the PV plant and the grid was out of the scope of this work.

5.5 Reference years

CES will enable the higher penetration of variable and undispatchable RE technologies [60, 95]. At the same time, the value of ES depends on the RE technologies penetration [49]. As a consequence, the business case of CES performing PV management applications depends on the PV penetration. This was the main reason why three different reference years were considered in this study: 2012, 2020 and a hypothetical zero carbon year.

2012 was selected for the baseline scenario and it describes the current state of CES in the UK; 2020 was chosen as a transition year because manufacturers expect that research advances, government support and customers demand help ES in general and CES in particular to take off. Also, the UK Government has already established quantifiable objectives for the penetration of RE technologies by 2020 [34]. Specifically, the 15% of the total demand should be met by RE sources and 30% of the total electricity generation should come from RE technologies. Finally, the zero carbon scenario was selected to understand the potential role of mature CES with high levels of PV and low carbon heat penetration. Data from 2050 was utilised to model the zero carbon scenario because the UK Government stated that GHG emissions should reduce at least 80% by 2050 relative to 1990 levels [20].

Additionally, some of the parameters which play a role in the business case of CES including the domestic demand and energy prices will also evolve during this decarbonisation pathway. In fact, the domestic demand is expected to be cut as a result of energy efficiency savings such as better insulation, low energy appliances and lighting (passive measures) and reduction of the stand-by consumption of appliances. The progressive replacement of natural gas boilers by HPs and CHP systems (among others) will increase the use of electricity and H_2 to meet the heat demand load. Moreover, ES technologies are expected to continue progressing and becoming more attractive in terms of cost and durability. Overall, the three different reference years were used to understand the progress of CES according to the projected evolution of the main parameters which affect its performance and business case.

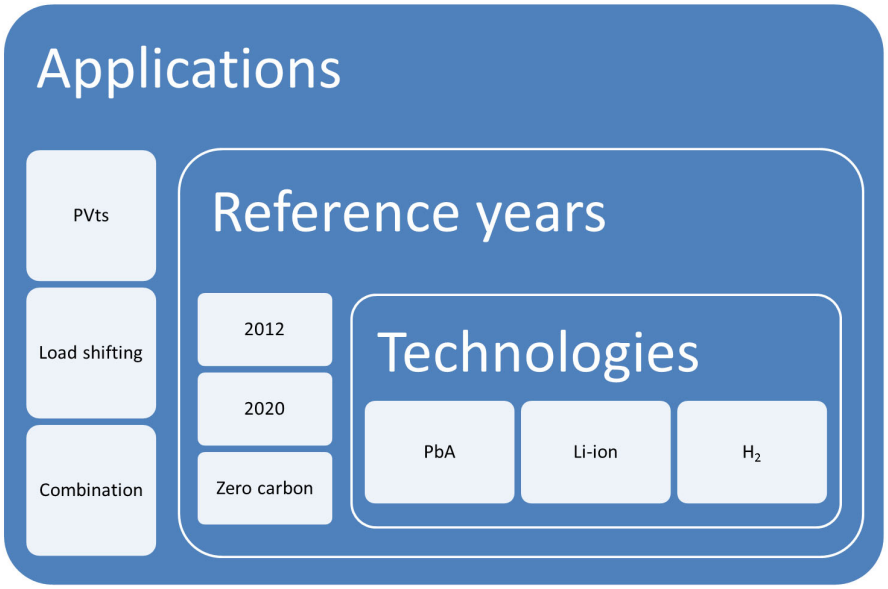

Figure 5.14: Schematic representation of the reference scenarios studied in this work.

5.6 Reference scenarios

Reference scenarios were defined in terms of the input data which describe the energy consumption level and the characteristics of ES technologies. A reference scenario included an ES application, ES technology and reference year as shown in Figure 5.14.

The reference scenario for 2012 aimed to represent the current situation of CES in the UK and therefore it is the baseline scenario. Likewise, the reference scenarios for 2020 and the zero carbon scenario were based on high levels of technological and economic ambition for CES and assumed important concerted effort to reduce the carbon intensity of the energy system (emission cuts of 18% on 2008 levels by 2020 [34]) and the domestic sector in particular. This effort was quantified by the UK Government for the domestic demand, PV generation and low carbon heat generation in a comprehensive report [20]. Although the reference scenarios for 2020 and the zero carbon scenario mean remarkable changes with regard to the baseline scenario (in 2012), only scenarios 2 and 3 from of this report were selected to limit the development of different technologies in the energy arena. The scenarios 2 and 3 were considered by the UK Government as the most plausible scenarios in comparison with scenarios 1 (the most pessimistic) and 4 (the most optimistic).

The input data used for the reference scenarios was structured depending on

Table 5.1: Cross-application parameters and reference values utilised in 2012, 2020 and the zero carbon year

Parameter	2012	2020	Zero carbon
Electricity price (p\kWh)[a]	13.0	16.3	31.0
Natural gas price (p\kWh)[a]	5.0	7.4	20.0
HP penetration[b]	1	14	100
Electricity demand (MWh\year)[c]	Current	up to 2.9	up to 2.4
Heating demand (MWh\year)[c]	Current	up to 10.3	up to 6.1
DHW demand (MWh\year)	Current[d]	Current	Current

[a] The price of the utilities was estimated using an average trend of those followed in the last 25 years and last seven years [164].
[b] The HP penetration in 2020 was obtained using a linear trend between 2012 and the total electrification of the heat sector by 2050.
[c] Domestic demands loads as predicted by DECC in the most plausible scenarios [20]. The HP electrical consumption is not included in the electricity demand here since it depends on the COP which is a result of the simulations presented in Chapter 6.
[d] It was assumed that DHW demand will not vary [20]. The typical DHW demand of a home varies between 3 MWh/year to 4 MWh/year [165].

the application, the ES cost and durability. Additionally, parameters which have the greatest impact on the business case were identified and a sensitivity analysis was included in order to tackle the uncertainty associated with them: ES cost, ES durability, PV penetration, export bonus and utility prices. Finally, battery and H_2 storage were not combined for any community in order to better compare both technologies. The study of a hybrid ES system for a 7-home community was analysed in a previous publication [138]. Next, the input data selected for the reference scenarios is introduced.

5.6.1 Cross-application parameters

There are some basic parameters which affect the business case for any ES technology and application such as the energy prices and the domestic demand. The values assumed for these cross-application parameters are shown in Table 5.1.

5.6.2 PVts parameters

In addition to the cross-application parameters, the parameters which specifically affect the performance and business case of a CES system performing PVts are the PV penetration and the export bonus as shown in Table 5.2. The PV penetration was defined as the percentage of homes in the UK with a PV installation.

Table 5.2: PVts parameters and reference values utilised in 2012, 2020 and the zero carbon year.

Parameter	2012	2020	Zero carbon
PV penetration (%)[a]	1	7.6	57.0
Export bonus (p\kWh)[b]	3.2	3.2	3.2
Curtailment obligation[c]	no	no	yes

[a] The PV penetration for the zero carbon scenario was obtained from the scenario 3 for PV micro-generation in 2050 from DECC [20]. However, the value for 2020 (7.6%) was obtained when considering that the PV capacity growths between 2012 and 2020 at the rate it did between 2010 and 2012.
[b]Export bonus in 2012.
[c]Power curtailment obligation was only considered on the reference scenarios for the zero carbon year.

Additionally, the power curtailment obligation as explained in Section 6.3.4 was considered in the zero carbon year.

5.6.3 LS parameters

The parameters which specifically affect the performance and economic benefits of CES when performing LS are the type of tariff (the number of periods and the electricity prices) and the forecast of the community demand load as shown in Table 5.3. As explained in Section 3.5.2 , the ratio between the off-peak and peak prices was kept constant for both tariffs and only the average price was increased when creating the prices for 2020 and the zero carbon year. Perfect foresight was assumed for the demand load forecast in order to quantify the maximum LS requirements and making the calculation independent on any forecast technique.

Finally, the parameters which affect the results obtained by the combination of applications were the same parameters already discussed for PVts and LS separately. Additionally, the forecast of the PV generation was also integrated. Perfect foresight was used for same reasons as above.

Table 5.3: LS parameters and reference values utilised in 2020 and the zero carbon year

Parameter	2020	Zero carbon
Economy 7 prices (p\kWh)	18.9-8.9	35.9-16.9
NETA average price (p\kWh)	16.3	31
Load forecast	perfect	perfect

5.6.4 Energy storage technologies parameters

Table 5.4: ES technologies parameters and reference values utilised in 2012, 2020 and the zero carbon year

Technology	Parameter	2012	2020	Zero carbon
PbA	**EFC**	1000	1250	1500
	Calendar losses (%/month)[a]	0.17	0.15	0.12
	ES medium cost (£\kWh)	260	150	65
Li-ion	**EFC**	2400	3000	3600
	Calendar losses (%/month)[a]	0.10	0.009	0.008
	ES medium cost (£\kWh)	1300	310	160
H_2	**Operational hours (h)**	5000	30000	60000
	Degradation (μV\(h·cell))	5	2	1
	Stack cost (£\kW)	3400	1300	980
	Tank cost (£\kg)	650	360	200
All	**Electronics cost**	Current[b]	-25%[c]	-30%[c]
	BoP cost (£\kW)	65	50	45
	Maintenance cost (£\kW)	6.5	6.5	6.5

[a]Monthly battery capacity percentage reduction as discussed in Section 4.7.1.
[b]Based on current manufacturer data shown in Figure 4.10.
[c]Cost reduction over cost in 2012 based on the historic trend [166].

As presented in Section 4.4, the models of different ES technologies were comprised of performance, durability and economic sub-models. While the same sub-models were utilized for all the scenarios, the input data for the durability and economic submodels varied depending on the reference year. Table 5.4 shows the ES properties which play a role in the business case. A comprehensive literature review was made for the battery storage medium cost and *EFC* as shown in Appendix B and for the electrolyser cost, tank cost and operational hours of the electrolyser for H_2 technology as shown in Appendix C.

The input data for the baseline scenario reflects the current state of art for different ES technologies. The reference values in 2020 were based on the estimations from manufacturers or research institutes based on the consolidation of the CES industry and the existence of mass production. The most promising and optimistic values from this literature review were used to model ES technologies in the zero carbon year. The cost reduction for the electronics was based on the cost reduction of PV inverters over the last 15 years [166].

However, there is much uncertainty related to the current cost and the potential reduction of the cost for battery technology especially Li-ion technology.

This is reflected in variety of values shown in Table B.2 in Appendix . It has been reported that the cost of Li-ion chemistry can reduce down to 290 £/kWh and 175 £/kWh by 2020 according to German and a Japanese sources respectively [105]. In the case of the durability, it is established by manufacturers including Saft and Hitachi that Li-ion batteries can last up to 15-20 years according to the control parameters presented in Table 4.1. Finally, there is less uncertainty in other cost of inverters because this a well established industry and the moment and other cost components including the BoP and maintenance costs.

5.7 Sensitivity analysis

CES for end user applications is not a mature market yet and several of the suitable technologies such as Li-ion battery and PEM electrolysers are still under research and development. In other cases, ES technologies are still in previous phases to the deployment (market pull) such as demonstration, development and research (technology push). This is one of the reasons why the durability and cost data for ES technologies can vary significantly depending on the source. Moreover, the lack of pilot projects which have been running for several years and related results from the field which are available in the literature complicates the characterization of CES systems.

The CES analysis presented in this thesis was developed for three different reference years and therefore the evolution of ES parameters and other parameters which influence the economics was quantified. However, there is high uncertainty related to these parameters due to the temporal scale of the analysis. Secondly, the fact that the ES industry but also the PV industry, HP industry and the FC industry are currently developing increases the uncertainty on CES. As a result, quantifying the uncertainty related to the reference input data and designing a method to tackle this uncertainty were key elements of this work.

The uncertainty related to the modeling results was related to the accuracy of the reference input data selected for the reference scenarios. The main parameters which affect the performance and business case of CES were identified for this study and the uncertainty associated with them was quantified by means of a comprehensive literature review as shown in Appendices B and C in the case of battery and H_2 technology respectively. These parameters included in the sensitivity analysis are: cost, durability, PV penetration, HP penetration, utility prices, export bonus and curtailment obligation.

A robust model for any type of system should include some analysis to quantifying how uncertainty may affect the results. Therefore, several techniques have

been used in the literature to assess the uncertainty related to different systems including sensitivity analysis [167], probability analysis [168] and stochastic simulation [169]. In this work, a sensitivity analysis was designed to tackle the uncertainty because:

- The impact of any parameter on the performance and economic benefits of CES was quantified when other parameters did not vary.
- The sensitivity analysis helped to identify the maximum and minimum value for any CES result (performance and economic benefits) depending on the variation of any parameter in addition to quantify the whole range of possibilities in between.
- Results from the sensitivity analysis are easy to understand and different stakeholders can visualize the impact of any input data on the performance and economic benefits.
- The sensitivity analysis could be easily integrated with the long-term deterministic scenario analysis of this study.

The advantages outlined above were the reasons why sensitivity analyses have been the most used technique when assessing the potential economic benefits of ES in the literature [49, 97–99, 105]. The main difficulty related to the application of the sensitivity analysis was the computational time related to running the algorithms several times. Therefore, the sensitivity analysis was computational intensive but the required time could be managed during this study.

Table 5.5: Parameters included in the cost and durability sensitivities for battery technology for 2020 and the zero carbon year.

Technology	Parameter	2020	Zero carbon
PbA	**ES medium cost (£/kWh)**	150-230	65-150
	***EFC* (cycle)**	1000-1250	1250-1500
	Calendar losses (%/month)	0.15-0.17	0.12-0.15
Li-ion	**ES medium cost (£/kWh)**	310-1300	160-1300
	***EFC* (cycle)**	2400-3000	3000-3600
	Calendar losses (%/month)	0.09-0.10	0.08-0.09

Similarly to the reference scenarios presented above, a sensitivity analysis was also developed for any combination of ES application, reference year and ES technology as a function of the size of the community. The level of sensitivity performed with the different parameters was related to the level of uncertainty associated with them. Specifically, the sensitivity analysis for 2020 considered the

parameters used in the baseline scenario (2012) and the sensitivity analysis for the zero carbon year considered the input data utilised for the reference scenarios in 2020 unless others considerations applied. A comment is included in the next sections in this case. The sensitivity analysis was not performed with the baseline scenario.

5.7.1 Energy storage technology sensitivity

Table 5.6: Parameters included in the cost and durability sensitivities for H_2 technology for 2020 and the zero carbon year.

Parameter	2020	Zero carbon
Stack cost (£/kW)	1300-3400	980-1300
Tank cost (£/kg)	360-650	200-360
Operational hours (h)	20000-30000	40000-60000

The cost and the durability parameters were modified separately according to the input data reflected in Tables 5.5 and 5.6 for battery and H_2 technologies respectively. The uncertainty related to the cost was higher than that related to the durability according to the literature review performed in Appendixes B and C. Therefore, the sensitivity of the cost of the storage medium accounted for a larger percentage modification (up to 325% for Li-ion technology in 2020). Finally, Table 5.7 summarizes the sensitivity of the cost of the electronics and the BoP which affected all ES technologies. The maintenance cost was not considered in the sensitivity analysis.

Table 5.7: Parameters included in the cost and durability sensitivities for battery and H_2 technologies for 2020 and the zero carbon year.

Year	2020	Zero carbon
Electronics cost reduction (%)	0-25	25-30
BoP cost (£/kW)	50-65	45-50

5.7.2 Demand and PV generation sensitivity

The sensitivity of the PV generation was based on the PV penetration in the UK according the scenarios defined by DECC as seen in Table 5.8. The sensitivity of the PV penetration in 2020 and the zero carbon year were based on the scenario 3 (2.3%) and 2 (53%) of the DECC analysis respectively. Likewise, the demand

sensitivity was based on the penetration of HPs in the UK and it was only applied to 2020. The demand sensitivity considered that the HP penetration was equal to 0% in 2020 in order to evaluate the impact of HPs on the CES performance and business case.

Table 5.8: PV and HP penetration sensitivity and the respective value for 2020 and the zero carbon target.

Parameter	2020	Zero carbon
PV Penetration (%)[a]	2.3-7.6	53-57
HP Penetration (%)[a]	0-14	100

[a]PV penetration and HP penetration based on estimations from DECC [20].

5.7.3 Energy prices sensitivity

The energy prices for the different reference years were summarized in Table 5.1. The sensitivity analysis included the following scenarios which are summarized in Table 5.9 according to the records of energy prices from the UK Government [170]:

- The electricity price and the natural gas price increase with the rate they have done for the last 25 years (lowest values in Table 5.9).
- The electricity price and the natural gas price increase with the rate they have done for the last last seven years (highest values in Table 5.9).
- The export bonus is equal to 0.045 £/kWh (i.e the export bonus in 2013).
- The export bonus is equal to 0 £/kWh.

However, the energy prices are dynamic variables and future energy prices will be affected by different factors including the electrification of the heating and transport sectors and the penetration of RE technologies. It is expected that

Table 5.9: Different energy prices and export bonus considered in the sensitivity analysis depending on the reference year.

Parameter	2020	Zero carbon
Electricity price (£/kWh)	0.136-0.19	0.167-0.452
Natural gas price (£/kWh)	0.052-0.094	0.102-0.289
Export bonus (£/kWh)	0-0.045	0-0.045

electricity will be more expensive if new demand loads are introduced in periods of peak demand if prices reflect the marginal cost of generating electricity [171]. Additionally, the *LCOES* of renewable energy technologies is less competitive that other traditional generator plants but from a merit order perspective they offer low marginal cost in comparison with generators which use fossil fuels [47]. The accurate modelling of the future electricity price dynamics is out of the scope of this work.

5.7.4 PV generation curtailment sensitivity

As argued in Section 6.3.4, the curtailment of PV generation can be integrated by a CES system which performs PVts when there is a curtailment obligation on place. The addition of this application is considered in the sensitivity analysis in 2020, while it was considered by the reference scenario in the zero carbon year.

5.8 Community approach

Figure 5.15: Ten homes of which eight of them have a PV plant on the roof. This schematic was used to illustrate the self-select community approach together with Figure 5.16.

One of the key aspects of this analysis is that it was performed as a function of the size of the community. The objective was to understand the impact of the aggregation of demands on the performance and economic benefits of CES. However, the domestic demand loads were not the only parameters which varied with the size of the community and the community approach selected for the PV generation and the low carbon heat generators are also explained in this section.

The domestic demand loads and the local PV generation were added as community size increased. The optimization method and methodology presented in this work were tested using real demand data up to a 100-home community as seen Section 3.10.1. A community size resolution of 5 homes was used from a single

home up to the 100-home community following this series: 1, 5, 10, 15, ..., 100. This community resolution allowed the accurate investigation of the effect of the community size on the CES performance and economic benefits while managing the overall computational time of the investigation.

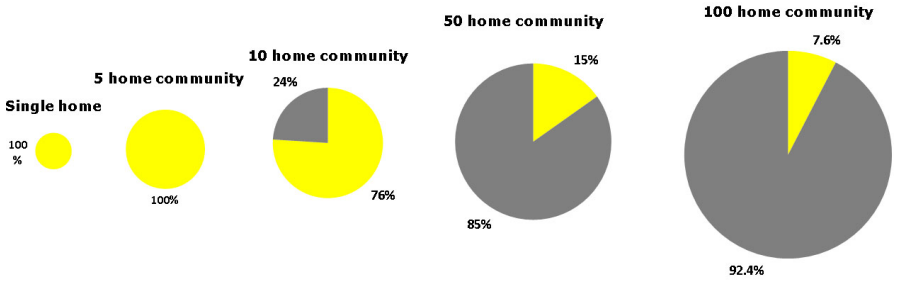

Figure 5.16: Evolution of the community PV percentage (yellow are in the pie charts) as a function of the size of the community in 2020 when the PV penetration in the UK was assumed to be 7.6%.

For any community size, the community PV percentage refers to the fraction of homes in the community with a PV array and it was calculated based on the PV penetration in the UK as shown in Table 5.10. A self-select connected community approach was utilised to obtain the PV percentage for any community size. This means that any CES system was first connected to the homes with PV panels when PVts was investigated. The main reason for this is that homes with PV panels are more likely to form an energy community with a CES system. Additionally, the PV penetration in the UK (less than 1% at the moment and less than 10% by 2020 even in the most optimistic scenarios predicted by DECC) suggested that this is the most sensible approach to follow. For example, Figure 5.15 shows 10 homes in 2020 which eight of them have a PV array according to the projected PV penetration in the UK equal to 7.6%. It was assumed that the PV array of the eighth home had a rating which was 60% of that used for the rest of the homes (3 kW_p).

A home with a PV array was utilised for investigating PVts in the single home scenario due to the fact that the PV penetration (7.6%) is higher than 1% (the community PV percentage is equal to 100%). The home with the most representative annual demand was selected among all homes. The 5-home community was comprised of the home selected for the single home scenario and other four homes with a PV array. The community PV percentage of the 5-home community was equal to 100% because the size of the community is lower than the PV penetration. The community demand loads were obtained when aggregating the different demand loads of the five homes. Finally, the 10-home community was comprised of the 5 homes which represented the 5-home community plus the rest of the

Table 5.10: Community PV and HP percentages based on the PV and HP penetration in the UK. PV penetration and HP penetration are based on estimations from DECC [20]

Parameter	2012	2020	Zero carbon
PV Penetration (%)[a]	< 1	7.6	57
Community PV percentage (%)	100[b]	7.6→100	57→100[c]
HP Penetration (%)[a]	< 1	14	100
Community HP percentage[d] (%)	0	14→100[c]	100

[a]PV penetration and HP penetration based on estimations from DECC [20].
[b]Only a single home with a PV array and without a HP was simulated in 2012.
[c]The minimum and maximum percentages were obtained according to the rationale illustrated in Figure 5.16. The minimum always corresponded to the 100-home community.
[d]The community PV percentage was randomised for any community size larger than 1 home.

homes in Figure 5.15. The community PV percentage was equal to 76%. The community domestic loads were obtained when aggregating the different loads of the 10 homes. Following the same procedure up to a 100 home community, Figure 5.16 shows the community PV percentages obtained for the single home, 5-home, 10-home, 50-home and 100-home communities.

Regarding HPs, they were randomly introduced as the size of the community increased based on the HP penetration for a given reference year. The single home scenario integrated a HP in 2020 to investigate the performance and business case of battery technology in a single home with a HP. Table 5.10 shows the relationship between the PV and HP penetrations in the UK and the PV and HP community percentages respectively. Finally, a total H_2 scenario was considered for studying H_2 storage. This means that the PEMFC system was sized and supplied electricity and heat to all the homes in the community as explained in Section 3.11.1.

5.9 Summary

A novel method was designed to obtain an optimum CES system for end user applications. The method evaluates the performance (round trip efficiency and annual discharge values amongst others), durability and economic benefits of suitable ES technologies by obtaining the *LCOES*, *IRR* and *LVOES*. The method is intrinsically flexible and obtains the CES system which optimizes any performance and economic parameter. The algorithms which implemented the method depending of the ES technology and application using a temporal resolution of 1 minute were discussed in this chapter.

A complimentary methodology was developed including three reference years

(2012, 2020 and a hypothetical zero carbon target) to show the evolution of the business case during the decarbonisation pathway. Reference scenarios together with a sensitivity analysis were designed in order to tackle the uncertainty associated with the main parameters which affect the economic benefits of CES. The reference scenarios and the sensitivity analysis were defined for each combination of ES application, ES technology and reference year based on a selection of demand data, PV penetration, HP penetration and ES technologies characteristics. The method followed a community approach and the optimum CES system was calculated as a function of the size of the community. Robustness is a key characteristics of this optimisation method and it is emphasized by the integration of different ES applications, ES technologies with different time scales and different communities sizes.

Chapter 6

Performance, economic benefits and optimum CES system for end user applications

In this chapter, the results of the application of the optimisation method are presented for the different scenarios defined in Chapter 5. Firstly, results from the baseline scenario are utilised to analyse ES systems located at single homes in 2012. After it, the performance and the economic benefits of CES are discussed depending on the application, PVts and LS, when projected to the year 2020 and to a hypothetical zero carbon target. For both applications, the results from the reference scenarios are firstly presented and then compared with those from the sensitivity analysis defined in Section 5.7. After investigating PVts and LS independently, the last part of this chapter discusses the repercussions of the combination of applications on the performance, economic benefits and optimum CES system.

For any application, performance results are firstly introduced for the different ES technologies as a function of the CES size (electrolyser rating or battery capacity) and the size of the community. When keeping the size of the community constant, understanding the variation * of any parameter with the CES size is possible and vice versa. The analysis of the performance results is then utilised to understand the economic results. For any application, the performance and economic benefits of different ES technologies are compared. Finally, the impact of the size of the community on the performance and economic benefits of CES systems is evaluated.

A key aspect of the performance parameters defined in Section 4.8 is they are dimensionless parameters or parameters which are not proportional to the scale of the CES system. This allowed the direct comparison of the results for any

CES system regardless the size of the community. This consideration can also be extended for the economic parameters. The *LCOES* and *LVOES* are measured in £/kWh, while the *IRR* is a percentage.

6.1 Baseline scenario

As explained in Section 5.5, the baseline scenario describes the current situation of CES in the UK. At the moment, a water tank in a single homes is the only ES system which is widespread in the UK together with electrical storage heaters as discussed in Section 2.4. Alternatively, some companies such as Solom, Hitachi, Saft and SMA Solar Technology AG are launching new battery systems which target single homes, Germany being the country in which the first solutions were offered due to the self-consumption incentives. In the UK the company Power one is launching the first battery system for single homes in 2014 called REACT® which consists of a 4.6 kW single-phase grid connected inverter and a Li-ion battery providing 2 kWh of usable capacity. As a consequence, a water tank and a battery system including PbA and Li-ion technologies performing PVts in a single home are compared for 2012. H_2 technology was not considered in 2012. The battery system only meets the electrical demand load while the water tank only meets the DHW demand load as indicated in Sections 4.5.3 and 5.7.2 respectively. The home selected had an annual electrical demand and DHW demand equal to 3 MWh and 3.3 MWh respectively.

6.1.1 Performance results of battery systems in a single home in 2012

Figure 6.1 shows the *EFC*, round trip efficiency, PV_{ES} and D_{ES} for PbA and Li-ion batteries in a single home. The battery capacity ranged between 1.9 kWh and 19 kWh. The round trip efficiency, PV_{ES} and D_{ES} followed a similar positive logarithmic trend with the capacity and this trend reduced with the capacity, specially in the case of the round trip efficiency of Li-ion technology. A 19 kWh Li-ion battery was able to absorb the 43% of the annual PV generation (PV_{ES}=0.43) and meet the 41% of the annual electrical demand (D_{ES}=0.41) as seen in Table 6.1.

Alternatively, the pattern followed by the *EFC* was different for both battery technologies. In the case of PbA batteries, the *EFC* increased up to a capacity which maximized them. Beyond this capacity, the capacity was misused and increasing the capacity did not increase the *EFC*. Specifically, the maximum *EFC* were 532 EFC and 1883 EFC for a 9.5 kWh PbA and a 1.9 kWh Li-ion battery respectively. According to this result, Li-ion technology used the smallest battery system to maximize the *EFC* while PbA technology needed a capacity which was 5 times larger. This was related to the higher *SOC* range, discharge rating (shown

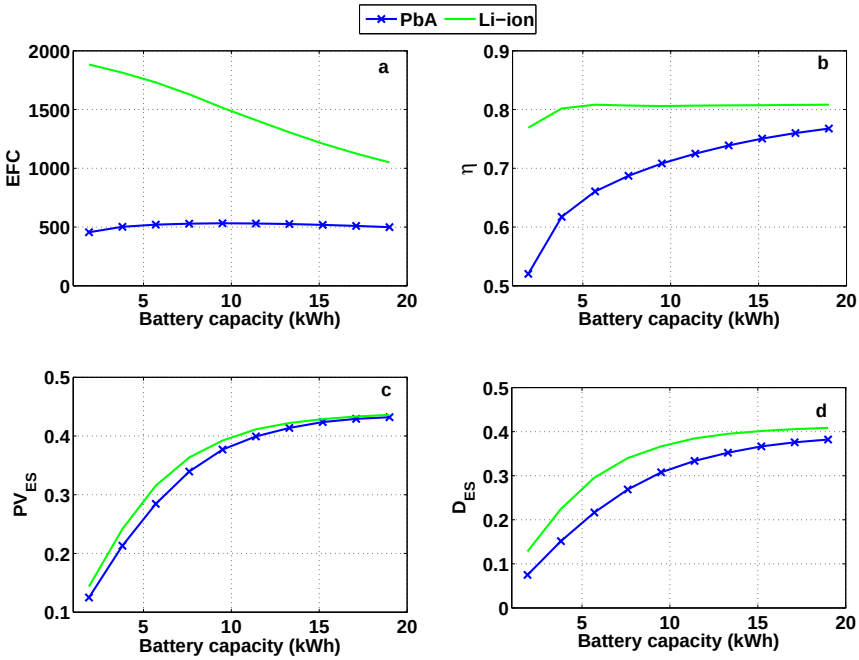

Figure 6.1: Performance results of PbA and Li-ion batteries performing PVts in 2012 as a function of the battery capacity: (a) equivalent full cycles, (b) round trip efficiency, (c) PV_{ES} and (d) D_{ES}.

in Table 4.1) and round trip efficiency up to 0.8 of Li-ion batteries. Li-ion batteries achieved better performance results for any of the parameters as summarized in Table 6.1.

Table 6.1: Performance parameters optimised for PbA, Li-ion and water tank technologies using PVts in 2012. The capacity of the battery (kWh) and the water tank (l) which achieved the optimum values is shown in brackets.

Technology	***EFC***	η	$\boldsymbol{PV}_{ES}$	$\boldsymbol{D}_{ES}$
PbA	532 (9.5)	0.77 (19)	0.43 (19)	0.38 (19)
Li-ion	1883 (1.9)	0.8 (19)	0.44 (19)	0.41 (19)
Hot water tank		0.83 (19)	0.69 (1000)	0.45 (500)

6.1.2 Performance results of hot water tanks in a single home in 2012

As seen in Figure 6.2, the efficiency of the hot water tank decreased with the tank capacity because the water was stored for longer periods despite the ratio between the external area of the tank and the tank volume reduces with the capacity (the external area of the 100 l and 1000 l water tank is 1.59 m^2 and 6.1 m^2 respectively).

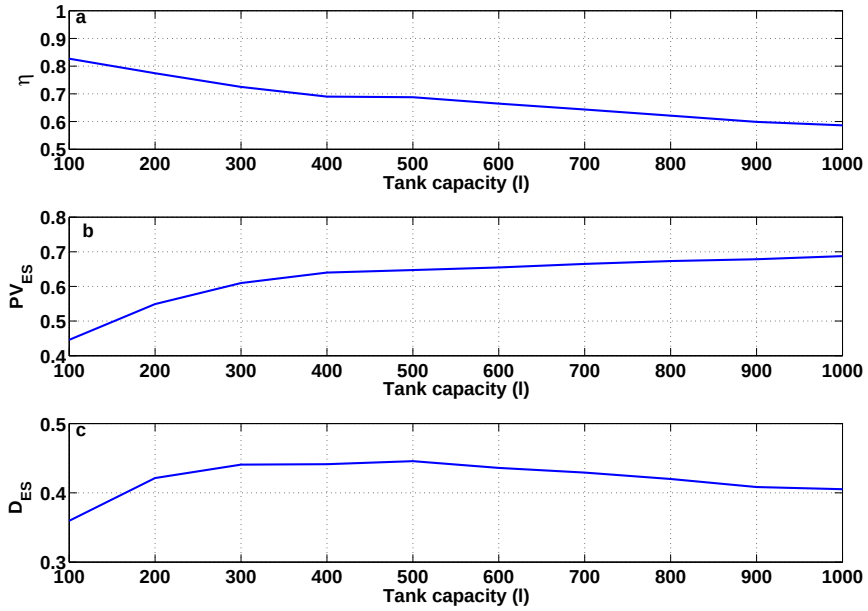

Figure 6.2: Performance results of hot water tanks performing PVts in 2012 as a function of the tank capacity: (a) tank efficiency, (b) PV_{ES} and (c) D_{ES}.

The PV_{ES} followed a logarithmic pattern similar to the one followed by battery systems and grew with the capacity of the tank up to 0.69. Similarly, the D_{ES} grew faster for small capacities but it reached a maximum of 0.45 for a hot water tank capacity equal to 500 l. Beyond this capacity, the efficiency was lower than 0.7 and this affected the final DHW met by hot water tank using PV generation. In other words, the self-discharge of the water tank became important and reduced the D_{ES}.

6.1.3 Economic results for ES systems in a single home in 2012

Based on the performance results, Figure 6.3 shows the *LCOES*, *IRR* and *LVOES* for the three ES technologies in a single home in 2012. For both battery technologies, there was an optimum battery capacity which minimized the *LCOES* of performing PVts. This result was related with the maximum *EFC* discussed above but also the round trip efficiency played a role. While the battery capacities which maximized the *EFC* were 9.5 kWh and 1.9 kWh for PbA and Li-ion technologies, the battery capacities which minimized the *LCOES* were 13.3 kWh and 3.8 kWh respectively as shown in Table 6.2. The minimum *LCOES* were 0.97 £/kWh and 1.5 £/kWh for PbA and Li-ion technologies respectively. The high initial cost of the Li-ion storage medium equal to 1300 £/kWh (260 £/kWh for PbA batteries) was the main reason for the 55% increase.

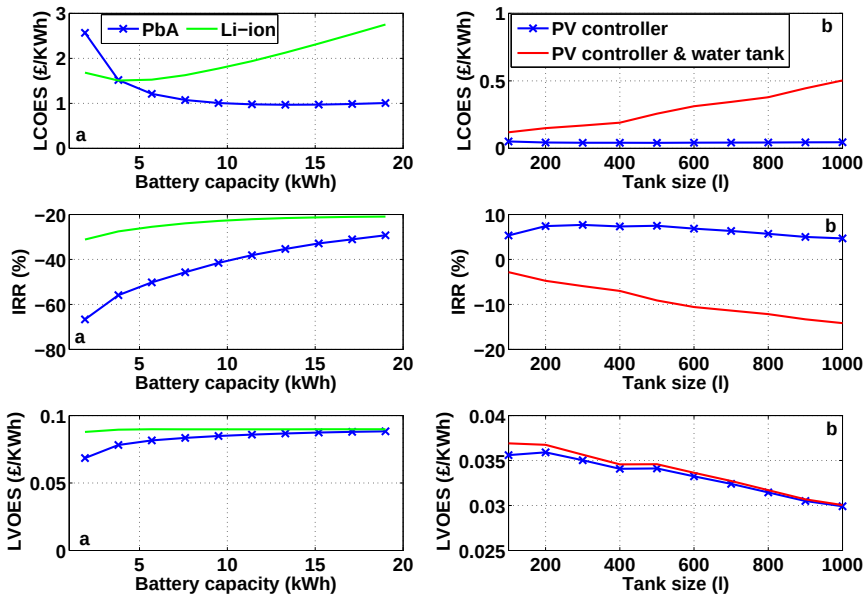

Figure 6.3: (a) *LCOES*, (b) *IRR* and (c) *LVOES* optimised for PbA, Li-ion and water tank technologies using PVts in 2012. The capacity of the battery (kWh) and the water tank (l) which achieved the optimum values is shown in brackets.

The maximum *IRR* was equal to -29.3% and -20.9% for PbA and Li-ion batteries respectively. The longer durability of Li-ion batteries (up to 16 years for the 19 kWh battery) made the *IRR* less negative. The *IRR* increased with battery capacity because the durability was proportional to the battery capacity. However, this should not be used as a conclusion because when the *IRR* is negative, the investment is not attractive and therefore selecting the largest battery capacity should not be the final decision.

Finally, the *LVOES* increased with the battery capacity until it reached a constant plateau. As suggested by Equation 3.2, the revenue obtained by performing PVts i.e the *LVOES* is proportional to the round trip efficiency. The round trip efficiency increases with the battery capacity according to Figure 6.1. The round trip efficiency dependency meant that Li-ion batteries achieved higher *LVOES* than PbA batteries up to 0.09 £/kWh as seen in Figure 6.3.

As explained in Section 4.9.4, two different situations were considered for evaluating the economic results of hot water tanks: the initial cost of the installation only includes the PV controller necessary to divert the surplus PV generation and the initial cost also considers the hot water tank. The *LVOES* of using PV generation to meet the DHW demand load was lower (up to 0.04 £/kWh) than the *LVOES* of using it to meet the electrical demand load (up to 0.09 £/kWh) due to

Table 6.2: Economic parameters optimised for PbA, Li-ion and hot water tank technologies using PVts in 2012. The capacity of the battery (kWh) and the hot water tank (l) which achieved the optimum values is shown in brackets. If the hot water tank already exits, only a PV controller is installed to divert the surplus PV generation.

Technology	***LCOES*** **(£/kWh)**	***IRR*** **(%)**	***LVOES*** **(£/kWh)**
PbA	0.97 (13.3)	-29.3 (19)	0.09 (19)
Li-ion	1.50 (3.8)	-20.9 (19)	0.09 (19)
Tank & PV controller	0.12 (100)	-2.8 (100)	0.04 (100)
PV controller	0.04 (500)	7.5 (500)	0.04 (100)

the lower price of the natural gas as shown in Table 5.1. However, the *IRR* was less negative or even positive when the hot water tank was not considered in the investment. Specifically, a house with a 200-l hot water tank minimized the *LCOES* to 0.04 £/kWh and achieved an *IRR* equal to 7.5% after installing a PV controller.

6.2 PV energy time shift: reference scenarios

Performance results are presented as a function of the battery capacity or the electrolyser rating for battery and H_2 systems, and as function of the size of the community. Ten different battery capacities or electrolyser ratings, as a percentage of the maximum CES demand according to Figure 5.3, were tested for each community. When keeping the size of the community constant, understanding the variation of a parameter with the battery capacity or the electrolyser rating is possible and vice versa.

6.2.1 Performance results of PbA batteries performing PVts when projected to the year 2020

Figure 6.4 shows the *EFC*, round trip efficiency, PV_{ES} and D_{ES} for PbA batteries in 2020 as a function of the size of the community and the battery capacity. The community size only went up to 50 homes due to the low PV penetration in the UK meaning that the community PV percentage had become very small for this size of community (i.e. 15.2% of the homes have a PV installation in the 50-home community). Similarly to the results in a single home, there was an optimum battery capacity which maximized the *EFC* for any community. When the battery capacity was smaller than the optimum, the battery discharged deeper and this impacted on its longevity. If the battery capacity was larger than the optimum, the community did not make use of the whole capacity most days. This increased the operational years but reduced the *EFC*. To illustrate this argument, a PbA

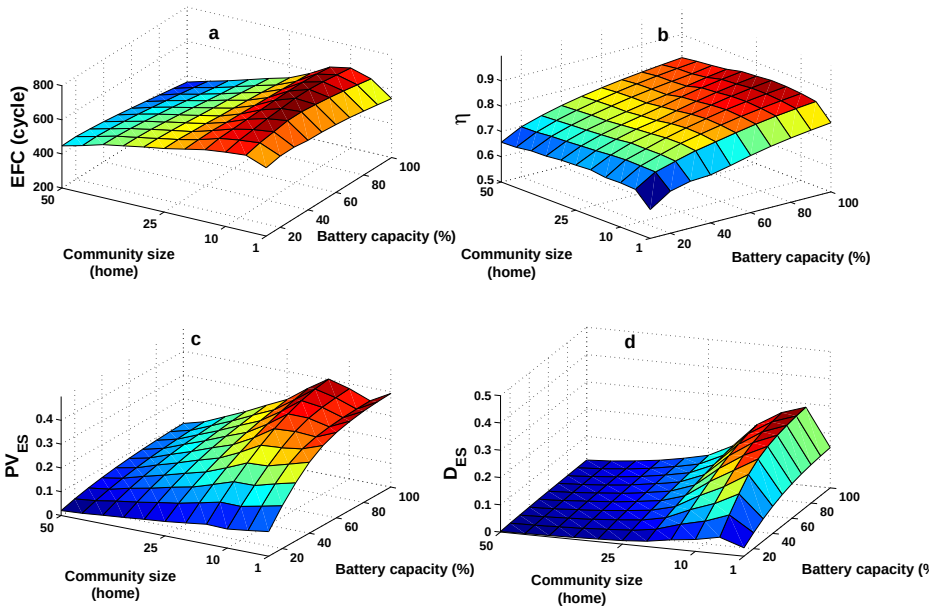

Figure 6.4: Performance results of PbA batteries performing PVts in 2020 as a function of the size of the community and the battery capacity: (a) equivalent full cycles, (b) round trip efficiency, (c) PV_{ES} and (d) D_{ES}. The battery capacity is given as a percentage of the maximum ES demand.

battery with a capacity of 10.4 kWh, 72.8 kWh and 104 kWh achieved 636 EFC, 697 EFC and 669 EFC respectively when performing in the 10-home community. The maximum *EFC* values, 696 EFC and 697 EFC, were obtained in the 5-home and 10-home communities in which the community PV percentage was 100% and 76% respectively. Specifically, a 72.8 kWh PbA battery performing in the 10-home community achieved 697 EFC because it managed more energy on a daily basis and the calendar losses were less relevant. In this case, the ratio between the battery capacity and the maximum discharge rating equal to 11.3 kW (the inverter rating) was more conservative than for the rest of communities. In the case of the 5-home community, the inverter rating was 8.6 kW.

The round trip efficiency increased with the battery capacity for any community. This suggests that the optimum battery capacity is a trade-off between the round trip efficiency and the *EFC*. The round trip efficiency was slightly affected by the size of the community and it remained stable for communities bigger than 25 homes in which the community PV percentage was low (<30%) because the ES management system limited the maximum charge and discharge as explained in Table 4.1. There was only a marked improvement from the single home to the 5-home community due the important effect of the aggregation of demands in this transition. A 1.8 kWh and 18 kWh battery achieved round trip efficiencies equal to 0.61 and 0.77 respectively in the single home while a 7.9 kWh and 79

kWh achieved round trip efficiencies equal to 0.67 and 0.84 respectively in the 5-home community. A PbA battery performing in a single home should cope with relatively high discharge rates for the given battery capacity due to the random demand. The maximum annual round trip efficiency was 0.85 obtained by a 104 kWh PbA battery when performing in the 20-home community.

Figure 6.4 shows that the PV_{ES} increased with the battery capacity for any community. As it was expected, the PV_{ES} was also higher in communities with high community PV percentage. When comparing communities with high community PV percentage, the higher rating of the inverter in those which were bigger increased the PV_{ES}. For example, the PV_{ES} was 0.08 and 0.4 for a 11 kWh and a 100 kWh battery in the 15-home community, 0.4 being the maximum result in 2020. The single home offered the highest mismatch between the PV generation and the demand load (30%) and this meant that the PV_{ES} was slightly higher than for the 5-home community and equal to 0.39 for a 79 kWh battery. Likewise, the D_{ES} followed a similar pattern to the PV_{ES}. It increased with the battery capacity for any community size and it was proportional to the community PV percentage. The maximum D_{ES} equal to 0.29 was obtained by a 79 kWh battery in the 5-home community.

6.2.2 Performance results of Li-ion batteries performing PVts when projected to the year 2020

Figure 6.5 shows the performance parameters for Li-ion batteries in 2020. The PV_{ES} and D_{ES} were equally affected by the capacity and the community size as they were for PbA technology. However, Li-ion technology achieved higher absolute values due to the higher SOC range, discharge capability and round trip efficiency. The maximum PV_{ES} and D_{ES} were 0.41 and 0.29 for a 110 kWh battery in the 15-home community and 79 kWh battery in the 5-home community respectively. However, the *EFC* and the round trip efficiency followed different patterns in addition to be greater.

The *EFC* reduced with the battery capacity in comparison with PbA technology which offered a more constant plateau with the battery capacity for any community size. For PbA technology, the maximum *EFC* were achieved by middle-sized batteries i.e. capacities in the middle of the capacity range: 12.6 kWh, 39.5 kWh 72.8 kWh for the single home, 5-home community and 10-home community respectively. However, the greatest *EFC* were obtained by the smallest battery system for Li-ion technology (7.2 kWh, 23.7 kWh 31.2 kWh for the single home, 5-home community and 10-home community respectively). Li-ion batteries did not need large capacities to cope with high charge and discharge rates and avoid

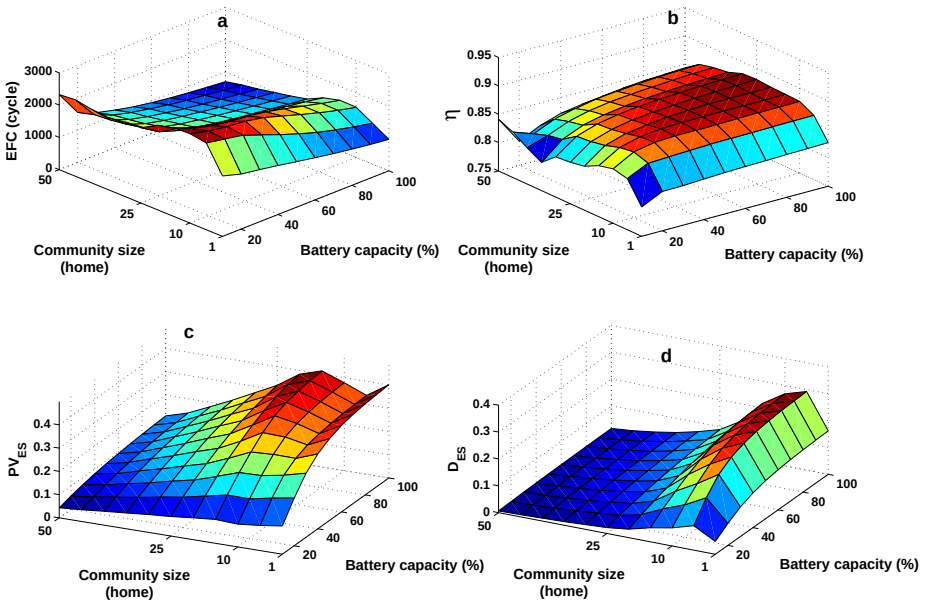

Figure 6.5: Performance results of Li-ion batteries performing PVts in 2020 as a function of the size of the community and the battery capacity: (a) equivalent full cycles, (b) round trip efficiency, (c) PV_{ES} and (d) D_{ES}. The battery capacity is given as a percentage of the maximum ES demand.

severe ageing in comparison with PbA technology. In fact, 2770 EFC were obtained by a 10.4 kWh battery in the 10-home community, this value being the highest. Regarding the round trip efficiency, it was less affected by the battery capacity for any community. There was also clear evidence of efficiency improvement in the transition between the single home to the 5-home community. The maximum round trip efficiency was 0.88 for a 88 kWh battery in the 25-home community.

6.2.3 Performance results of H_2 systems performing PVts when projected to the year 2020

Figure 6.6 shows the C_{factor}, electrolyser efficiency, PV_{ES} and H_{2ratio} as defined in Section 4.8.2. For any community, the C_{factor} i.e. the number of operational hours slightly reduced with the electrolyser rating since a bigger electrolyser did not take advantage of the PV generation when it is lower than its parasitic losses (which were assumed equal to the 10% of the electrolyser rating in Section 4.5.2). For example, the C_{factor} of a 1.1 kW and a 12.9 kW electrolysers were 0.3 and 0.22 respectively in the 5-home community. Likewise, the efficiency of the 1.1 kW electrolyser was 0.66 while only 0.58 for the 12.9 kW electrolyser. According to Figure 6.6, the electrolyser efficiency reduced with the rating for any community

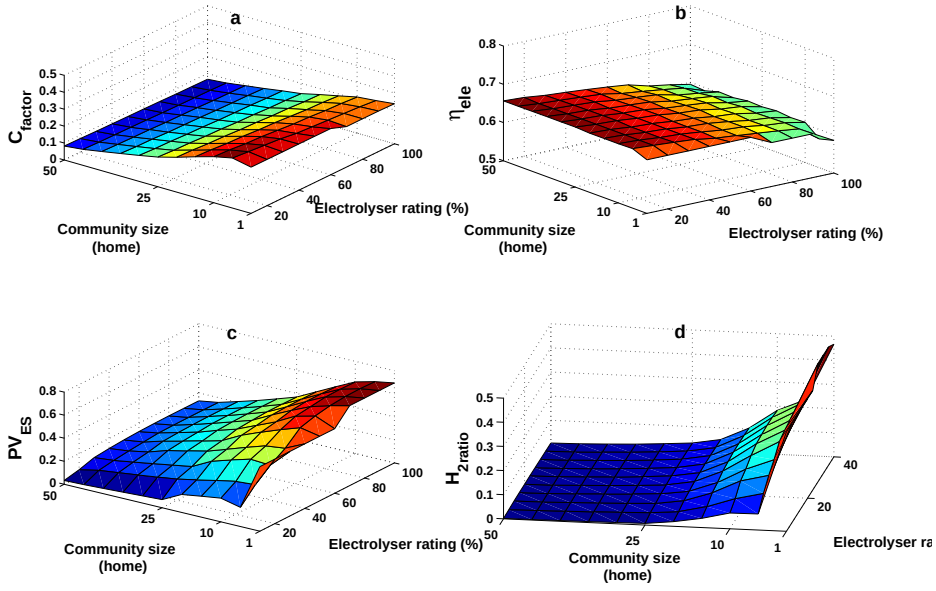

Figure 6.6: Performance results of H_2 systems performing PVts in 2020 as a function of the size of the community and the electrolyser rating: (a) capacity factor, (b) electrolyser efficiency, (c) PV_{ES} and (d) H_{2ratio}. The electrolyser rating is given as a percentage of the maximum ES demand.

and kept constant with the community size. For any community, the partial load operation became more important as the electrolyser rating increased.

The PV_{ES} followed a similar trend to those described with battery technology but values were considerably higher because the power rating of a H_2 storage system does not limit the maximum daily charge (kWh, as it happened with battery technology). For example, a 2.3 kW and a 12.8 kW electrolysers were able to utilise 69% and 66% of the total PV generation for the single home and the 5-home community respectively.

According to Figure 6.6, the H_{2ratio} did not increase significantly with the electrolyser rating for any community but it reduced markedly with the size of the community. In order to understand these effects, the H_{2ratio} obtained by a 2.2 kW electrolyser and a 18.0 kW electrolyser in the 10-home community was 0.07 and 0.18 respectively while the H_{2ratio} of a 1.1 kW electrolyser in the single home and in the 5-home community was 0.41 and 0.07 respectively. As it was argued in Section 3.11.1, the ratio between the size of the PEMFC system and the community size increased with the size of the community due to the positive impact of the aggregation of demands. As a result, the relatively weight of the H_2 generated by the electrolysers reduced with the community size. Moreover, the community PV percentage which is a measurement of the surplus available PV generation for

the CES system also affected the H_2 generated by the PEM electrolyser and the H_{2ratio} as a result.

Consequently, increasing the electrolyser rating had two opposite effects on the H_2 generation for any community. On the one hand, a larger electrolyser is able to absorb more PV generation when this is high (typically at midday). On the other hand, the parasitic losses become more important and this reduces the electrolyser efficiency, specifically its ability to make use of the low PV generation on cloudy days, when the sun rises and during the sunset periods.

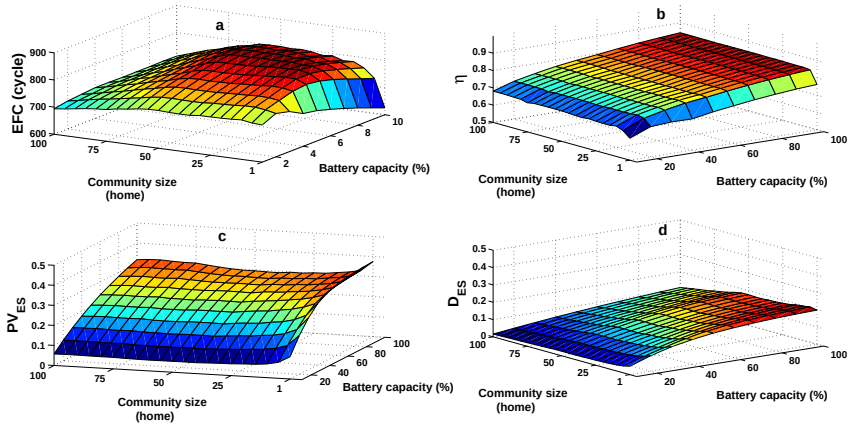

Figure 6.7: Performance results of PbA batteries performing PVts in the zero carbon year as a function of the size of the community and the battery capacity: (a) equivalent full cycles, (b) round trip efficiency, (c) PV_{ES} and (d) D_{ES}. The battery capacity is given as a percentage of the maximum ES demand.

6.2.4 Performance results of PbA, Li-ion and H_2 technologies performing PVts when projected to a hypothetical zero carbon year

Figures 6.7, 6.8 and 6.9 show the same performance parameters discussed in 2020 for PbA, Li-ion and H_2 technologies respectively in the zero carbon year. There are two main aspects to consider when comparing these results to those in 2020. Results are shown up to the 100-home community because the PV penetration in the UK was assumed to be 57% (much higher than 7.6% in 2020). Secondly, the reduction of the ES technology cost and the durability improvement assumed for the zero carbon target defined in Table 5.4 impacted on the performance results.

The community PV percentage was 100% up to the 55-home community and results were less affected by the community PV percentage than in 2020. This

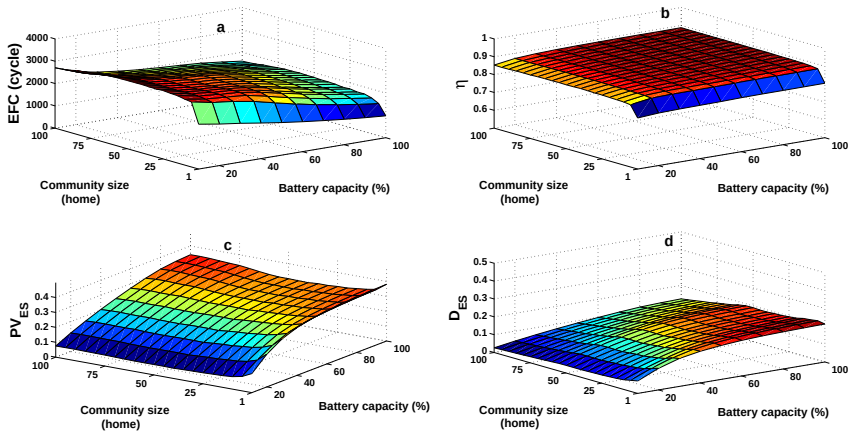

Figure 6.8: Performance results of Li-ion batteries performing PVts in the zero carbon year as a function of the size of the community and the battery capacity: (a) equivalent full cycles, (b) round trip efficiency, (c) PV_{ES} and (d) D_{ES}. The battery capacity is given as a percentage of the maximum ES demand.

allowed to investigate the impact of the community size for a constant community PV percentage (100%). The different performance parameters followed a similar pattern to that followed in 2020 over a wider community size range. The highest PV_{ES} equal to 0.39 for a 55 kWh battery occurred at the single home due to

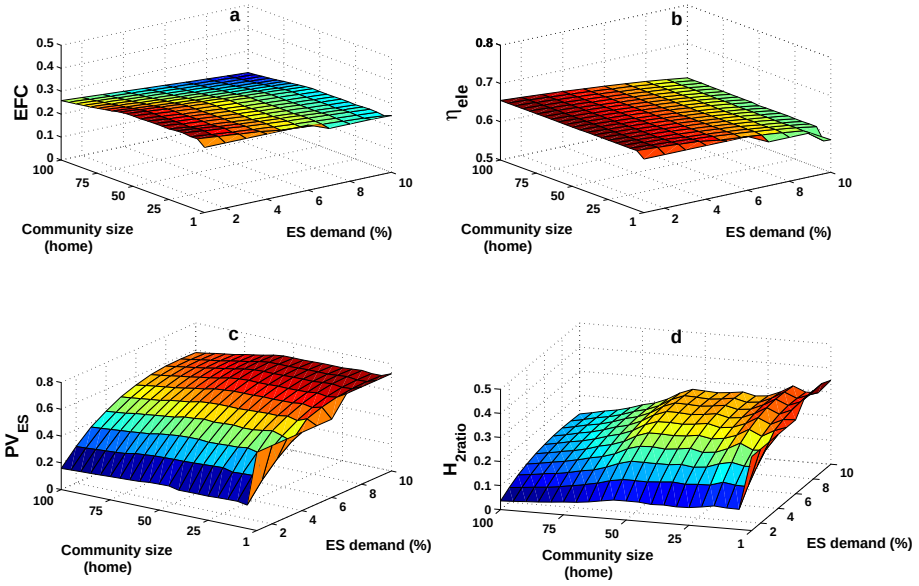

Figure 6.9: Performance results of H_2 systems performing PVts in the zero carbon year as a function of the size of the community and the electrolyser rating: (a) capacity factor, (b) electrolyser efficiency, (c) PV_{ES} and (d) H_{2ratio}. The electrolyser rating is given as a percentage of the maximum ES demand.

Table 6.3: Performance parameters optimised for PbA batteries, Li-ion batteries and H_2 systems performing PVts in the zero carbon year. The size of the community and the capacity of the battery (kWh) or the rating of the electrolyser (kW) which achieved the optimum values is shown in brackets.

Year	technology	$\boldsymbol{EFC/C_{ratio}}$	η/η_{ele}	$\boldsymbol{PV_{ES}}$	$\boldsymbol{D_{ES}/H_{2ratio}}$
2020	PbA	697 (10,72.8)	0.85 (20,702)	0.40 (15,100)	0.29 (5,79)
	Li-ion	2770 (10,10.4)	0.88 (25,88)	0.41 (15,110)	0.30 (5,79)
	H_2	0.30 (5,1.1)	0.66 (25,1.1)	0.69 (1,2.3)	0.49 (1,2.2)
Zero carbon	PbA	827 (15,102.6)	0.84 (95,702)	0.37 (1,19)	0.20 (5,72)
	Li-ion	3065 (25,26.6)	0.89 (100,704)	0.38 (1,19)	0.22 (5,72)
	H_2	0.31 (15,3.4)	0.66 (95,13.5)	0.73 (1,2.3)	0.37 (1,2.2)

the mismatch between the PV generation and the demand (70%) and then the PV_{ES} followed a quite constant plateau up to the 60-home community. Table 6.3 compares the optimum values for each performance parameter obtained by each technology.

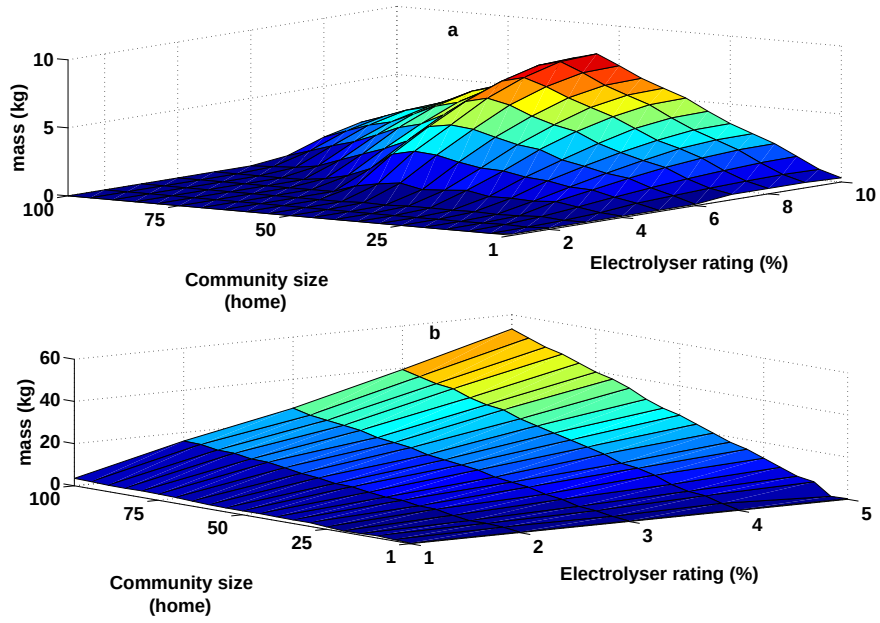

Figure 6.10: Required H_2 tank size for PVts (a) and LS (b) as a function of electrolyser rating and the size of the community in the zero carbon year.

Finally, Figure 6.10 shows the H_2 tank size for PVts in the zero carbon year as a function of the electrolyser rating and the size of the community. H_2 storage requirements were limited by the performance of the PEMFC systems for any community, for example an 80 kW electrolyser performing in a 60-home community

the tank storage capacity was 7.8 kg of H_2. Although the rating of the electrolyser (shown in Figure 6.14) was always higher than the rating of the PEMFC system for any community (shown in Figure 3.10), the PEMFC systems run continuously each day of the year. Secondly, the round trip efficiency of H_2 storage also played role. Only up to 66% of the electricity consumed by the electrolysers was transformed into H_2 as shown in Figure 6.9 and the total efficiency of the PEMFC systems was around 73% as shown in Figure 3.11 (round trip efficiency of 48%).

6.2.5 Economic results of PbA, Li-ion and H_2 technologies performing PVts when projected to the year 2020

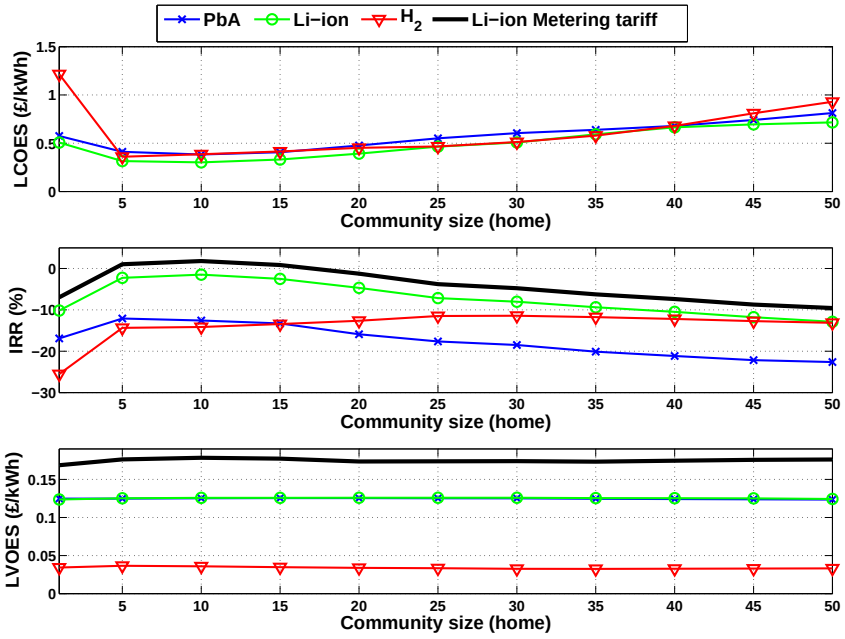

Figure 6.11: (a) *LCOES*, (b) *IRR* and (c) *LVOES* optimised for PbA batteries, Li-ion batteries and H_2 systems performing PVts in 2020 as a function of the size of the community.

Figures 6.11 shows the optimum values of the *LCOES*, *IRR* and *LVOES* for PbA, Li-ion and H_2 technologies when performing PVts in 2020 as a function of the size of the community. The *LCOES* and the *LVOES* associated with electricity generation in shown for H_2 technology. The pattern followed by the *LCOES* and the *IRR* (in less extent) was drastically affected by the community PV percentage. For communities with more than 25 homes in 2020, the low community PV percentage (<15%) limited the charge of the CES system. In 2020, PbA, Li-ion and H_2 technologies offered the lowest *LCOES* (0.38 £/kWh, 0.30 £/kWh 0.36 £/kWh$_e$ respectively) and the highest *IRR* (-12.1%, -1.5% and -12.1% respectively) for the 5-home and 10-home communities with a community PV percentage higher than 75%.

The minimum *LCOES* and the minimum *IRR* were found at the 10-home community because in addition to the high surplus PV generation (PV percentage equal to 76%), the higher rating of the inverter increased the annual charge (and the *EFC*) in comparison with the 5-home community (with a community PV percentage of 100%). This fact also maximized the *EFC* as discussed in the previous section. In the case of H_2 storage, the converter of the electrolyser was sized according to the surplus PV power generation and therefore the *LCOES* was minimized for the 5-home community in which more surplus PV generation was available (community PV percentage equal to 100%). If the cost of the storage medium for Li-ion reduces down to 310 £/kWh by 2020, Li-ion will be the most attractive technology for performing PVts.

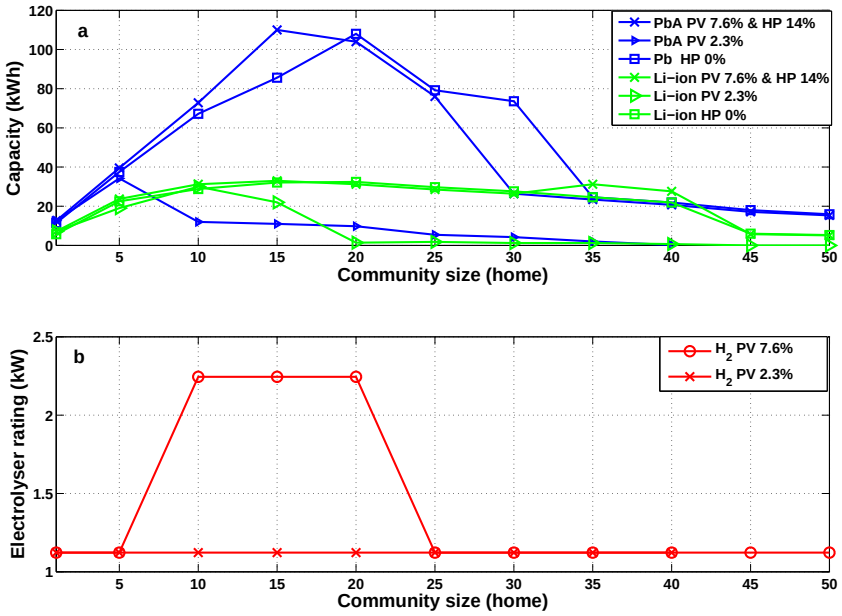

Figure 6.12: Optimum CES system which minimised the levelised cost, *LCOES*, associated with PVts as a function of the community size for (a) PbA and Li-ion batteries; (b) and H_2 systems in 2020.

The optimum battery capacity and electrolyser rating which reduced the cost of performing PVts is represented as a function of the size of the community in Figure 6.12. The optimum sizes increased steadily up to 72.8 kWh, 31.2 kWh and 1.1 kW for PbA, Li-ion and H_2 technologies in the 10-home community. For communities with more than 10 homes, the optimum sizes reduced due to the lower community PV percentage (<50%). The change in the trend was more sharply for PbA technology than for Li-ion technology due to its lower round trip efficiency, discharge rating and *SOC* range according to the values defined in Table 4.1.

Table 6.4: Economic parameters optimised for PbA batteries, Li-ion batteries and H_2 systems performing PVts in the zero carbon year. The size of the community and the capacity of the battery (kWh) or the rating of the electrolyser (kW) which achieved the optimum values is shown in brackets.

Year	**Technology**	***LCOES*** **(£/kWH)**	***IRR*****(%)**	***LVOES*****(£/kWH)**
2020	PbA	0.38 (10,72.8)	-12.1 (5,79)	0.13 (15,110)
	Li-ion	0.30 (10,31.2)	-1.5 (10,41.6)	0.13 (15,110)
	H_2	0.36_e (5,1.1)	-14.1 (10,2.2)	0.04 (5,1.1)
Zero carbon	PbA	0.11 (60,569)	39.1 (60,512.1)	0.27 (60,569)
	Li-ion	0.13 (60,341.4)	25.0 (60,341.4)	0.27 (60,569)
	H_2	0.18_e (60,26.9)	24.5 (60,26.9)	0.14 (5,1.1)

Even with the ES technology cost reduction assumed for 2020, the *IRR* was negative for any community in 2020. However, Li-ion batteries with a capacity of 24 kWh and 31 kWh in the 5-home and 10-home communities achieved *IRR* values equal to -2.3% and -1.5% respectively. This means that relatively financial support would be necessary to make the *IRR* positive. However, the *IRR* was much lower than the discount rate used in the economic model (10%). Therefore, the minimum value of the *LCOES* obtained in 2020 (0.30 £/kWh for a 31 kWh Li-ion battery in the 10-home community) was always higher than the *LVOES* (0.13 £/kWh). The *LCOES* for PbA and H_2 technologies increased up to 0.38 £/kWh (a 73 kWh battery in the 10-home community) and 0.36 £/kWh_e (a 1.1 kW electrolyser in the 5-home community) respectively. In addition to the initial cost, the other main reason why the *LCOES* was higher than the *LVOES* was CES systems only performed for some hours around midday (8 hours maximum considering the charge and discharge) due to the daily pattern followed by the solar irradiance and the demand load (in less extent) as shown in Figure 3.2.

The maximum *LVOES* was quite flat no matter the size of the community. As Equations 3.2 and 3.4 indicate, the maximum *LVOES* is achieved by the CES system which performs more efficiently for any community. The maximum efficiency kept constant with the community size as seen in Figures 6.4, 6.5 and 6.6. For the battery technology, the maximum round trip efficiency was achieved by the largest battery system for any community and the values achieved by both battery technologies were quite similar. As discussed above, the maximum electrolyser efficiency was achieved by the smallest electrolyser for any community. The maximum *LVOES* ranged between 0.12 £/kWh and 0.13 £/kWh for PbA and Li-ion battery technologies when the price of the electricity was 0.165 £/kWh and the export tariff was 0.032 £/kWh in 2020. The maximum *LVOES* value associated with H_2 was lower than for the battery technology because the PEMFC system efficiency (shown in Figure 3.11) reduced the round trip efficiency. Secondly, H_2

storage generates electricity and heat and the heat generated had a lower value since the price of the natural gas is lower (7.4 £/kWh in 2020). This reduced the *LVOES* to 0.04 £/kWh in 2020.

6.2.6 Economic results of PbA, Li-ion and H_2 technologies performing PVts when projected to a hypothetical zero carbon year

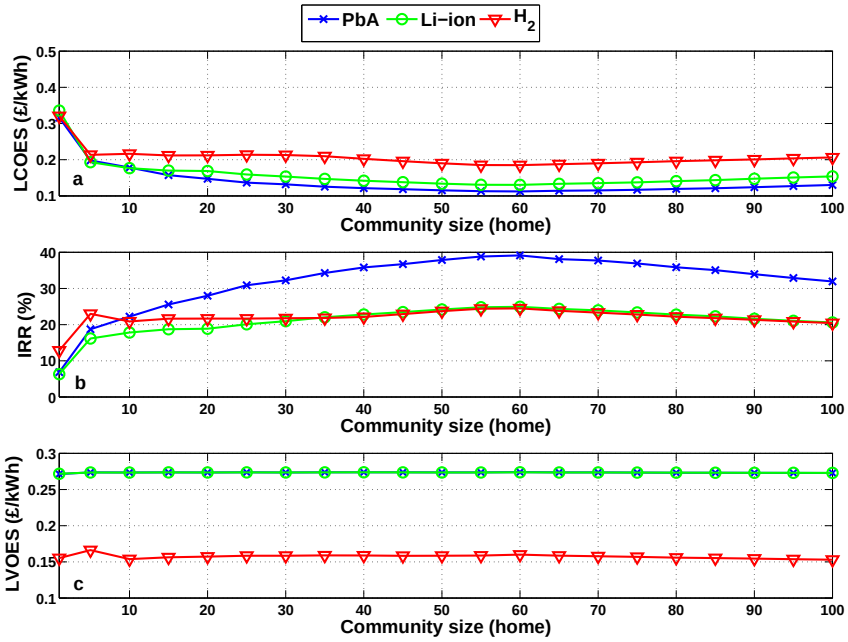

Figure 6.13: (a) *LCOES*, (b) *IRR* and (c) *LVOES* optimised for PbA batteries, Li-ion batteries and H_2 systems performing PVts in the zero carbon year as a function of the size of the community.

Opposite to 2020, there was a business case for any community in the zero carbon year and just for the single home the *LCOES* (0.32 £/kWh, 0.34 £/kWh and 0.31 £/kWh for PbA, Li-ion and H_2 technologies respectively) was higher than the *LVOES* (0.27 £/kWh for both battery technologies and 0.13 £/kWh for H_2 technology). However, the optimum case was given by the 60-home community (with a community PV percentage equal to 95%). Considering an initial cost of 65 £/kWh for PbA batteries, the minimum *LCOES* was equal to 0.11 £/kWh and it was achieved by a 569 kWh battery in this community. The effect of the community PV percentage was smoothed in the zero carbon year due to the higher PV penetration.

The maximum *LVOES* which ranged around 0.27 £/kWh was higher than the

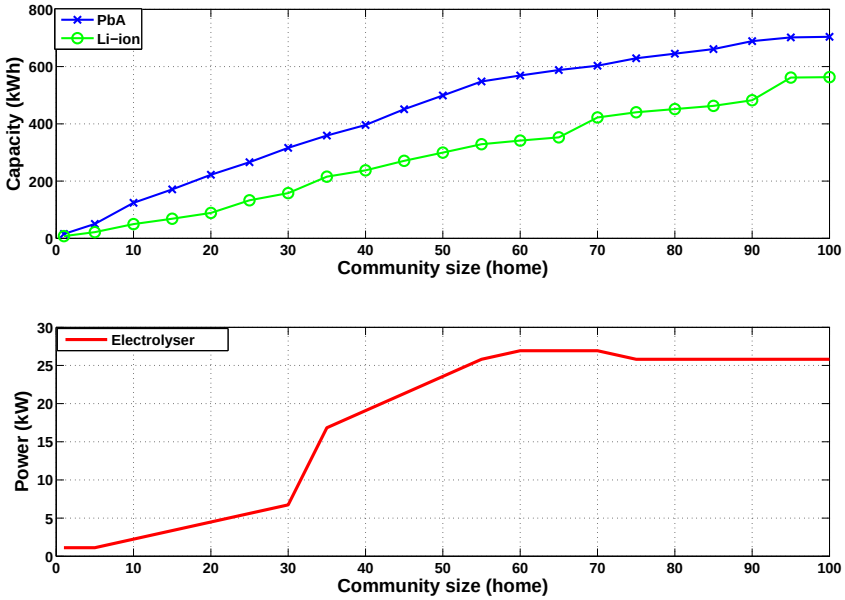

Figure 6.14: Optimum CES system which minimised the levelised cost, *LCOES*, associated with PVts as a function of the community size for (a) PbA and Li-ion batteries; (b) and H_2 systems in the zero carbon year.

LCOES and this created very positive *IRR* up to 39% for a 512 kWh PbA battery in a 60-home community. Likewise, a 341 kWh Li-ion battery minimized the *LCOES* to 0.13 £/kWh and maximized the *IRR* to 25%. Finally, a 27 kW electrolyser minimized the *LCOES* to 0.18 £/kWh$_e$ while the *LVOES* ranged between 0.15 £/kWh and 0.17 £/kWh for H_2 technology. Figure 6.10 demonstrates that optimum electrolyser also minimized the H_2 tank requirements and therefore minimized the initial cost of the H_2 system.

Figure 6.14 shows the battery capacities and electrolyser ratings which minimized the *LCOES* associated with PVts in the zero carbon year. The ratio between the optimum battery capacity and the number of homes did not reduce markedly with the size of the community for a constant community PV percentage. However, the positive impact of the aggregation of demands on the performance improved the economic results with the size of the community. The steep change in the optimum electrolyser rating between the 30-home and the 35-home community was due to the reduction of cost assumed for electrolyser with a rating higher than 10 kW explained in Section 4.9.4.

The cost reduction expected for the three ES technologies will determine the best option for PVts. With the input data selected, Li-ion (310 £/kWh) technology was the best option in 2020 and PbA (65 £/kWh) was the best option for zero carbon scenario. Similarly to what happened in 2020, there was a change

in the trend of the optimum CES system at the 60-home community due to the reduction of the community PV percentage. This change in the trend was very clear for the electrolyser rating because the rating is proportional to the maximum surplus PV power. The trend variation was also more marked for PbA technology than for Li-ion technology as it happened in 2020. According to this figure, PbA batteries needed from 2.5 to 1.5 times more capacity than Li-ion batteries to reduce the *LCOES*, 2.5 being related to the smallest communities in which the random demand load requested larger PbA battery capacities.

6.3 PV energy time shift results: Sensitivity analysis

6.3.1 Energy storage technology sensitivity

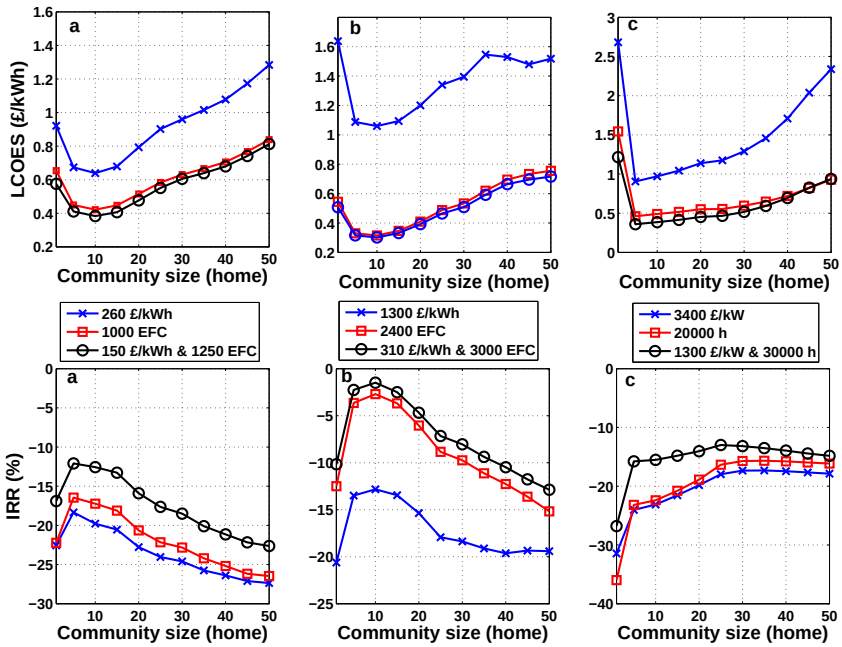

Figure 6.15: *LCOES* and *IRR* optimised for (a) PbA, (b) Li-ion and (c) H_2 technologies using PVts in 2020 depending on the cost and durability characteristics.

The results of the ES technology sensitivity analysis are based on the data presented in Tables 5.5 and 5.6 for battery and H_2 technologies respectively. Results for 2020 are presented in Figure 6.15. The cost and durability of the technology affected the *LCOES* and the *IRR* associated with PVts but they did not affected the *LVOES* (the durability of the project is considered in the calculation but its effect can be neglected). As a consequence, the *LVOES* was not shown in the results. While the cost and durability affected the absolute values of the

LCOES and the *IRR*, the pattern of the curves were not affected. According to this, the optimum CES systems obtained for the reference scenarios were not affected by the cost and durability.

Figure 6.15 demonstrates that the technology cost affected more the *LCOES* and the *IRR* than the durability. This was especially marked for Li-ion technology for which the cost of the storage medium varied between 310 £/kWh and 1300 £/kWh. If the results from the reference scenarios pointed out the great potential of Li-ion batteries for PVts and this technology maximized the *IRR* (-1.5%) and reduced the *LCOES* (0.30 £/kWh) when the cost went down to 310 £/kWh in 2020, Figure 6.15 indicates that the *IRR* reduced to -12.8% and the *LCOES* increased to 1.1 £/kWh when the cost of the storage medium goes up to 1300 £/kWh. This meant a 250% increase in the *LCOES* of Li-ion technology regarding the reference scenario. H_2 cost uncertainty also had a great impact on the results. The optimum *LCOES* of H_2 grew to 0.9 £/kWh$_e$ and the *IRR* declined to -17.3% respectively. The *LCOES* rose to 0.64 £/kWh in the case of PbA technology which is the technology with less cost uncertainty. Results indicated that if the technology costs keep constant, PVts should not be considered as a business case maker.

In addition to the lower uncertainty assumed for the technology durability presented in Tables 5.5 and 5.6, the impact of the durability in the *LCOES* was not as marked as the impact of the cost because the time value of money. Figure 6.15 shows that he *IRR* was more sensitive to the durability than the *LCOES*. Specifically, the maximum *IRR* reduce down to -16.4%, -2.7% and -15.7% for PbA, Li-ion and H_2 technologies when the durability characteristics kept constant with the baseline scenario.

Figure 6.16 shows the results of the sensitivity of the ES technology characteristics in the zero carbon year. If the cost keeps constant with those assumed for the reference scenarios in 2020, the minimum *LCOES* is 0.22 £/kWh (+96%), 0.35 £/kWh (+169%) and 0.12 £/kWh (-31%) and the maximum *IRR* is 16.1% (-59%) , 6.5% (-74%) and 17.7% (-26%) for PbA, Li-ion and H_2 technologies respectively. The *IRR* was still positive for the three ES technologies in most community sizes, but it was negative for the PbA (-2.4%) and Li-ion (-5.7%) technologies in the single home. However, the durability did not affected the business case and the value of the economic parameters varied scarcely and only for H_2 there was a 15% increase in the *LCOES*.

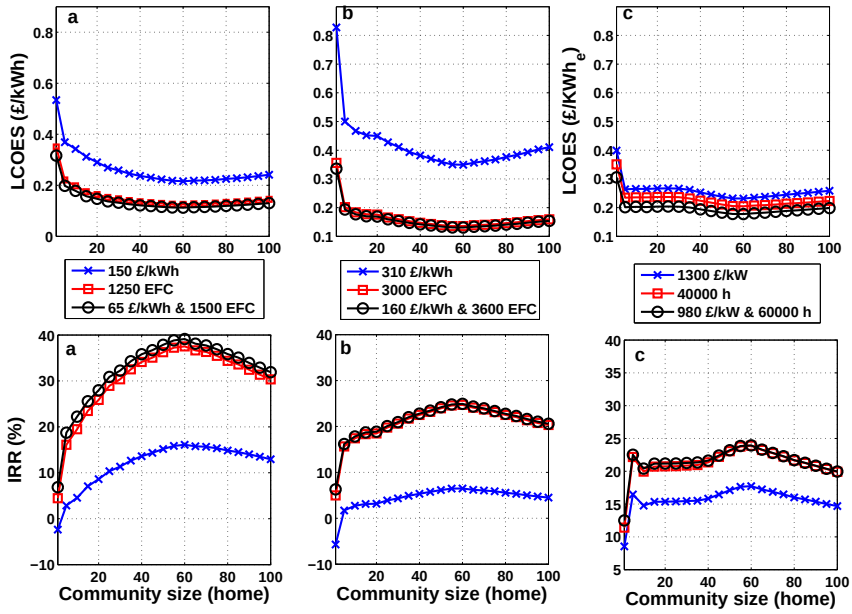

Figure 6.16: *LCOES* and *IRR* optimised for (a) PbA, (b) Li-ion and (c) H_2 technologies using PVts in the zero carbon year depending on the cost and durability characteristics.

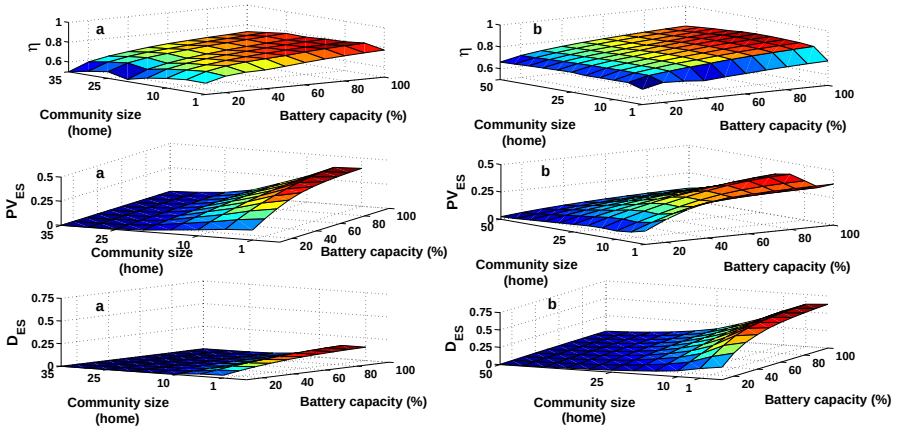

Figure 6.17: Performance results of PbA batteries performing PVts in the zero carbon year as a function of the size of the community and the battery capacity when (a) the PV penetration was assumed to be 2.3% and (b) the HP penetration was assumed to be 0% in the UK.

6.3.2 Demand and PV sensitivity

PVts is an application which increases the amount of PV generation consumed on-site and therefore results are affected by the community PV percentage and the demand. The community PV percentage was based on the PV penetration as explained in Section 5.8. The maximum surplus PV power determined the electrolyser rating and the maximum demand load fixed the the inverter rating of battery systems as detailed in Section 4.6. According to the results from the

reference scenarios, the business case for PVts was dramatically affected by the community PV percentage and the optimum results occurred when this was higher than 75%. The reference scenarios for 2020 assumed a PV penetration equal to 7.6% and a HP penetration of 14%. The sensitivity presented in this section analyses how the performance and economic results were affected when the PV penetration reduced to 2.3% and the HP penetrations reduced to 0% independently in 2020.

Results from PbA technology are utilised here to explain how the PV penetration and the HP penetration affected the performance as shown in Figure 6.17. The round trip efficiency, PV_{ES} and D_{ES} were selected to illustrate the effect on the performance. According to Figure 6.17, the round trip efficiency was not affected due to the way that the CES systems were sized based on the available surplus PV energy and the management system on place defined in Table 4.1. The maximum round trip efficiency, 0.81, was achieved by a 38 kWh battery in the 5-home community.

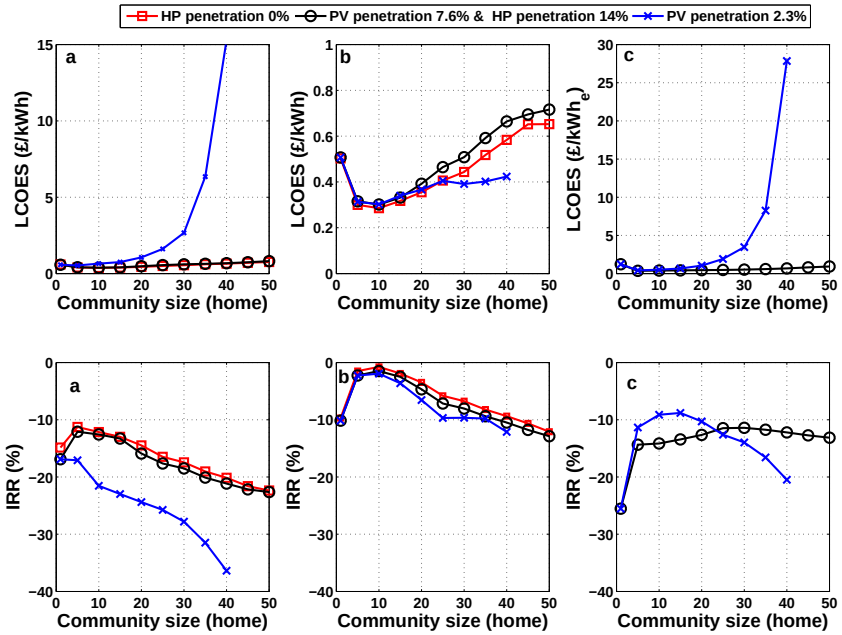

Figure 6.18: *LCOES* and *IRR* optimised for (a) PbA, (b) Li-ion and (c) H_2 technologies using PVts in 2020 depending on the PV and HP penetration.

The lower PV penetration and HP penetration had a greater impact on the PV_{ES} and the D_{ES}. The PV_{ES} reduced steadily as the the PV generation did for communities of more than 10 homes since a higher fraction of the PV generation was directly taken by the demand load. When comparing two CES systems of the same size in the same community but with different community PV percentages,

the PV_{ES} was lower when the community PV percentage was higher due to the dramatically increase of the total community PV generation which is not utilised by the CES. For example, a 30 kWh PbA battery (maximum capacity) offered a PV_{ES} equal to 0.27 in the 10-home community with a community PV percentage of 24%. When the PV percentage was 76%, a 104 kWh battery (maximum capacity) and a 33 kWh battery only utilised 37% and 20% of the total PV generation respectively in the same community.

The D_{ES} was also reduced when the PV penetration was 2.3% because the annual discharge reduced sharply as the community size increased. Only the 6% of the total electrical demand was met by the 30 kWh PbA battery in the 10-home community when the community PV percentage was 24%. However, a 31 kWh and a 104 kWh battery were able to meet 12% and 26% of the total demand respectively when the community PV percentage was 76%.

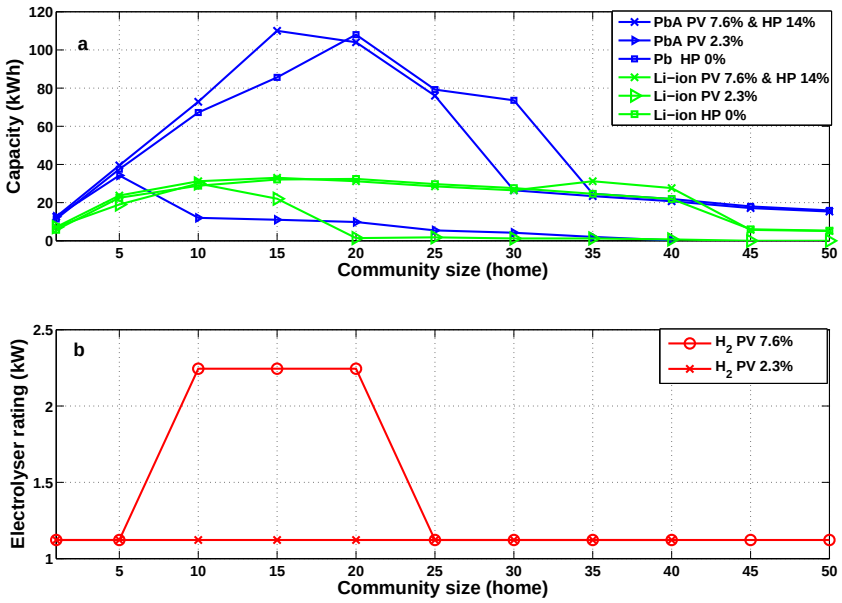

Figure 6.19: Optimum CES system which minimised the levelised cost, *LCOES*, associated with PVts as a function of the community size for (a) PbA, (a) Li-ion and (b) H_2 technologies depending on the PV and HP penetration in 2020.

Likewise, the PV_{ES} and the D_{ES} were affected by the HP penetration in 2020. The PV_{ES} did not vary significantly regarding the reference scenario because HP introduced two opposite effects on the community. Firstly, the amount of surplus PV energy available for charging the CES reduced when HPs were utilised. However, the inverter rating of the battery system increased as shown in Figure 4.7 and this allowed the faster charging of the CES system. In fact, the consideration of HPs increased the demand load and more energy was stored when possible to

meet the larger demand requirement. These effects counterbalanced each other and the PV_{ES} did not vary markedly when the HP penetration varied from 14% to 0%. The PV_{ES} of a 96 kWh PbA battery in the 10-home community was 0.36 without HPs while it was 0.38 for a 104 kWh PbA battery with a HP penetration of 14%. Regarding the D_{ES}, it rose steeply without HPs due to the much lower electrical demand. The same batteries as before were able to supply 26% and 49% of the total demand of the 10-home community with or without HPs respectively.

Figure 6.18 analyses the impact of the PV and HP penetrations in the *LCOES* and the *IRR*. The HP penetration was not discussed for H_2. For PbA and H_2 technologies, the PV penetration steeply changed the *LCOES* and *IRR* results in comparison with the reference scenario. In the case of H_2, the lower community PV percentage reduced the C_{factor}, the maximum value being 0.23 at the single home. As a consequence, results were only represented up to the 40-home community because the trend became asymptotic for the *LCOES*. The minimum *LCOES* increased to 0.53 £/kWh (+39%) and 0.42 £/kWh (+17%) and the maximum *IRR* declined to -16.9 % (-40%) and -8.8 % (-38%) for PbA and H_2 technologies when compared with the reference scenarios. For PbA technology, the community approach did not add value due to the low PV penetration and the lowest *LCOES* (0.58 £/kWh) and highest *IRR* (-16.9%) were given at a single home.

Li-ion batteries offered the best response with the 2.4% PV penetration and a 30 kWh battery achieved the minimum *LCOES* and the maximum *IRR* equal to 0.30 £/kWh and -1.9 % respectively in the 10-home community. However, the trend of the *LCOES* and the *IRR* also changed after the 25-home community. Li-ion chemistry performed better when high discharges were demanded (the inverter rating for the 10-home community was 11.3 kW) for the given capacity. However, the impact of the Li-ion CES system on the community would be very limited as discussed previously with the PV_{ES} and the D_{ES}. Figure 6.19 compares the CES systems which reduced the *LCOES* associated with PVts depending on the PV and HP penetration in 2020.

The *LCOES* slightly reduced while the *IRR* slightly increased when HPs were removed from the analysis. The main reason for the *LCOES* reduction relied on the increase of the *EFC* based on larger surplus PV energy available and the lower discharge rates when HPs were not considered. In order to illustrate this effect, the *EFC* of the optimum PbA battery for the 5-home community were 696 EFC and 707 EFC with and without HP. As a result, the associated *LCOES* were 0.40 £/kWh and 0.41 £/kWh respectively. Specifically, the optimum *LCOES* reduced to 0.37 £/kWh (-3%) and 0.29 £/kWh (-5%) and the *IRR* increased to 11.25% (+7%) and -0.77% (+49%) for PbA and Li-ion respectively. In fact, the heat demand load has a high seasonal pattern which affected the cycling characteristics

and the *DOD* of the (larger) battery sized to supply the heat demand load.

Regarding the sizing of the battery, Figure 6.19 shows that the optimum battery capacity slightly reduced without HPs. The optimum PbA battery was 39.5 kWh and 72.8 kWh for the 5-home and 10-home communities with a HP penetration of 14% while 37.5 kWh and 67.2 kWh without HPs. When the battery did not have to cope with the HP demand load, the inverter rating (as shown in Figure 4.7) and the optimum battery capacity reduced as a result. There was a great impact only for a single home in which the community HP penetration varied from 100% to 0%. A 12.6 kWh and a 7.2 kWh battery (a 11.4 kWh and a 5.7 kWh) minimized the cost of performing PVts for PbA (Li-ion) technology when HP were considered or not in a single home respectively. The still low HP penetration assumed by 2020 for the reference scenarios (14%) accounted for the small absolute impact of the presence or not of HP on the economic parameters.

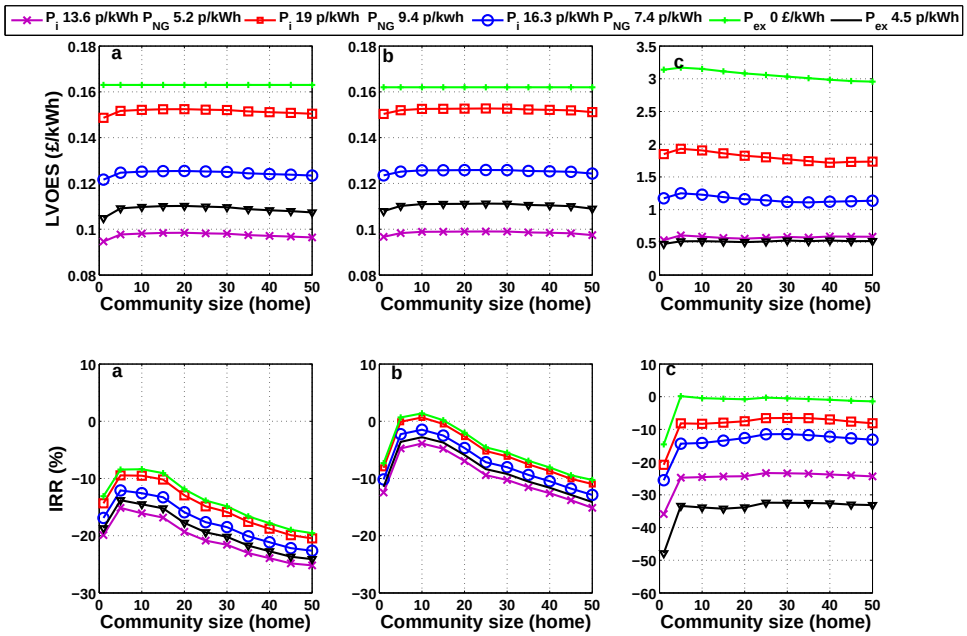

Figure 6.20: *LVOES* and *IRR* optimised for (a) PbA, (b) Li-ion and (c) H_2 technologies using PVts in 2020 depending on the energy prices and the export bonus.

6.3.3 Energy prices sensitivity

The effect of the energy prices and the export tariff paid to the PV electricity injected into the grid is discussed in this section. Neither the performance nor the *LCOES* were affected by the energy prices only the revenue was. As a consequence, the *IRR* and the *LVOES* are discussed in this sensitivity analysis.

The energy prices and the export tariff did not affect the pattern of the curves as seen in Figure 6.20. However, the energy prices and the export tariff affected the *LVOES* and the *IRR* markedly. The effect on the *LVOES* is derived from Equations 3.2 and 3.4 for the battery and H_2 technologies respectively. The *IRR* became positive (0.7%) for Li-ion technology for the 10-home community when the price of the electricity and the natural gas were assumed to be 0.19 £/kWh and 0.095 £/kWh respectively. Likewise, if the export bonus disappears in a hypothetical scenario in which only the self-consumption is supported, the *IRR* would be 0.7% and 1.4% in the 5-home and 10-home communities. If the export is not paid, H_2 technology was able to achieve a neutral *IRR* for the 5-home community due to is great flexibility to store surplus PV energy.

6.3.4 PV generation curtailment sensitivity

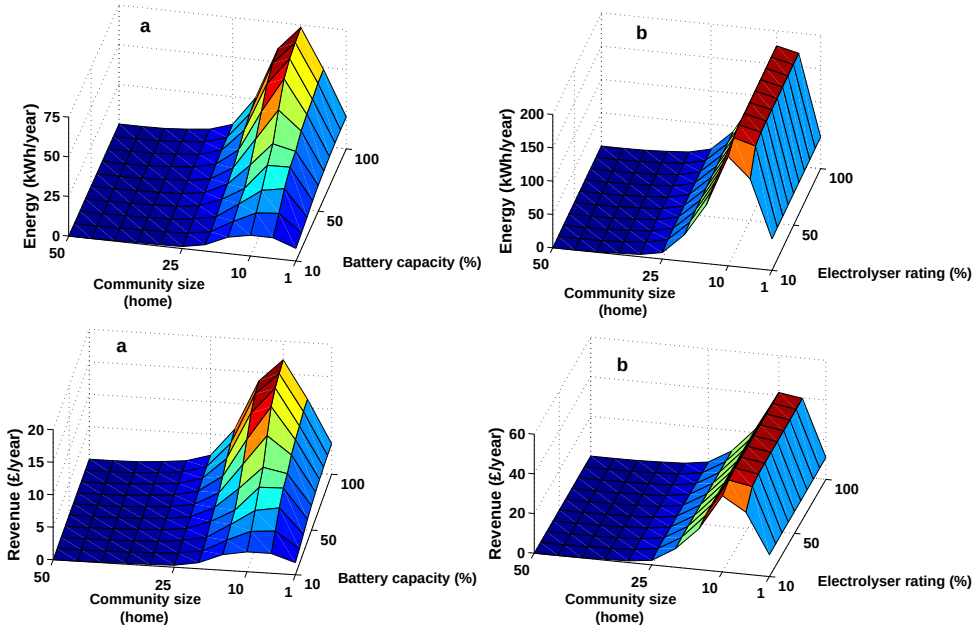

Figure 6.21: PV generation curtailment avoided and revenue associated with it for (a) PbA and (b) H_2 technologies performing PVts in 2020 as a function of the size of the community and the CES size.

Figure 6.21 shows the curtailment avoided by PbA batteries and H_2 systems and the revenue calculated according to Equation 3.10 if the curtailment obligation applies in 2020 as explained in Section 6.3.4. Li-ion battery results are not shown in this figure but they were on the same scale that those from PbA batteries. H_2 technology was more effective than battery technology to avoid any curtailment due to the decoupling of the power and energy ratings. The results obtained from the 5-home community can be used to illustrate these two conclusions. The largest PbA and Li-ion systems with a capacity of 104 kWh were able to avoid 48

kWh/year and 44 kWh/year curtailed respectively while a 12.9 kW electrolyser was able to avoid up to 170 kWh/year. These energy flows meant 15 £/year, 13 £/year and 35 £/year for PbA, Li-ion, and H_2 technologies respectively. This revenue could be added to the revenue obtained from PVts when the curtailment obligation is considered. This new revenue affected the *IRR* and *LVOES* as seen in Figure 6.22 but only in the case of H_2, this application had an impact on the *LVOES* and *IRR* which grew by 47% and 67% respectively.

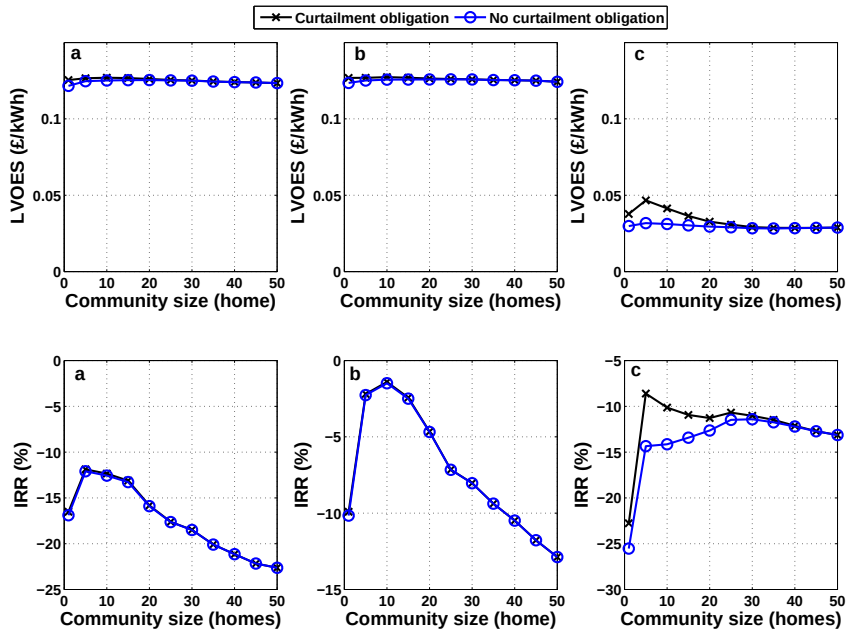

Figure 6.22: *LVOES* and *IRR* optimised for (a) PbA, (b) Li-ion and (c) H_2 technologies using PVts in 2020 depending on if the curtailment obligation is applies.

Finally, Figure 6.23 can be used to further understand the relationship between the *IRR* and two key parameters, the storage medium cost and electricity prices with the *IRR*. But also to identify break-even points and present key sensitivity results to decision makers. Results from the optimum Li-ion battery (42 kWh) in a 10-home community are utilised for this purpose, this being the optimum community by 2020 due to the PV penetration assumed for this reference year. According to the slope of the curves, the relationship is more linear with the electricity price than the storage medium cost but also the *IRR* is more sensitive to the storage medium. A cost of the storage medium of 260 £/kWh is the break-even point for an electricity price of 16.3 p/kWh, while 310 £/kWh is the break-even point for an electricity price of 19 p/kWh. When the storage medium cost was 260 £/kWh, the *IRR* values were positive for any electricity price projected by 2020 up to 9.2% when the electricity price is 31 p/kWh. However, there is not a break-even point if the storage medium cost is 780 £/kWh (the *IRR* was -1.6% when the electricity price was 31 p/kWh).

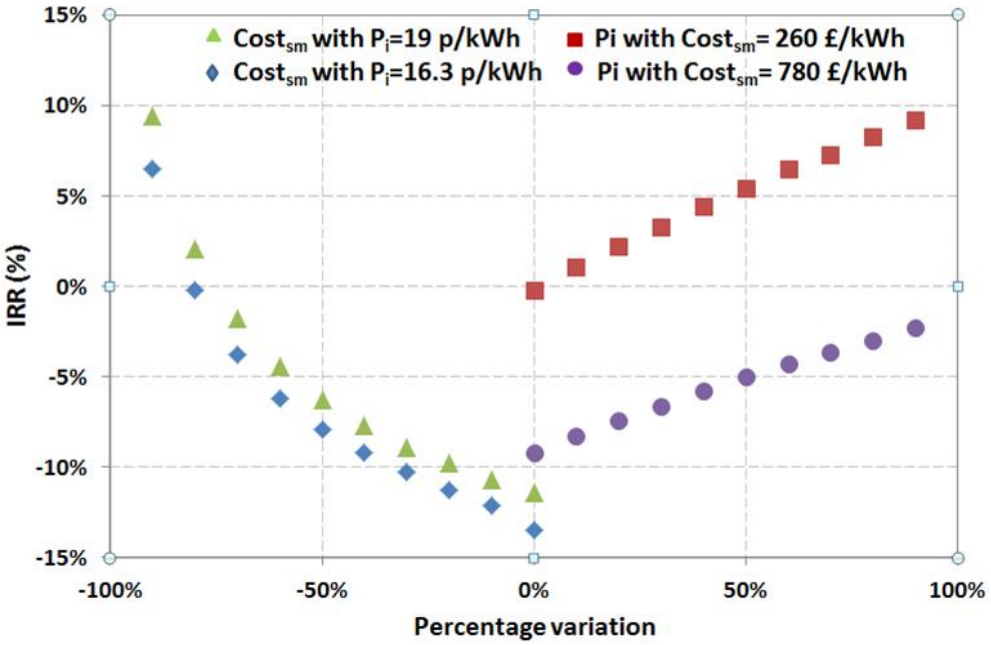

Figure 6.23: *IRR* of the optimum Li-ion battery (41.6 kWh) performing PVts in a 10-home community in 2020 (community PV percentage of 76%) as a function of the storage medium cost (percentage variation over a reference cost of 1300 £/kWh i.e. 0% variation) for an electricity price of 16.3 p/kWh and 19 p/kWh; and as a function of the electricity price (percentage variation over a reference price of 16.3 p/kWh i.e. 0% variation) for a storage medium cost of 260 £/kWh and 780 £/kWh.

6.3.5 Comparison of the reference case with a metering tariff

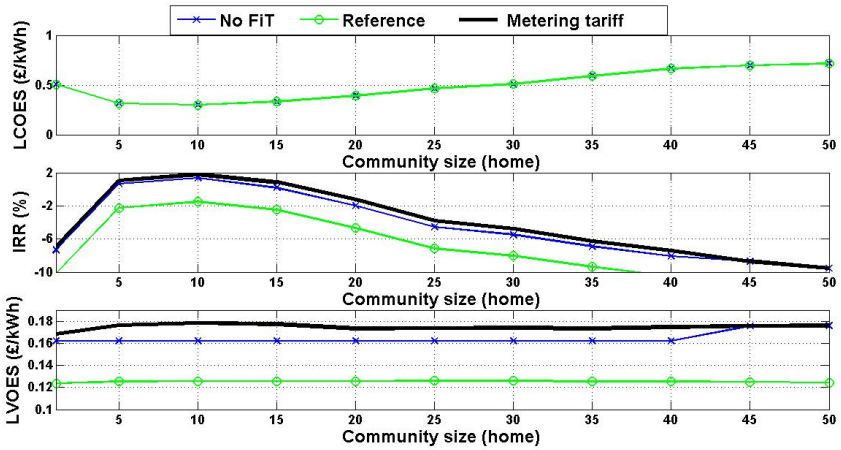

Figure 6.24: (a) *LCOES*, (b) *IRR* and (c) *LVOES* optimised for Li-ion batteries performing PVts depending on the tariff in 2020 as a function of the size of the community.

In this section, the reference case is compared with two scenarios in which FiTs and/or discounts for PV energy do not exist in order to reflect this future

possible policy scenario. Also, CES systems can export to the grid and they are paid the price established by the tariff considered. The first alternative scenario is represented by a "Metering tariff" which follows the prices from the NETA marked presented in Figure 3.4 i.e. the "Metering tariff" contains 48 different prices per day. The second alternative is based on the reference scenario but the export rate utilised in Section 3.4 (3.2 p/kWh) does not apply. The comparison of these three different tariffs is only shown for Li-ion batteries performing PVts in 2020 for the shake of simplicity. Figure 6.24 represents the economic results obtained in the three different scenarios. The two new scenarios achieved better economic results and the *IRR* and *LVOES* were greater. According to Equation 3.2, the revenue obtained from PVts in the reference scenario was proportional to the difference between the import and export electricity prices but in these two new scenarios the revenue was proportional to the import and export tariffs (which were assumed to be identical).

When comparing the two new scenarios, Figure 6.24 shows that the "Metering tariff" obtained higher *IRR* (up to 1.8%) and *LVOES* (up to 0.18 £/kWh) than the new flat rate tariff (*IRR* and *LVOES* equal to 1.4% and 0.16 £/kWh respectively). The reason for this was that a battery performing PVts usually discharges in the afternoon and evening and the "Metering tariff" reflects the higher cost of the electricity generation at this time (higher electricity generation's marginal) cost as seen in Figure 3.4. Finally, same *LCOES* were achieved in the three different scenarios, the minimum being 0.30 £/kWh for the 10-home community hence Li-ion battery capacities were optimised according to the reference tariff and therefore the capacities (e.g. 23.7 kWh and 31.2 kWh for the 5-home and 10-home communities respectively) were much smaller than the community demand load requirements on a daily basis. As a result, all electricity supplied by the batteries was consumed internally in the communities in reality.

6.4 Load shifting: reference scenarios

The same performance and economic parameters presented for PVts above were analysed for LS and only the PV_{ES} did not apply for LS. Different from PVts, LS economic results for 2020 and the zero carbon year are presented in the same graphs below because there was no parameter like the PV penetration which changed the scale of the results in both reference years. Likewise, the size of the community went up to 100 homes for both reference years.

The same input data utilised with the reference scenarios and the sensitivity analysis for PVts was also utilised with LS. The most important addition was the consideration of the two different tariffs presented in Section 3.5, Economy 7 and the *NETA* tariff. The electricity and heat efficiency of the PEMFC systems

ranged between 0.37 and 0.35 respectively as represented in Figure 3.11 and the maximum electrolyser efficiency obtained with PVts was 0.66 as reported in Table 6.3. When considering these efficiencies, the ratio between the valley price and the peak price of Economy 7 (0.47) and the price of the natural gas (7.4 p/kWh, the price of heat being 8.7 p/kWh), the LS condition ($\eta_e + \eta_h \times (P_{iv}/P_h) > P_{iv}/P_{ip}$) given by Equation 3.8 was not met for H_2 storage. As a consequence, results from H_2 technology performing LS with Economy 7 are not included below.

6.4.1 Performance results of PbA batteries performing LS when projected to the year 2020

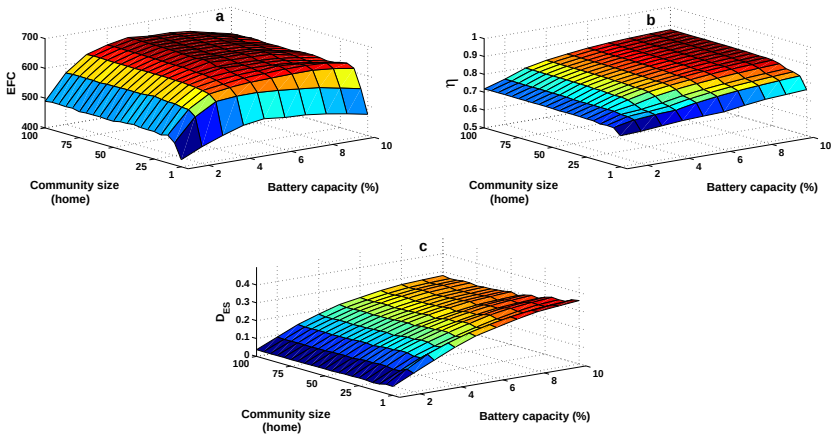

Figure 6.25: Performance results of PbA batteries performing LS with the NETA tariff in 2020 as a function of the size of the community and the battery capacity: (a) equivalent full cycles, (b) round trip efficiency and (c) D_{ES}. The battery capacity is given as a percentage of the maximum ES demand.

Figures 6.25 and 6.26 show the *EFC*, round trip efficiency and D_{ES} for PbA technology when performing LS with the NETA tariff and Economy 7 respectively. The *EFC* were affected by the size of the community and the battery capacity, the capacity effect being already discussed for PVts. Similarly, there was also an intermediate capacity which maximized the *EFC* for any community. LS results were not affected by the community PV percentage and this allowed the clear observation of the positive effect of the community size on the *EFC*. The *EFC* gently grew with the size of the community and there was only a sharp increase in the transition from a single home to the 10-home community. The maximum *EFC* of the 10-home and 100-home communities were equal to 630 EFC and 657 EFC respectively with the NETA tariff. These figures were on the range of the *EFC* obtained by PbA technology for PVts when the community PV percentage was equal to 100% as indicated in Table 6.3.

Figure 6.26 demonstrated that PbA batteries performing LS with Economy 7 achieved the greatest *EFC*. This was a consequence of the ratio between the off-peak and the peak prices for Economy 7, 0.47, which was always lower than the round trip efficiency shown in this figure. Additionally, the peak period of Economy 7 lasts for 17 hours and therefore a high fraction of the demand is shifted. The maximum *EFC* equal to 914 EFC were achieved by a 99 kWh battery in the 10-home community. This was related to the higher weight of the peak demand load for small communities as explained with the D_{ES} below.

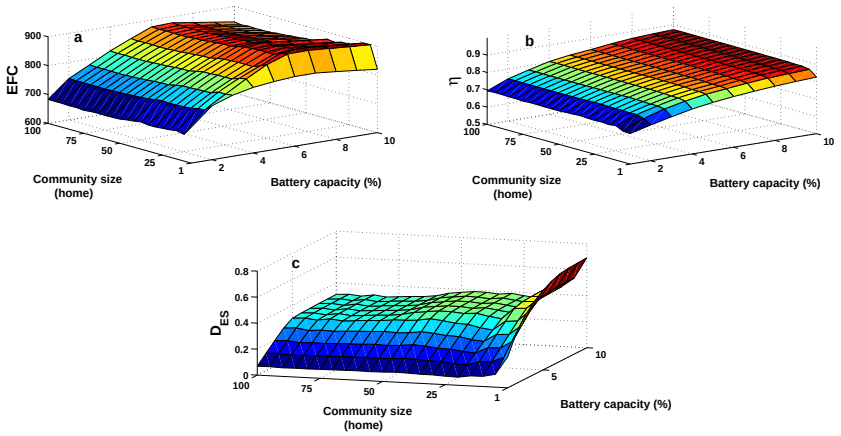

Figure 6.26: Performance results of PbA batteries performing LS with Economy 7 in 2020 as a function of the size of the community and the battery capacity: (a) equivalent full cycles, (b) round trip efficiency and (c) D_{ES}. The battery capacity is given as a percentage of the maximum ES demand.

The round trip efficiency increased with the capacity steadily and with the size of the community for the two tariffs. Again, the transition was more abrupt for the smaller communities. For any community, the *DOD* and the relative discharge rating reduced with the battery capacity and this had a positive impact on the round trip efficiency. Regarding the community size, the positive effect of the aggregations of demands reduced the discharge rates in relation to the battery capacity as suggested by Figure 4.7. The maximum round trip efficiency evolved from 76% for the single home (57 kWh) to 88% for the 100-home community (1340 kWh) in the case of the *NETA* tariff. It went up to 0.83 for a 73 kWh battery performing in the single home, this value also being achieved at the 100-home community. The maximum round trip efficiency achieved in the 100-home community with the two tariffs was a 4% higher than the maximum round trip efficiency obtained with PVts as shown in Tables 6.5 and 6.3.

Finally, the D_{ES} increased with the battery capacity but it slightly decreased with the size of the community. The main reason for this relied on the fact that the aggregation of demands reduced the relative weight of the peak demand load

in the daily demand as seen in Figure 3.7 (the community profile became smoother and flatter). Specifically, the fraction of the daily peak demand was up to 97% for the single home and up to 85% for the 100 community with Economy 7. The battery was charged to supply the peak demand when performing LS and this was reflected in the results. The maximum D_{ES} for the single home was 0.32 while it reduced to 0.27 for the 100-home community. This effect was strengthened in the case of Economy 7 due to the longer duration of the peak period and the higher battery activity, the maximum D_{ES} being equal to 0.69 for the single home.

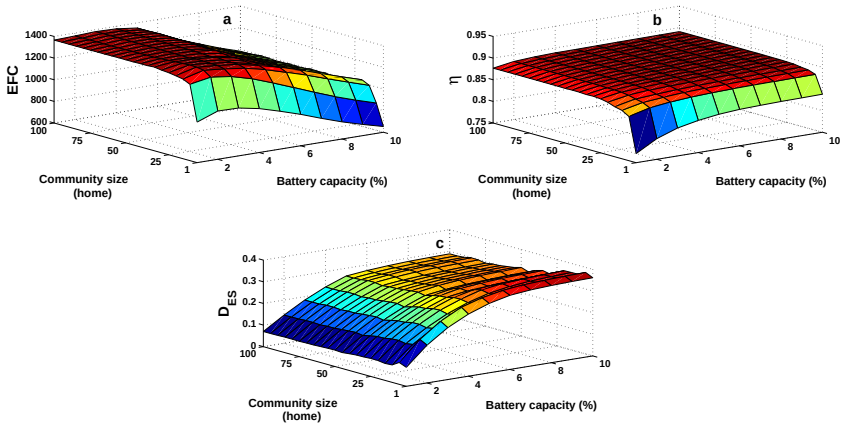

Figure 6.27: Performance results of Li-ion batteries performing LS with the NETA tariff in 2020 as a function of the size of the community and the battery capacity: (a) equivalent full cycles, (b) round trip efficiency and (c) D_{ES}. The battery capacity is given as a percentage of the maximum ES demand.

6.4.2 Performance results of Li-ion batteries performing LS when projected to the year 2020

Figures 6.27 and 6.28 show the *EFC*, round trip efficiency and D_{ES} of Li-ion technology when performing LS with the NETA tariff and Economy 7 respectively. In addition to obtaining higher performance values than PbA technology, as summarized in Table 6.5, the most important difference was Li-ion batteries required smaller capacities to obtain the maximum *EFC* for any community with the two tariffs. In the case of the NETA tariff, a 64.8 kWh, a 192 kWh and a 637 kWh Li-ion batteries achieved 1368 EFC, 1381 EFC and 998 EFC respectively in the 50-home community, the maximum being equal to 1400 *EFC* for a 59 kWh in the 20-home community. Another difference was the different *EFC* pattern followed by Li-ion batteries performing LS with Economy 7 for small communities. The relatively higher peak demand load of the smaller communities (in comparison with the flatter profile of bigger communities, as shown above) meant that the *EFC* did not reduce with the capacity as shown in Figure 6.28. In fact, a 174.6 kWh

Li-ion battery achieved 1942 EFC in the 20-home community, the maximum result.

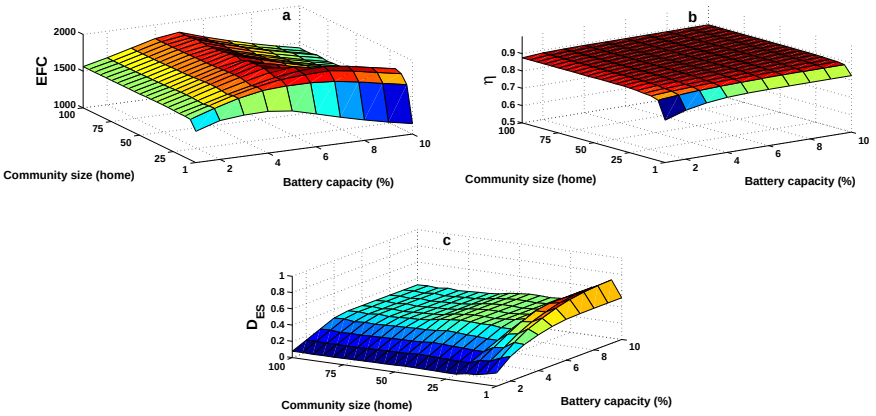

Figure 6.28: Performance results of Li-ion batteries performing LS with the Economy 7 in 2020 as a function of the size of the community and the battery capacity: (a) equivalent full cycles, (b) round trip efficiency and (c) D_{ES}. The battery capacity is given as a percentage of the maximum ES demand.

In terms of the round trip efficiency, Li-ion batteries behaved similar to when performing PVts. Results did not vary significantly with the battery capacity and the community size as seen in Figures 6.27 and 6.28 except for the transition between the single home and the 5-home community. Related to this, the minimum round trip efficiency of Li-ion batteries performing with the NETA tariff was 0.77 (for a 6.1 kWh battery), 0.85 (for a 11 kWh battery) and 0.85 (for a 121 kWh battery) for the single home, 5-home and 100-home communities respectively. Finally, the D_{ES} values were similar to those obtained by PbA technology as compared in Table 6.5. PbA batteries counterbalanced the lower round trip efficiency with the use of larger capacities as quantified in Figure 6.30 (battery systems were sized according the demand load requirements for LS).

6.4.3 Performance results of H_2 systems performing LS when projected to the year 2020

Figure 6.29 shows the performance results for H_2 technology performing LS with the NETA tariff. A H_2 system should perform with a round trip efficiency high enough to meet the LS condition derived from Equation 3.8, $\eta_e + \eta_h \times (P_{iv}/P_h) > P_{iv}/P_{ip}$. The electrolyser efficiency reduced with the electrolyser rating because parasitic losses were assumed to be directly proportional to the rating of the electrolyser and as a result, the C_{factor} reduced steadily with the electrolyser rating. In fact, there was an electrolyser for which the efficiency was not high enough to perform LS for any community e.g. a 1.1 kW, 4.7 kW, 8.2 kW and 100 kW

for the single home, 5-home, 10-home and 100-home communities. This was the reason why only six PEM electrolysers were tested for each community as shown in Figure 6.29.

The highest capacity factor equal to 0.36 was achieved in the 5-home community by a 2.5 kW electrolyser because the electrical efficiency of the PEMFC system (0.37) was the highest for this community as presented in Figure 3.9. In larger communities, the PEMFC systems run at full load longer i.e. at higher current densities according to Figure 3.9 due to the positive effect of the aggregation of demands. At full load, the electrical efficiency reduced, the heat efficiency increased and the total efficiency kept constant. According to Equation 3.8, the electrical round trip efficiency of a H_2 system necessary to meet the LS condition weights more than the heat efficiency because the price of the electricity at peak time is several times higher than the price of the heat (8.7 p/kWh). Finally, the reduced H_2 consumption of the PEMFC system in the single home due to the randomness of the heat demand load quantified in Section 3.11.1 was the reason why the capacity factor of the electrolyser performing at the single home was the lowest (0.27) in comparison with the rest of communities.

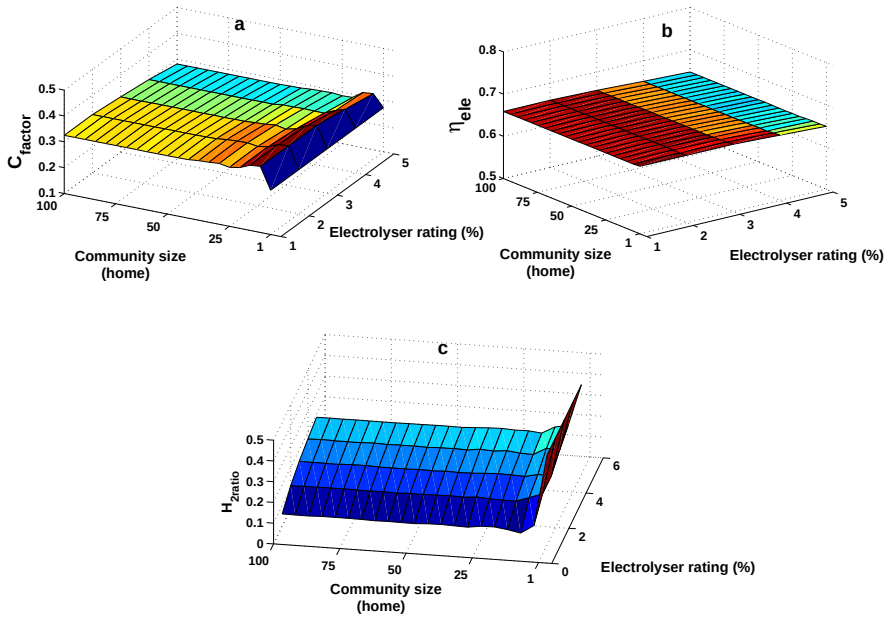

Figure 6.29: Performance results of H_2 systems performing LS with the NETA tariff in 2020 as a function of the size of the community and the battery capacity: (a) capacity factor, (b) electrolyser efficiency and (c) $H2_{ratio}$. The electrolyser rating is given as a percentage of the maximum ES demand.

The electrolyser efficiency reduced with the electrolyser rating for any community because the electrolyser ran at partial load more often as discussed in the PVts analysis. In order to illustrate this effect, the electrolyser efficiency ranged

Table 6.5: Performance parameters optimised for PbA, Li-ion and H_2 technologies using LS depending on the tariff in 2020 and the zero carbon year. The size of the community and the capacity of the battery (kWh) or the rating of the electrolyser (kW) which achieved the optimum values is shown in brackets.

Year	***Technology***	**Tariff**	$\boldsymbol{EFC/C_{ratio}}$	η/η_{ele}	$\boldsymbol{D_{ES}/H_{2ratio}}$
2020	**PbA**	NETA	658 (100,710)	0.88 (100,1340)	0.35 (5,116)
		Eco7	914 (10,99)	0.88 (100,1073)	0.69 (1,73)
	Li-ion	**NETA**	1399 (20,60)	0.89 (100,1194)	0.38 (5,106)
		Eco7	1942 (20, 175)	0.89 (100,1133)	0.72 (5,108)
	H_2	**NETA**	0.36 (5,2.5)	0.68 (1,1.1)	0.49 (1,1.1)
Zero Carbon	**PbA**	**NETA**	778 (100,1226)	0.88 (100,1340)	0.37 (1,39)
		Eco7	1008 (15,223)	0.88 (100,2038)	0.51 (1,51)
	Li-ion	**NETA**	1586 (100,636)	0.89 (100,636)	0.39 (5,140)
		Eco7	2164 (40,364)	0.89 (100,2034)	0.90 (1,66)
	H_2	**NETA**	0.45 (10,1.1)	0.66 (20,1.1)	0.37 (10,14.6)

from 0.66 to 0.63 for a 9.0 kW and 94.3 kW electrolysers running at the 50-home community. The size of the community did not affect the electrolyser efficiency and electrolysers run at maximum load when the LS condition for H_2 storage was met.

Finally, the pattern followed by the $H2_{ratio}$ responded to same factors discussed for the C_{factor} and the electrolyser efficiency but different rules applied. The $H2_{ratio}$ evolved similar to the electrolyser efficiency as a function of the size of the community. However, the electrolyser rating had an opposite effect on the $H2_{ratio}$ ratio and it increased steadily with the electrolyser rating. The $H2_{ratio}$ ratio was 0.06 and 0.26 when considering the same electrolyser ratings as above for the 50-home community. The $H2_{ratio}$ was higher in the single home due to the lower H_2 consumption of the PEMFC system. The maximum $H2_{ratio}$ was equal to 0.49 for a 1.1 kW electrolyser in the single home.

6.4.4 Performance results of PbA, Li-ion and H_2 technologies performing LS in the zero carbon year

The performance results in the zero carbon year are not discussed because same patterns than those represented above for 2020 were obtained. Table 6.5 summarizes and compares the optimised values of the performance results in 2020 and the zero carbon year.

The size of the H_2 tank for LS in the zero carbon year is shown in Figure

6.10. The most noticeable difference with the tank size obtained with PVts was the larger storage requirements for the largest electrolysers performing LS for any community, up to 53 kg for a 100 kW electrolyser in the 100-home community. However, the optimum H_2 system comprised an electrolyser and H_2 tank in which the tank size was much smaller than the maximum for any community as shown in Figure 6.31. For example, the optimum H_2 system for the 100-home community comprised a 19 kW electrolyser and a 3.6 kg H_2 tank.

6.4.5 Economic results of PbA, Li-ion and H_2 technologies performing LS when projected to the year 2020 and a hypothetical zero carbon year

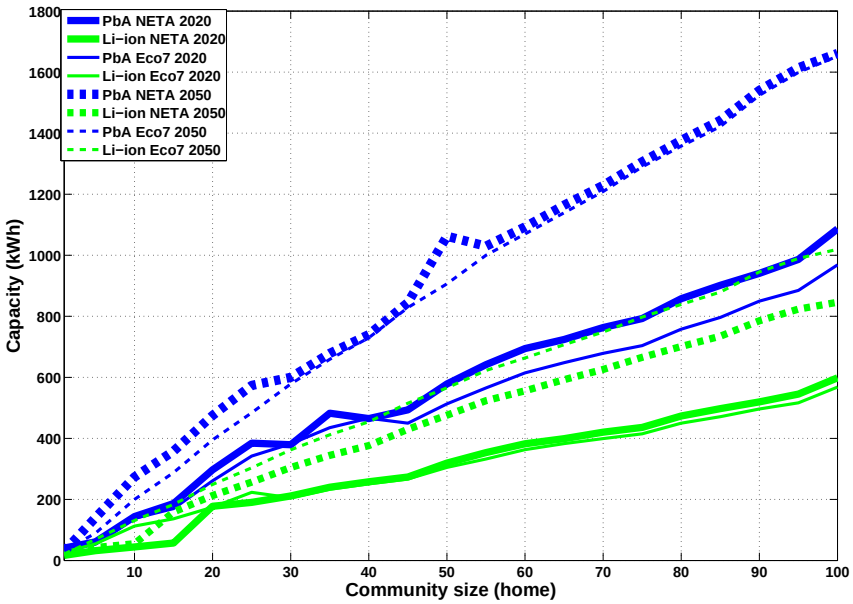

Figure 6.30: Optimum battery capacity which minimised the levelised cost, *LCOES*, associated with LS with Economy 7 and the NETA tariff as a function of the community size for PbA and Li-ion technologies in 2020 and the zero carbon year.

Figure 6.30 shows the battery capacities which reduced the *LCOES* of performing LS for PbA and Li-ion technologies depending on the tariff. Equally to PVts, PbA batteries required larger capacities than Li-ion batteries to reduce the cost with the two tariffs. The PbA capacity which reduced the cost of performing LS with Economy 7 in the 50-home community was 513 kWh, while it reduced to 305 kWh for Li-ion technology in 2020. According to the results represented in Figure 6.30, the optimum PbA capacity was approximately twice the optimum Li-ion capacity in the case of the NETA tariff and around 1.6 times for Economy 7 for any community except for the single home in the case of Economy 7. The

reason why the ratio was slightly higher with the NETA tariff was larger battery capacities were necessary to increase the round trip efficiency and meet the LS condition given by Equation 3.6. The optimum PbA and Li-ion battery capacities were similar with Economy 7 in the single home because PbA technology was not able to meet the relatively high peaks which randomly occurred in the demand. This reduced the optimum capacity for PbA technology to 30.5 kWh, the optimum capacity of Li-ion battery being 27 kWh.

Figure 6.30 also shows that the optimum battery capacity was very similar with the two tariffs for both battery technologies for any community. Specifically, Li-ion capacity was slightly larger for Economy 7 due to the higher duration of the peak period while slightly larger capacities were necessary for PbA batteries with the NETA tariff as discussed above. The optimum capacity profile was less uniform for the NETA tariff since the prices of the NETA market and the round trip efficiency determined if LS was performed or not on a daily basis. This modified the annual results and the optimum size varied more steeply as a result. The optimum battery capacities required in the zero carbon year were around 50%-60% and 75-85% larger than for 2020 for the NETA tariff and Economy 7 respectively. In order to illustrate the impact of the HP penetration, the optimum Li-ion battery capacities performing Economy 7 for the 100-home community were 568 kWh (HP penetration equal to 14%) and 1020 kWh (HP penetration equal to 100%) in 2020 and the zero carbon year respectively.

In the case of H_2 technology, Figure 6.31 shows that the optimum electrolyser rating increased steadily with the size of the community. The electrolyser rating for the 5-home, 25-home and 100-home communities were 1.1 kW, 5.6 kW and 19.1 kW in 2020 respectively. The PEMFC systems were sized according to the electrical demand and the lower electrical demand requirements in the zero carbon year according to the demand input data selected in Table 5.1 justifies the larger electrolyser rating in 2020. The electrolyser ratings were 9.0 kW and 7.9 kW in for the 50-home community in 2020 and the zero carbon year respectively.

Figures 6.32 and 6.33 show the *LCOES*, *IRR* and *LVOES* optimised for PbA, Li-ion and H_2 technologies performing LS depending on the tariff as a function of the size of the community in 2020 and the zero carbon target respectively. The *LCOES* associated with electricity generation is shown for H_2 technology. The pattern followed by the *LCOES* and the *IRR* was similar for the two battery technologies and for the two tariffs considered. The pattern demonstrates the positive effect of the community size. The *LCOES* followed a negative logarithmic trend while the *IRR* followed a positive logarithmic trend as a function of the size of the community. The positive effect of the aggregation of demands impacted on the *IRR* and *LCOES* but the effect became smoother as the community size increased.

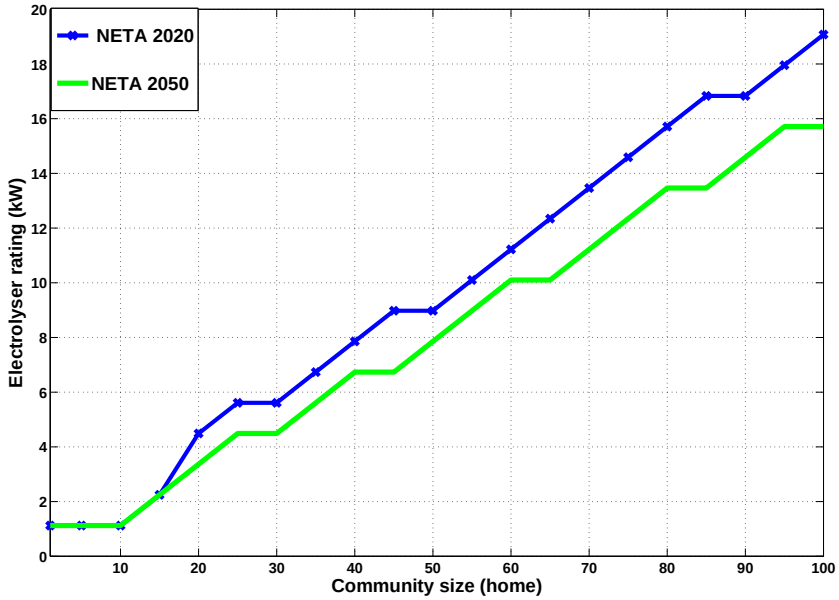

Figure 6.31: Optimum electrolyser which minimised the levelised cost, *LCOES*, associated with LS with Economy 7 and the NETA tariff as a function of the community size in 2020 and the zero carbon year.

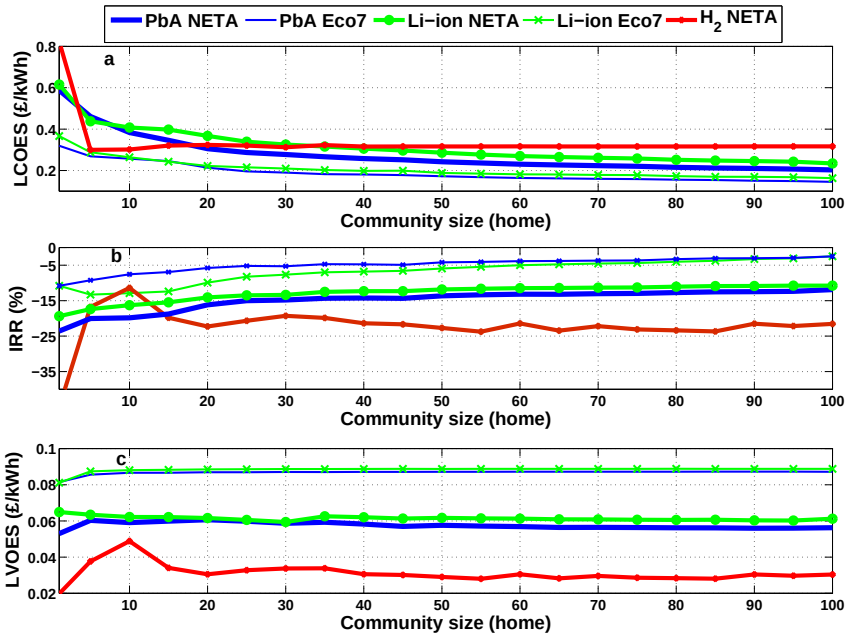

Figure 6.32: (a) *LCOES*, (b) *IRR* and (c) *LVOES* optimised for PbA, Li-ion and H_2 technologies using LS in 2020 depending on the tariff.

The best economic results were obtained in the 100-home community while the maximum *LCOES* and the minimum *IRR* were achieved in the single home. The two battery technologies achieved better economic results with Economy 7. As

discussed in Section 6.4.1, the ratio between the prices of the electricity at the valley and peak periods offered by Economy 7, 0.47, and the duration of the peak period (17 h) are very attractive for LS. The *LCOES* and the *IRR* of a 342 kWh PbA battery in the 25-home community were 0.20 £/kWh and -8% for Economy 7, these results being negatively modified to 0.29 £/kWh and -16% for a 384 kWh PbA battery with the NETA tariff.

For H_2 systems, the economic results were also affected by the PEMFC systems performance. As previously discussed with the performance results, PEMFC systems which operated at the single home, 5-home and 10-home communities operated more often at partial load achieving higher electrical efficiency as represented in 3.11. This allowed electrolysers operating in these small communities to meet the LS condition more often due to the higher weight of the price of the electricity on the LS decision. As a consequence, the *LCOES* and the *IRR* reached 0.30 £/kWh$_e$ and -11.4% for the 10-home community, varying to 0.32 £/kWh$_e$ and -21.5% for the 100 home community. For those communities in which the electrical efficiency of the PEMFC system was higher, the *LCOES* and the *IRR* became more attractive due the flexibility of H_2 storage. According to this flexibility, the electrolyser could run at full load whenever the price of the electricity was low enough to meet the LS condition (according to Equation 3.8).

PbA was the technology which obtained the lowest *LCOES* and the highest *IRR* equal to 0.14 £/kWh and -2.5% respectively in the 100-home community, yet Li-ion values were very similar as indicated in Table 6.6. Li-ion technology obtained slightly lower *LCOES* values with the NETA tariff just for the single home and the 5-home community. The main reason for this was the round trip efficiency of PbA battery system was a bit lower for these communities and this reduced the *EFC*. Specifically, the round trip efficiency of the optimum PbA systems was 0.72 (35 kWh) and 0.77 (61 kWh), while the round trip efficiency of Li-ion technology was 0.81 (17 kWh) and 0.87 (31 kWh) for the single home and the 5-home community respectively.

Economy 7 was the tariff with the higher *LVOES* because the valley and peak prices of the NETA tariff were not as attractive as those from Economy 7 on a daily basis. The maximum *LVOES* obtained for PbA and Li-ion batteries performing Economy 7 was 0.09 £/kWh, while this value fell to 0.06 £/kWh in the case of the NETA tariff. The *LVOES* did not depend on the community size for the reasons explained with PVts. The *LVOES* of H_2 technology was around 0.04 £/kWh for any community. Despite the prices in the Imbalance Market (NETA) being much more variable, those variations were averaged and smoothed when the NETA tariff was created. The variability of the prices may increase in the future due to the penetration of wind energy [172], the presence of smart meters and

intelligent sockets [55].

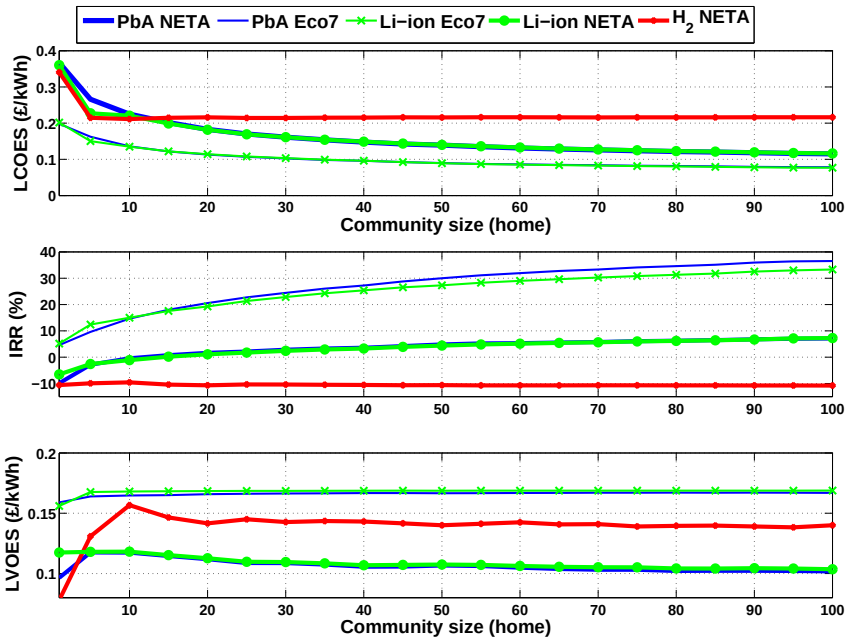

Figure 6.33: (a) *LCOES*, (b) *IRR* and (c) *LVOES* optimised for PbA, Li-ion and H_2 technologies using LS in the zero carbon year depending on the tariff.

Similarly to PVts, the improvement of the ES properties assumed for the reference scenarios in the zero carbon year together with the increase of the energy prices (as summarized in Table 5.1) made the business case more widespread ($IRR>0$) for any technology, tariff and size of the community as shown in Figure 6.33. PbA and Li-ion batteries performing LS with Economy 7 achieved positive *IRR* for any community, the maximum values 36.5% and 33.2% respectively achieved in the 100-home community. However, communities with less than 15 homes did not achieve positive *IRR* with the NETA tariff. Additionally, the *LCOES* went down markedly by the zero carbon year and reached the minimum value for the two battery technologies, 0.08 £/kWh, at the 100-home community. Optimised economic results in 2020 and the zero carbon year are summarized in Table 6.6. In the case of the NETA tariff, the *LCOES* was always higher than the *LVOES* i.e. the *IRR* was lower than the discount rate assumed (10%). The trend of the curves was steeper for small communities and they became smoother as the size of the community increased. The *LVOES* related to Economy 7 and the NETA tariff was 0.17 £/kWh and 0.11 £/kWh respectively for both battery technologies. In the case of H_2 storage, it only obtained a negative *IRR* in the single home, the *IRR* being higher for small community sizes up to 31.1% for the 10-home community. H_2 storage achieved a *LCOES* of 0.21 £/kWh$_e$ and a *LVOES* of 0.16 £/kWh in the 10-home community.

Table 6.6: Economic parameters optimised for PbA, Li-ion and H_2 technologies using LS with Economy 7 and the NETA tariff in 2020 and the zero carbon year. The size of the community and the capacity of the battery (kWh) or the rating of the electrolyser (kW) which achieved the optimum values is shown in brackets.

Year	Technology	Tariff	*LCOES* (£/kWh)	*IRR*(%)	*LVOES*(£/kWh)
2020	**PbA**	**NETA**	0.20 (100,1086)	-12.4 (100,1340)	0.06 (20,328)
		Eco7	0.14 (100,969)	-2.5 (100,1073)	0.09 (95,981)
	Li-ion	**NETA**	0.24 (100,359)	-10.8 (100,896)	0.06 (1,36)
		Eco7	0.16 (100,568)	-2.5 (100,1024)	0.09 (100,1133)
	H_2	**NETA**	0.30_e(10,1.1)	-11.4 (10,1.1)	0.04 (10,1.1)
Zero carbon	**PbA**	**NETA**	0.12 (100,1611)	7.0 (100,2109)	0.12 (5,155)
		Eco7	0.08 (100,1652)	36.5 (100,1277)	0.17 (90,1880)
	Li-ion	**NETA**	0.12 (100,846)	7.1 (100,1058)	0.12 (10,272)
		Eco7	0.08 (100,1020)	33.2 (100,815)	0.17 (100,2034)
	H_2	**NETA**	0.21_e (10,1.1)	31.1 (10,1.1)	0.14 (10,1.1)

6.5 Load shifting results: sensitivity analysis

The NETA tariff is used in this section to illustrate the LS sensitivity analysis. Although the values of the economic parameters depended on the tariff, results presented bellow allow the understanding of the impact of key parameters on the performance and economic benefits of CES systems performing LS. Likewise, only results in 2020 are presented in this section.

6.5.1 Energy storage technology sensitivity

The initial cost of the CES systems had a remarkable impact on the *LCOES* and the *IRR* associated with LS as illustrated in Figure 6.34. Neither the cost or the durability changed the pattern and they only affected the absolute values. The minimum *LCOES* increased to 0.23 £/kWh (+15%) and 0.39 £/kWh (+95%) for PbA technology, 0.27 £/kWh (+12.5%) and 0.99 £/kWh (+312.5%) for Li-ion technology and 0.39 £/kWh$_e$ (+30%) and 0.79 £/kWhh$_e$ (+163%) for H_2 technology when assuming that the durability and cost respectively keep constant with those in 2012, according to the data presented in Table 5.5. Likewise, the maximum *IRR* reduced to -17.3% and -19.9% if the durability and cost properties are those of the baseline scenario for PbA technology in 2020. Similarly, the optimum IRR was equal to -16.1%, and -24.1% respectively for Li-ion technology and -19.3%, and -38.5% respectively for H_2 technology.

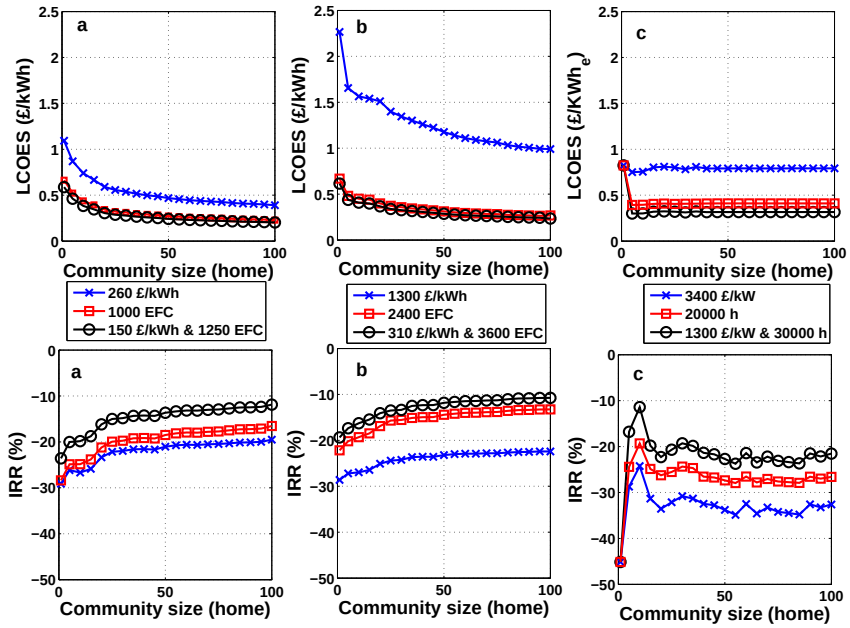

Figure 6.34: *LCOES* and *IRR* optimised for (a) PbA, (b) Li-ion and (c) H_2 technologies using LS with the NETA tariff in 2020 depending on the ES cost and durability characteristics.

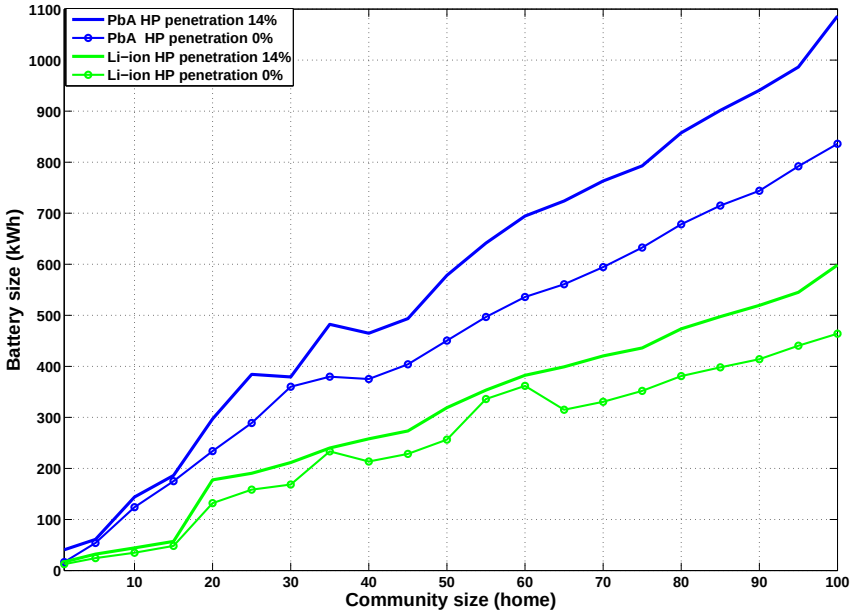

Figure 6.35: Optimum CES system which minimised the levelised cost, *LCOES*, when performing LS as a function of the size of the community for the three technologies depending on the HP penetration in 2020.

6.5.2 Demand sensitivity

The impact of the heat demand load on the optimum battery capacity and the economic benefits with LS is quantified in this section. LS is an ES application which manages the domestic load demand and therefore the demand is a key factor to understand the performance and economic benefits. Figure 6.35 shows the optimum battery capacity which reduced the cost of performing LS for PbA and Li-ion batteries depending whether the heat demand load was considered (HP penetration equal to 14%) or not (HP penetration equal to 0%). The optimum capacities were similar for small communities and then the trend became more steady and slightly more positive for a HP penetration of 14% for both battery technologies. The battery capacity reduced by 21% and 20% for PbA and Li-ion technologies which is consistent with the two different chemistries considering that the absolute capacity was larger for PbA technology. This can be illustrated with the 90-home community in which the optimum battery capacities were 941 kWh and 744 kWh for PbA technology and 519 kWh and 414 kWh for Li-ion technology when considering or not the heat demand load.

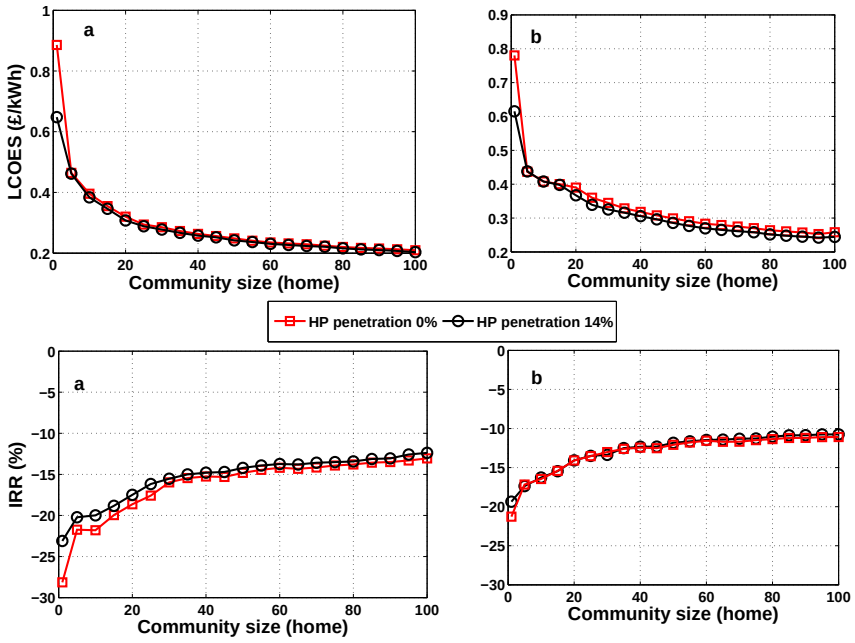

Figure 6.36: *LCOES* and *IRR* optimised for (a) PbA and (b) Li-ion technologies as a function of the size of the community when performing LS with the NETA tariff depending on the HP penetration in 2020.

Figure 6.36 shows how the HP penetration affected the economic parameters in 2020. There was not a great impact on the results for any community and just the single home was considerably affected by the use of a HP. The larger battery capacity necessary to deal with the heat demand load was the most significant

difference. In fact, the *EFC* achieved by both technologies were on the same range as before. The presence of HPs was partially minimised in the optimum results because the optimization method selected a battery capacity which is not markedly affected by the seasonal pattern of heat demand load. The case of PbA technology in the single home can be used to illustrate the impact of the heat demand load. While the optimum capacity reduced significantly from 35.4 kWh to 16.5 kWh when a HP was not considered, the *EFC* also went down from 471 EFC to 417 EFC respectively.

Figure 6.36 shows that the *LCOES* and the *IRR* slightly reduced and increased respectively with a HP penetration of 14%. In this scenario, battery systems were able to manage more energy on a annul basis per kWh of capacity. Specifically, the *LCOES* and the *IRR* achieved by the PbA technology in the case of the 100-home community were 0.21 £/kWh (+5.0%) and -13.0% (-4.8%), changing to 0.26 £/kWh (+8.3%) and -14.0% (-12.9%) for Li-ion technology when the HP penetration was 0%. In the case of the single home, the *LCOES* increased to 0.89 £/kWh (+37%) and 0.98 £/kWh (+58%) for PbA and Li-ion batteries, while the *IRR* reduced to -28.1% (-21.6%) and -21.3% (-9.8%) respectively without HP.

6.5.3 Energy prices sensitivity

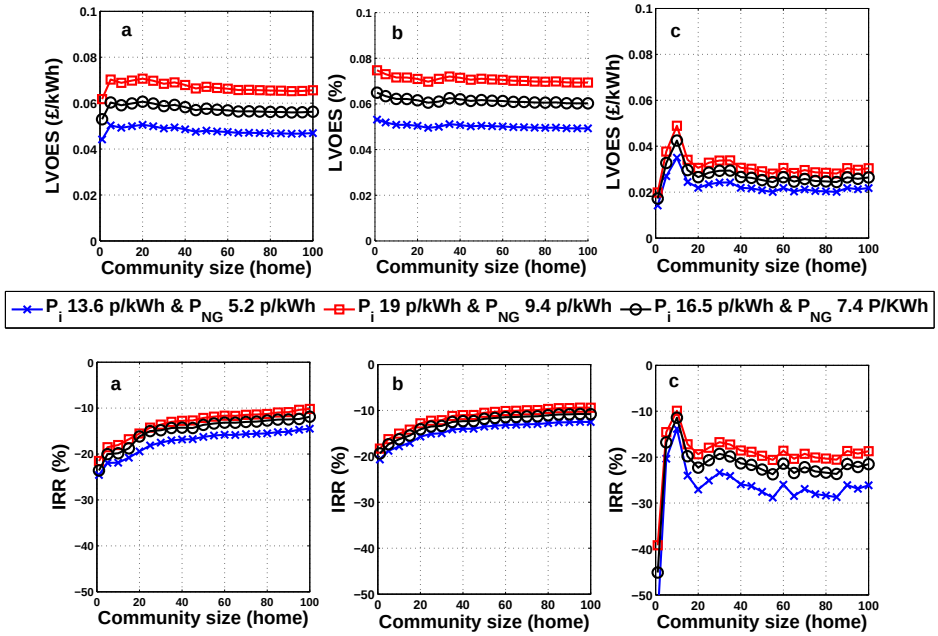

Figure 6.37: *LCOES* and *IRR* optimised for (a) PbA, (b) Li-ion and (c) H_2 technologies as a function of the size of the community when performing LS with the NETA tariff depending on the energy prices in 2020.

Figure 6.37 shows the influence of the energy prices on the *LVOES* and the *IRR*. The input data for this sensitivity analysis was introduced in Table 5.9. The *LVOES* slightly oscillated around 0.06 £/kWh in the reference scenarios for the two battery technologies and was modified to 0.05 £/kWh or 0.07 £/kWh when the average price of the electricity was 13.6 p/kWh or 19.0 p/kWh respectively. This means a 17% absolute variation with regard the reference case. Likewise, the maximum *LVOES* was modified to 0.035 £/kWh or 0.049 £/kWh for H_2 technology when the price of the electricity was 13.6 p/kWh (price of natural gas equal to 5.2 p/kWh) or 19.0 p/kWh (price of natural gas equal to 9.4 p/kWh), the *LVOES* being equal to 0.043 £/kWh in the reference scenario.

The energy prices also affected the *IRR*. The maximum *IRR* increased to -10.2% (+17.8%), -9.4% (+24.8%) and -9.9% (+13.2%) for PbA, Li-ion and H_2 technologies respectively when the electricity price increased to 19 p/kWh. Likewise, the *IRR* reduced to -14.5% (-16.9%), -10.8% (-13.6%) and -13.8% (-21.0%) respectively with a electricity price equal to 0.136 £/kWh. These optimum values were given at the 100-home and 10-home communities for battery and H_2 technologies respectively. The impact of the electricity prices in the profitability and the value of CES was buffered by the fact that the ratio of the prices kept constant in the sensitivity analysis. This meant that the revenue per discharge varied but the number of discharges was kept constant.

6.6 Combination of applications: PVts and load shifting

If previous sections discussed PVts and LS independently, the final part of this chapter focuses on the case in which CES systems perform both applications at the same time. PVts will be combined with the NETA tariff and Economy 7. A sensitivity analysis is not presented here and only results from the reference scenarios are discussed. The performance and the economic benefits of the combination of applications are affected by the same parameters included in the PVts and LS sensitivity analyses and therefore same conclusions apply here. The integration of PVts and LS including the NETA tariff and Economy 7 as function of the size of the community is discussed below when considering that the PV generation has priority over the grid import.

6.7 Combination of applications: reference scenarios

6.7.1 Performance results of PbA and Li-ion batteries performing PVts and LS when projected to the year 2020

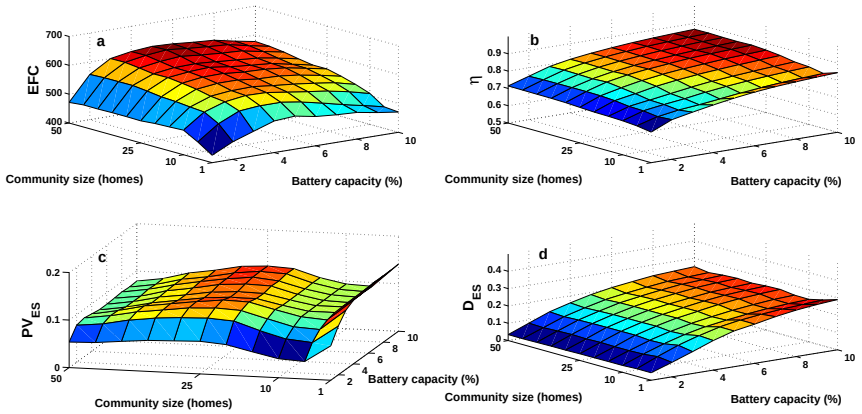

Figure 6.38: Performance results of PbA batteries performing PVts and LS with the NETA tariff in 2020 as a function of the size of the community and the battery capacity: (a) equivalent full cycles, (b) round trip efficiency, (c) PV_{ES} and (d) D_{ES}. The battery capacity is given as a percentage of the maximum ES demand.

The same performance parameters calculated for the PVts analysis were also included in this section. Only graphs showing the PbA results are presented here to illustrate the impact of the combination of applications on the battery technology. Figure 6.38 shows the performance results of PbA batteries in 2020 and it demonstrates that results were a combination of those discussed for PVts and LS independently. Specifically, the battery capacity and the community size determined what application was predominant and this was reflected on the values and patterns. The community PV percentage was higher than 76% up to the 10-home community and as a consequence, the *EFC*, round trip efficiency and D_{ES} were more affected by the energy charged from surplus PV generation. The PV_{ES} reached a low when the PV penetration was higher than 76% because PV electricity was only discharged at peak times. For the communities with more than 20 homes in which the community PV percentage was lower than 40%, the results of the combination of applications were very similar to those discussed for LS.

Figure 6.39 shows the same results when PVts was combined with Economy 7. As it was seen during the LS analysis, better results were obtained with Eco-

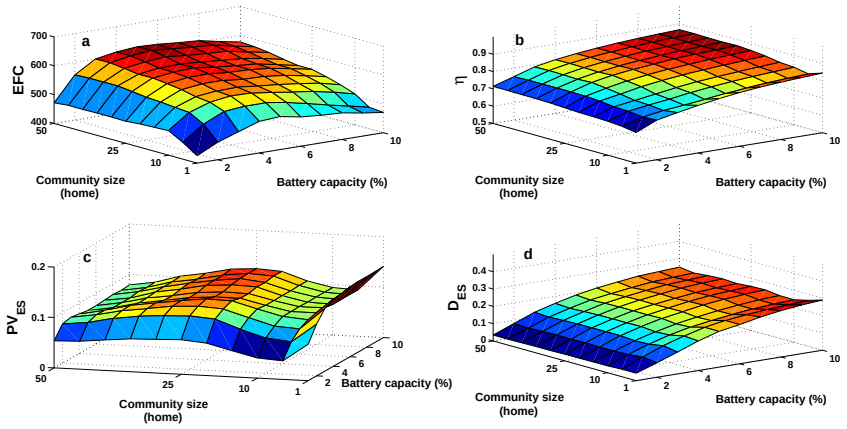

Figure 6.39: Performance results of PbA batteries performing PVts and LS with Economy 7 in 2020 as a function of the size of the community and the battery capacity: (a) equivalent full cycles, (b) round trip efficiency, (c) PV_{ES} and (d) D_{ES}. The battery capacity is given as a percentage of the maximum ES demand.

nomy 7. The PV_{ES} was much higher when Economy 7 was combined with PVts due to the longer peak period. As discussed in Section 5.4, batteries were sized according to the LS requirements but subtracting the peak demand load which is met directly by the PV arrays and the electricity charged from the PV arrays (PVts). As a consequence, battery capacities were much larger than those which performed PVts and the PV_{ES} had a much flatter profile for any community size as a consequence. In fact, the PV_{ES} reached its maximum (0.35) for medium battery capacities (105 kWh battery in the 20-home community) in Figure 6.39 and then it slightly declined.

Same conclusions to those extracted from PbA results apply for Li-ion batteries in terms of the impact of the size of the community and the battery capacity when considering the higher round trip efficiency and discharge ratings of Li-ion chemistry discussed in previous sections.

6.7.2 Performance results of H_2 systems performing PVts and LS when projected to the year 2020

Figure 6.40 shows the C_{factor}, electrolyser efficiency, PV_{ES} and $H2_{ratio}$ for H_2 technology when performing PVts and LS with the NETA tariff. Mid and long-term storage was put into practice when H_2 systems performed PVts and LS simultaneously using the flexibility given by the decoupling of the power and energy ratings. While PVts and LS were supplementary applications for battery technology even when the charge from the PV plants and the grid occurred at different times, LS was only displaced by PVts when PV generation met the peak demand load

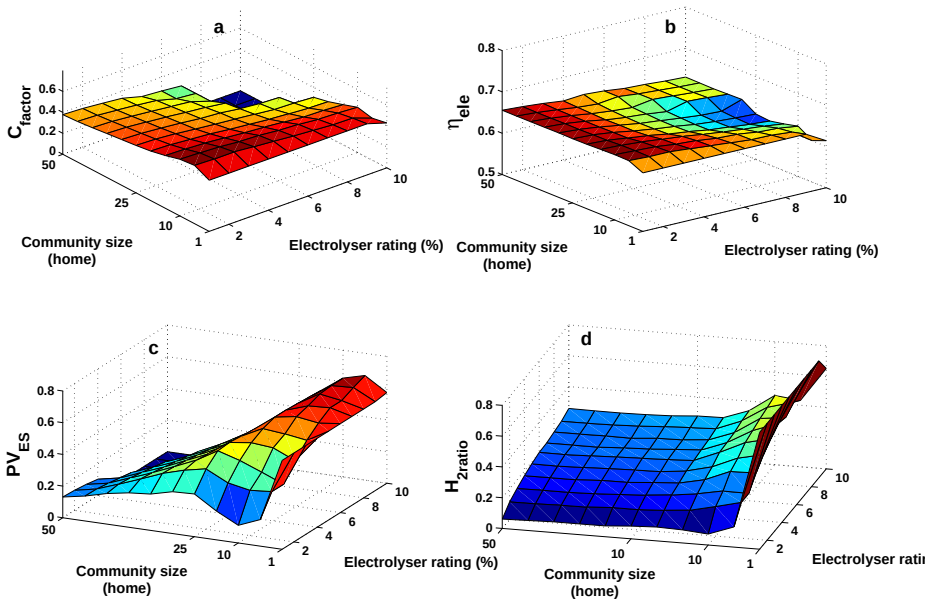

Figure 6.40: Performance results of H_2 systems performing PVts and LS with the NETA tariff in 2020 as a function of the size of the community and the electrolyser rating: (a) capacity factor, (b) electrolyser efficiency, (c) PV_{ES} and (d) H_{2ratio}. The electrolyser rating is given as a percentage of the maximum ES demand.

directly for H_2 storage. Additionally, the flexibility given by the tank size contributed to cope with the larger H_2 generation from both sources (PV generation and grid import). This is the reason why the C_{factor} increased when compared with values achieved for LS only. Regarding the rest of the parameters, they behaved as shown for PVts and LS depending on the community PV percentage which determined which application prevailed. The optimum value of the performance results together with the CES system which achieved them and the community size are shown in Table 6.7.

6.7.3 Economic results of PbA, Li-ion and H_2 technologies performing PVts and LS when projected to the year 2020

The figures presented below differ from those included in the PVts and the LS analyses in which each figure compared the economic results of different technologies when performing an application. Here, the greatest interest was in investigating the impact of adding a second (main) application to the business case. Figure 6.41 shows the optimum battery capacity which minimized the cost of performing PVts, LS and the combination of applications with the NETA tariff and Economy 7 for PbA technology in 2020 and the zero carbon year. The optimum capacity which minimized the cost of meeting the demand load with PVts and the NETA

Table 6.7: Performance parameters optimised for PbA, Li-ion and H_2 technologies using PVts and LS in 2020 and the zero carbon year. The size of the community and the capacity of the battery (kWh) or the rating of the electrolyser (kW) which achieved the optimum values is shown in brackets.

Year	technology	Tariff	EFC/C_{ratio}	η/η_{ele}	PV_{ES}	$D_{\%ES}/H2_{ratio}$
2020	**PbA**	NETA	616 (50,440)	0.87 (45,598)	0.14 (1,49)	0.29 (1,49)
		Eco7	905.3 (50,564)	0.88 (100,1073)	0.34 (15,101)	0.64 (1,7)
	Li-ion	NETA	1442 (20,29)	0.89 (45,536)	0.14 (1,48)	0.41 (1,48)
		Eco7	1836 (10, 261)	0.89 (1,88)	0.33 (5,81)	0.89 (1,88 kWh)
	H_2	**NETA**	0.56 (5, 1.1)	0.66 (10,2.2)	0.66 (5, 2.8)	0.76 (1,2.2)
Zero carbon	**PbA**	NETA	705 (100,974)	0.87 (90,2106)	0.13 (1,18)	0.30 (1,38)
		Eco7	1005 (100, 866)	0.88 (75,1557)	0.31 (1,11.8)	0.67 (1,50)
	Li-ion	NETA	1639 (100,208)	0.89 (70,1506)	0.12 (1,16)	0.31 (1,36)
		Eco7	1907 (100,797)	0.89 (60,631)	0.30 (1,27)	0.68 (1,66)
	H_2	**NETA**	0.62 (5,1.1)	0.66 (85,13.5)	0.73 (1,2.3)	0.77 (15,34.7)

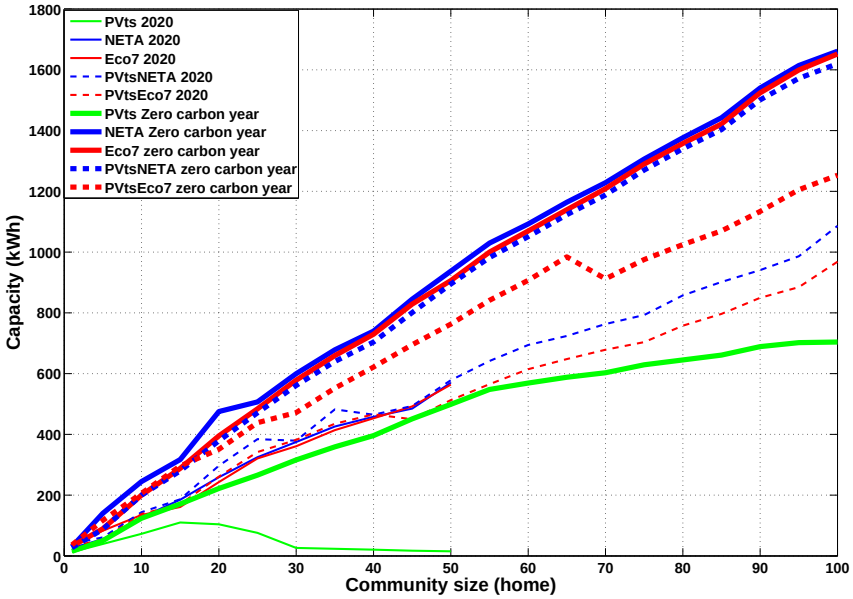

Figure 6.41: Optimum PbA battery capacity which minimised the levelised cost, *LCOES*, associated with PVts, LS and both applications combined with the NETA tariff and Economy 7 as a function of the size of the community in 2020 and the zero carbon year.

tariff was 95% the capacity when only considering LS in the zero carbon year when the PV penetration was 57%. This percentage reduced to 75% for Economy 7. This suggested that results from LS should be used as the starting point to analyse the results from the combination of applications. According to this, analysing the impact of adding the PV management to the demand load management in terms of cost, profitability and revenue is discussed next.

Figures 6.42 and 6.43 compare the optimum *LCOES*, *LVOES* and the *IRR* for

PbA technology when performing PVts, LS and both application simultaneously with the NETA tariff and Economy 7 respectively. For any community, the optimum battery capacity performing PVts and LS simultaneously slightly decreased regarding the case in which only LS was performed but the energy managed by the battery reduced more due to the PV energy supplied directly to the demand load. For example, while a 185 kWh battery performing PVts and LS simultaneously minimized the cost of meeting the demand load by annually supplying 9763 kWh in the 15-home community, a 186 kWh battery performing only LS was able to annually shift 12866 kWh in the same community. As a result, the management of the PV generation in addition to the management of the demand load reduced the *EFC* from 635 EFC to 542 EFC in this case. Secondly, CES systems only discharged at peak times and this reduced the overall charge of the battery from the PV plants and the grid. As a result, the *LCOES* increased from 0.35 £/kWh to 0.42 £/kWh when the battery performed PVts in addition to LS.

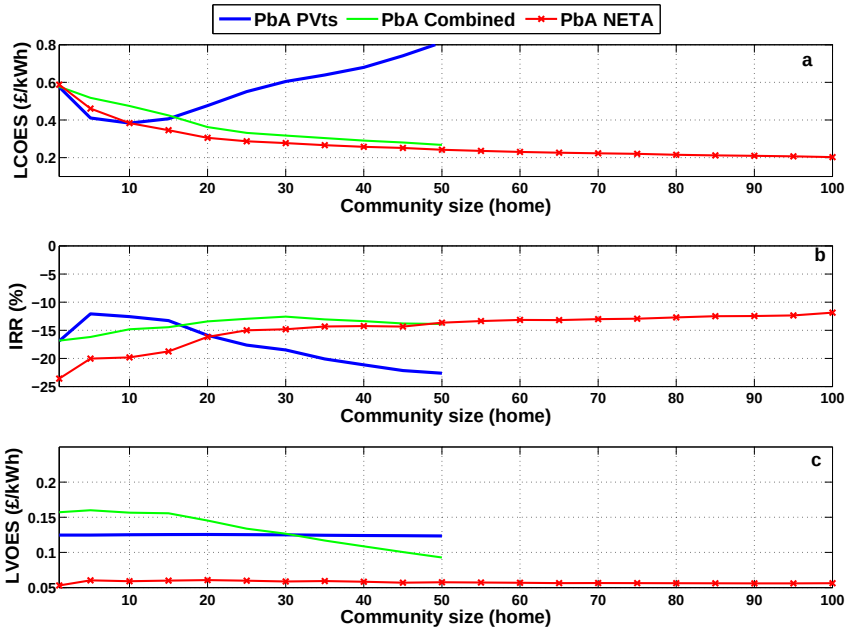

Figure 6.42: Optimised (a) *LCOES*, (b) *IRR* and (c) *LVOES* as a function of the size of the community for PbA technology depending on the application developed when considering the NETA tariff in 2020.

Moreover, the consideration of the PV management increased the profitability of the investment and the value of the discharge. The use of the local PV generation was more attractive from a financial point of view than shifting the demand load with the NETA tariff. For the 5-home community with a community PV percentage equal to 100%, the *IRR* and the *LVOES* increased up to -16.2% and 0.16 £/kWh respectively, which means a 19% and 167% increase regarding the LS values (-20.0% and 0.06 £/kWh respectively). The remarkable increase in the

LVOES was related to the fact that PV energy was only discharged at peak time. This effect was more remarkable for community with community PV percentages higher than 75%.

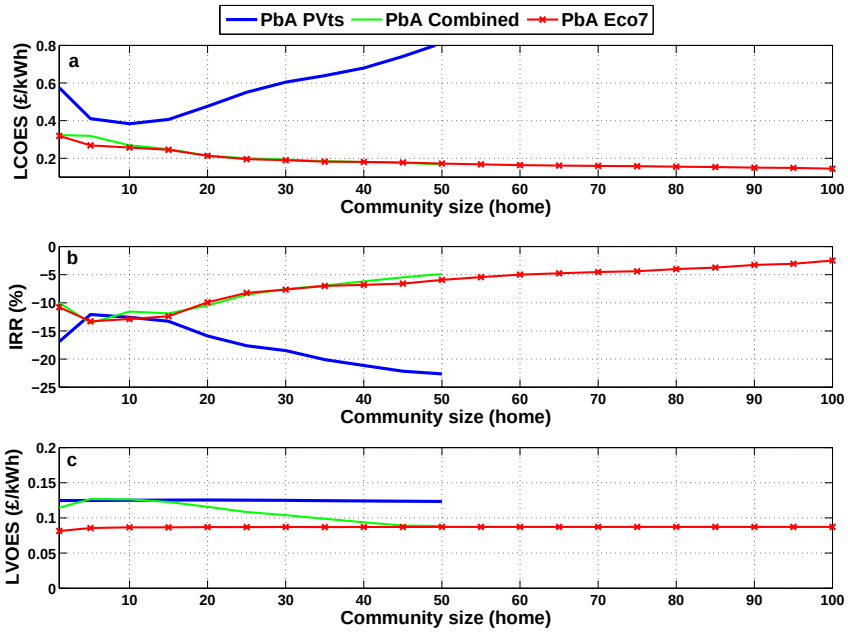

Figure 6.43: (a) *LCOES*, (b) *IRR* and (c) *LVOES* optimised for PbA technology as a function of the size of the community depending on the application when considering Economy 7 in 2020.

Same effects where introduced by PVts when incorporated to LS with Economy 7. However, the larger annual discharge achieved with this tariff buffered the impact of adding PVts. Additionally, charging from the grid was not limited as it was with the NETA tariff due to the much longer peak period of Economy 7. As a consequence, the cost of meeting the demand load just slightly increased because the electricity generated from the PV plants counterbalanced the reduction of the shifted demand load. In the case of the 5-home community (100% of PV percentage), the *LCOES* increased by 19% (from 0.27 £/kWh to 0.32 £/kWh). Again, PVts markedly increased the value associated with the battery discharge to 0.128 £/kWh for the 5-home community (it was equal to 0.086 £/kWh with Economy 7). Also, the *LVOES* was higher than when only PVts was considered (0.125 £/kWh) for community PV percentages higher than 75% since the electricity charged from the PV plants was discharged only at peak time. The consideration of PVts did not modify the profitability of the project remarkably and the *IRR* only increased from -12.9% to -11.6% (10%) for the 10-home community due to the lower impact of the electricity charged from the PV plants on an annual basis.

Figures 6.44 and 6.45 show the results for Li-ion batteries when combining

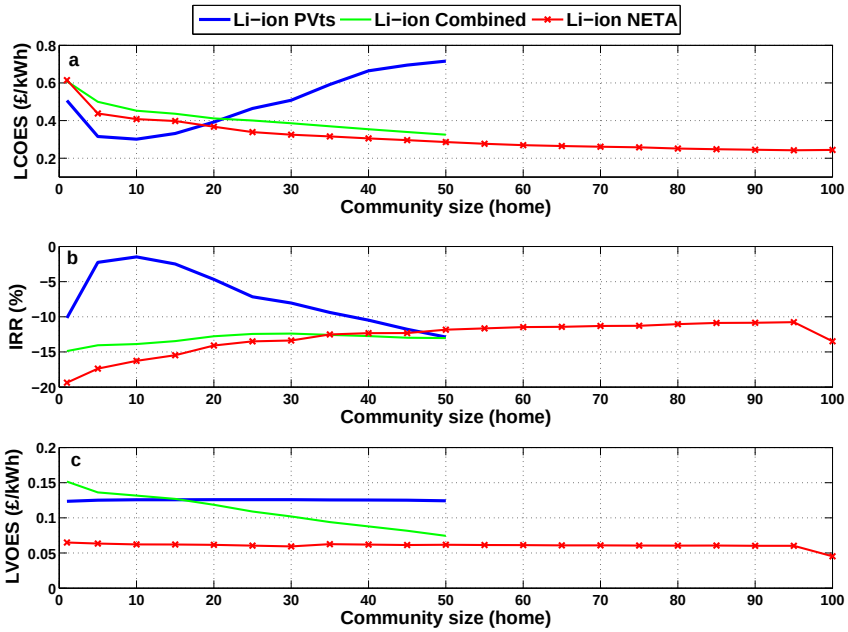

Figure 6.44: (a) *LCOES*, (b) *IRR* and (c) *LVOES* optimised for Li-ion technology as a function of the size of the community depending on the application when considering the NETA tariff in 2020.

PVts with the NETA tariff and Economy 7 respectively. The combination of applications made the maximum *LVOES* obtained by PbA and Li-ion batteries different. The *LVOES* is proportional to the round trip efficiency. Therefore, the maximum *LVOES* was achieved by the battery with the largest capacity when PVts and LS were investigated independently, the maximum round trip efficiency of PbA and Li-ion technologies being very similar as shown in Figures 6.4 and 6.5. When both applications were combined, the maximum *LVOES* was obtained by the batteries with the smallest capacity in which the fraction of energy charged from the PV plants managed by the battery was higher for any community. While Li-ion batteries offered high round trip efficiency for low capacities for any community size (as shown in Figure 6.5), PbA technology required larger capacities to achieve similar values. This was the reason why the maximum *LVOES* achieved by Li-ion technology (0.141 £/kWh) when being charged from the PV plants and the grid using Economy 7 was higher than the value achieved by PbA technology (0.126 £/kWh). In the case of the NETA tariff, the round trip efficiency played the same role but this time the peak and valley prices were variable on a daily basis. PbA technology only discharged when the peak prices were much higher than the off-peak prices and this impacted on the revenue obtained by PVts i.e. increased its *LVOES* up to (0.16 £/kWh). The maximum *LVOES* of Li-ion technology was 0.136 £/kWh.

H_2 results are presented in Figure 6.46 including the *LCOES* and the *LVOES*

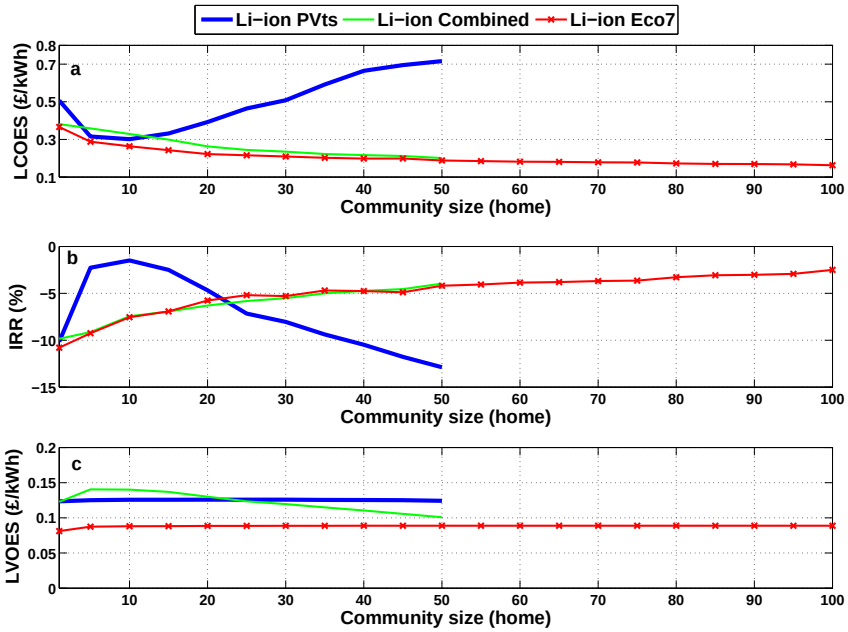

Figure 6.45: (a) *LCOES*, (b) *IRR* and (c) *LVOES* optimised for Li-ion technology as a function of the size of the community depending on the application when considering Economy 7 in 2020

associated with electricity generation. The flexibility of H_2 storage varied some of the patterns followed by the economic parameters in comparison with those of the battery technology. By adding PVts to LS, the *LCOES* just slightly reduced for those communities with more than 75% due to the similar ratings of the electrololysers for LS and for LS with PVts. Specifically the minimum *LCOES* of the electrolysers performing LS and LS with PVts was 0.30 £/kWh$_e$ in the 10-home community.

The *IRR* was between the values achieved by PVts and LS independently and only for the 10-home community, in which the efficiency of the PEMFC system was higher, adding PVts reduced the profitability to -16.1% (-11.4% for LS). PV energy was given priority to run the electrolyser at any time and the electrolyser missed periods in which the valley prices were very attractive. For the rest of communities, the incorporation of the PV management increased the value although this effect was more marked for high community PV percentages. Main results for the three technologies are compared in Table 6.8.

6.8 Summary and conclusions

The method and methodology presented in Section 5.1 have been tested using the demand data, PV generation and heat generation models introduced in the second part of Chapter 3. The performance, economic benefits and optimum CES system

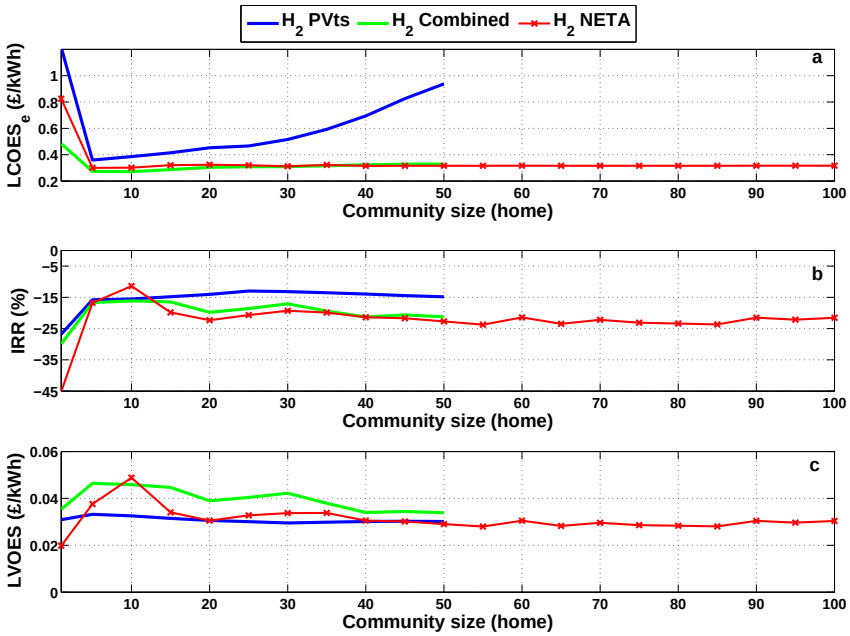

Figure 6.46: (a) *LCOES*, (b) *IRR* and (c) *LVOES* optimised for H_2 technology as a function of the size of the community depending on the application when considering the NETA tariff in 2020.

for end user applications were quantified as a function of the size of the community. The application of the method and the methodology allowed the comparison of different technologies, applications, the evaluation of the aggregation of benefits by the consideration of several applications and the impact of the aggregation of demands in the performance and economic benefits of CES.

One of the key conclusions according to the results derived from the application of the method, PVts increases the *LVOES* of CES and LS has the potential to reduce the *LCOES* as demonstrated with Economy 7. The maximum *LVOES* associated with PVts was up to 0.13 £/kWh when projected to the year 2020 according to the reference scenarios, reducing to 0.06 £/kWh and 0.09 £/kWh for LS with Economy 7 and the NETA tariff respectively. In the case of the *LCOES*, the minimum values were 0.3 £/kWh, 0.14 £/kWh, 0.2 £/kWh for PVts in 2020, LS with Economy 7 and LS with the NETA tariff respectively.

The *IRR* depends on the balance between the *LVOES* and the *LCOES*. According to the figures above, the *IRR* was negative for any of the reference scenarios considered in 2020 and only when the price of the electricity and the natural gas went up to 0.194 £/kWh and 0.094 £/kWh respectively or the export bonus disappeared, the *IRR* became positive for PVts and LS with Economy 7 in 2020. Another important result is that battery systems performing PVts also needed community PV percentages higher than 75% in order to achieve positive *IRR* val-

Table 6.8: Economic parameters optimised for PbA, Li-ion and H_2 technologies using PVts and LS in 2020 and the zero carbon year. The size of the community and the capacity of the battery (kWh) or the rating of the electrolyser (kW) which achieved the optimum values is shown in brackets.

Year	technology	Tariff	*LCOES* (£/kWh)	*IRR*(%)	*LVOES*(£/kWh)
2020	**PbA**	**NETA**	0.27 (50,570)	-12.6 (30,463)	0.16 (5,13)
		Eco7	0.17 (50,564)	-5.0 (50,564)	0.13 (5,20)
	Li-ion	**NETA**	0.33 (50,316)	-12.4 (30,417)	0.15 (1,5)
		Eco7	0.20(50,358)	-1.5 (10,159)	0.14 (5,11)
	H_2	**NETA**	0.27_e(10,1.1)	-16.1 (10,1.1)	0.05 (5,1.1)
Zero carbon	**PbA**	**NETA**	0.10 (100,1620)	24.2 (60,631)	0.33 (1,4)
		Eco7	0.06 (100,1253)	64.2 (100,674)	0.27 (25,68)
	Li-ion	**NETA**	0.14 (100,821)	16.0 (70,304)	0.31 (1,3)
		Eco7	0.09(100,996)	34.4 (100,559)	0.29 (15,34)
	H_2	**NETA**	0.21_e(100,15.7)	39.2 (10,2.2)	0.16 (10,2.2)

ues, while those performing LS with Economy 7 also needed communities with more than 75 homes. Likewise, the highest the electrical efficiency of PEMFC systems, the highest the revenue for H_2 systems due to the higher price of the electricity. Alternatively, CES became a profitable energy option when project to a hypothetical zero carbon target even when the technology cost kept constant with the 2020 levels.

CES requirements per home reduced with the community size due to the better matching between PV generation and the demand load for PVts and the less importance of the peak period for LS. These two community effects made some performance parameters such as he *EFC*, PV_{ES} and D_{ES} higher for small communities up to 20 homes. However, the community approach helped to increase the range of CES sizes which achieved high performance values as the community size increases. This helped to reduced the *LCOES* associated with any application when considering that the optimum CES system is a trade-off decision between the *EFC* and the round trip efficiency for battery technology and C_{factor} and the electrolyser efficiency for H_2 technology. The larger the community, the higher the *IRR* and the lower the *LCOES* although the benefits introduced by the community approach were more marked for communities up to 25 homes. This was a consequence of the randomness associated with the demand loads for the small communities.

When CES systems perform PVts and LS simultaneously, the performance results are the result of the combination of effects introduced by both applications. Which applications is more relevant depends on the management system and the CES size. The management system determines which application has priority for charging the CES system (PVts in this work) and if RE is only discharged at peak periods (this was assumed in this work). Then, increasing the size of the CES

system intensifies the importance of the application which does not have priority and effects from both applications are combined.

Interestingly, a water tank with a PV controller which shifts the surplus PV generation in a single home was the CES system which obtained better economic results in 2012 ans 2020, especially when the property already has a water tank (maximum *IRR* equal to 7.5%). H_2 demonstrated its flexibility for applications such as heat decarbonisation, the prevent of power curtailment and the combination of applications. The consideration of PV power curtailment obligation increased the *LVOES* and the *IRR* by 47% and 67% respectively with regard to the same H_2 system performing only PVts. When PVts and LS were combined, the impact of H_2 storage in the community was boosted and the PV_{ES} kept constant while the H_{2ratio} doubled regarding only *PVts* or *LS*. Finally, PbA technology demonstrated good performance and better economic behaviour than Li-ion technology for LS because CES systems are sized according to the demand load for this application. Larger battery systems were necessary as a consequence and the performance of PbA and Li-ion batteries approximated, being the initial cost of PbA batteries lower. However, Li-ion should be the preferred option for PVts in communities when the initial cost reduces as manufacturers expect (310 £/kWh in 2020). Li-ion chemistry performs PVts significantly better than PbA chemistry considering PVts requests smaller capacities, larger charge ratings and similar discharge ratings than LS.

Chapter 7

Design, construction, testing and evaluation of a community hydrogen storage system

A community hydrogen storage system (H-CES) was designed, built and tested for a low carbon community. This chapter begins with the motivation for building a H-CES system and the community in which it was installed is described, the Creative Energy Homes. Secondly, the three main components which comprise the H-CES system (electrolyser, H_2 tank and PEMFC system) are presented together with the other elements which are part of the balance of the plant (BoP).

The H-CES system performed the end user applications introduced in Chapter 3 (PVts, LS and the combination of them) and results of those tests are presented and analysed in this chapter. Long term ES was demonstrated when the H-CES performed LS and H_2 was stored for the day after. Additionally, the C_{factor} of the electrolyser increased by 116% when PVts was added to LS. Differences between simulation and experimental results were addressed for H_2 technology. The design and construction of this H-CES system complemented the insights gained from the modeling and simulation results shown in Chapter 6 and the complementary findings were emphasized.

7.1 Hydrogen technology for a community energy storage system

The flexibility of the optimization method and methodology presented in Chapter 5 was utilised to compare different ES technologies, applications and the optimum CES system as a function of the size of the community for different end user applications in different scenarios. This modeling work was complemented with the design, construction and testing of a H-CES system in a 7-home community.

The Creative Energy Homes are a group of seven energy efficient dwellings located at The University of Nottingham which have RE technologies on-site together with other low carbon technologies such as a FC systems and HPs. The Intelligent Smart Energy Community project was developed to manage the community's RE generation and electrical demand using ES and demand side management. One of the key decisions to take when building any CES system is what ES technology is utilised. As discussed in Chapter 5, battery, H_2 and thermal storage are the most suitable technologies for end user applications. Six of the dwellings already have a water tank which is integrated with solar thermal installations on place.

Battery and H_2 technologies were suggested as suitable ES technologies for this community. From a project perspective, the objective is comparing both technologies from an experimental point of view and finally integrate them in a hybrid CES system. Both CES systems were finally commissioned in October 2013 and the author of this thesis was the project manager in charge of the design, construction, testing, procurement, delivery and maintenance of the H-CES system.

The modelling work and the simulation results were considered during the design process however the rating of the different components of the H-CES system was not the optimum. This was due, in part to the still limited range of H_2 systems on the market at the moment. When referring to H_2 storage as a market product which is being developed, it is still in the research and/or demonstration stages. Additionally, there were other economic and technological factors which constrained the design and construction processes. However, this H-CES system was a unique example to:

- Test the real performance of a H-CES system when performing end user applications: PVts, LS and the combination of them.
- Compare simulation and experimental results and use the latter as a feedback to the modeling assumptions.
- Understand the practical implications of some modelling assumptions and vice versa.
- Inform stakeholders who are interested in CES about key aspects of the design, construction and commissioning process which can be improved in future systems.

7.2 The Creative Energy Homes

The Creative Energy Homes are a group of seven dwellings located at University Park, the main campus of The University of Nottingham. Figure 7.1 shows a

Figure 7.1: Panoramic view of the Creative Energy Homes at the University on Nottingham. The H-CES system was installed for this community.

panoramic view of the Creative Energy Homes. They are located at Green Close in the School of the Built Environment. The Creative Energy Homes are a real platform for research and education on sustainability applied to the architecture and built environment as well as showcasing the state of the art in energy efficient homes. The houses were built and designed to various degrees of innovation and flexibility to allow the testing of different aspects of construction including passive design, cladding materials, glazing materials, thermal performance, building services systems, RE technologies and sustainable water supply systems. The homes are occupied and are being instrumented in order to provide comprehensive post occupancy evaluation data. The houses were promoted and built by The University of Nottingham with the support of different industrial partners, each having different research or commercial interests as reflected in the houses designs and construction. The partners are David Wilson Homes, TARMAC, E.ON, BASF, The Mark Group, Saint-Gobain and The department of Architecture of The University of Nottingham. As a consequence, each house is a different project in which different sustainability aspects are showcased. A step further is the creation of a microgrid among all houses in which RE generation and demand are managed using a community approach. ES comprising battery and H_2 technologies together with demand side management are being integrated at the moment in this micro grid as schematically represented in Figure 7.2.

7.2.1 Microgeneration at the Creative Energy Homes

The Creative Energy Homes is an efficient community in 2014 but can also be considered as a new development after 2016 (new homes should be zero carbon homes after 2016 [34] or an average community in 2050 (all homes should be zero carbon by then [34]). Different types of electricity and heat generators are located

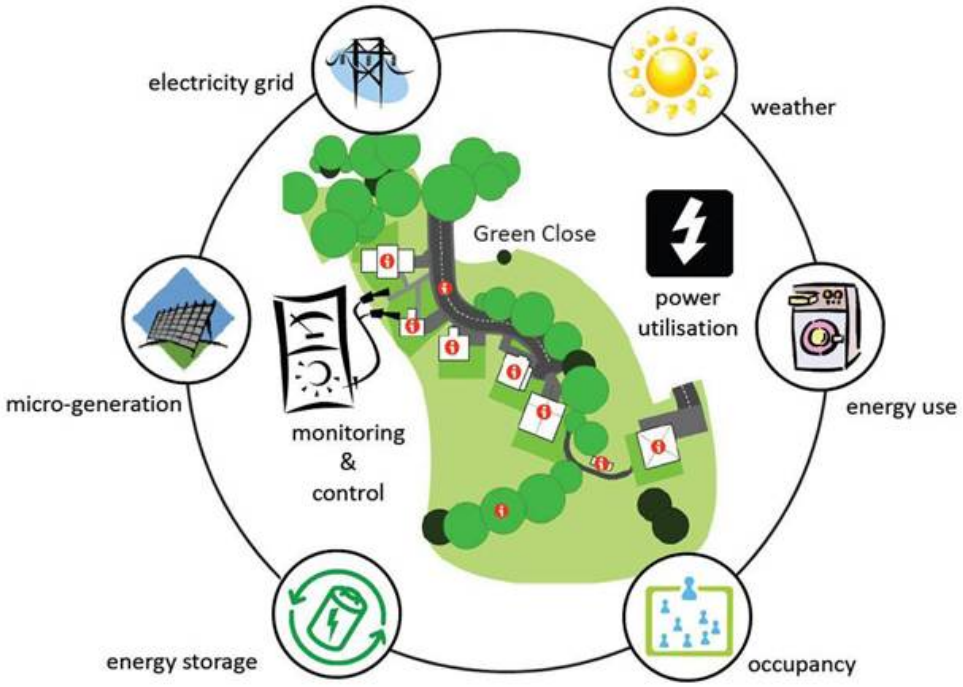

Figure 7.2: Schematic representation of the microgrid which is being created at the Creative Energy Homes community with a battery system, H_2 system and demand side management.

Table 7.1: PV arrays located at the Creative Energy Homes and their maximum power.

Home	**PV array rating (kW_p)**
David Wilson	1.5
Tarmac Code 6	3.6
Nottingham HOUSE	4
The Mark Group Eco House	3.8

on-site. Regarding RE generation on-site, PV technology is the most widespread among the seven dwellings being integrated in four of the homes. Additionally, there are also two micro-wind turbines on the area and a 1.2 kW_e SOFC system in the David Wilson Home which was installed in November 2013 running as a CHP generator. Regarding the heat generation, the BASF House and the Mark Group Eco House use air-source HPs, Tarmac Code 4 and Code 6 share a biomass boiler, the E.ON retrofit research home has a condensing gas boiler and the Nottingham HOUSE uses a heat recovery system with a back-up condensing natural gas boiler. Also, there are solar thermal collectors for DHW and mechanical ventilation heat recovery for ventilation. Table 7.1 summarizes the peak rating of the PV arrays installed in the community.

Table 7.2: Different electrical demand loads with the electrical rating in one of the Creative Energy Homes, the Tarmac Code 6

Room	**Appliance (Amount)**	**Power (W)**	**Total (W)**
Hall	Light Bulb (1)	13	13
Living room	Light Bulb (3)	13	39
Living room	Laptop (1)	360	360
Kitchen	Hot plates (4)	2200, 1400, 1800, 1800	7200
Kitchen	Kettle	(1)	2000
Kitchen	Toaster	(1)	750
Kitchen	Oven (1)	2075	2075
Kitchen	Hood (1)	250	250
Kitchen	Refrigeration and freezer (1)	87	87
Kitchen	Washing machine (1)	2050	2050
Kitchen	Fluorescent lamp (1)	20	20
Utility room	Light Bulb (1)	13	13
Toilet	Light Bulb (1)	13	13
Bedroom 1	Light Bulb (1)	13	13
Bedroom 1	laptop (1)	250	250
Bedroom 2	Light Bulb (1)	13	13
Bedroom 3	Light Bulb (1)	13	13

7.2.2 Demand at the Creative Energy Homes

The seven dwellings of the community are used for different purposes. The David Wilson Home is used as an office where six staff members of the University of Nottingham work. The Mark Group Eco House and the Nottingham house have just been launched and they are empty at the moment but they are expected to be offices too. The BASF House is the residence of three PhD students; TARMAC Code 4 is the residence of one research fellow and his family (three members in total) and TARMAC Code 6 is the residence of one PhD student and his family (three members in total). Finally, the E.ON retrofit research home is empty most time and many thermal tests are developed with it but it is also used as a temporal residence for master students in the summer. As an example, Table 7.2 represents permanent appliances and electrical equipment used in TARMAC Code 6. The total power capacity installed is more than 15 kW. Other small devices and gadgets are not included in this summary.

However, all these appliances are never used at the same time. Figure 7.3 shows real demand data of the TARMAC Code 6 house in two different days, the 17^th February, 2011 and 16^th June, 2011. The total electricity consumption was

10.2 kWh and 8.1 kWh respectively. This figure also shows the PV generation in both days and the two profiles emphasize the marked seasonal pattern of PV generation (the PV array is also partially shaded). The daily PV generation was 1.2 kWh and 16.3 kWh respectively.

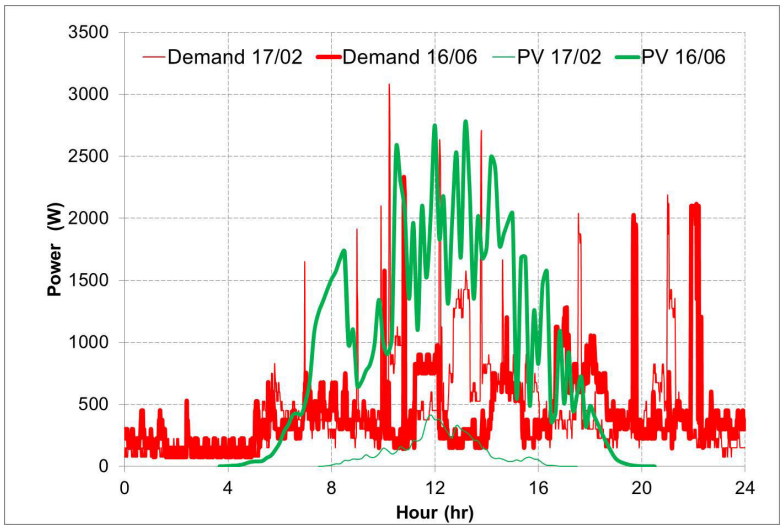

Figure 7.3: Electrical consumption and PV generation in one of the Creative Energy Homes, the Tarmac Code 6, in two different days.

7.3 Community hydrogen storage system at The University of Nottingham

The H-CES system comprises three main components: an electrolyser, H_2 tank and a FC system. Next, these three systems are described in terms of the chemistry they utilise to generate, store and use H_2 respectively and their BoP.

7.3.1 Electrolyser system

A PEM electrolyser manufactured and commissioned by ITM Power is utilised to generate H_2. The model is the HBox-PV which was designed for direct coupling to a PV array. Figure 7.4 shows the HBox-PV electrolyser in its final location at The University of Nottingham. The PEM electrolyser is both voltage and current limited with a peak voltage of 60 VDC and a peak current of 75 ADC. The maximum electricity peak capacity of the electrolyser is 1.1 kW_e. This corresponds to the electrolyser rating which reduced the LCOES associated with PVts for a 5-home community as indicated in Table 6.4.

The system was designed for PV off-grid applications therefore uses DC power as the system input. It is capable of operating without supervision using only the

Figure 7.4: PEM electrolyser at The University of Nottingham. The model is the 1.1 kW_e HBox-PV manufactured by ITM Power.

PV input and coping with the fluctuating nature of a PV power source. From the PV array perspective, the electrolyser can be viewed as a variable demand load which conducts maximum power point tracking in order to maximize the power from the DC source by varying the voltage. The parasitic losses were minimized to approximately 6% of the electrolyser electrical rating according to the design. This allows the electrolyser to be able to generate H_2 with a minimum PV input equal to 40 W according to theoretical design. The electrolyser system integrates the H_2 generation, pressurisation, water-gas separation and cooling. All these different processes are managed by an internal control system which monitors different performance variables such as pressure and temperature and supervises the performance. Table 7.3 summarizes the main performance parameters which describe the electrolyser performance according to the design specifications.

There are two additional elements necessary for the operation of the electrolyser which are briefly introduced next; the deionised water system and the electrical

Table 7.3: Electrolyser performance parameters and values reported by the manufacturer.

Parameter (unit)	Value
H_2 generation (g/h)	up to 18
Input voltage (VDC)	up to 45
Input current (ADC)	up to 30
System working pressure (bar)	up to 15
H_2 Gas Purity (%)	99.99
Cell voltage at 1 A/cm^2 and 55 °C (V)	2.1
Minimum η_{ele} (kWh/Nm^3)	4.9
PV Power Rating (kW)	1.2
Maximum water consumption (cc/h)	150
Deionised water quality	ASTM Type 2 DI water

converter.

Deionised water unit

The electrolyser needs deionised water for generating H_2 and therefore a deionised water unit was installed for this purpose. The deioniser selected was supplied by the company Elga Water Process. It supplies deionised ASTM type 2 DI water (water purity higher than 1 MΩ/cm and total organic carbon, TOC, level <50 ppb). The water is supplied to the electrolyser with a pressure just above atmospheric. A feed pump was incorporated in order to supply water at the pressure specified. The deionised water unit has a 35 litre water tank to guarantee the supply, the maximum water production rate being 7.5 l/hour. Table 7.4 summarizes the main parameters which define the deioniser water unit characteristics in relation to the electrolyser requirements seen in the previous section.

Table 7.4: Deioniser water unit performance parameters and values reported by the manufacturer.

Parameter (unit)	Value
Resistivity (MΩ/cm)	>1
Total organic carbon (ppb)	≤ 50
Pressure supply (bar)	1-3
Electrical consumption (W)	43

DC converter

The electrolyser was designed for direct coupling with a PV array and therefore an additional component was necessary for its integration into an AC microgrid. The electrolyser DC input voltage should always be lower than 60 VDC but the PV arrays on the roof of the houses, summarized on Table 7.1, generate DC electricity at a voltage higher than 230 VDC and they are directly coupled to a grid tie DC/AC inverter. As a consequence, direct coupling between the electrolyser and any of the PV arrays was not possible. There were two possibilities to connect the electrolyser to the microgrid: install a DC/DC voltage converter between one of the PV arrays and the electrolyser or an AC/DC converter between the grid and the electrolyser. Finally, the second option was selected due to two main reasons. Firstly, an AC/DC converter enables utilisation of the PV generation from all PV arrays located in the area following a community approach as suggested in this thesis. Secondly, finding a suitable AC/DC converter on the market for the required voltage and current input ranges of the electrolyser was possible, while a specific DC/DC converter suitable for this project would have been custom-built, making this choice more expensive and time-consuming. The AC/DC converter selected for this project was supplied by the company Power Solve. Table 7.5 shows the main performance parameters of the rectifier related to the electrolyser requirements.

Table 7.5: AC/DC converter performance parameters and values reported by the manufacturer

Parameter (unit)	Value
Power rate (W)	1500
DC supply voltage (V)	up to 48
DC supply current (A)	up to 31.3
Efficiency (%)	90

7.3.2 The hydrogen tank

The H_2 generated by the electrolyser should be stored until there is an economic driver for using it related to the different end user applications the H-CES system performs. As it was explained in Section 2.6.3, there are three main H_2 storage categories in the market: compressed gas, liquefied H_2 and solid state (metal hydrides). The H_2 tank used in this project uses Mg to store H_2 as a metal hydride. This decision was made considering that the H_2 tank is part of a H-CES system located in a residential area. Metal hydrides have two characteristics which make them more attractive and potentially safer in comparison with the other alternatives. Firstly, metal hydrides do not store H_2 at high pressure while achieving

similar energy densities to compress gas technology. In addition to this, it is possible to benefit from the thermodynamics which govern the performance of the MgH_2 tank to reduce and/or stop any potential leak. Heat is necessary to promote the desorption of H_2 and cutting the heat supply can be used to stop the discharge in the case of any H_2 leak. This technique is utilised in the system at The University of Nottingham.

The H_2 tank was manufactured by McPhy Energy and is able to store up to 4 kg of H_2 using of Mg powder. MgH_2 has scientific significance because it has the highest energy density equal to 9 MJ/kg of all reversible hydrides [79]. It can be considered as the benchmark technologies for solid state H_2 stores. Figure 7.5 shows the H_2 tank in its final location at The University of Nottingham. The main components of the H_2 tank system are: metal hydride, the thermal management, the gas panel and the electrical control system.

Metal hydride tank

The MgH_2 tank was designed to work under pressure up to 12 bar and at a temperature up to 390 °C. The MgH_2 tank is filled with Mg based pellets which react with H_2. The reaction direction is controlled by the temperature and pressure inside the MgH_2 tank. The Mg pellets are located inside a metallic cylinder which gives them mechanical stability and integrity. H_2 is absorbed or released by means of a coaxial pipe.

Thermal management system

The main disadvantage of MgH_2 is that a significant amount of heat should be managed at high temperature, typically between 300 °C and 500 °C due to the high enthalpy of reaction, around 70-75 kJ/mol [79]. In the H_2 tank at The University of Nottingham, the absorbed or released heat is managed using PCM. The heat storage system is divided in two semi-circular tanks in which the PCM was tightly applied around the MgH_2 tank. Additionally, the PCM is also used to measure the amount of H_2 in the MgH_2 tank. During the discharge, PCM (initially liquid) starts to become solid, which causes the pressure to increase in the heat storage system. As a result, measuring the pressure of the PCM gives information about the amount of PCM solidified and it can be related to the quantity of H_2 in the MgH_2 tank. The PCM is an alloy containing Tin (Sn), Zinc (Zn) and Magnesium (Mg). Both, the MgH_2 tank and the PCM are insulated from the exterior. The insulation keeps the thermal losses of the system to around 700 W.

The gas panel

The gas panel has two main functions: deliver H_2 at conditions which are suitable for the application during the discharge and supply H_2 at suitable conditions to the

Figure 7.5: Magnesium metal hydride tank at The University of Nottingham.

MgH_2 tank during the charge. During the discharge, H_2 is supplied cold (50 °C), filtered and with a pressure and/or flow according to the application, the MgH_2 tank being at 350 °C and 10 bar, approximately. Likewise, the cold H_2 provided by the electrolyser (around 40 °C – 50 °C) is regulated in flow and filtered before being supplied to the MgH_2 tank. The main components of the gas panel are:

- A cooler: H_2 is cooled using forced convection in a H_2-air heat exchanger composed of tubes with fins.
- A flow regulator: comprised of a mass flow controller, a control valve and

pneumatic two way valves in order to achieve the pressure or the flow required by the MgH_2 tank or by the PEMFC system depending on the storage cycle. The flow regulator is capable of regulating the H_2 flow between 1.2 g/h and 60 g/h in this H-CES system.

- A filter: a stainless steel filter is used to remove any impurity or potential particles.
- A buffer: the H_2 buffer is able to store 21 l of H_2 and it is used to supply H_2 when the flow is lower than 20 g/h.

This mass flow regulator was a special requirement of this project in order to integrate the tank with the electrolyser. A flow regulator between 20 g/h and 600 g/h is incorporated in other tank models. Due to the incorporation of this new flow controller, the buffer is not really necessary in this tank but it was finally incorporated in the commissioning due to the complexity of its removal.

The gas panel is shown in Figure 7.6. The buffer (which can be seen at the bottom right corner of this figure) impacts on the interaction between the H_2 tank, the electrolyser and the PEMFC system by modifying the flows among the three subsystems. The MgH_2 tank is not charged until the pressure inside the buffer is 8 bar. The H_2 flow transducer is located downstream the buffer during the charge. As a consequence, the electrolyser flow is only equal to the flow supplied to the MgH_2 tank once 8 bar is reached in the buffer and this is the reason why the H_2 stored in the MgH_2 tank does not increase at the beginning of the H_2 generation as shown in the results presented in Section 7.5.1. Similarly during the discharge, the flow supplied by the MgH_2 tank may be different than the real H_2 consumption of the PEMFC system, especially during the start-up. The buffer can supply H_2 to the PEMFC system and also accumulate part of the H_2 supplied by the MgH_2 tank.

The electrical unit

The H_2 tank uses electricity to keep the MgH_2 tank at the working temperature (350 °C) and to control the MgH_2 tank (absorption and desorption) and the rest of components (flow regulator, heat management system and some actuators). The H_2 tank also uses compressed air for the pneumatic valves. Table 7.6 summarizes the main specifications of the H_2 tank according to the manufacturer.

7.3.3 The PEMFC system

The PEMFC system uses the H_2 stored in the H_2 tank when there is an economic benefit derived from its operation. As it was explained in Section 2.6.3, there are different types of FC systems on the market, SOFC and PEMFC systems

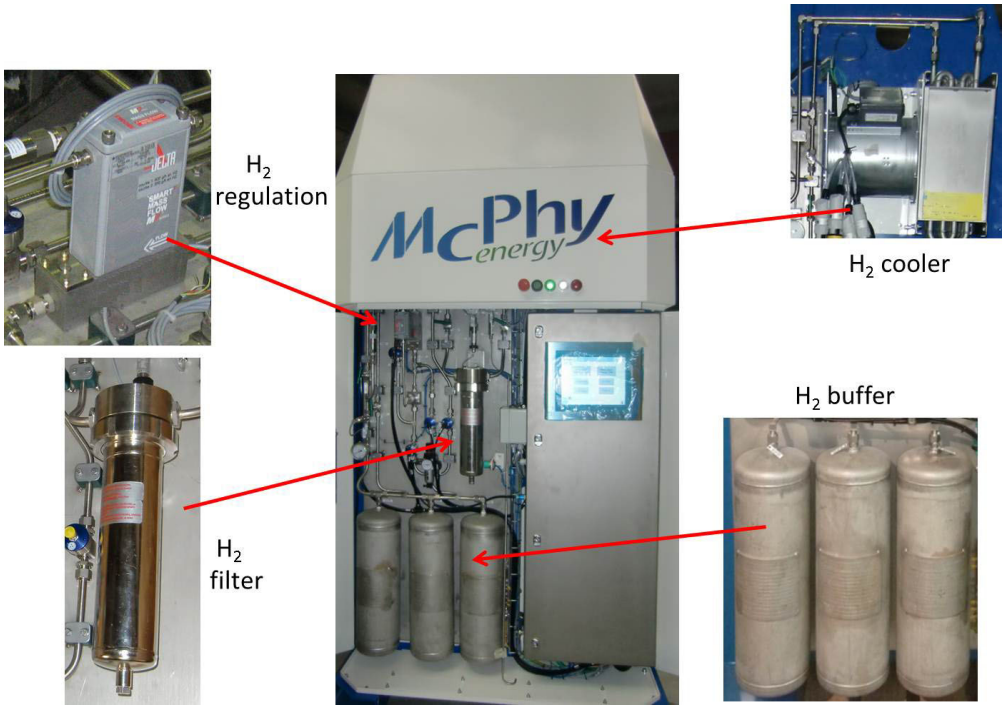

Figure 7.6: Gas panel of the H_2 tank including its main components.

Table 7.6: MgH_2 storage system specifications as reported by the manufacturer

Parameter (unit)	Value
Maximum capacity (kg)	4
Nominal inlet pressure (bar)	8-10
Nominal outlet pressure (bar)	1.5-2.5
Maximum flow rate (g/h)	600
Electrical consumption (W)	800

being the most widespread technologies. In this project, a 20-cell PEMFC stack manufactured by Ballard is used to generate electricity and heat as shown in Figure 7.7. This PEMFC system is able to generate up to 75 ADC at a voltage equal to 12 VDC, a maximum power rate equal to 0.9 kW_e approximately. According to the specifications, the heat generated by the PEMFC system at maximum current is a bit higher than the electrical output and equal to 1 kW_h. Unlike the electrolyser and the H_2 tank systems supplied by ITM Power and McPhy Energy, Ballard Power Systems only supplied the PEMFC stack. As a consequence, the whole BoP was designed and commissioned as part of this project following Ballard Power Systems specifications. Following the same system approach introduced in [76], the different elements which comprise the PEMFC system are introduced next.

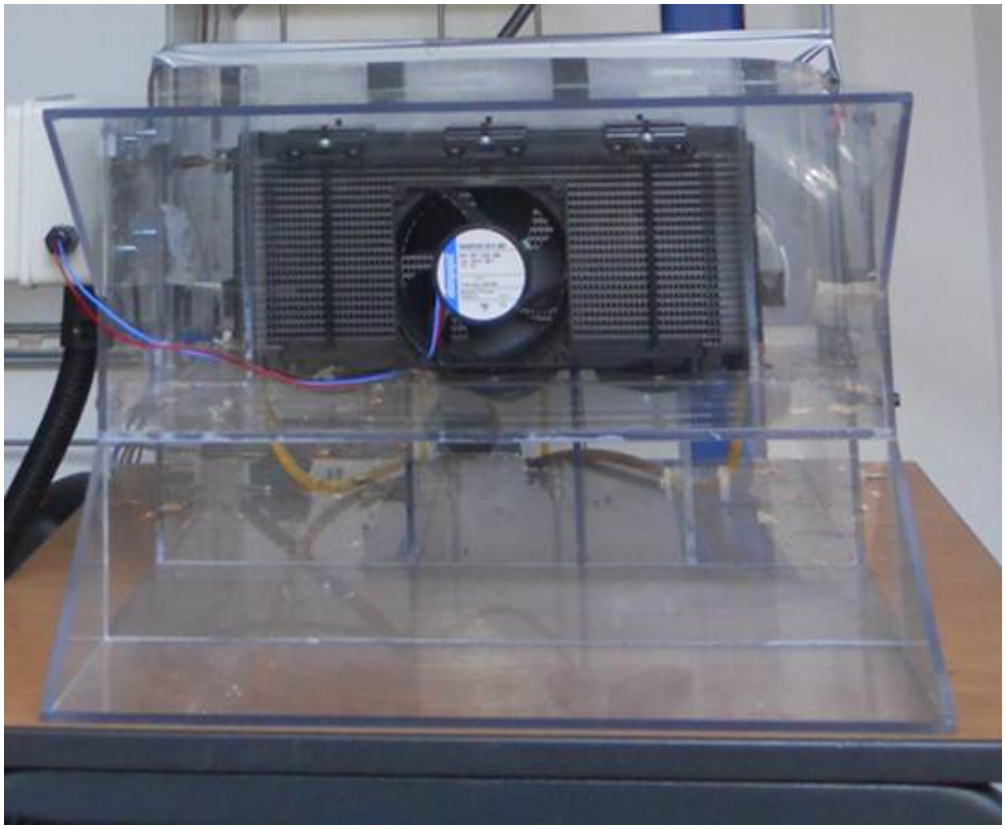

Figure 7.7: PEMFC system located at The University of Nottingham.

Fuel cell stack subsystem

The stack has 20 cells and generates the DC voltage and current by consuming the H_2 and oxygen from the air. Its performance is represented in Figure 7.8 by means of the voltage and current characteristic according to the manufacturer.

Hydrogen supply subsystem

The H_2 tank described above is the most important element of the H_2 supply subsystem. However, the H_2 stored in the H_2 tank should be supplied at a pressure and rate specified by the PEMFC system characteristics. In addition to this, impurities which build in the PEMFC anode need to be removed. The H_2 supply subsystem is comprised of five different elements:

- H_2 tank: it supplies the H_2.
- Pressure regulator (Swagelok): it reduces the pressure down to the optimum for the PEMFC stack equal to 0.4 barg.
- 1 l gas reservoir (Swagelok): located at the outlet of the pressure regulator. It helps to keep the pressure constant during the purge.

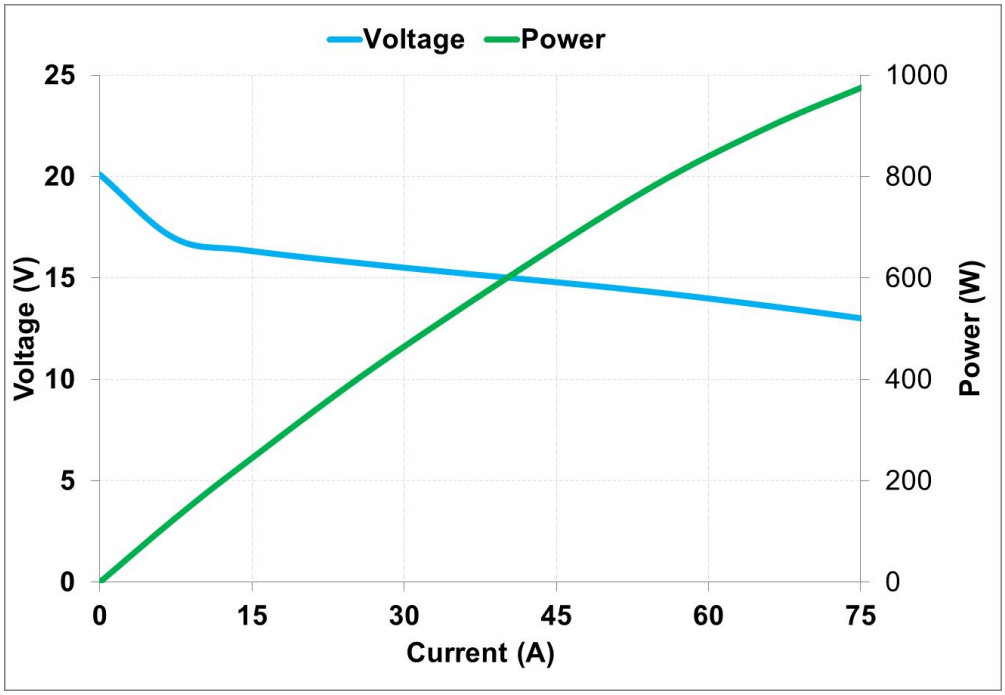

Figure 7.8: Voltage and power of the PEMFC stack as a function of the current generated based on the polarization curve of a single cell according to the manufacturer specification when considering the 20 cells.

- Supply valve (Burkert): a solenoid valve which allows the supply of H_2 to the PEMFC system or isolates the PEMFC stack when it is de-energized.
- Purge valve (Burkert): a solenoid valve which performs the purge in order to clean the impurities which build up in the anode.

Thermal management subsystem

This subsystem supplies the coolant to keep the PEMFC stack close to the optimum temperature and at the same time supplies the oxidant (oxygen) necessary for the reaction. In this configuration, the coolant and the oxidant are the same fluid (air) but coolant requirements are distinctly higher than the oxidant requirements, up to 80 times more air flow at maximum power. The main elements of this subsystem are:

- A fan (Ebm-Pabst): it supplies the air necessary for keeping the temperature close to the optimum and also supplies the oxidant for the reaction.
- A filter: it removes any particle or dust from the air which could damage the PEMFC stack.

The fan keeps the temperature of the stack in a safe temperature range and its speed is adjusted to meet the optimum temperature. Figure 7.9 shows the optimum temperature as a function of the current generated by the stack.

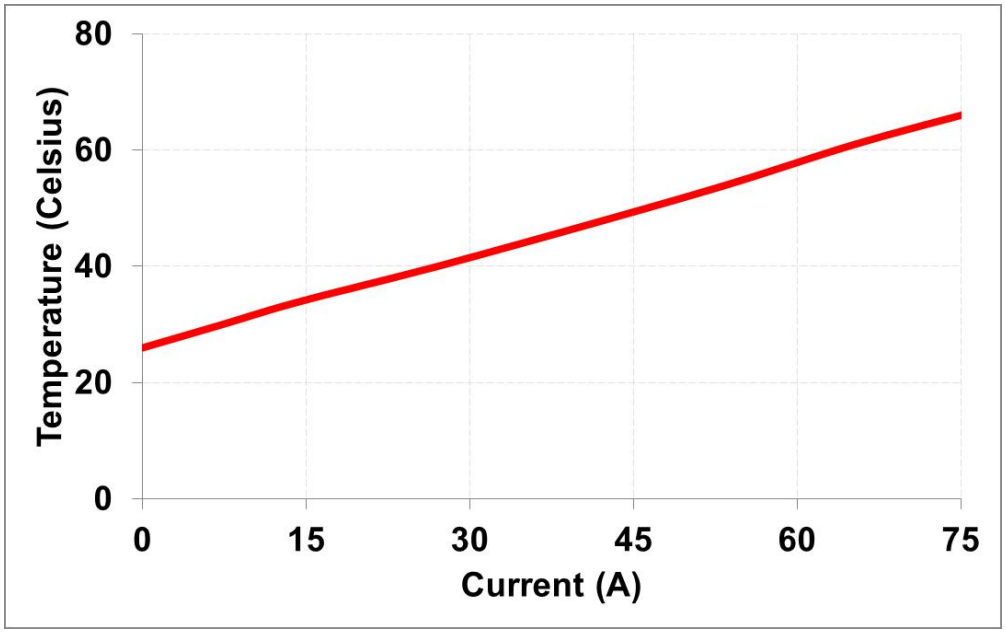

Figure 7.9: Optimum temperature of the PEMFC stack as a function of the current generated according to the manufacturer specification.

Power electronics and control subsystem

This subsystem is responsible for controlling the whole operation of the PEMFC system safely and efficiently and integrates the electrical demand load which is connected to the stack. The core of this subsystem is the algorithm which controls the PEMFC system based on the real variables together with the data acquisition (DAQ) hub with automation capability. The DAQ hub is the NI USB-6009 from National Instruments and the algorithm was implemented with the software LabVIEW. A printout of the code implemented in LabVIEW is shown in Appendix H. The DAQ hub was used to transmit the signals from the different transducers to the control algorithm, and the control commands generated by the algorithm to the different actuators on the other direction. Other necessary elements are:

- Thermistors (Maruta): two thermistors monitor the PEMFC stack temperature.
- Current transducer (Lem): monitors the current generated by the PEMFC stack.
- Voltage transducer (Lem): monitors the voltage generated by the PEMFC stack.
- Relays (Finder): command the operation of the fan, supply valve, purge valve and the contactor.
- DC contactor (Tyco): isolates the PEMFC stack from the demand load after the shutdown.

- Auxiliary supply (Weidmuller): all actuators, the current and voltage transducers use 24 VDC and demand some power. Overall, a 72 W auxiliary power supply at 24 VDC is used to run all the BoP.

The electrical demand load in this project is the DC/AC inverter connected to the grid. This PEMFC stack generates low DC voltage (between 12-18 VDC) and high AC current (up to 75 ADC). Finding a suitable DC/AC inverter for this stack was a challenge because despite inverters have been developed recently for RE technologies, most of them are designed for PV applications in which the input voltage is higher than 230 VDC. Even the only standard inverter available on the market for FC systems by SMA Solar Technology AG was designed for a voltage range between 20 and 50 VDC which is always higher than the voltage generated by the stack as shown in Figure 7.8. Finally, an inverter supplied by the company Power Solve was used in this project because it was the closest fit to this application. The characteristics of the inverter are shown in Table 7.7. Additionally, the PEMFC system needs a passive load at the start-up and a load bank is utilised for this purpose which is then disconnected with another contactor equal to the one introduced above.

Table 7.7: DC/AC inverter technical characteristics as reported by the manufacturers.

Parameter (unit)	**Value**
DC input voltage (V)	10.5-28
DC input current (A)	4-65
Power rating (kW)	1.2
Nominal efficiency (%)	90

Finally, the different equipment utilised to control and actuate the PEMFC system consumes electricity which should be considered as parasitic losses and reduces its final efficiency. The nominal electrical consumption of the parasitic loads is summarized in Table 7.8. The value of the fan consumption reflects the maximum power when it is spinning at maximum speed, 29 W. The two contactors consume 14 W each but only for one second approximately when they are engaged and disengaged. As a consequence, the consumption from the contactors can be neglected.

7.4 H-CES system integration, building and safety

The electrolyser, the H_2 tank and the PEMFC systems were integrated to perform as a safe, coordinated, reliable and efficient H-CES system. The H_2 only

Table 7.8: Parasitic loads and the nominal value as reported by the manufacturer.

Parasitic load	Value (W)
Maximum fan power	29
Voltage transducer	1.2
Current transducer	2.4

Figure 7.10: Cabinet where all electrical and electronic equipment was located.

flows between the electrolyser and the H_2 tank and the H_2 tank and the PEMFC system. A three way valve was allocated among the three systems in order to facilitate the flow in the proper direction depending on the storage cycle. All the different electrical and electronic components which are necessary for the safe and reliable performance of the PEMFC system were placed inside an electrical cabinet as shown in Figure 7.10. Figure 7.11 shows a schematic representation of the final layout of the installation with the different flows of the utilities used by the different systems.

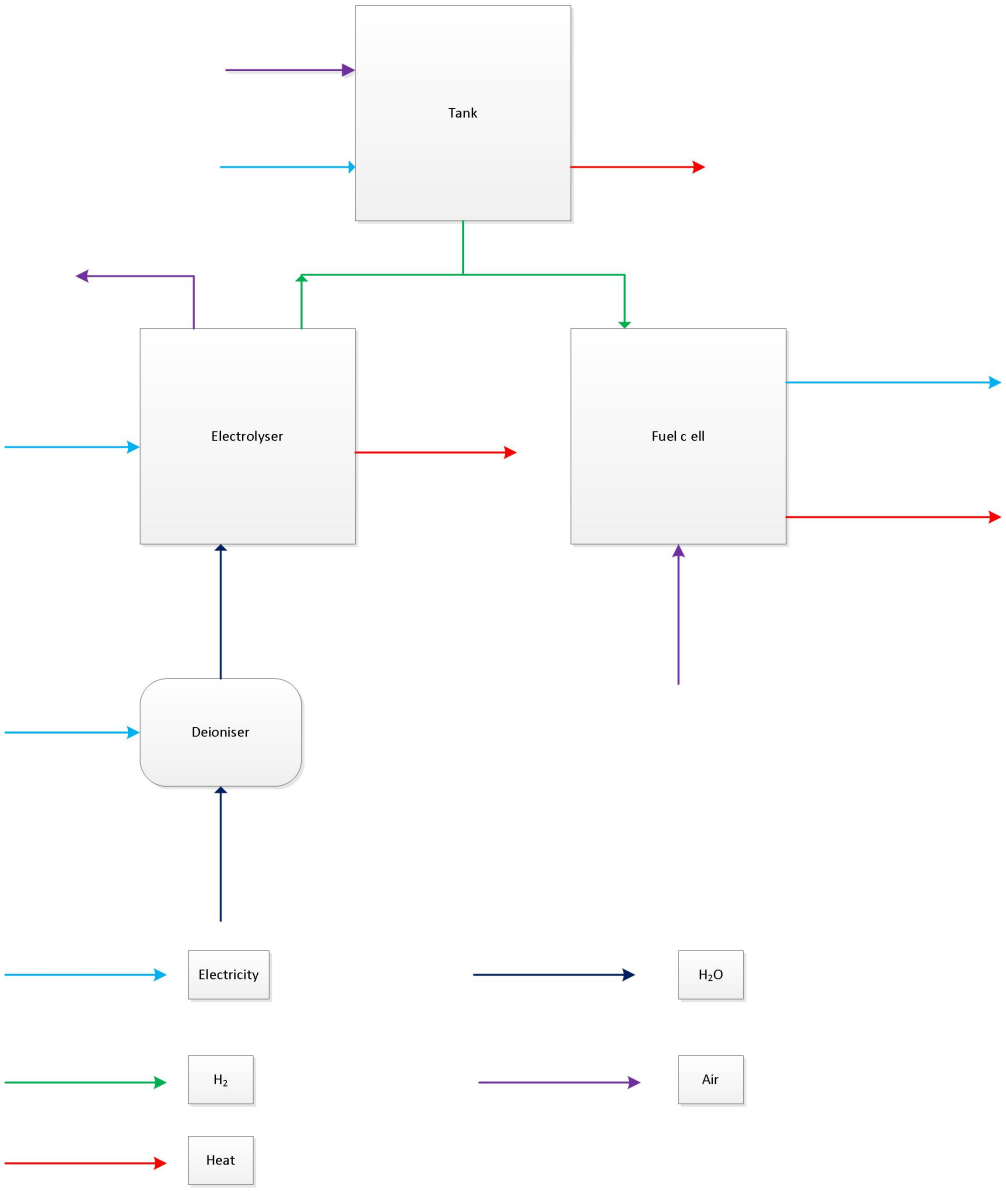

Figure 7.11: Schematic representation of the H-CES system with the main energy flows and fluids utilised by the electrolyser, H_2 tank and PEMFC systems.

H_2 is a highly flammable substance and the lightest, therefore the building was designed according to the dangerous substances and explosive atmospheres

regulations [173]. Additionally, risk assessments were designed for the three main subsystems and a global safety operation procedure is available at the location. Only personnel trained for this purpose can access the installation. The H-CES system is allocated inside a building which was selected for this application and it is integrated with the Creative Energy Homes as shown in 7.12. The main characteristics of the building are summarized below:

- The plant is big enough to allocate the different equipment, operate them and perform any necessary maintenance.
- The space taken by the different equipment was optimized in order to effectively integrate the H-CES in the community.
- The building selected is a metal shed which is 3.5 m width, 4 m long, 2.8 m eaves and it has a height of 3 m at the ridge height.
- The roof could be relieved in unlikely case of any explosion because it is fixed with bolts.
- The roof also has intrinsic ventilations which are necessary in case of any H_2 leak occurs. Specifically, it has 40 orifices which are 130×25 mm^2 each at the ridge and another 20 orifices which are 50×25 mm^2 at each eave on the sides.
- In order to increase the ventilation area, extra vents were created at the highest points of the front and the back facades, just below the Apexes. These vents are two circles with a diameter of 111 mm each and other two circles with a diameter of 75 mm per side.
- The floor was not completely sealed and some space between the ground and the building was left to create natural ventilation.
- The building has two roller doors which are 2.6 m wide by 2.4 m high. One of them is used as a front door to access the building. The back door is used in case that any maintenance is necessary in the H_2 tank. Both doors could be used to reduce the H_2 concentration in the unlikely event of any H_2 leak.
- The building has a H_2 detection system which detects the level of H_2 in the interior atmosphere. The detections system has a low level alarm and high level alarm and the doors can be operated to increase the ventilation in the unlikely event of a H_2 leak.

Figure 7.12: H-CES system at the Creative Energy Homes community of The University of Nottingham.

7.5 Experimental results

The H-CES system was designed to perform the end user applications presented in Chapter 3 i.e PVts and LS. According to Table 7.1, four of the seven Creative Energy Homes have a PV array (Community PV percentage equal to 57%). The community PV percentage of this community is representative of the scenarios considered in Chapter 5 in which the community PV percentages ranged between 48%-100% and 23%-76% for the 5-home and 10-home communities. This section shows the experimental results of this H-CES system depending on the application performed.

After the commissioning, the electrolyser failed due to a technical problem related to the control system. Additionally, the efficiency of the DC/DC converter supplied with the electrolyser was around 60% according to the first tests as shown in Appendix I. As a consequence, the tests were performed with an H_2 supply bottle simulating the electrolyser. Specifically, results from a 1.1 kW electrolyser performing in a 5-home community in which two of the homes have a PV installation were utilised. This corresponds with the current situation of the Creative Energy Homes in which the Mark Group Eco House and the Nottingham house haven just been launched and are unoccupied. The performance results obtained on the second step of the method introduced in Section 5.1.2 were utilised

to obtain the electrolyser H_2 flow and efficiency. When simulating the performance of the electrolyser at maximum power (1.1 kW_e) with the H_2 bottle, the H_2 flow, the power consumption and the electrolyser efficiency oscillated around 18 g/h, 1.1 kW and 66% in the graphs below due to the control in place with the H_2 bottle.

Other aspects which should be considered to better understand the experimental results presented in this chapter are the fact that the monitoring of demand, the RE generation and the environmental variables in the community is still under development and only data from the H-CES system is presented here. Finally, the heat generated by the PEMFC system is utilised to heat the building in which the H-CES system is located. Since the PV generation and the community demand were not monitored at the Creative Energy Homes, the PV_{ES} was not calculated. Similarly, the H_{2ratio} was not obtained since the PEMFC system only used H_2 supplied by the tank (the H_{2ratio} is equal to 1). Next, experimental results depending on the ES application are shown in the same order as in Chapter 6.

7.5.1 Results of the H-CES system performing PVts

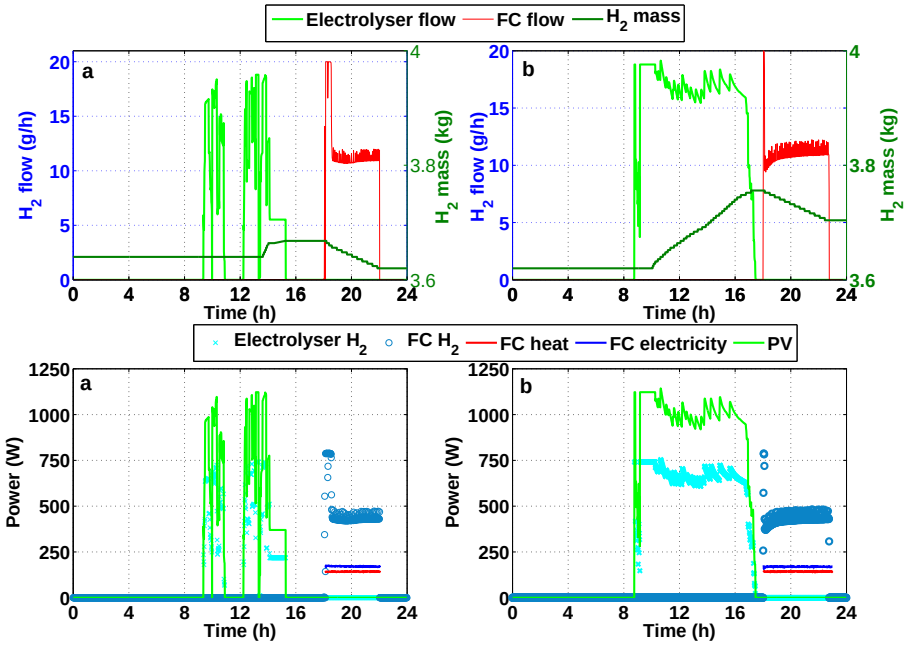

Figure 7.13: H_2 flows and related power flows of the electrolyser and PEMFC systems when performing PVts in two different days in a 5-home community. (a) The day 1 and (b) the day 2 represent a day with low (7.1 kWh) and high (22.0) PV generation respectively.

As reported in Section 6.2.5, the community PV percentage i.e. the surplus PV energy is the factor which affects more the performance of any CES system performing PVts. Therefore, two days with different solar resource were utilised

to understand the performance of the H-CES system when performing PVts. The first day, day 1, was a day in which the PV generation i.e. solar resource was lower and more variable (7.1 kWh in the 5-home community) while the second day, day 2, was a sunny day with higher PV generation (22.0 kWh in the 5-home community).

Figure 7.13 shows the H_2 flows and the related power flows (a) in day 1 and (b) day 2. The graphs with the H_2 flows also show the evolution of the mass in the H_2 tank according the charge and discharge cycles. At the beginning of the day 1 and 2, the H_2 mass in the tank was (a) 3.64 kg and (b) 3.62 kg respectively. The electrolyser started to generate H_2 at 9:22 am and 8:46 am respectively. In the day 2, the electrolyser could perform continuously until 5:29 pm. By then, the H_2 stored in the tank went up to 3.76 kg. However, the H_2 generation was interrupted for 1 hour and 20 minutes at 10:05 am in the day 1 when the H_2 mass in the tank was 3.64 kg. The electrolysis came to an end at 3:18 pm when the H_2 mass in the tank equal was 3.67 kg.

The electrolyser performed with a capacity ratio equal to 0.19 and 0.36 on (a) the day 1 and (b) day 2 respectively. Therefore, even in the day in with low community PV generation (7.1 kWh), the capacity ratio was attractive due to the community approach. The H-CES system is connected to all the homes in the community and this made that even in the day 1 the electrolyser ran for several hours at a rate close to its maximum rating equal to 1.1 kW_e. The maximum H_2 flow of the electrolyser was 18.8 g/h. Alternatively, the electrolyser run at full load and the C_{ratio} increased to 0.36 when the daily community PV generation was 22.0 kWh. In conclusion, the community approach together with the optimum rating of the electrolyser buffered the impact of the irradiance on the electrolyser performance and helped it to perform more continuously and at higher load even in days with low solar resource.

Opposite to the electrolyser, the PEMFC system ran at partial load generating around 170 W_e and 140 W_h between 6 pm and 10 pm in both days. The H_2 flow to the PEMFC system oscillated around 11.5 g/h and only during the start-up the flow was higher due to the dynamics the PEMFC system and the presence of the buffers in the H_2 tank. The longer term ES approach of this H-CES system is demonstrated when comparing the H_2 flows with the total H_2 tank capacity (4 kg) in Figure 7.13. The H_2 mass in the tank reduced to 3.62 kg at the end of the two days. The electrolyser and the PEMFC system only made use of around 5% of the total storage capacity in both days. Finally, the reason why the electrolyser flow did not increase the mass of the H_2 tank at the beginning of the charge was the fact that the electrolyser was filling the buffers located between the electrolyser and the MgH_2 tank as mentioned in Section 7.3.2.

Figure 7.14 shows the efficiencies of the electrolyser and the PEMFC systems in

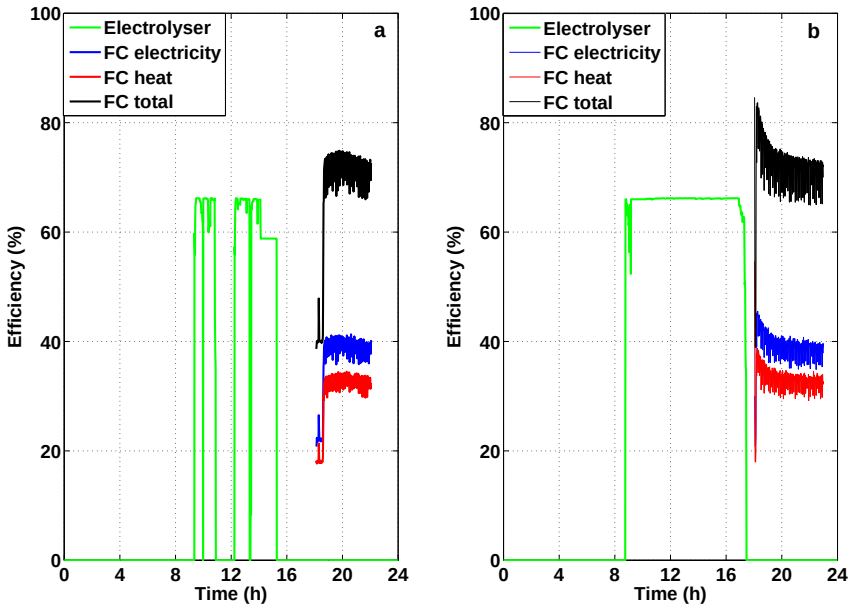

Figure 7.14: Electrolyser and PEMFC systems efficiency when performing PVts in a 5-home community in two different days in a 5-home community. (a) The day 1 and (b) the day 2 represent a day with low (7.1 kWh) and high (22.0) PV generation respectively.

both days. The efficiencies were derived from the power flows showed in Figure 7.13 and the H_2 power flow using the high heating value of H_2 equal to 39.4 kWh/kg. The community approach helped to keep the electrolyser efficiency higher than 60% most of the time, even in the day in which the solar resource was scarce. With regard to the PEMFC system, the H_2 flow was higher at the start-up due to the presence of the buffers as explained in Section 7.3.2. As a consequence, the PEMFC system efficiency experimentally measured was not representative at the start-up. After it, the electrical, heat and total efficiencies became constant around 0.38, 0.32 and 0.7 respectively. Finally, the daily efficiencies are shown in Table 7.10. The PEMFC system efficiency was calculated considering the performance in both days because its value only depends on the load factor (current generated by the PEMFC system) but not on the PV generation. The fact that the PEMFC system ran at very partial load with a current equal to 13 ADC in both days affected the performance and the total efficiency only was 70%. Table 7.10 shows the values of the main performance parameters achieved by the electrolyser and the PEMFC system when performing PVts considering the two different days.

7.5.2 Metal hydride tank performance

One of the novelties of this H-CES system is that it integrates a MgH_2 tank as H_2 store. As argued in Section 2.6.3, most H_2 systems installed in other projects utilised compressed gas. MgH_2 was introduced in Section 2.6.3 and it may be

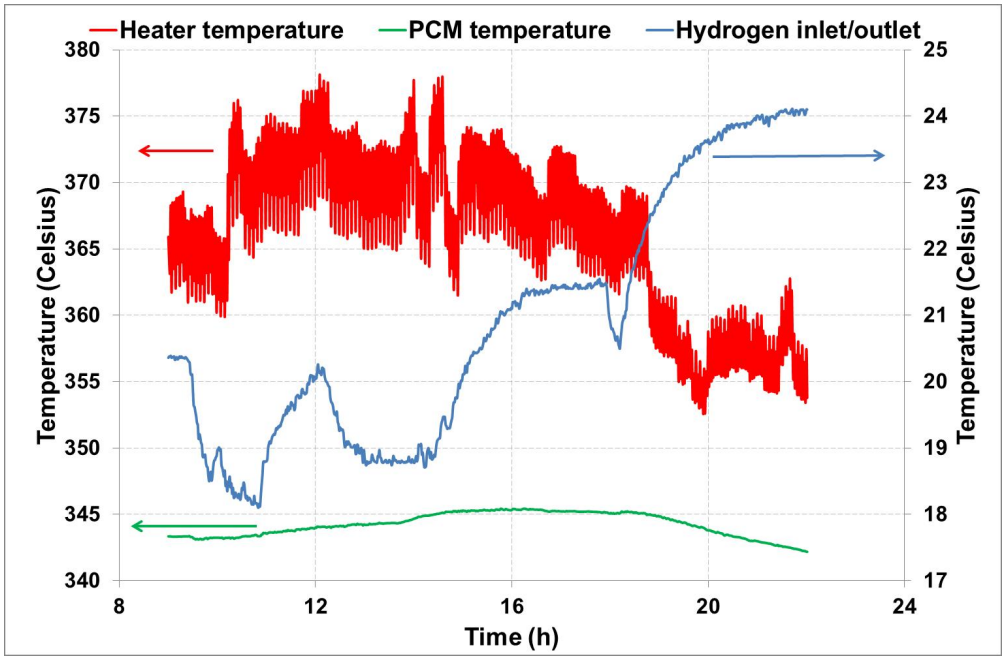

Figure 7.15: Temperatures of the H_2 tank when performing PVts according to the day 1 in the previous section.

considered as the baseline technology for metal hydrides due to its storage capacity (7.6 wt%), energy density (9 MJ/kg) and relatively low cost. Therefore, understanding the performance of a MgH_2 tank coupled with a PEM electrolyser and PEMFC system was a key priority to this investigation.

Figures 7.13 and 7.17 show the evolution of the H_2 mass in the MgH_2 tank depending on the application. In this section, the day 1 from the PVts analysis (the day in which the PV generation was 7.1 kWh) was used to show the evolution of the temperature and pressure of the MgH_2 tank. The description of the different components of the MgH_2 tank was made in Section 7.3.2 together with an explanation of the thermal management subsystem which is utilised to control the H_2 uptake and desorption.

Figure 7.15 shows three different temperature profiles which are relevant for the performance of the tank. The inlet/outlet H_2 flow temperature (buffers), the temperature of the PCM material utilised to manage the heat i.e. the storage cycle and the temperature of the heaters. Figure 7.16 shows the tank pressure and the pressure in the buffers i.e. pressure from H_2 supplied by the electrolyser (inlet) and to the PEMFC system (outlet). The temperature of the heaters oscillated due to the control employed by the H_2 tank. The H_2 tank uses a proportional-integrative-derivative (PID) control block with pulse-width modulation (PWM). This block controls the heat injected into the PCM using a thyristor. The temperature of the heaters vary as a function of the thyristor cycles (on and off).

Regarding the PCM temperature, the temperature was 344 °C at the beginning of the test. The pressure inside the buffer increased up to 8 bar and then H_2 was supplied to the MgH_2 tank as shown in Figure 7.16. As a result, the pressure in the buffers reduced and the pressure in the MgH_2 tank increased before they became equal. Heat was created during the charge cycle due to the exothermic nature of the absorption reaction [79], and this heat was utilised to melt the PCM material. The phase change occurs at constant temperature according to the thermodynamics around 343 °C, but in reality the PCM temperature was a bit higher in order to liquefy the alloy used as PCM as seen in Figure 7.15. Similarly, the temperature was a bit lower than the melting temperature in order to solidify the alloy. The PCM temperature is very similar to the MgH_2 tank temperature. When the electrolyser generation came to an end at 3:18 pm, the buffers and MgH_2 tank pressures decoupled and they slightly increased and reduced respectively.

Finally, the inlet/outlet H_2 flow temperature (buffers) depend on whether H_2 was flowing and the direction of the flow. During the charge cycle, the temperature reduced because H_2 was supplied cold from the bottle. This is the reason why the temperature reduced from 20 °C at the beginning of the test to 18 °C. Then, the electrolyser stopped generating H_2 as seen in Figure 7.13 and the temperature increased to behave as before the H_2 generation started. When the H_2 generation finished at 3:18 pm, this temperature increased steadily. When the discharge started at 6 pm, the pressure of the buffers was reduced to facilitate the discharge from the MgH_2 tank and then the MgH_2 tank supplied a flow around 18 g/h which was higher than the flow requested by the PEMFC system and as a consequence, the pressure of the buffers increased and became similar to the pressure of the MgH_2 tank. During the discharge, the temperature of the H_2 supplied by the MgH_2 tank was around 340 °C and then cooled down to $23-24$ °C approximately.

7.5.3 Results of the H-CES system performing LS

For the same reasons argued in Section 6.4, the H-CES system only perform LS by means of the NETA tariff. Specifically, the NETA prices used for the reference scenario in 2020 were utilised to illustrate the performance of the H-CES system when performing LS. However, the same performance results would be achieved with any other reference year due to the fact that the ratio between the valley and peak prices was always kept constant in this work as explained in Section 5.6.3. Two consecutive days were utilised to demonstrate the performance of the H-CES system when performing LS with this tariff, the 29 September and the 30 September. The prices of the four different periods in both consecutive days are shown in Table 7.9. Equivalent graphs to those shown above for PVts will be discussed in this section for LS with the NETA tariff.

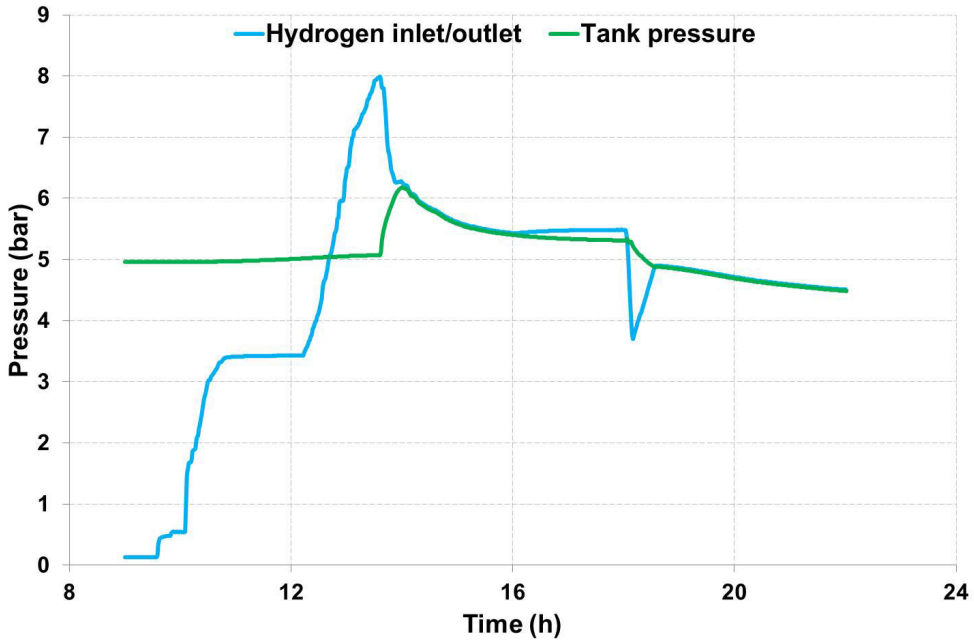

Figure 7.16: Evolution of the pressures of the H_2 tank when performing PVts according to the day 1 in the previous section.

Table 7.9: Prices for the four periods in the two consecutive days (29 September 2007 and 30 September 2011) utilised to demonstrate the performance of the H-CES system when performing LS with the NETA tariff.

	Day 1				**Day 2**			
Period	**1**	**2**	**3**	**4**	**1**	**2**	**3**	**4**
Price (£/kWh)	0.131	0.325	0.507	0.172	0.228	0.389	0.217	0.15

Figure 7.17 shows the H_2 flows and the related power flows of the electrolyser and the PEMFC system in the two consecutive days. Related to the H_2 flows, the evolution of mass in the H_2 tank according to the charge and discharge cycles is also represented. According to the prices shown in Table 7.9 and the LS condition derived from Equation 3.6, $\eta_e + \eta_h \times (P_{ev}/P_h) > P_{ev}/P_{ep}$, LS was performed with the grid import of the periods 2 and 3 of the first day by running the electrolyser during the period 1. Similarly, the grid import of the period 2 in the second day was shifted and the electrolyser ran during period 4 of the day 1. Running the electrolyser for the day after demonstrated the flexibility of H_2 technology as a mid-term/long term ES.

Additionally, H_2 storage flexibility is demonstrated in Figure 7.17 by means of the electrolyser performance. Specifically, the electrolyser ran at maximum load when the price of the electricity was low in periods 1 (0.131 £/kWh) and 4 (0.172

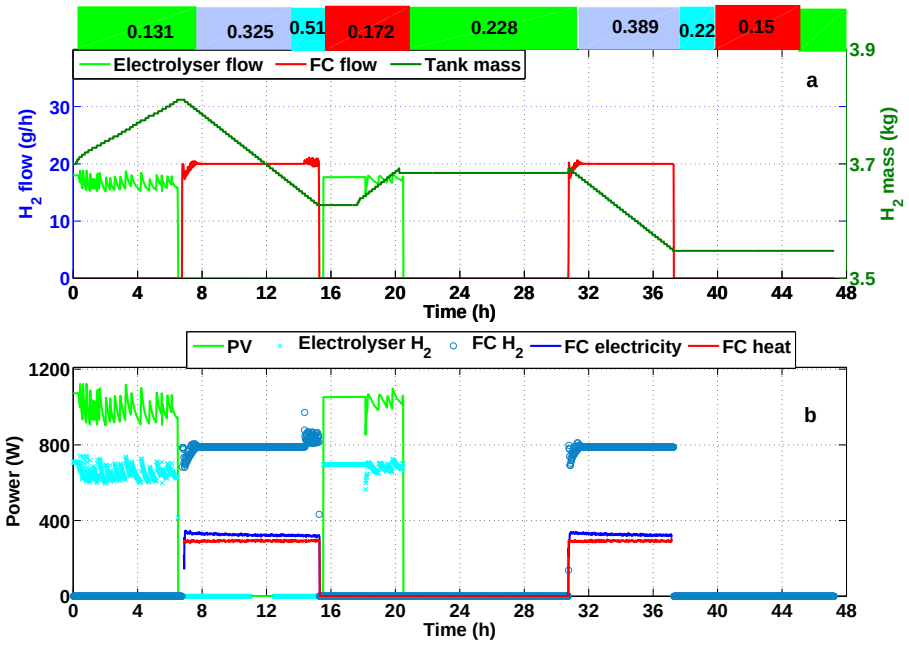

Figure 7.17: (a) H_2 flows and (b) related power flows of the H-CES system (electrolyser and PEMFC systems) in two consecutive days (29 September and 30 September) when performing LS with the NETA tariff.

£/kWh) of the first day. This was possible because the H_2 tank capacity (4 kg) is suitable for mid and long-term ES. The H_2 mass in the tank was equal to 3.7 kg at the beginning of the first day. The electrolyser generated around 18 g/h (at full load) when the price of the electricity was equal to 0.131 £/kWh, increasing the H_2 mass in the tank to 3.81 kg by the end of the period 1. In the second and third periods with a price equal to 0.325 £/kWh and 0.507 £/kWh respectively, the PEMFC system generated around 320 W_e. and 290 W_h when consuming 20 g/h of H_2. After the period 3, the H_2 mass in the tank was equal to 3.63 kg. Next, the electrolyser also ran at maximum load for 5 hours and the H_2 mass in the tank grew up to 3.7 kg. At the end of the first day and the beginning of the second day, the H-CES system rested and then the PEMFC system generated the same electricity and heat as before. By the end of period 2, the H_2 mass in the tank declined to 3.55 kg. The H-CES system did not perform during the rest of day. By running at full load when the price of the electricity was low, the electrolyser efficiency increases, as discussed in Sections 6.2.3 and 6.4.3, along with the economic benefit derived from LS according to Equation 3.8. Specifically, the H_2 flow generated by the electrolyser was around 18 g/h and the related electrical consumption power around 1.1 kW_e.

Figure 7.18 shows the efficiencies achieved by the electrolyser and the PEMFC system. When comparing these results with those obtained when performing PVts, the most important difference was the higher efficiency achieved by the two

systems, especially by the PEMFC system (around 79%). The reason for this marked improvement was the reduced impact of the parasitic losses introduced in Table 7.8 at higher load i.e. higher current (27 A). This efficiency was higher than the value obtained with the modelling simulation work shown in Figure 3.11 because the heat was supplied to the laboratory by means of the fan. In the modelling work, a heat exchanger is utilised to distribute the heat and it reduced the total efficiency [138]. In the case of the electrolyser, the electrolyser efficiency increases with the electrolyser load and the efficiency achieved was equal to that achieved with PVts in the day with high PV generation (day 2) in Figure 7.14. The main results from the LS tests are summarized in Table 7.10.

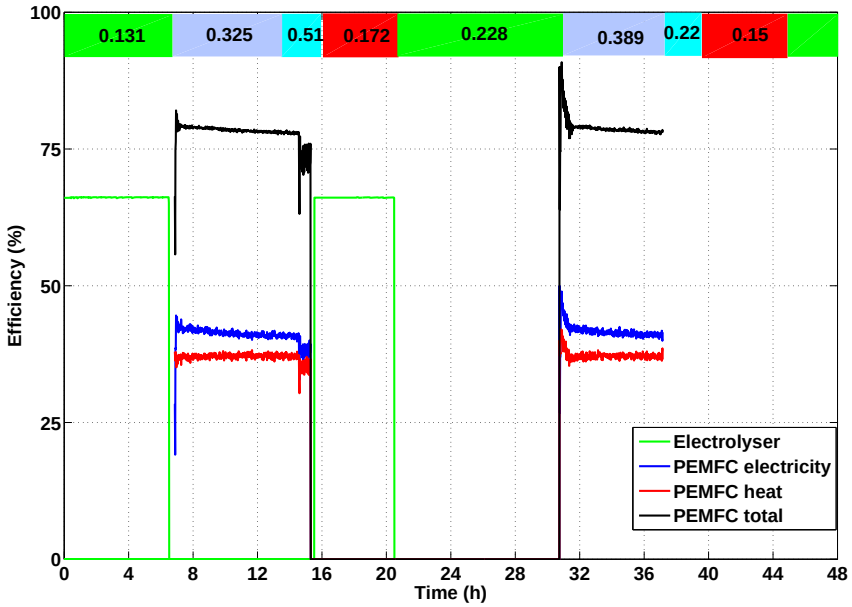

Figure 7.18: Electrolyser and PEMFC systems efficiency in two consecutive days (29 September 2007 and 30 September 2011) when performing LS with the NETA tariff.

7.5.4 Results of the H-CES system performing PVts and LS

The performance results of the H-CES system performing PVts and LS with the NETA tariff simultaneously in a day are detailed in this section. The prices of the electricity in the day selected, 26 December, were 0.085 £/kWh, 0.176 £/kWh, 0.146 £/kWh and 0.273 £/kWh for the periods 1,2,3 and 4 respectively as indicated in Figure 7.19. The lowest price was given by the first period, and the ratio between the minimum price and the rest of prices were 0.48 , 0.58 and 0.27. The price of the natural gas was 0.074 £/kWh. Considering the electrolyser efficiency and the efficiency of the PEMFC system when the H-CES system performed LS

summarized in Table 7.10, the grid import from periods 2 and 4 could be shifted using the period 1 to charge the H_2 tank by running the PEM electrolyser. Figure 7.19 shows the H_2 flows and the related power flows for this day.

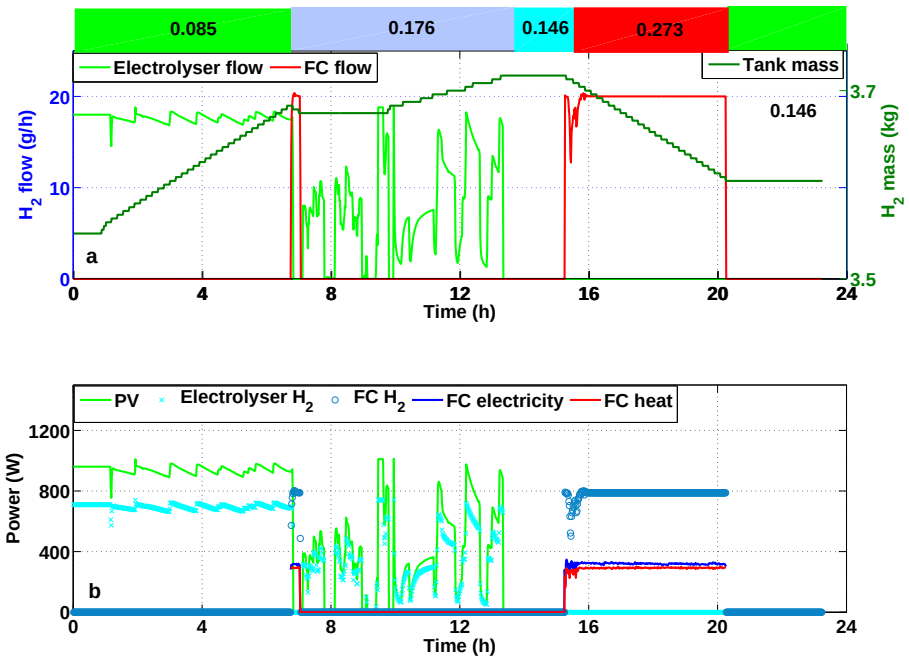

Figure 7.19: (a) H_2 flows and (b) related power flows of the electrolyser and PEMFC systems in a day when performing PVts and LS with the NETA tariff.

According to the four prices of the day selected, the electrolyser ran at maximum load during the period 1. The electrolyser flow generation was close to the maximum (around 18 g/h). As a result of the electrolyser performance, the H_2 mass in the H_2 tank increased from 3.55 kg to 3.69 kg. Once the valley period finished, the PEMFC system generated electricity and heat simultaneously but after 10 minutes there was surplus PV energy available at the community. As a consequence, the electrolyser ran again following the available surplus of PV generation in the community. At this time, the surplus electricity available for the electrolyser was very variable therefore it ran at partial load from 7:30 am to 2 pm when the variable PV surplus generation came to an end. In between, the electrolyser alternated periods of no generation with others running at full load. The H_2 generated from the PV plants increased the H_2 mass in the tank from 3.68 kg to 3.72 kg. Then, the H-CES system rested for one hour and a half until the peak period started and the PEMFC system generated heat and electricity simultaneously again. The electricity and heat generated was equal to 320 W_e and 290 W_h approximately respectively. The PEMFC system stopped at 9 pm.

The related efficiencies from the combination test are shown in Figure 7.20.

Table 7.10: Performance parameters obtained by the H-CES system depending on the application.

	PVts		LS	Combination
H_2 mass generation (g)	50.3	140.6	204	181
C_{factor}	0.19	0.36	0.25	0.54
η_{ele}	0.64	0.66	0.66	0.65
PEMFC electrical efficiency	0.38		0.39	0.40
PEMFC heat efficiency	0.32		0.38	0.36
PEMFC total efficiency	0.70		0.79	0.76

This figure demonstrates the impact of the partial load on the electrolyser efficiency because it kept constant at 0.66 when running with electricity from the grid, but fluctuated when running with the surplus PV generation. The daily electrolyser efficiency was equal to 0.65. Regarding the PEMFC system, the electricity and heat efficiencies were similar to the values shown when performing LS. Similarly to the LS test, the PEMFC system achieved a total efficiency of 79%.

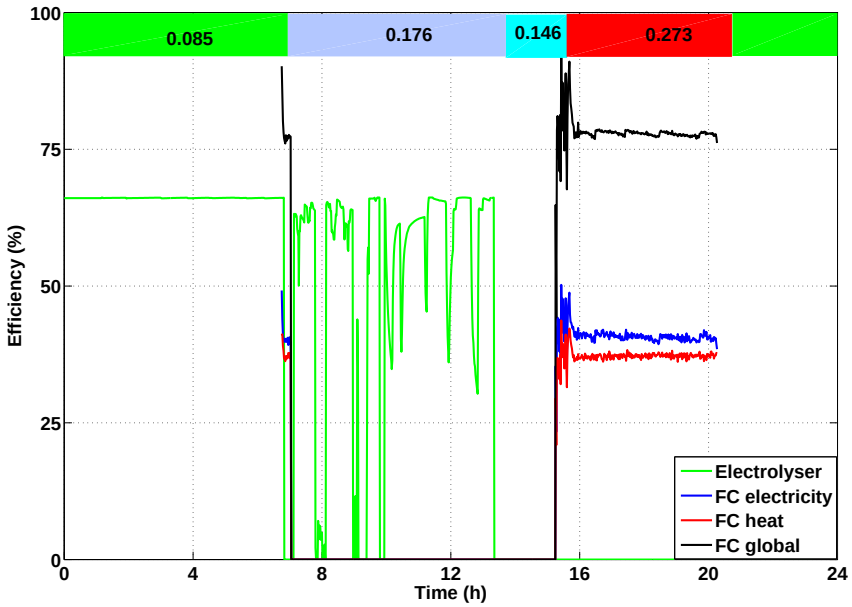

Figure 7.20: Electrolyser and PEMFC system heat and electricity efficiencies when performing PVts and load shifting with the NETA tariff.

7.6 Practical considerations and learnings from the H-CES system

The integration of the different elements which make up this H-CES system was a key part of the design and construction phases. Interesting learnings were concluded from these phases and they were shared with the three manufacturers ITM Power, McPhy Energy and Ballard Power System. Some of these learnings were related with specific problems which were necessary to be solved prior the commissioning of the whole H-CES system and others with improvements which should be included in subsequent H-CES systems. Some of the points discussed in this section are specifically related to H_2 technology but others can be extended to others ES technologies.

The power electronics (inverters and converters) is a key element for the optimum performance of any CES system connected to the network or any different alternative micro-grid as argued in Section 4.6. Therefore, manufacturers of ES technologies should consider the power electronics specifications during the design process for a successful integration of their systems according to the final application. This aspect should be improved in the case of the electrolyser and PEMFC system. The efficiency of the DC/DC converter supplied with the electrolyser was around 60% according to the first tests as shown in Figure I.2. This efficiency dramatically drops the *LVOES* and increases the *LCOES* of a CES system as discussed in Chapter 6. The revenue obtained by performing PVts and LS is proportional to the round trip efficiency as indicated by Equations 3.2 and 3.6 and the C_{factor} of the electrolyser also depends on the efficiency in the case of LS.

As discussed in Section 7.3.1, the PEM electrolyser was designed for direct coupling with a specific PV array and it is both voltage and current limited. These two characteristics meant that the final location should have a PV array which matches the electrolyser specifications or the end user should buy some a DC/DC converter in order to connect the PV array to the electrolyser. Additionally, this configuration limits the range of applications that the electrolyser can be integrated to. The manufacturer was informed that an AC connection to the mains would convert the electrolyser into a more flexible product which is not directly linked to the characteristics of a PV array. For example, the electrolyser could be integrated following a community approach as suggested in this thesis. In this H-CES system, an AC/DC converter was purchased for the integration of the electrolyser into the microgrid schematically represented in Figure 7.2.

Another important factor to bear in mind is that the final round trip efficiency and the reliability of CES system reduce when the different electronic components are not custom-made. This was the case of this H-CES system in which the

PEMFC system was integrated with a solar inverter which does not extract the maximum power from the PEMFC stack as it was designed for a solar array as shown in the results above. Additionally, the electrolyser failed due to the non-optimum integration of the AC/DC converter added to connect the system into the grid.

Similarly, it has been suggested to the manufacturers that the design should minimize any additional requirement by CES systems. For example, the H_2 tank needs compressed air for activating some pneumatic valves and this requirement can be difficult to meet depending on the final location. In the case of any intrinsic requirement like the need of deionised water for the electrolyser, the manufacturer should also incorporate this into its final design. Otherwise, the end user should look for a suitable product in the market and as discussed above the integration is not always optimum.

Finally, the adoption of consistent standards by different manufacturers working in the same industry would also be appreciated by final users. The different pipe connections of the electrolyser, tank and PEMFC systems used different sizes and units (imperial and metric) depending on the manufacturer and different diameters. This increased the cost and complexity of the piping work related with the installation.

These different issues were translated into future improvements for the different manufacturers. As discussed in Section 2.4, most ES technologies and H_2 technology in particular are not mature yet and these suggestions should be incorporated as the sector seeks to take a stronger position in the market.

7.7 Summary and conclusions

A H-CES system was designed, built, tested and evaluated in a low carbon community when performing end user applications. The PEM electrolyser, the H_2 tank and the PEMFC system which comprise the H-CES system were presented and their integration was discussed in this chapter. Spacial emphasis was given to the total BoP necessary for the integration of the different equipment. The building in which the H-CES system is allocated at the Creative Energy Homes community was also constructed with the proper safety measures in place.

PVts, LS with the NETA tariff and the combination of both them were performed successfully with the H-CES system. A H_2 bottle was utilised to simulate the electrolyser following electrolyser failure. The main conclusions extracted from the experimental tests are the low round trip efficiency (0.52) of H_2 technology, its flexibility and capability for mid-term and long term ES. The mid-term ES

approach was demonstrated with the test in which the H-CES system performed PVts and LS simultaneously. In fact, the C_{factor} increased more than 50% when both applications were executed by the H-CES system with regard to only one application. This improvement was possible due to the decoupling of the electrolyser rating and the H_2 tank capacity. The increase of the C_{factor} reduces the *LCOES* as discussed in Chapter 6. The electrolyser and the PEMFC systems achieved efficiencies up to 66% and 79% respectively. The impact of the partial operation in the efficiency was experimentally demonstrated, especially by the PEMFC system in which the total efficiency drop by 9% when the electrical output reduced from 390 W to 170 W. In the case of the electrolyser, the community approach kept the electrolyser efficiency higher than 60% even in the day in which the PV generation was more variable.

Additionally, the demonstration of the performance of the MgH_2 tank depending on the storage cycle has also been addressed. The analysis of the behaviour of the temperature and the pressure in relation to the thermal management was included. The H_2 tank consumes 700 W of electricity which were not considered in the round trip efficiency because they are specific related to the technology selected for the metal hydride. However, this amount, which is a great penalty for this system, could be dramatically reduced when increasing the size of the tank. According to McPhy Energy, the efficiency per kg of H_2 storage increases exponentially with the size of the system and a 25 kg H_2 storage would only have a thermal loss of 2.4 kW to the surroundings.

Learnings gained from the design and construction phases were shared with the manufacturers and are explained here for different stakeholders such as manufacturers, installers, governments and end users. Among the different improvements, the consideration of the optimum electronic equipment for the chemistry and rating of the CES system was considered a key factor to maximize the CES system discharge rating, round trip efficiency and reliability.

Chapter 8

Conclusions, outlook and future work

CES refers to ES located very close to customers and develops different applications which are useful for different stakeholders such as end users, utility companies, DNO and governments. This chapter summarizes the contribution of this work and analyses the main conclusions derived from:

- the application of the optimization method and methodology to obtain the optimum CES system as a function of the size of the community.
- and the design, construction and testing of a CES system which uses H_2 technology.

Additionally, the related implications of the conclusions and the outlook for CES are addressed. Finally, recommendations for future research work are suggested.

8.1 Contribution

The main contributions of this thesis are:

1. a comprehensive review of ES technologies and applications with a special focus on end user applications.
2. an optimization method which obtains the optimum CES system when performing end user applications as a function of the community size.
3. the application of this method using a complimentary methodology with real demand data up to a 100-home community. Simulation results demonstrated the positive effect of the community approach and conclusions for ES technologies and applications were reached.

4. the quantitative and qualitative assessment of a new H-CES system integrated in a low carbon community which was designed and built as part of this study and performs end user applications.

8.1.1 Review of the role of energy storage in new energy systems: end user applications

A comprehensive review of ES in the context of new energy systems was performed in Chapter 2 and gave a better understanding of how ES could support the integration of different RE technologies. RE technologies were characterized depending on their temporal and spatial variability in Chapter 1. Different technological options available for minimizing the impact of their variability such as demand side management, flexible generation and interconnection were compared.

In this context, ES applications which help RE technologies to behave as traditional generators and play a role in different electricity markets were explained in Chapter 2. These markets assure the reliability of the network and the optimum performance of different assets. ES applications were classified depending on the scale of the ES cycles in energy applications and power applications. Related to this classification, different technologies available in the market were suggested for different types of applications.

While the review included in this work is similar to others undertaken before in terms of number of applications and technologies included, it paid special emphasis to end user applications and the suitable technologies for them. A meta review of CES was undertaken by considering different end user applications, technologies, the economic benefits derived from them and other service and strategic benefits in Chapters 3 and 4. Although strategic benefits are linked with wide and eclectic concepts like sustainability and reliability, they should also be considered by different stakeholders such as governments and utility companies since they are becoming more important for end users.

The holistic CES approach followed in this study is schematically represented in Figure 4.11. Among different ES applications, PVts and LS were optimised because they are energy applications which are performed on a daily basis and manage the RE generation and the demand of customers respectively. Additionally, the integration of other applications such as the decarbonisation of the heating sector and avoiding PV power curtailment were also investigated.

The ability to discharge for several hours at maximum rating and the modularity in size from kWh to MWh are the main characteristics required for ES technologies to perform end user applications and play the role of CES. According

to these requirements, battery, H_2 and thermal storage technologies were selected and different technology options were discussed. Specifically, PbA batteries and hot water tanks were selected as more mature technologies considering PbA batteries have already been integrated in autonomous RE installations and hot water tanks have been widely used with natural gas boilers and solar DHW installations. Additionally, PEM electrolysers and Li-ion chemistry were chosen as promising alternatives when considering their performance characteristics and the cost reduction expected by manufacturers.

8.1.2 An optimisation method for obtaining the optimum CES system

A method was designed to obtain the optimum CES system for end user applications as a function of the size of the community as explained in Chapter 5. The method firstly obtains the largest CES system when determining the maximum ES demand throughout the year depending on the application. Then, it tests 10 different CES systems and obtains the performance and ageing of suitable ES technologies. Subsequently, the seasonal performance and durability are calculated based on the performance and then input as data for calculating the economic benefits of CES.

From a simulation point of view, deterministic models based on time-series data in which uncertainty was tackled by a sensitivity analysis were utilised. However, randomness was introduced in models by the use of real demand data. Robustness is a key characteristic of this optimisation method and it was demonstrated by the integration of different applications and technologies. PVts, LS by means of two different tariffs (Economy 7 and a four-period tariff derived from the prices from the NETA market), heat decarbonisation, the prevention of power curtailment and combination of them were included. These end user applications were defined according to current market structures, government incentives and future trends. Additionally, comprehensive models of ES technologies which quantify the performance, durability and economic benefits were incorporated. While each ES technology uses different chemical and physical principles to store energy, the same approach and philosophy were shared by the different ES technology models.

This method contributes to the engineering and scientific knowledge of CES (and ES in general) because it obtains the economic behaviour of CES systems based on the performance and ageing of suitable ES technologies without assuming any performance parameter. Additionally, all relevant components of a CES system such as the storage medium, electronics, BoP and maintenance were considered in the initial cost.

The method included the calculation of key performance and economic parameters which are interesting for different stakeholders as defined in Chapter 4. The performance parameters quantify how well the asset is used (EFC and C_{factor}), the round trip efficiency and the impact on the community (PV_{ES}, D_{ES} and H_{2ratio} for battery and H_2 technologies respectively). The levelised cost, $LCOES$, levelised value, $LVOES$, and profitability, IRR, of CES were quantified by the method.

8.1.3 Comprehensive CES methodology

A comprehensive methodology was developed in parallel with the method in order to increase the learnings extracted from the application of the method. The economic benefits of CES were quantified in the UK using a long-term time horizon (up to a hypothetical zero carbon target) to investigate the optimum CES. The aim of the methodology was to:

- Define the community approach e.g. how PV generation, domestic demand and heat generation add up as the community size increases.
- Understand the evolution of CES during the decarbonisation pathway in the UK.
- Tackle the uncertainty related to the performance, durability and economic benefits of CES.

The methodology achieved these three requirements by:

- Considering different community sizes ranging from a single home to a 100-home community. The homes with PV generation were assumed to be more likely to form an energy community as explained in Chapter 5.
- Using three different reference years: 2012, 2020 and a hypothetical zero carbon scenario. All parameters were modified in these reference years.
- Defining reference scenarios and a complementary sensitivity analysis. A reference scenario combines an ES application, ES technology and reference year. The sensitivity analysis included main parameters which affect the economic benefits such as ES technology cost, durability, PV generation, heat generation, demand and energy prices.

A limitation of this work is energy prices were forecasted based on current trends projections. However, energy prices will not be directly proportional to carbon abatement achievement and most expensive technologies may be required to achieve further carbon dioxide emissions reduction in the long term. Energy prices utilised in this work could be considered as pessimistic, specially for the zero carbon year.

8.1.4 A CES system for a 7-home community

The last contribution of this work has been the integration and assessment of a H-CES system performing end user applications in a low carbon community at The University of Nottingham. The H-CES system comprises a PEM electrolyser, MgH_2 tank and a PEMFC system. The community (the Creative Energy Homes) have RE generation on-site and the H-CES system performed different end user applications such as PVts, LS and the combination of them. Practical knowledge gained from the construction and field-tests of CES systems, like those presented in this thesis, are necessary for the optimization of CES systems and may contribute to the uptake of CES in the coming years.

8.2 Conclusions

This section highlights the main conclusions from the application of the method and the methodology on the one hand; and the design, construction and testing of the H-CES system on the other hand. The main objective of this thesis was to establish the optimum CES system and this was undertaken by using modelling and experimental methods.

8.2.1 Conclusions from the CES modelling work

PV energy time-shift

An evaluation of the available PV generation should be made prior to any CES project in which PVts is considered. Performance and economic results emphasized that optimum CES was given by community PV percentages higher than >75%. However, when comparing communities with same community PV percentage e.g. 100%, the *LCOES* reduced and the *IRR* increased with the size of the community. Simulation results also demonstrated that the single home is never the optimum case and even communities with lower community PV percentage obtained better economic results. In order to illustrate this conclusion, a 33 kWh Li-ion battery resulted in a *LCOES* equal to 0.33 £/kWh in the 20-home community with a community PV percentage of 38% while a 7.2 kWh Li-ion battery offered a *LCOES* equal to 0.51 £/kWh at the single home with a community PV percentage equal to 100% when projected to the year 2020. In fact, the single home obtained the highest *LCOES* and lowest *IRR* in 2020 and the hypothetical zero carbon year.

Load shifting

There are two basic reasons why Economy 7 is a very attractive tariff for LS with battery technologies:

- In Economy 7, the ratio between the off-peak price and the peak price is always lower than the round trip efficiency of any battery system and therefore LS can be performed on a daily basis (even with PbA batteries).
- The peak period lasts for 17 hours and therefore a high fraction of the daily demand can be shifted. Specifically, the fraction of the daily peak demand was up to 97% for a single home and up to 85% for a 100-home community.

Additionally, end users know the electricity prices before hand and the logic and control necessary to implement this tariff is simple. In the case of the four-period tariff, the ratio between the valley and peak prices was not always attractive on a daily basis but also the peak period was shorter.

The optimum battery capacity (including PbA and Li-ion batteries) was very similar for LS with Economy 7 and the NETA tariff. Specifically, Li-ion capacity was slightly larger for Economy 7 (up to 20%) due to the higher duration of the peak period while PbA technology needed slightly larger capacities (up to 19%) with the NETA tariff in order to increase the round trip efficiency and meet the LS condition given by Equation 3.6.

Comparison of PV energy time-shift and load shifting

Another interesting research output came from the comparison between PVts and LS. Results in 2020 are utilised to compare both applications here. LS has the potential to reduce the *LCOES* of CES (down to 0.14 £/kWh with Economy 7 in 2020) due to the larger amount of energy managed on a daily basis. In order to achieve low LCOES values, the *EFC* and C_{factor} should be as high as possible for battery and hydrogen technologies. The amount of energy managed by a CES system performing PVts is limited by the amount of surplus generation which depends on the community PV percentage and the solar radiation (which follows a daily and seasonal pattern). The *LCOES* associated with PVts increases as a result, the minimum equal to 0.30 £/kWh when projected to the year 2020. This conclusion was clearly emphasized by Economy 7 and less by the NETA tariff (minimum *LCOES* equal to 0.20 £/kWh in 2020) due to the different price variability and tariff structure as discussed in the previous section.

However, the *IRR* and the *LVOES* associated with PVts are higher than those associated with LS. For PVts, the maximum *IRR* achieved by Li-ion and PbA batteries was equal to -1.5% and -12.1% respectively in 2020. These values were higher than the *IRR* obtained with LS, even with Economy 7. The maximum *IRR* related to Economy 7 was equal to -2.5% for PbA and Li-ion batteries. Finally, the *LVOES* of PVts in 2020 (around 0.15 £/kWh) also indicates that managing the PV electricity adds more value than managing the electricity from the national

grid, the *LVOES* of LS being equal to 0.09 £/kWh and 0.06 £/kWh for Economy 7 and the NETA tariff respectively.

Heat decarbonisation

Heat decarbonisation was considered in this thesis as a strategic benefit because there is not a direct revenue associated with any CES system which manages RE generation to meet the heat demand load. However, this approach may be reviewed in the future. Heat decarbonisation is intrinsically provided by H_2 CES systems which integrate a FC system as seen in this work.

For battery technology, the integration of HPs affect the economic benefits of CES but especially the required battery capacity. HPs increase the required optimum battery capacity, although this effect is more marked for LS because CES systems are sized according to the demand load requirements. The size of the optimum battery system which performs LS increased by 20% when the HP penetration varied from 0% to 14% in 2020, while similar capacities were required for PVts. Likewise, the size of the optimum battery system which performs LS increased around 75% when the HP penetration varied from 14% in 2020 to 100% in the zero carbon year.

How HPs affect the economic performance of battery systems also depends on the type of application. HPs reduce the *LCOES* and increase the *IRR* of battery systems which perform LS while introducing opposite effects on battery systems which perform PVts. The sensitivity analysis from 2020 demonstrated that the *LCOES* reduced by 5-8% and increased by 3-5% for LS and PVts respectively depending on the size of the community when the HP penetration varied from 0% to 14%.

Power curtailment

The prevention of PV power curtailment is an application which does not modify the business case of battery systems which perform PVts. Only in the case of H_2 technology, the *LVOES* grew up by 47% due to the ability of H_2 to store surplus electricity even in days with high PV generation. However, the curtailment of RE generation already faces strong rejection by the public and customers want to maximize the amount of electricity generated at home which is utilised on-site. Therefore, this application may be considered as strategic by stakeholders such as utility companies, DNOs and governments.

Combination of applications and aggregation of benefits

The combination of applications developed by the same CES system has been studied in this work as introduced in Section 5.4. Modelling results obtained in

Section 6.7 indicated that ES applications can be classified as complimentary and supplementary depending how they integrate between them when combined by a CES system.

Complimentary applications are those which can be performed by any CES system simultaneously and they do not limit the economic benefits of each other. An example of complimentary applications was studied with PVts and the prevent of power curtailment from PV arrays. When the curtailment of the PV generation was considered, the economic revenue related to PVts did not decrease. Both revenues were added to obtain the total annual revenue. Another example of complimentary applications was given by the consideration of the heat demand load (heat decarbonisation) by a CES system performing LS. The heat demand load increased the *IRR* and reduced the *LCOES* of performing LS regarding the case in which only the electrical demand load was met. The consideration of the heat demand load impacted on the optimum size of battery systems as discussed in the previous section.

However, PVts and LS are supplementary applications. PVts reduces the amount of community grid import which is shifted because a fraction of it is directly met by the PV generation (ranging from 26% for a single home with a HP to 30% for communities with more than 30 homes). Secondly, the combination of PVts and LS introduces a dilemma related to the different nature of the electricity which is managed by a CES system. When only PVts was considered, electricity charged from the PV plants was discharged whenever the demand was higher than the PV generation. Likewise, electricity which is charged from the grid when the price of the electricity is low is discharged at peak times when only LS is performed.

Nevertheless, when electricity is charged from the PV plants and the grid simultaneously, the fraction charged from the PV plants could also be discharged during the valley period while the fraction charged from the grid should strictly be discharged at peak time as discussed in Section 6.6. However, the difference between the valley and the peak price may make the annual revenue higher when the PV electricity is only discharged at peak time. Results obtained with the NETA tariff and PVts shown in Section 6.7.3 suggests that discharging only at peak time is not the optimum solution when the peak period is not long enough to integrate the discharges associated with PVts and LS (<8 h). In order to illustrate this conclusion, the *LCOES* of the optimum PbA battery performing in the 5-home community increased from 0.35 £/kWh to 0.42 £/kWh (20%) when PVts was added to LS with the NETA tariff.

Energy storage technologies

The combination of a hot water tank and a PV controller is the CES system which obtained better economic results in 2012 especially when the domestic property already has a water tank (*IRR* equal to 7.5% for a 500 l water tank). This result was based on the substitution of natural gas by electricity generated by PV arrays but it would be even more attractive for those households which are not connected to the gas utility because electricity prices are higher than natural gases.

When comparing alternative ES technologies such as PbA, Li-ion and H_2, Li-ion was the most promising for performing PVts (*LCOES* equal to 0.30 £/kWh and *IRR* equal to -1.5% in 2020). PVts requires relatively small capacities and large charge and discharge ratings and Li-ion chemistry performs better under these requirements. However, PbA technology reduced the *LCOES* associated with LS down to 0.14 £/kWh in 2020 (for Economy 7) due to the fact that CES systems were sized according to the demand load requirements. LS requirements prevailed over PVts when both applications were performed simultaneously and as a consequence PbA technology also obtained better results (*LCOES* equal to 0.17 £/kWh for a 564 kWh PbA battery performing Economy 7 with PVts in a 50-home community in 2020).

H_2 technology demonstrated which is a very interesting ES technology when extra flexibility is required e.g. the price of electricity is variable, the CES system performs PVts and LS simultaneously and/or power curtailment is considered. The C_{factor} increased from 0.36 to 0.56 when PVts was added to LS with the NETA tariff. Also, the *LVOES* increased up to 0.05 £/kWh and the *LCOES* reduced to 0.27 £/kWh$_e$ with regard to the same system performing only PVts (*LVOES* equal to 0.04 £/kWh and *LCOES* equal to 0.36 £/kWh$_e$). When power curtailment was considered, H_2 technology was the only ES technology in which the *LVOES* increased significantly (up to 47%) when this application was added to PVts as demonstrated in Section 6.3.4.

Seasonal ES was not required in any of the optimum scenarios due to the balance between the H_2 generation from the electrolyser and the H_2 consumption from the PEMFC system. H_2 generation by electrolysers was limited by the C_{factor} (up to 0.56) and electrolyser efficiency (up to 0.66), while PEMFC systems operated 24 h per day with an efficiency up to 0.79, as seen with the H-CES system at the Creative Energy Homes in Chapter 7.

Finally, a cost of the storage medium of 260 £/kWh for Li-ion batteries (equivalent to a 16% subsidy over the assumed cost in the reference scenario, 310 £/kWh) is the break-even point (IRR$>$ 0) for Li-ion batteries by 2020 for an

electricity price equal to 16.3 p/kWh. If the price of the electricity is equal to 19 p/kWh by 2020, the break-even point modifies to 310 £/kWh. The cost of the storage medium should be equal to 75 £/kWh (55% subsidy) and 750 £/kW (63% subsidy) for PbA batteries and PEM electrolysers by 2020 respectively for an electricity price equal to 16.3 p/kWh.

Community approach

The benefits of the community approach were demonstrated by the results obtained from the PVts and LS analyses. In the case of PVts, the more uncorrelated the demand among different homes, the more benefits are introduced by the community approach, the transition between the single home and the 5-home community being the best example (the *LCOES* reduced by 38%). The impact of increasing the size of the community was gentler in the zero carbon year (56%) than in 2020 (7.6%) due to much lower PV penetration in 2020. The community approach reduced the *LCOES* down to 0.30 £/kWh and 0.11 £/kWh in 2020 and the zero carbon target respectively. These values meant a cost reduction by 37% and 66% regarding the single home. Results demonstrated that PbA batteries need from 2.5 to 1.5 more capacity than Li-ion batteries to reduce the *LCOES*, 2.5 being related to the smallest communities in which the random demand load requested larger PbA capacities.

The ratio between the optimum CES size and the number of homes did not reduce markedly with the size of the community for a constant community PV percentage for PVts despite the ratio between the maximum battery capacity and the number of homes reduce as the community sizes increases (19 kWh/home, 14.4 kWh/home and 10.0 kWh/home for the single home, 5-home and 50-home communities). However, the demand of a single home is the most random and this impacts negatively on the performance. The importance of the randomness of the demand for the small communities was demonstrated by the PV_{ES}, D_{ES}, *EFC* (in less extent) and the round trip efficiency. As the size of the community increases, high *EFC* were achieved for a wider range of CES sizes. This effect together with the cost reduction assumed with the battery capacity according to Equation 4.17 kept the ratio between optimum CES size and the community size (kWh/home) constant with the size of the community or even slightly increased it (7.6 kWh/home, 4.3 kWh/home and 6.0 kWh/home for the single home, 5-home and 50-home communities). However, the power rating of the battery (kW) reduced with the community size. This ratio was 3 kW/home, 1.6 kW/home and 1 kW/home for the single home, 5-home and 50-home communities.

The positive effect of the aggregation of demands was clearer for LS (as it was not affected by the community PV percentage). The *LCOES* followed a

negative logarithmic trend while the *IRR* followed a positive logarithmic trend as a function of the size of the community. The positive effect of the aggregation of the demands became smoother as the community size increased. The minimum *LCOES* (0.14 £/kWh) and the maximum *IRR* (-2.5%) were obtained by the 100-home community while the maximum *LCOES* (0.32 £/kWh in 2020) and the minimum *IRR* (-10.8% in 2020) were achieved in a single home. The optimum PbA capacity was approximately twice the optimum Li-ion capacity in the case of the NETA tariff and around 1.6 times for Economy 7 for any community size except the single home in the case of Economy 7.

8.2.2 Conclusions from the design, construction and testing of the CES using H_2 technology

Experimental results confirmed the low round trip efficiency (52%) and the high flexibility of H_2 storage indicated by the simulation results. The importance of the different parasitic losses on the round trip efficiency was emphasized by days in which the electrolyser and the PEMFC system performed at partial-load operation. When operating a full load, the round trip efficiency achieved by the electrolyser and the PEMFC system was the highest. The electrolyser and the PEMFC system achieved efficiencies up to 66% and 79% respectively.

The flexibility of H_2 storage was emphasized when the H-CES perform PVts and LS simultaneously. The C_{factor} increased from 0.25 to 0.54 when PVts was added to LS (with the NETA tariff) due to the decoupling of the electrolyser rating and the H_2 tank capacity. One of the main novelties of this H-CES was in the inclusion of a MgH_2 tank. Experience and results demonstrated that this is a reliable technology which integrated safely in the community.

Knowledge gained from the design and construction phases were shared with the manufacturers and explained in this thesis for different stakeholders such as manufacturers, installers, government and end users. Among different improvements, the consideration of the optimum electronic equipment for the chemistry and rating of the ES technology was considering a key factor to optimise the CES charge and discharge rating, round trip efficiency and reliability.

8.3 CES Outlook

In addition to the improvement of the efficiency related to the different energy processes such as generation, conversion, storage and transport, RE technologies are the most sustainable option for meeting the increasing demand requirements as argued in Chapter 1. Additionally, technologies like PV generators allow customers to generate their own RE and technologies such as HPs and FC systems

allow them to use it to meet the space heating load. CES impacts positively on communities by shifting the local RE generation (as quantified by the PV_{ES}) and meeting the local demand (as quantified by the D_{ES}). Additionally, the community approach improves the performance of CES systems as seen with the *EFC* and the C_{factor} for battery and H_2 technologies respectively. The main drawback for the uptake of CES is the still high cost of ES technologies. In fact, it was demonstrated that the installation a PV controller in homes which already have a hot water tank is the only CES system which is financially attractive at the moment.

If the cost of ES technologies reduce down to levels which manufacturers expect by 2020 (310 £/kWh, 150 £/kWh and 1300 £/kW for PbA, Li-ion and PEM electrolyser respectively) and the energy prices continue increasing at the rate they have done for the last seven years, CES becomes economically attractive by then ($IRR>0$). Related to this, all utility companies increased the energy prices ranging by 3.7% and 12% at the beginning of 2014 in the UK [174]. Similar increases are also taking place in other European countries.

Even if energy price increases slow down (as considered in the reference scenarios of this study), the positive impact of the aggregation of demands on the performance of CES systems helped the *IRR* to be almost positive for large communities in the case of LS with Economy 7 (-2.5% for a 1073 kWh PbA battery in the 100-home community), and for communities with community PV percentage higher than 75% in the case of PVts (-1.5% for a 41.6 kWh Li-ion battery in the 10-home community). The cost reduction expected for the three ES technologies will determine the best option. With the input data selected, Li-ion (310 £/kWh) technology was the best option for PVts in 2020 and PbA (150 £/kWh) was the best option for LS. H_2 storage should be the choice if the community already has a system running as a CHP generator.

There are additional factors which should be considered by different stakeholders in order to understand the scope of CES. Despite being the most profitable option, different stakeholders should understand that shifting PV generation to meet the DHW using hot water tanks means that the electrical and heat demand loads are not met by local RE generation. This approach would not tackle the space heating demand which accounts for 66% of the domestic energy consumption in the UK in 2009 [165].

The final location of CES systems should also be considered for the uptake of CES. Locations such as single homes (1 home), block of flats (10-20 homes), developments (20-50 homes) and 11/0.4 kV substations (150-500 homes) are some of the potential final locations for CES in the UK. Alternatively, CES systems

can also be integrated in refueling points for electric drive vehicles in the case of battery and H_2 technologies. At the moment, the lack of infrastructure to install CES systems in many of the locations suggested above together with the general opinion in favour of ES in single homes made individual homes the first option for the deployment of CES as single home systems, Germany being the best example. The interest in "single family" ES systems is related to the *autarky* concept. This work gives conclusive evidences for alternative sizing.

The deployment of reliable, efficient and cost effective CES, the selection of the optimum sizes according to the application or applications (as discussed in this work) together with the installation of CES systems in suitable locations outlined above requires the collaboration of different stakeholders.

8.4 Future work

This study set out to investigate CES comprehensively using modeling and experimental work. The work here presented can be expanded in different ways as suggested below.

8.4.1 Energy storage applications

Other ES applications could be investigated following the same method and methodology. For example, the decarbonisation of the transport sector using electricity and H_2 as energy vectors could be analysed following the method and methodology presented here when considering the transport requirements as a different demand load.

It is hoped that that further research focuses on the combination of applications and the aggregation of benefits. Future research should determine whether surplus PV generation should be discharged only at peak time or at peak and valley time when a CES system performs PVts and LS simultaneously depending on the ES technology and the tariff structure (prices, number of periods and durations).

8.4.2 Energy storage technologies

Although this study covers the whole range of suitable technology families for end user applications, additional types of thermal, battery and H_2 technologies could being investigated using the same method and methodology. Thermal storage could be investigated by community thermal storage (district heating) or even water tanks in individual homes could be managed using community, regional or national strategies for RE generation and demand management. H_2 storage could also be expanded when comparing PEMFC and SOFC systems. Finally, modifying

the heat to electricity ratio of FC systems may make sense for H_2 technology performing LS when taking into account that electricity is more expensive than natural gas.

8.4.3 Method

The method developed in this work could be used to solve other problems using the same rationale. For example, instead of obtaining the optimum CES system and related community size depending on the PV and HP penetration, the method can be utilised to obtain the optimum community for a given CES system. This option may be relevant when electric drive vehicles are widespread and a second hand market is developed for battery and FC systems which are not any longer valid for transport applications but still useful for stationary applications.

8.4.4 Methodology

The methodology used input data from the UK for modeling PV generation, demand and heat generation. These input data should be updated when possible for 2020 and the hypothetical carbon year. Likewise, the methodology could be given a wider scope by using input data from different countries.

From another perspective, this methodology could be implemented for local communities or developments in which there is not uncertainty in the input data. This could be very useful for utility companies, energy service companies and consultancies which want to design, built and integrate the optimum CES system for a community or development which specific RE generation and demand load requirements.

There are some aspects of the methodology which could be expanded or approached in a different direction. Future work could investigate further the impact of carbon abatement on the future energy prices i.e how sensitive energy prices are to CO_2 emissions reduction's measures. According to this, more accurate projections based on statistics and econometrics could be used to reassess the economic benefits of CES in the decarbonisation roadmap. Also, uncertainty can be tackled with alternative techniques to the one used in this (one-at-a-time sensitivity analysis). Probability analysis including global sensitivity analysis and Bayesian probabilistic methods consider the uncertainty of several different parameters simultaneously, the full range of input parameters interval, as well as the combined variability and their probability distribution; and stochastic models e.g. Monte Carlo method represent variables states by probability of distributions instead of unique values. These techniques can be used to analyse further the uncertainty on the economic benefits of CES. Finally, the HP model utilised in this

work could be given an application scope to include different HP performances in the field depending on the final installation and application by using statistical tools e.g. Gaussian distributed values to the COP at each time step.

8.4.5 Community hydrogen storage system and Creative Energy Homes

A Li-ion battery has just being installed at the Creative Energy Homes. Therefore the optimum use of the community H_2 storage system presented in this thesis and the Li-ion battery, as a hybrid system, should be part of the future work.

Appendix A

Air source Heat Pump model

As represented in Figure 3.12, a HP is comprised of four main components: condenser, expansion valve, evaporator and compressor. The HP model obtains the enthalpy of the refrigerant at the inlet and outlet of the main components of the cycle as represented in Figure 3.12. In order to do it, it uses the equations which governs the thermodynamic performance of each component (derived from the first principle of the thermodynamics), the pressure-enthalpy diagram of the R-134A refrigerant, and performance parameters such as temperature differences between fluids in heat exchangers and efficiencies based on previous experimental research. All these equations and parameters where taken from two reference books for HPs [175, 176].

A.1 Evaporator

Equation A.1 represents the performance of the evaporator. In the evaporator, the heat transfer occurs from the outdoor air to the refrigerant as forced convection. The evaporator is a heat exchanger with a fan which pushes the air through the tubes with fins where the refrigerant changes from liquid to gas. The difference between the temperature of the air and the refrigerant at the outlet of the evaporator is typically between 8 °C and 10 °C due to the relatively low conductivity of the air. In this work, a difference of 9 °C was assumed. In order to avoid the presence of liquid at the compressor inlet, the refrigerant should leave the evaporator completely dry. The refrigerant is superheated for this purpose. In this work, the superheating was assumed to be equal to 9 °C. The temperature of the refrigerant is used to obtain its enthalpy at the inlet h'_2 and outlet of the evaporator h_3.

$$q_e = (h_3 - h'_2) \tag{A.1}$$

A.2 Compressor

The compressor increases the pressure of the refrigerant between the evaporator and the condenser. The overall compressor efficiency can be broken down into indicative (due to entropy generation), mechanical (due to friction) and electrical efficiency (due to the motor losses). Based on standard values, 0.8, 0.9 and 0.85 were chosen respectively. The indicative efficiency (η_i) is used to obtain the enthalpy of the refrigerant at the compressor outlet (h_5) using the isentropic compression (h_4) as a reference as shown in Equation :

$$\eta_i = \frac{(h_4 - h_3)}{(h_5 - h_3)} \tag{A.2}$$

A.3 Condenser

In the condenser, the water is heated for the heat application using heat released by the refrigerant. The most important parameter to quantify is the temperature at which the hot water is distributed. In this work, the heat is generated at two different temperatures depending on if it is instantaneously supplied to the application or stored, 40 °C and 60 °C respectively. Based on the experimental performance of HPs, it was assumed that the temperature of the water increases by 6 °C in the condenser. The temperature difference between the refrigerant and the hot water is 6 °C based on a shell and tubes heat exchanger using forced convection. A subcooling equal to 5 °C was considered to improve the performance of the expansion valve. These assumptions were used to obtain the enthalpy of the refrigerant at the condenser outlet h_1).

$$q_c = (h_5 - h_1') \tag{A.3}$$

A.4 Expansion valve

The expansion valve is modelled as an element which decreases the pressure keeping the enthalpy constant as shown in Equation A.4:

$$h_2' = h_1' \tag{A.4}$$

In addition to the main components, the friction losses in the pipes were considered by reducing the inlet pressure of the compressor a 5% and increasing the discharge pressure of the compressor by 5%. The fan necessary to push the air through the evaporator and the pump which circulates the water through the condenser conform the BoP of the HP. The fan in the evaporator was assumed to have an efficiency of 0.6 and the water pump which circulates the water an efficiency equal to 0.6 based on typical values of small HPs.

Appendix B

PbA and Li-ion literature review: EFC and cost

B.1 Maximum equivalent full cycles for battery technologies

As explained in Section 4.7.1, calendar losses were modelled considering a linear relationship between the capacity losses and the *EFC* characteristic of the technology. Therefore, a literature review was performed in order to quantify the *EFC* that PbA and Li-ion technologies can achieve. The *EFC* refer to the maximum discharge performed for any battery system if only cycle losses play a role. Table B.1 show the variety of results published in the literature for PbA and Li-ion batteries.

B.2 Battery system cost

A different literature review was performed in order to select the cost of the storage medium for batteries, $cost_{sm}$, which is utilised as input data by the economic submodel as defined in Section 4.9.4. There is much uncertainty related to the current cost of battery technologies and the potential reduction of the cost. This is reflected in variety of values shown in Table B.2. M. Braun et al. reported that the cost of Li-ion chemistry can reduce down to 290 £/kWh or 175 £/kWh using a German and a Japanese source respectively [105].

Table B.1: Equivalent full cycles data for PbA and Li-ion batteries reported in the literature.

Reference	**PbA battery**	**Li-ion battery**
[144]	300 cycles at 80% DOD	3000 cycles at 80% DOD
[18]	500 deep cycles	
[64]		between 3000 and 9000 cycles
[17]	2500 cycles at 60% DOD	5000-7000 at 80% DOD
[177]	560 EFC	
[97]	2100-3000 cycles at 80%	7000-10000 cycles at 80%
[158]	2000 cycles	4000 cycles
[74]	2000 cycles at 80% DOD	
[178]	$<$ 1500 deep cycles	$>$ 1500 cycles
[19]	200-1000 cycles	4000-100000 cycles

Table B.2: Cost of the storage medium data for PbA and Li-ion batteries reported in the literature.

Reference	**PbA battery (£/kWh)**	**Li-ion battery (£/kWh)**
[144]	45-170	610-870
[97]	90-150	260-570
[49]	1040-2430	620-2350
[11]		230-1040
[67]	110-160	
[17]	200-650	520-1960
[178]	30-70	590-850
[158]		
[19]	130-260	390-2480

Appendix C

Hydrogen literature review: durability and cost

C.1 Hydrogen durability

I. Stafell concluded that the durability of PEMFC systems was up to 10000 h in 2010 [134]. However, there is not much specific data regarding the durability of electrolysers technology. According to the energy storage report prepared by the Centre for Low Carbon Futures, H_2 storage lasts between 5 and 20 years [19]. This data was modified in another report by Enea to 5 and 10 years [11].

Without entering into specific technological details, a FC system for a vehicle should last for 15 years in order to be commercially competitive according to the Carbon Trust [179]. The DOE stated that FC systems should last between 60000 h-80000 h and 5000 h for stationary and vehicle applications respectively in the Fuel cell and hydrogen program [180]. The European Commission research program on hydrogen and fuel cells stated that stationary FC systems should last for 40000 h by 2015 [181].

C.2 Hydrogen cost

There was great variety on the figures reported by I. Stafell about the cost of production for PEMFC systems and SOFC systems, assuming that mass production occurred. Figures ranged from more than 8700 £/kW and less than 4350 £/kW for FC system including the BoP [134]. According to independent analysis commissioned by the Carbon Trust [179], the current state of PEMFC systems is predicted to cost 32 £/kW in automotive applications when manufactured at mass scale (i.e. 500,000 units per year). However, in order to be competitive with ICE vehicles, automotive FC systems must reach approximately 23 £/kW. Cost savings can be achieved by reducing material costs (notably platinum use), increasing power density, reducing system complexity and improving durability.

Table C.1: Comparison between the targets set by the European Commission for 2010 and 2020 for FC technology.

Parameter	**2010**	**2020**
Durability FC vehicle (h)	2000-2500	>5000
Durability FC stationary (h)	12000	30000
System cost FC vehicle (£/kW)	>870	45
System cost stationary μFC (£/kW)		3480-4350
System cost stationary FC (£/kW)		1310-2180

The DOE was more ambitious and set 490 £/kW and 20 £/kW for stationary and vehicle applications respectively.

According to the DOE program, the cost of FC systems must be reduced and their durability improved in order to be competitive with current technologies [180]. Specifically, the cost targets for stationary and automotive applications were 20 £/kW and 650-980 £/kW depending on size and application. The European Commission established the following costs: 3480-4350 £/kW for μCHP, 1300-1740 £/kW for industrial or commercial systems by 2015 [181]. In its Strategic Energy Technologies Information System, the European commission also reviewed FC systems and hydrogen objectives and compared them with those from DOE [81] which are more ambitious. The European Commissions objectives for 2010 and 2020 are summarized in Table C.1. For example, the durability target for stationary FC systems is 60000 h in 2020 for the DOE.

The European Commission also specified the cost of the the H_2 delivery at refueling stations to be lower than 4.4 £/kg (0.13 £/kWh) by 2015 [181]. For the production cost of distributed electrolysis, the European Commission determined 4.8 £/kg by 2030 [81]. The Carbon trust argued that the cost of electrolysis is expected to reduce due to efficiency and design improvements. A cost of 0.14 £/kWh was assumed for a H_2 vehicle in the Carbon Trust report [179]. This price reflects that electrolyser systems run intermittently, providing a balancing solution for the power grid, although this is dependent on scale and location. Finally, cost objectives for gaseous and solid state H_2 storage were 440 £/kg and 4350 £/kg for 2010 and 350 £/kg and 720 £/kg for 2020 according to the European Commission [81].

As reported here, most of the available data for H_2 technologies refers to FC systems. When describing electrolysis cost, all the targets referred to the cost of the H_2 generation (£/kg) but they did not mentioned the initial cost of the

electrolyser system. Alternatively, other ES reports reported the current initial cost of electrolysers which range between 195-390 £/kW [67], between 1960-3260 £/kW [182], 4-470 £/kW for large scale and 980-6500 £/kW for small scale [19].

Appendix D

PEM Electrolyser model

D.1 Electrolysis and PEM electrolysers

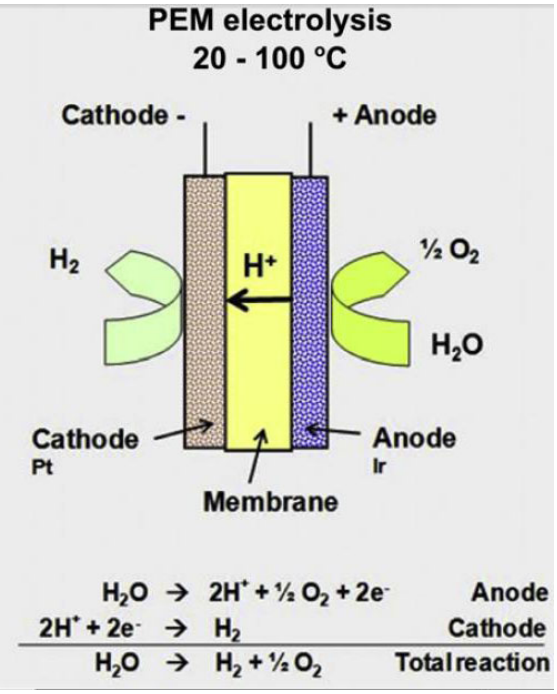

Figure D.1: Schematic representation of the PEM electrolysis with the different reactants, products, reaction sites and reactions [15].

The water electrolysis process consists of electrochemically splitting water into its constituents, namely hydrogen and oxygen and it is an endothermic reaction. A PEM electrolyser uses perfluorosulfonic acid polymer (Nafion (TM)®) as a solid electrolyte to separate the anode and the cathode where hydrogen and oxygen are generated respectively as shown in Figure D.1. Titanium is widely used for the stack components (bipolar plates, current collector plates, etc.) because of its resistance to corrosion [159]. In an electrolyser, deionised water is firstly fed into the electrolyser cell at the anode side. Using DC current as second input, the

oxidation of water molecules takes place generating oxygen, protons and electrons in the anode. For this, the DC voltage applied must be higher than the reference voltage, V_{ref} (1.229 V at standard conditions), which is related to the change in Gibb's free energy, ΔG, according to Equation D.1 in which F is the Faraday constant (96485 C/mol). Next, protons are transported from the anode to the cathode through the electrolyte and electrons are conducted through an external circuit. At the cathode surface, protons are converted into hydrogen molecules when reacting with electrons.

$$V_{ref} = \frac{\Delta G}{2 \cdot F} \tag{D.1}$$

The water electrolysis process also requires some heat to occur. The total amount of energy necessary is given by the enthalpy change of the reaction according to Equation D.2 in which ΔS is the entropy change. Considering this additional heat supply, the total voltage required, namely thermoneutral voltage, V_{tn}=ΔH/(n·F), is equal to 1.482 V at standard conditions.

$$\Delta H = \Delta G + T \cdot \Delta S \tag{D.2}$$

The ideal catalyst for the cathode and the anode should increase the reaction rate in addition to have high porosity, mechanical strength, electricity conductivity and prevent corrosion. In conventional PEM electrolysers, platinum is used as a catalyst, specially for the cathode, despite its high cost. However, platinum alloys are necessary for the anode because the reactions is more sluggish: platinum/ruthenium, platinum/iridium and even iridium are also used for the anode [155].

D.2 Polarisation voltage of PEM electrolysers

The performance of an electrolyser is explained by the current and voltage graph shown in Figure 4.3. This graph gives information about the voltage which is necessary to generate a certain current value, which is directly proportional to the hydrogen flow rate. An ideal electrolyser would require a voltage which is derived from the thermodynamics principles. However, several voltage losses occur during the electrolysis process. Next, the thermodynamic voltage and the different voltage losses which occur in an electrolyser are modelled. Additionally, the most important operational parameters which affect the electrolyser performance are explained together with the typical operational range.

D.2.1 Thermodynamic voltage

The Nernst potential or thermodynamic voltage, defined in Equation D.1, describes the potential of the electrolyser when no voltage is applied. This voltage varies with temperature and pressure at which the electrolyser is operating. Different approaches have been adopted in the literature in order to quantify the variation of Gibb's free energy with the temperature and pressure. In Equation D.3, ΔG^T is the Gibbs free energy change at any temperature but at standard pressure and the second factor refer to pressure variation [154]. Additionally, T_{ele} is the temperature of the electrolyser, p_{H2} is the partial pressure of H_2, p_{O2} is the partial pressure of oxygen and p_{H2O} is the partial pressure of water.

$$\Delta G = \Delta G^T + T_{ele} \times ln(\frac{p_{H2} \times p_{O2}^{0.5}}{p_{H2O}}) \tag{D.3}$$

Marangio et al. used experimental data fitting for determining the enthalpy and entropy of the reaction to obtain the Gibb's free energy for the Nernst voltage [154]. Alternatively, it has been argued that the variation of Nernst potential is negligible (around 3-4% of total electrolyser voltage variation) and based on this the Nerst voltage was assumed to be constant [159]. However, other authors argued that considering the temperature and pressure effects is necessary because electrolysers operate far from standard conditions and the reversible voltage increases with pressure and decreases with temperature. [183]. As a consequence, different models have been developed to obtain the Nerst voltage [78, 155, 159]. In this work, the Nerst voltage was obtained using the equation suggested by Agbli et al., Equation D.4, in which a_{H2O} is the activity of water (assumed equal to 1) and R is the universal gas constant (8.31 J/(mol·K).

$$E_0 = \frac{\Delta G}{2 \times F} + \frac{R \times T_{ele}}{2 \times F} \times ln(\frac{p_{H2} \times p_{O2}^{0.5}}{a_{H2O}}) \tag{D.4}$$

D.2.2 Activation voltage

The Butler-Volmer equation, D.5, is the basic equation to describe the electrochemical reactions occurring at electrolysers (and FCs) at the cathode and the anode [154, 183]. In this equation, i is the cell current density (A/cm^2), i_0 is the exchange current density (A/cm^2), α_1 and α_2 are the charge transfer coefficients of the reaction in two directions (products and reactants).

$$i = i_0 \times [exp(\frac{\alpha_1 \times F \times \eta_{act}}{R \times T_{ele}}) - exp(\frac{\alpha_2 \times F \times \eta_{act}}{R \times T_{ele}})] \tag{D.5}$$

Typically, the transfer coefficient, α is assumed to be the same in both directions (symmetric reactions) and this assumption simplifies the expression and

gives Equation D.6 [27]:

$$\eta_{act} = \frac{R \times T_{ele}}{\alpha \times F} \times arcsinh(\frac{i}{2 \times i_0}) \tag{D.6}$$

Alternatively, a simplification of the Butler-Volmer equation has also been suggested when the current density is much higher than the exchange current density, i $>$i$_0$, as shown in Equation D.7:

$$V_{act} = \frac{R \times T_{ele}}{2 \times \alpha \times F} \times ln(\frac{i}{i_0}) \tag{D.7}$$

The activation overvoltage caused at the cathode layer has been neglected in the literature because the cathode exchange current density is up to six orders of magnitude higher than the anode exchange current density [184]. However, other authors considered both overvoltages assuming different values for the the transfer coefficients including 0.5 for the anode and the cathode [155, 185], 2 for the anode and 0.5 for the cathode [154], 0.5 for the cathode and between 0.1 and 0.6 for the anode depending on the temperature [183], and 0.7 and 0.6 for the anode and the cathode respectively [153].

Regarding the exchange current densities, different values have been suggested for the anode ranging from 10^{-7} A/cm^2 for platinum/iridium and 10^{-12} A/cm^2 for platinum while there was more agreement for the cathode, specifically a value of 10^{-3} A/cm^2 has been widely used [155, 184, 185]. Alternatively, Ni et al. suggested an expression to determine the exchange current density as a function of the temperature. They used reference values for the exchange current densities found in the literature, 10^{-9} A/cm^2 and 10^{-3} A/cm^2 for the anode and cathode respectively based on platinum electrodes as shown in Equation D.8. The value of the activation energies used to obtain the real exchange current densities were 76 kJ/mol and 18 kJ/mol for the anode and cathode respectively.

$$i = i_{ref} \times exp(\frac{-E_{act}}{R \times T_{ele}}) \tag{D.8}$$

In this work, the variation of the exchange current density with the temperature and the roughness factor of the electrodes was considered for the anode and the cathode according to Equation D.9 based on a previous model [153].

$$i_0 = i_0^{ref} \times \gamma_m \times exp(\frac{E_{act}}{R} \times (\frac{1}{T_{ele}} - \frac{1}{T_{ref}}) \tag{D.9}$$

In this equation, the roughness factor of the electrodes, γ_m, was assumed to be 150, while the reference exchange current density, i$_0^{ref}$, was assumed to be 10^{-3}

for the cathode (platinum) and 10^{-7} for the anode (platinum/iridium). The activation energy, E_{act}, was assumed to be 76 kJ/mol for the anode and 18 kJ/mol for the cathode. Finally, the transfer coefficient, α, had a value of 0.5 for both the anode and cathode.

D.2.3 Ohmic voltage

Ohmic losses refer to the voltage which is necessary to transport electrons and protons through the electrolyser stack. In an electrolyser stack, electrons and protons are generated at the anode. The protons and electrons must be transported to the cathode in order to generate H_2. Electrons are transported using an external circuit and protons are transported through the polymer membrane. The ohmic resistance includes the resistance from the electrodes, electrolyte and interconnects. However, it is usually dominated by the electrolyte resistance [27]. Typically, Nafion (TM)® is used as the raw material for membranes, but there are several types of Nafion (TM)® membranes [153, 154].

The electrolyte resistance is inversely proportional to the membrane's conductivity. Water content and temperature are the parameters which affect the conductivity. In general, conductivity improves when both temperature and water content increases. PEMs have negative fixed charge sites and free volume to allow protons to move through the polymer structure, the latter characteristic being intrinsic to polymer materials. The transport of protons in the membrane is enhanced by water molecules which acts as a proton carrier (vehicle mechanism) [27]. Water movement through PEMs is due to two forces: electro-osmotic drag and diffusion from the anode to the cathode [78]. Alternatively, it has also been argued that the pressure gradient between the anode and the cathode causes a water flow in the reverse direction [154]. However, Agbli et al. argued this effect should be neglected when both sides have similar pressures [153].The diffusion phenomena which affects the the water transport is driven by the concentration gradient and the Fick's first law has been used to describe it [78].

Electro-osmotic drag by protons is the main phenomenon occurring in PEMs. Protons moving through the membrane carry water molecules with them. This transport is proportional to the amount of water in the membrane. The water content of the membrane, λ, is quantified as the ratio of water molecules to the number of charge sites. The water content is a function of the water activity, a_{H2O}, which is defined as the ratio between the pressure of the water vapour and the saturation water vapour pressure. Typically, water content at the membrane is assumed to be in equilibrium with saturated water vapour. Zawodzinski et al. measured the conductivity of Nafion (TM)TM 117 at 30 °C and 80 °C and they

obtained a relation among the conductivity, temperature and water content [186]. Gurau et al. empirically obtained the conductivity of the PEM, σ_{mem} as shown in Equation D.10 in which $\lambda(x)$ is the water content in the membrane as a function of the distance to the cathode interface.

$$\sigma[\lambda(x)]_{mem} = [0.5139 \times \lambda(x) - 0.326] \times exp[1268 \times (\frac{1}{303} - \frac{1}{T_{ele}})] \tag{D.10}$$

The arithmetic mean between the water content at the anode and the cathode has also been used to obtain the content in the membrane [78]. Alternatively, the water content has been estimated using a linear correlation between the values at the anode and the cathode as shown in D.11. L is the membrane thickness, λ_a and λ_c are the water contents at the anode and cathode interfaces which were assumed to be 14 and 10 respectively. Different thickness values reported in the literature are 50 μm, 130 μm and 178 μm, 100 μm used in this work.

$$\lambda(x) = \frac{\lambda_a - \lambda_c}{L} \times x + \lambda_c \tag{D.11}$$

The number of water molecules transported by a proton i.e. electro-osmotic drag coefficient, n_{drag} , is given by Equation D.12. Marangio et al. assumed a value of 7 for the electro-osmotic drag coefficient [154], but Agbli et al. considered that this parameter was a function of temperature [153]. Once the the electro-osmotic drag coefficient is known, the electro-osmotic drag can be obtained using Equation D.13

$$n_{drag} = n_{drag}^{sat} \times \frac{\lambda}{22} \tag{D.12}$$

$$J_{H2O,drag} = 2 \times n_{drag} \times \frac{j}{2 \times F} \tag{D.13}$$

There have been different approaches for the conductivity of the membrane based on experimental research and/or modelling assumptions. Choi et al. modelled a 178 μm polymer membrane with a conductivity equal to 0.14 S/cm assuming a constant temperature of 80 °C and the membrane was immersed in water. Harrison et al. obtained that the conductivity of a commercial PEM electrolyser with a membrane of 178 μm was 0.075 S/cm. Dale et al. experimentally obtained the membrane conductivity between 10 °C and 60 °C degrees and a quadratic expression was suggested to explain this relationship as shown in Equation D.15:

$$\sigma = 0.0480257 + 8.15178 \times 10^{-4} \times T_{ele} + 5.11692 \times 10^{-7} \times T_{ele}^2 \tag{D.14}$$

In this work, the membrane conductivity was modelled by means of mobility of the protons according to Equation D.15 in which C_{H^+} and D_{H^+} are the concen-

tration and diffusivity of protons. These parameters were based on Nafion (TM)® 117 technology [154].

$$\sigma = \frac{F^2 \times C_{H^+} \times D_{H^+}}{R \times T_{ele}} \tag{D.15}$$

The membrane resistance was obtained from above parameters and the ohmic resistance was the product of current and membrane's resistance. Once the conductivity is known, the membrane's resistance is obtained by using Equation D.16 and the ohmic voltage is the product of the current and this resistance:

$$R_{PEM} = \int_a^b \frac{dx}{\sigma} \tag{D.16}$$

$$V_{ohm} = i \times R_{PEM} \tag{D.17}$$

D.2.4 Concentration voltage

In an electrolyser, reactants should be conducted to the anode and cathode to the achieve oxidation and reduction reactions respectively. At the same time, products should be removed from the reaction sites in order to allow reactants to reach the catalyst layer where the reaction takes place. However, if supply and removal of reactants and products in electrolyser stacks are not optimum, there is a voltage loss related to it. The concentration losses are quantified by the limiting current density defined as the current which causes the reactant concentrations fall to zero. The concentration of the reactants and the removal of products are improved using sophisticated flow channels in the electrolyser (convection) and electrodes (diffusion).

Electrolysers typically perform in an area of the current-voltage curve which is far from the limiting current density i.e. current densities smaller than 15000 A/m^2. As a consequence, concentration losses have been neglected in many previous models in the literature [155, 184, 185]. However, reactant depletion affects both the Nerst cell voltage and the kinetic reaction rate. Depletion leads to a similar loss in both cases. This concentration loss has been modelled using the limiting current density, i_L, as shown in Equation D.18 in which c is a constant which depends on the geometry and mass transport properties [27].

$$V_{con} = c \times \frac{i_l}{i_L - i} \tag{D.18}$$

In this work, concentration effects have been considered by obtaining the difference between the concentration of the reactants at the electrolyser inlet and outlet with the concentration of the reactants at the reaction sites [154]. This approach focuses on diffusion process at electrodes using the Fick's first law to describe the

concentration changes. In order to obtain the concentration of hydrogen, oxygen and water at the anode and the cathode, the model firstly obtains their partial pressures. Then, the concentrations at the reaction sites were obtained from the concentration at the channels. In channels, convective effects were neglected and the concentration losses were assumed to depend on the diffusion. A molar balance was utilised to obtain the concentration at the channels [154].

D.3 Performance parameters

D.3.1 Current density

Different maximum current density values have been utilised in models in the literature or in real systems. Among others, 1.6 A/cm^2 and 1.4 A/cm^2 or even values lower than 1 A/cm^2 have been applied into models or real systems [154, 159, 183–185]. In this work, a maximum current density equal to 1.5 A/cm^2, in the range of the values reported in the literature, was selected.

D.3.2 Temperature

The temperature is a key parameter for the performance of electrolysers as it affects all different voltages explained above and the efficiency as a result. It has been reported that the cell voltage reduces with temperature mainly due to improvement in kinetics, but also conduction of protons in the membrane improves exponentially as temperature does [153, 185]. Selamet et al. experimentally measured the efficiency of an electrolyser cell as a function of the temperature. The efficiency increased from from 74% at 20 °C to 87% at 80 °C, mainly due to the better catalyst's activity and much better ionic conductivity.

Typically, electrolyser operates at a nominal temperature which ranges between 50 °C and 80 °C [154, 159, 183–185]. Regarding simulation studies, most models found in the literature assumed uniform temperature [78, 185]. However, the temperature varied from 25 °C to 37 °C when the current increased from 70 A to 140 A in the tests performed by Harrison et al. [184].

In this work, the temperature is derived from the energy balance performed to the electrolyser system. However, a maximum temperature of 80 °C was set as control variable for the electrolyser. The specific heat capacity of the stack was assumed to be equal to 814 J/kg·K [187]. The convective heat transfer coefficient was assumed to be 50 W/m·K [153]and it was assumed that the electrolyser starts at room temperature.

In order to keep the temperature close to the optimum, a thermal management system is utilised for the electrolyser. Water electrolysis is an endothermic reac-

tion. However, during cell operation, heat is generated due to the different losses enumerated above. PEM electrolysers usually operate in exothermic mode as the heat production due to losses exceeds energy demand [185].

D.3.3 Pressure

Electrolysers can be classified according to the operational pressure as low-pressure (typically below 30 bar) and high-pressure (above 30 bar). Additionally, some electrolysers are designed with a pressure gradient between the anode and the cathode (higher) [184] while others use the same pressure in both sides. Gorgun et al. assumed atmospheric pressure for the whole electrolyser [78]. However, it is more attractive when the electrolyser generates H_2 at higher pressure and values such as 10 bar, 14 bar, 35 bar and 70 bar have been found in the literature [154,183]. The pressure gradient of the electrolyser presented in Chapter 7 was assumed for the modeling work in this study with a cathode pressure of 15 bar and an anode pressure of 1 bar.

D.3.4 Efficiency

This section reports how the efficiency of an electrolyser is calculated and different values reported in the literature. Using parametric analysis, Ni et al. found that the electrolyser efficiency increases with temperature and the anode exchange current density while decreases with the electrolyte's thickness [185].

The thermoneutral voltage of the electrolyser, V_{eleth}, has been used to obtain the electrolyser's efficiency according to Equation D.19 [159]. The thermodynamic voltage considers the Nernst voltage in addition to the heat necessary for the reaction. The thermoneutral v voltage has been modelled as a polynomian function of the temperature [183].

$$\eta_{ele} = \frac{V_{eleth}}{V_{cell}} \tag{D.19}$$

Alternatively, the efficiency of the electrolyser has been obtained using the first principle of the thermodynamics which is the method used in this study [185]. Table D.1 summerizes the system efficiencies of some electrolysers avalaible in the market

Table D.1: Efficiency of different commercial electrolysers available in the market based on HHV of hydrogen.

Company	**Model**	Technology	**System efficiency (%)**
Stuart	IMET 1000	Alkaline	73
Teledyne	EC-750	Alkaline	63
Proton	HOGEN 380		56
ITM Power	H-Box Solar	PEM	72
Norsk Hydro	Atm type 5040	Alkaline	73
Avalence	Hydro 175	Alkaline	64

Appendix E

Applications not considered in the analysis

E.1 Applications not considered in this work

PVts and LS were identified as key applications to create a potential business case for CES. They were considered as the game changer for CES. But there are other potential applications which could be developed by CES systems and they were not analysed in this work. Potentially, a CES system could also develop the applications presented below in the future and they may help to increase its profitability and/or value.

E.1.1 Peak shaving

In previous legislations in Germany, the curtailment capability was only a requirement for PV generators which installed capacity was equal or higher than 100 kW_p. Due to the successful implementation of PV arrays of smaller sizes in domestic and commercial properties, the new amendment of the German legislation introduced the curtailment capability for domestic applications [112]. Therefore, a rule which only applied for large PV generators has been applied to smaller generators when the domestics installation became very widespread (voltage and power flow issues are arising related to these domestic installations) and curtailment technology was available for small scale installations. A similar approach could occur with peak shaving.

At the moment, only companies with high power capacities are charged for their peak power demand. Typically, they are middle or big industrial customers which have special contracts with a power-peak component [60]. However, the penetration of HPs and electric drive vehicles will change the peak demand of the residential and commercial areas and the peak could be 3-4 times higher than before according to the demand data managed in this work (heat demand loads

are less random than electrical demand loads). Secondly, the rolling out of smart meters (by 2020 in every house in the UK [34]) will give more information about the customer demand profile and peak demand load. For all these reasons, demand charges for residential customers could be also applied in the future. Peak shaving can be accomplished by customers by means of CES.

Peak shaving is a capacity application which requires that the CES system is not completely charged when the maximum peak occurs on a daily basis (as it happened with the avoidance of power curtailment). The reduction of the peak in the power demand offers several advantages to the energy system. The peak demand is met by less efficient generators which only run during peak time as discussed in Section 2.5.2. For any utility company, the reduction of the peak power means purchasing less electricity when the price is higher. In addition to this, it allows the use of less expensive equipment in the house (such us measurement and other auxiliary equipment) but also the deferral of investment in low voltage lines to increase its capacity.

E.1.2 Decarbonisation of the transport sector

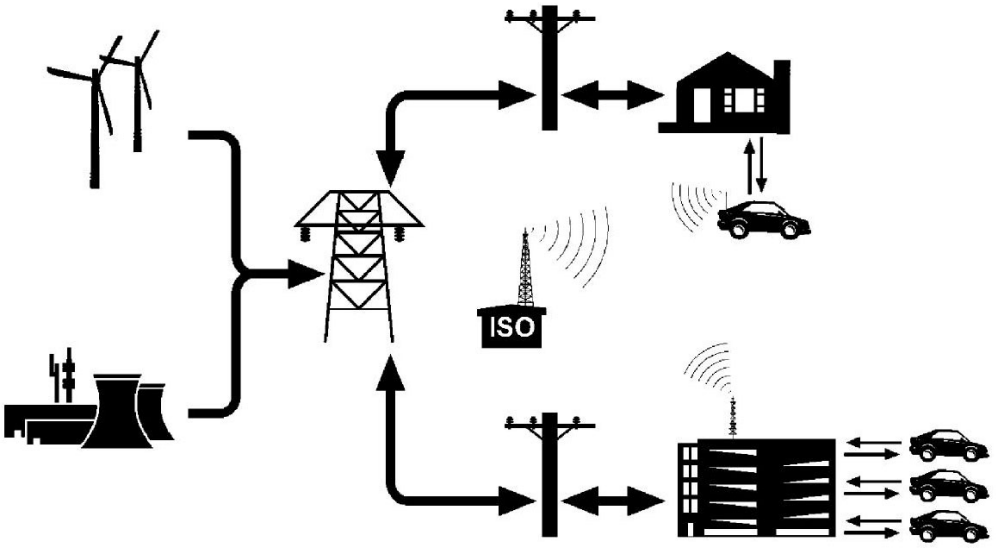

Figure E.1: Illustrative schematic representation of the power line and wireless control connections between electric drive vehicles and the electric power grid for vehicle to grid applications [16].

Similar approach followed with the heating sector could be utilised to investigate the decarbonisation of the transport sector. In fact, electricity and H_2 will be two of the key energy vectors utilised for this purpose. Same method as presented in Section 5.1 could be utilised for the transport sector when considering the vehicle fleet requirements as an additional load. However, the focus of this work

was in stationary applications related to the domestic sector.

Additionally, electric drive vehicles can be used for power systems applications with related economic benefits such as spinning reserves, frequency control and peak shaving by implementing vehicle to grid (V2G) infrastructure and communication [16]. However, the required infrastructure to manage the communication between the general control and the fleet of vehicles is still under research. Understanding the different applications and the related performance and economic benefits depending on the type of electric drive vehicle is a key aspect for the deployment of vehicle to grid applications.

E.1.3 Distributed energy storage applications

Some distributed ES applications presented in Chapter 2 can be developed by CES such as voltage control, power flow management, restoration, islanding capability (network management). However, the integration of these applications would make the CES management more complex. Secondly, the consideration of the end user applications discussed in this work (PVts and LS) by CES systems helps to reduce the likelihood of the events in which other distributed ES applications are based on. Alternatively, CES could also offer additional generation capacity to the grid operator and act as an alternative spinning reserve.

E.1.4 Power to gas

Power to gas is a promising option to decarbonise the heating and transport sectors. Both sectors accounted for 20.7% and 15% of the total emissions of the UK in 2010. As discussed in Section 1.2.1, most RE generation comes in the form of electricity. As a consequence, using RE electricity to generated fuel for vehicles and heating for buildings seems very promising. Additionally, power to gas can also contribute to reduce integration problems of RE technologies discussed in Sections 1.2.1, 2.5.4 and 3.2 without using electrical ES which is a costly asset as discussed in this thesis.

The fuel generated can be either H_2 by means of an electrolyser as it is discussed in this work and/or biomethane if H_2 reacts with carbon. P2G implies the connection of the electrical network with the gas distribution system. Current research and first demonstration plants suggest that power to gas requires large scale installations from a technological but especially economic point of view. Power to gas can introduce benefits to the future smart grid by integrating variable RE generation and help to decarbonise the transport and heating sectors by providing sustainable fuels using the current infrastructure.

Appendix F

Performance battery models in the literature

F.1 Performance lead-acid battery models in the literature

Many PbA models used in previous works were integrated with stand-alone applications. The models were developed for RE technology applications with temporal resolutions ranging from one minute to one hour in order to quantify the instantaneous, daily and seasonal performance, but neglecting the transient response.

The Shepherd model is one of the most well-known models and is considered a basic model which other more sophisticated were based on [188]. This model describes the electrochemical behavior of a PbA cell in terms of voltage and current relationship. Ross reported that Shepherd model by using Equation F.1 [189] in which K is the coefficient of polarization and t is the discharge time.

$$V_b = V_0 - K \times \frac{Q}{Q - I_b \times t} \times I_b - R_b \times I_b \tag{F.1}$$

According to Doumbia et al. [190], the main parameters which determine the PbA battery performance are the internal resistance, the polarization effect, and self-discharge. The self-discharge is difficult to estimate because is related to different factors such as operating temperature, operation cycles, materials and technology. Cherif et al. obtained an empirical model which related the battery voltage with the battery current and the SOC using parameters based on experimental research [157]. However, this model should only be applied to the specific battery model used to obtain the parameters empirically, unless those tests are repeated with a different battery. A more simple voltage and current relationship was also utilised to determine the annual energy balances for PbA technology as part of an optimization problem [103]. It as assumed that the battery voltage is linear with the SOC based on experimental results.

PbA models have also been integrated in RE softwares for helping designers and engineers to calculate and optimise stand-alone RE technologies installations mainly. RETScreen® assumed constant efficiency and that the usable battery capacity is a function of the nominal battery capacity, the temperature and the discharge rate [191]. PSspice® is an engineering software for modelling and simulating batteries among many other electrical devices. A voltage source with a resistance has been suggested to model a PbA battery using this software [192]. The voltage source and the resistance were obtained using the maximum SOC, the number of cells in series, the empirical battery efficiency and the empirical self-discharge.

In the case of Trnsys®, a sofwtare to simulate the performance of grid connected and stand-alone PV systems, a voltage of 2 V was assumed per cell [193]. Then, the battery was modeled using the Hyman model and a self-discharge model considering temperature effects was added [194]. It was argued that PbA models must be complex enough to describe both charging and discharging cycles but easy to use and employ parameters which are supplied by manufacturers [195]. PVsyst® incorporated the voltage characteristics depending on the charge and discharge for a great range of commercial PbA batteries together with maintenance details. The input data used in PVsyst® are: type of technology, voltage or number of elements, nominal capacity, internal resistance and Faradic efficiency. This model was not used in this work because it was based on specific empirical data and battery capacities.

F.2 Performance lithium-ion models used in the literature

Li-ion models have been used in the literature for a wide range of application such as mobile, stationary (RE technologies applications) and electric drive vehicles. Special emphasis was given to mobile and transport applications due to the attractive dynamic response, high energy density (up to 2000 Wh/kg [17]) and (relatively) high power density (up to 100 W/kg [64]) of Li-ion batteries. Li-ion batteries have been mainly modeled using the equivalent electrical circuit shown in Figure 4.2 but incorporating more components for the battery impedance such as capacitors and coils conforming a RC network as shown in Figure F.1. These additional elements were used to describe the dynamic response.

Three different type of modelling approaches (Thevenin-based, an Impedance-based and Runtime-Based electrical models) were compared in a compressive work as a starting point and then different elements and approaches from the three raw

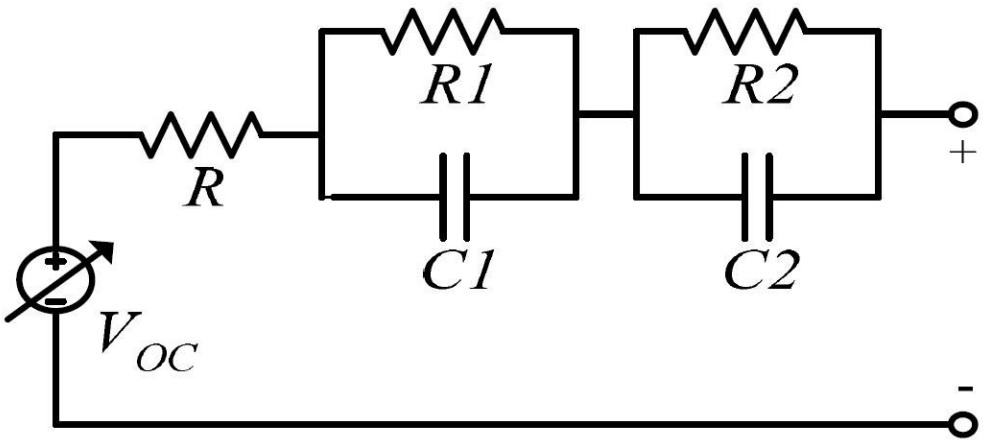

Figure F.1: Equivalent electrical circuit of a Li-ion battery considering capacitors and coils conforming a RC network

models were combined to create a more sophisticated model [146]. The model was validated using experimental research. The final model accounted for all the dynamic characteristics of Li-ion technology in order to model the transient response: non-linear open-circuit voltage, current, temperature, cycle number and storage time dependent capacity (dynamic capacity and self-discharge). All parameters of the model depended on the *SOC*, current, temperature and cycle number. Finally, it was argued that a simplification of the model could be extended to low-power applications neglecting the effects of self-discharging, cycle number and temperature.

Gao et al. focused on portable application and developed a model which paid attention to electrical and thermal aspects but included different electrochemical processes by assuming uniformity inside the battery (bulk values) [150]. In order to use this model with any specific Li-ion battery, obtaining the V_b-I_b curves during discharges at constant temperature is necessary. In order to incorporate the dynamic response to this model, the voltage answer of the battery to a step change in the current is necessary. The thermal behavior of the Li-ion battery was obtained using the first principle of thermodynamics.

Modelling the transient behavior of Li-ion batteries derived from power applications was a objective for in two different works [118, 151]. It was argued that the voltage of the battery depends strongly on the *SOC* and as a result the voltage source and the impedance used in the model shared this dependence. The impedance included as seen in Figure F.1:

- A conducting resistance and resistance from leading wires.
- A resistance and capacitor representing mass transport effects.
- A resistance in parallel with a capacitor representing the charge transfer and

the electrochemical double layer.

A very similar approach was followed by Braun et al. with a voltage source, a single resistance representing the electronic conductivity of the current collectors, the active materials, the electrolyte and three RC parallel circuits modelling [105]:

- The double layer capacitor: transition of the charge carriers at the electrode interface.
- The diffusion effects: concentration gradients of the charge carrier within the electrolyte and the electrodes.
- The active materials.

All parameters depended on the *SOC*. The open circuit voltage was a liner function of the SOC. The behavior of the other parameters was also assumed linear. In this work, the authors could access specific battery parameters supplied by the manufacturer SAFT who collaborated in the project.

Appendix G

CES discretizaton utilised by the optimization method

This appendix shows the different CES systems tested by the optimization method presented in Chapter 4 depending on the application, technology and the reference year. Specifically, the different CES systems were derived from the first step of the optimization method as explained in Section 5.1.1.

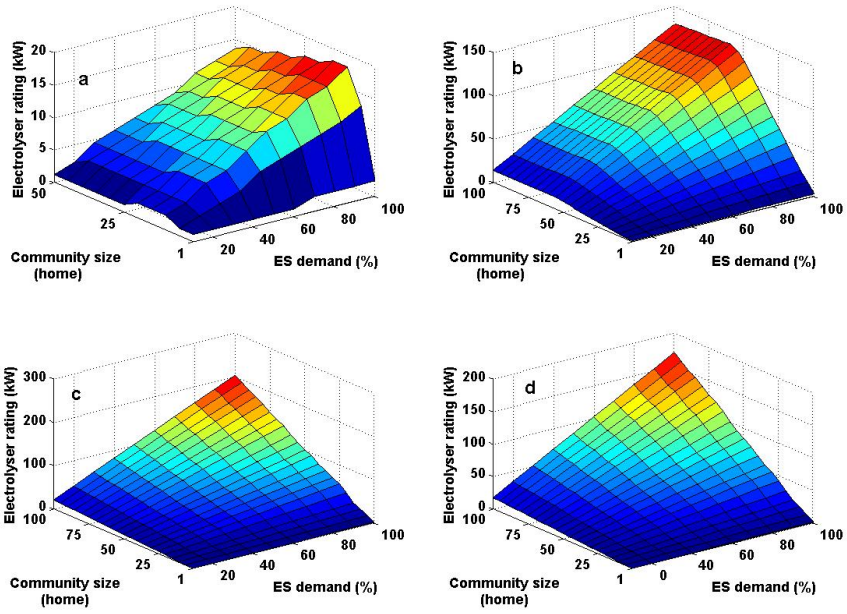

Figure G.1: PEM electrolyser rating as a percentage of the ES demand for different communities for (a) PVts and (b) LS with the NETA tariff in 2020, and (c) PVts and (d) LS with the NETA tariff in the zero carbon year. Ten electrolysers were tested for each community.

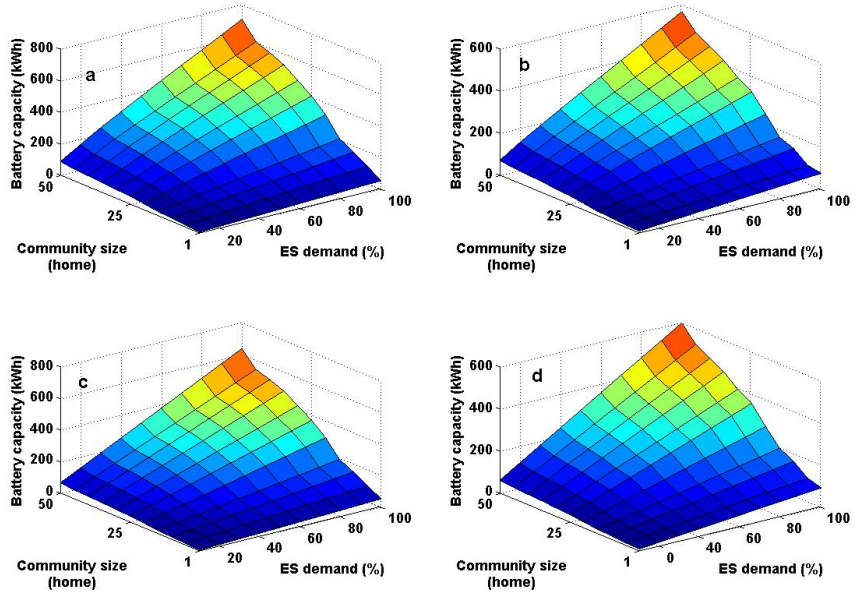

Figure G.2: Battery capacity as a percentage of the ES demand for different communities in 2020 for PbA batteries performing (a) PVts and LS with the NETA tariff and (b) PVts and LS with Economy; and for Li-ion batteries performing (c) PVts and LS with the NETA tariff and (d) PVts and LS with Economy.

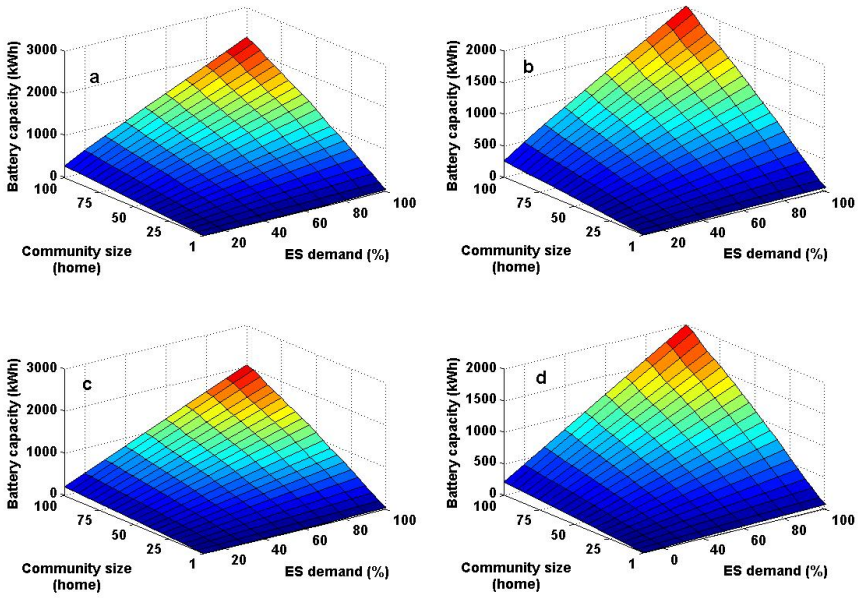

Figure G.3: Battery capacity as a percentage of the ES demand for different communities in the zero carbon year for PbA batteries performing (a) PVts and LS with the NETA tariff and (b) PVts and LS with Economy; and for Li-ion batteries performing (c) PVts and LS with the NETA tariff and (d) PVts and LS with Economy.

Appendix H

Control of the PEMFC system

This appendix shows the LabVIEW code developed to control the PEMFC system.

Appendix I

Efficiency of the converter of the electrolyser

The DC/DC converter integrated in the electrolyser has a rating of 1.2 kW. Figure I.1 shows the efficiency of the DC/DC converter of the electrolyser in one of the tests. The efficiency depends on the input DC power and went up to 0.61. Additionally, the efficiency reached 0.74 due to the dynamics of the electrolyser when the input DC power decreased. However, these data should be considered as part of the transient response of the electrolyser. Secondly, the DC power input increased every hour because

Figure I.2 shows the he efficiency of the DC/DC converter versus the input DC power. The data plotted in this figure was selected from Figure I.2. According to this figure, the efficiency of the converter is proportional to the DC power input. No data was resented between between a input DC power ranging from 300 W to 600 W because the efficiency available was lower than 0.2, therefore it is not representative. The main differences between these data and the efficiency assumed in the modelling work, represented in Figure 4.5, are that the efficiency of this DC/DC converter is significantly lower, around 35% lower and the efficiency also became constant for a much higher load, specifically for a input DC power equal to 840 W i.e. a load factor equal to 0.7. According to Figure 4.5, the efficiency keeps constant for a load factor equal to 0.3 while

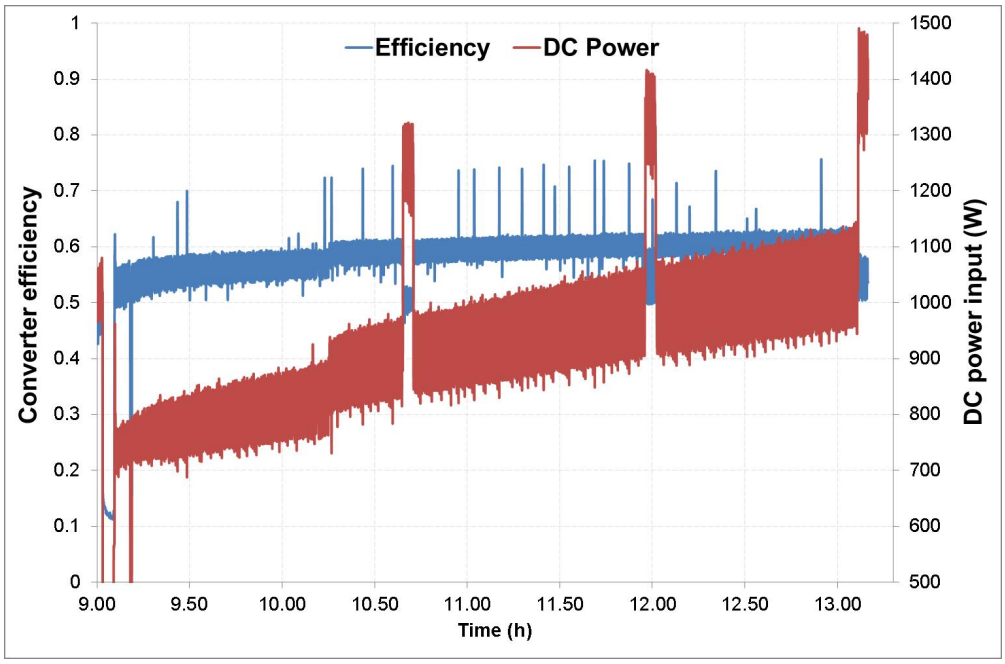

Figure I.1: Efficiency of the DC/DC converter of the electrolyser and input DC power test during a test.

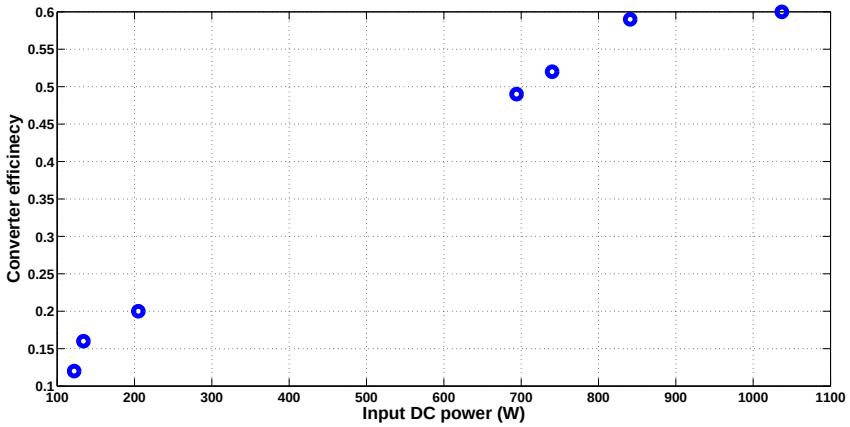

Figure I.2: Efficiency of the DC/DC converter of the electrolyser versus the input DC power.

Appendix J

CES system which optimizes different performance and economic parameter

Figures J.1 and J.2 show the battery systems which optimised different performance parameters depending on the application for PbA and Li-ion technologies respectively in the zero carbon year. The battery system which optimized the round trip efficiency, PV_{ES}, D_{ES} and the $LVOES$ was the same that optimized the round trip efficiency for the two battery technologies when performing PVts or LS.

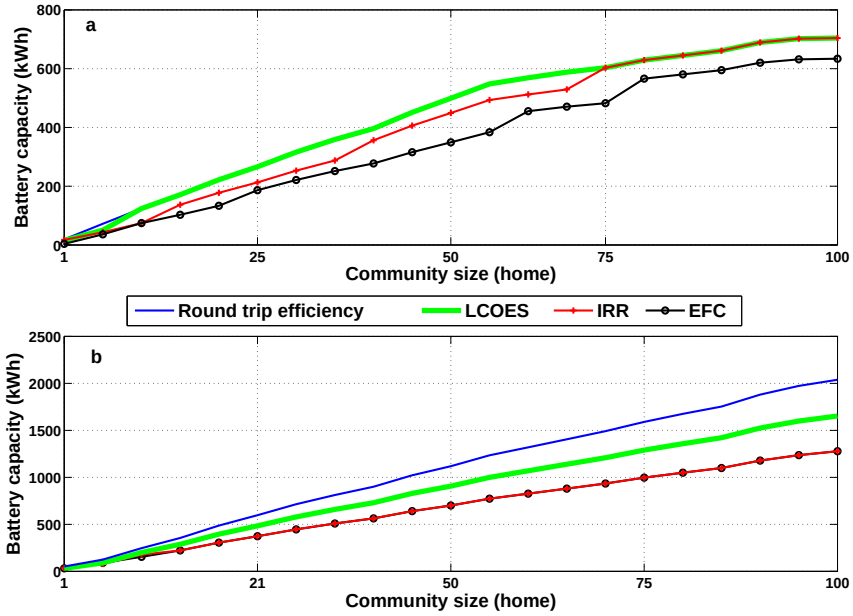

Figure J.1: PbA battery system which optimized different performance and economic parameters as a function of the size of the community when performing (a) PVts and (b) LS with Economy 7 in the zero carbon year.

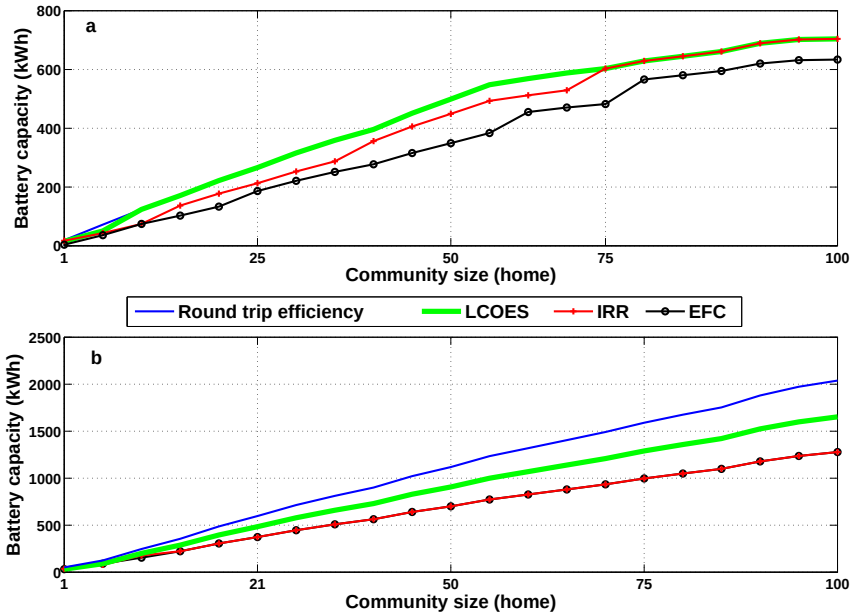

Figure J.2: Li-ion battery system which optimized different performance and economic parameters as a function of the size of the community when performing (a) PVts and (b) LS with Economy 7 in the zero carbon year.

Figure J.3 shows the electrolyser which optimised different performance parameters depending on the application in the zero carbon year.

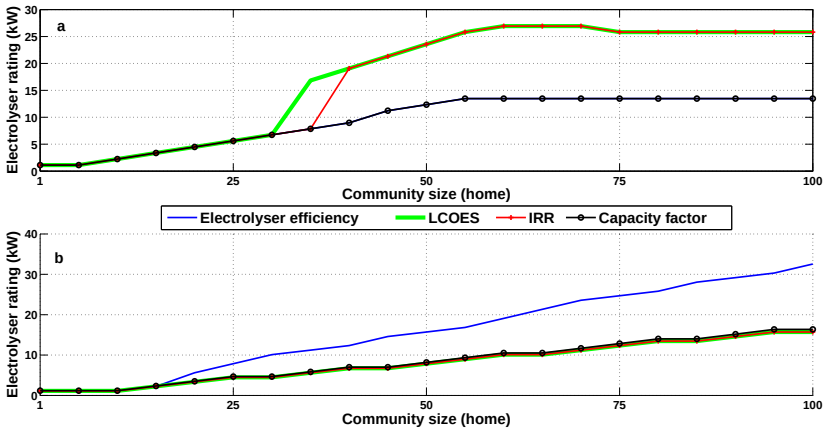

Figure J.3: Electrolyser which optimized different performance and economic parameters as a function of the size of the community when performing (a) PVts and (b) LS with the NETA tariff in the zero carbon year.

Appendix K

Algorithms developed for the CES optimisation

K.1 Algorithm for obtaining the maximum battery capacity for PVts and discretizes the capacity

Contents

- Importing the community surplus PV generaton and the unmet demand
- Importing the inverter rating for any community size
- Importing the inverter efficiency curve
- Comparing the community surplus PV energy with the inverter rating
- Obtaining the daily surplus PV energy
- Discretization of the battery capacity

```
%  Code created by David Parra for the Thesis: "Optimum Community Energy
% storage for end user utility applications"

%   Code to obtain the ES demand or maximum capacity
% for battery technology peforming PVts


clear all
clc
%=========================================================================
year=365;
day=24;
hour=60;
minute=1;
h=1440;
```

```
Community=21;
```

Importing the community surplus PV generaton and the unmet demand

```
W_PVplus_com=importdata('C:\Folder\W_PVplus_com_2020_WQB.mat');
W_daux_com=importdata('C:\Folder\W_daux_com_2020_WQB.mat');

W_PVplus_com=importdata('C:\Folder\W_PVplus_com_2020_WQB.mat');
```

Importing the inverter rating for any community size

```
P_invLaB_WQ_50_nom=importdata('C:\Folder\P_invLaB_WQ_50_nom_2020.mat');
```

Importing the inverter efficiency curve

```
In_aux=importdata('C:\Folder\In_aux.mat');
eta_conv_aux=importdata('C:\Folder\eta_conv_aux_HE.mat');
Out_aux=importdata('C:\Folder\Out_aux_HE.mat');

eta_conv_bat=zeros(hour*day*year,Community);
W_PVDC=zeros(hour*day*year,Community);
W_PVplus_com2=zeros(hour*day*year,Community);

E_dif_char=zeros(year,Community);
E_dif_disc=zeros(year,Community);


for k=1:1:Community

    W_PVplus_com2(:,k)=W_PVplus_com(:,k);
```

Comparing the community surplus PV energy with the inverter rating

```
    for i=1:1:hour*day*year

                if W_PVplus_com2(i,k)>(1.05*P_invLaB_WQ_50_nom(k,1))*...
                        eta_conv_aux(22,1)
                    W_PVplus_com2(i,k)=(1.05*P_invLaB_WQ_50_nom(k,1))*...
                        eta_conv_aux(22,1);
                end


    end
```

```
    In_conv=W_PVplus_com2(:,k)./P_invLaB_WQ_50_nom(k,1);
    eta_conv_bat(:,k)=interp1(In_aux,eta_conv_aux,In_conv);
    W_PVDC(:,k)=W_PVplus_com2(:,k).*eta_conv_bat(:,k);
```

Obtaining the daily surplus PV energy

```
    for n=1:year
                E_dif_char(n,k)=sum(W_PVDC(((n-1)*hour*day+1):...
                    ((n-1)*hour*day+hour*day),k))/60000;
                E_dif_disc(n,k)=sum(W_daux_com(((n-1)*hour*day+1):...
                    ((n-1)*hour*day+hour*day),k))/60000;
    end

end

E_char_max=max(E_dif_char);
E_disc_max=max(E_dif_disc);
LaB_Com_REts_2020_max=round(E_char_max);
```

Discretization of the battery capacity

```
var=10;

LaB_Com_REts_2020_var=zeros(Community,var);

for k=1:1:Community
    for j=1:1:var

        LaB_Com_REts_2020_var(k,j)=j*LaB_Com_REts_2020_max(1,k)/var;
    end
end

%
```

K.2 Algorithm for obtaining the optimum battery capacity for PVts

Contents

- Code created by David Parra for the Thesis: "Optimum Community Energy storage for end user utility applications"
- Importing input data and defining main variables

- Optimization
- Defining time for Simulik
- Economic analysis
- Power curtailment without energy storage
- Battery voltage definition according to Community size
- Defining battery operation parameters
- Battery cost
- Energy balances for battery charging and discharging
- Preparing the data
- Calling the Battery model in Simulink
- Loading the results from Simulink
- Managing the results from Simulink
- Calculating the performance results
- Calculating the daily results
- Calculating the annual results
- Assessing the durability
- Obtaining the economic parameters
- Searching for the optimum for each community

Code created by David Parra for the Thesis: "Optimum Community Energy storage for end user utility applications"

```
%   Code to obtain the ES demand or maximum capacity for battery
%  technology performing PVts
clear all
clc

Community=21;

for Number=1:1:Community
```

Importing input data and defining main variables

```
Iteration=1;
var=10;
%   Importing 10 different battery capacities for each community
LaB_Com_REts_2020_var=importdata('C:\Folder\LaB_Com_2020_WQB_var.mat');

Capacity_initial=importdata('C:\Folder\LaB_Capacity_initial_2020_WQB.mat');
Max_Dis=zeros(Community,var);
Max_Char=zeros(Community,var);
```

```
Cells_Number=24*ones(Community,1);
V_cell=2;
Life_factor=0.7;

%  Importing community PV and demand data
E_PVy_com=importdata('C:\Folder\E_PVy_com_2020_WQB.mat');
E_dy_com=importdata('C:\Folder\E_dy_com_2020_WQB.mat');
Demand_ratio=importdata('C:\Folder\Demand_ratio_LaB_REts_2020_WQB.mat');
PV_ratio=importdata('C:\Folder\PV_ratio_LaB_REts_2020_WQB_Inv50.mat');
W_PVplus_com=importdata('C:\Folder\W_PVplus_com_2020_WQB.mat');
W_daux_com=importdata('C:\Folder\W_daux_com_2020_WQB.mat');
W_com_100_HP=importdata('C:\Folder\W_com_100_HP_2020.mat');


%  Electricity price and export bonus
Price_W=0.163;
ExportBonus=0.032;
Revenue_REts=importdata('C:\Folder\Revenue_REts_LaB_REts_2020_WQB.mat');
%=========================================================================
year=365;
day=24;
hour=60;
minute=1;
h=1440;
%   Battery management system
SOC_min=0.4;
SOC_max=0.9;
Z_LaB_2020=2.4;
CL_factor=17*year*h;
P_max_dis=2/5;
P_max_char=1/5;

%  Power curtailment
Peak_Power_com=importdata('C:\Folder\Peak_Power_com_2020_WQB.mat');
PC_factor=0.7;
W_Ct_set=PC_factor*Peak_Power_com;
Revenue_Ct=importdata('C:\Folder\Revenue_Ct_LaB_REts_2020_WQB_Inv50.mat');
Generation_bonus=0.16;
```

```
%  Converter and inverter data
In_aux=importdata('C:\Folder\In_aux.mat');
eta_conv_aux=importdata('C:\Folder\eta_conv_aux_HE.mat');
Out_aux=importdata('C:\Folder\Out_aux_HE.mat');
P_invLaB_WQ_50_nom=importdata('C:\Folder\P_invLaB_WQ_50_nom_2020.mat');
eta_inv_mean=importdata('C:\Folder\eta_inv_com_2020_WQB.mat');
Out_conv=zeros(hour*day*year,1);
In_inv=zeros(hour*day*year,1);

W_daux2=zeros(hour*day*year,Iteration);
W_PVplus_com2=zeros(hour*day*year,Iteration);
W_batout_aux=zeros(hour*day*year,Iteration,var);
W_batin_aux=zeros(hour*day*year,Iteration,var);

%   Battery parameters
V_bat=zeros(hour*day*year,Iteration,var);
I_bat=zeros(hour*day*year,Iteration,var);
W_bat=zeros(hour*day*year,Iteration,var);
SOC=zeros(hour*day*year,Iteration,var);
Capacity=zeros(hour*day*year,Iteration,var);
W_bat_dis=zeros(hour*day*year,Iteration,var);
W_bat_char=zeros(hour*day*year,Iteration,var);
W_dbat=zeros(hour*day*year,Iteration,var);
W_PVbat_DC=zeros(hour*day*year,Iteration,var);
W_PVbat_AC=zeros(hour*day*year,Iteration,var);
W_bat_aux=zeros(hour*day*year,Iteration,var);
W_batPV=zeros(hour*day*year,Iteration,var);
% %%%%%%%%%%%%%%%%%%%%%%%%%%%%%%%%%%%%%%%%%%%%%%%%%%%%%%%%%%%%%%%%%%%%%%%%%%%%%%%

%   Daily results definitnion

%   Daily results related to PV energy

E_PVbat=zeros(year,Community,var);
E_PVgrid=zeros(year,Community,var);

%   Daily results related to the battery
E_char=zeros(year,Community,var);
E_dis=zeros(year,Community,var);
E_batPV=zeros(year,Community,var);

%   Daily results related to the type of carge
```

```
E_charPV=zeros(year,var);

%   Daily results related to the demand
E_dbat=zeros(year,Community,var);
E_dgrid=zeros(year,Community,var);


%   Daily results related to the grid
E_CtPV=zeros(year,Community);
E_Ct=zeros(year,Community,var);
E_CtES=zeros(year,Community,var);

 W_dgrid=zeros(hour*day*year,Iteration,var);
W_gridPV=zeros(hour*day*year,Iteration,var);
W_CtPV=zeros(hour*day*year,Iteration);
W_CtES=zeros(hour*day*year,Iteration,var);
W_gridCt=zeros(hour*day*year,Iteration,var);
W_PVgrid=zeros(hour*day*year,Iteration,var);


%   Battery efficiency
LaB_eff_AC=importdata('C:\Folder\LaB_eff_AC_REts_2020_WQB.mat');
LaB_eff_DC=importdata('C:\Folder\LaB_eff_DC_REts_2020_WQB.mat');
Capacity_fin=importdata('C:\Folder\LaB_Capacity_fin_REts_2020_WQB.mat');
Life=importdata('C:\Folder\Life_LaB_REts_2020_WQB.mat');
EFC=importdata('C:\Folder\EFC_LaB_REts_2020_WQB.mat');

%  Annual resuls
E_PVbaty=importdata('C:\Folder\E_PVbaty_LaB_REts_2020_WQB.mat');
E_PVgridy=importdata('C:\Folder\E_PVgridy_LaB_REts_2020_WQB.mat');
E_chary=importdata('C:\Folder\E_chary_LaB_REts_2020_WQB.mat');
E_disy=importdata('C:\Folder\E_disy_LaB_REts_2020_WQB.mat');
Discharge_REts=importdata('C:\Folder\Discharge_REts_LaB_REts_2020.mat');
E_batPVy=importdata('C:\Folder\E_batPVy_LaB_REts_2020_WQB.mat');
E_dgridy=importdata('C:\Folder\E_dgridy_LaB_REts_2020_WQB.mat');
E_CtPVy=zeros(Community,1);
E_CtESy=zeros(Community,var);
E_Cty=importdata('C:\Folder\E_Cty_LaB_REts_2020_WQB_Inv50.mat');


LaB_Com_REts_2020_var=importdata('C:\Folder\LaB_Com_2020_WQB_var.mat');
```

Optimization

```
PV_ratio_max=importdata('C:\PV_ratio_max_LaB_REts_2020.mat');
Demand_ratio_max=importdata('C:\Demand_ratio_max_LaB_REts.mat');
Efficiency_max=importdata('C:\Efficiency_max_LaB_REts.mat');
IRR_max=importdata('C:\IRR_max_LaB_REts_2020_WQB_Inv50.mat');
NPV_max=importdata('C:\NPV_max_LaB_REts_2020_WQB_Inv50.mat');
Life_max=importdata('C:\Life_max_LaB_REts_2020_WQB_Inv50.mat');
EFC_max=importdata('C:\EFC_max_LaB_REts_2020_WQB_Inv50.mat');
LCOES_PS_min=importdata('C:\LCOES_PS_min_LaB_REts_2020_WQ.mat');
LCOES_REts_min=importdata('C:\LCOES_REts_min_LaB_REts.mat');
LCOES_Ct_min=importdata('C:\LCOES_Ct_min_LaB_REts_2020.mat');
LVOES_max=importdata('C:\LVOES_max_LaB_REts_2020_WQB.mat');

I_PV_ratio=zeros(Community,1);
I_Demand_ratio=zeros(Community,1);
I_IRR=zeros(Community,1);
I_NPV=zeros(Community,1);
I_Mass_ratio=zeros(Community,1);
I_Efficiency=zeros(Community,1);
I_Life=zeros(Community,1);
I_EFC=zeros(Community,1);
I_LCOES_REts=zeros(Community,1);
I_LCOES_PS=zeros(Community,1);
I_LCOES_Ct=zeros(Community,1);
I_LVOES=zeros(Community,1);


Capacity_PV_ratio=zeros(Community,1);
Capacity_Demand_ratio=zeros(Community,1);
Capacity_IRR=zeros(Community,1);
Capacity_Life=zeros(Community,1);
Capacity_EFC=zeros(Community,1);
Capacity_Efficiency=zeros(Community,1);
Capacity_LCOES_REts=zeros(Community,1);
Capacity_LCOES_Ct=zeros(Community,1);
Capacity_LVOES=zeros(Community,1);
```

Defining time for Simulik

```
t_year_aux=minute*hour*day*year;
t_year=1:minute:(minute*hour*day*year);
t_year=t_year';
```

```
t_day_aux=minute*hour*day;
t_day=1:minute:(minute*hour*day);
t_day=t_day';
```

Economic analysis

```
%   Cost
LaB_cost_2020=150;%£/kWh
LaB_cost_BoP=100;%$/kW
BoP_cost_var=zeros(Community,var);
Maintenance_cost_var=zeros(Community,var);
ConversionDollardtoPound=150/230;
LaB_cost_BoP=ConversionDollardtoPound*LaB_cost_BoP;
LaB_cost_Maintenance=10;%$/kW
LaB_cost_Maintenance=LaB_cost_Maintenance*ConversionDollardtoPound;
LaB_W_ref=100;%kWh
LaB_cost_var=importdata('C:\Folder\LaB_cost_var_REts_2020_WQB_Inv50.mat');
Elec_size=importdata('C:\Folder\Elec_size.mat');
Elec_cost=importdata('C:\Folder\Elec_cost.mat');
Elec_cost_f_2020=0.25;
Elec_cost=Elec_cost*(1-Elec_cost_f_2020);
LaB_cost_BoP=LaB_cost_BoP*(1-Elec_cost_f_2020);

Elec_cost_var=importdata('C:\Folder\LaB_Elec_cost_var_REts_2020_WQB.mat');
LaB_system_cost_var=zeros(Community,var);
P_inv_var=importdata('C:\Folder\P_inv_var_2020_WQB_Inv50.mat');
p_bat=0.7;

%   Levelized cost of energy sotrage
LCOES_REts=importdata('C:\Folder\LCOES_REts_LaB_REts_2020_WQB_Inv50.mat');
LCOES_Ct=importdata('C:\Folder\LCOES_Ct_LaB_REts_2020_WQB_Inv50.mat');
LVOES=importdata('C:\Folder\LVOES_LaB_REts_2020_WQB_Inv50.mat');
Revenue_y=importdata('C:\Folder\Revenue_y_LaB_REts_2020_WQB_Inv50.mat');
IRR=importdata('C:\Folder\IRR_LaB_REts_2020_WQB_Inv50.mat');
CFy=0;
NPV=importdata('C:\Folder\NPV_LaB_REts_2020_WQB_Inv50.mat');
Num_EFREtsy=zeros(Community,var);
Num_EFPSy=zeros(Community,var);
Num_EFCty=zeros(Community,var);
r=0.1;% Interest rate

  k=Number
```

```
      q=k-(Number-1);
```

Power curtailment without energy storage

```
        for i=1:1:(hour*day*year)
            if W_PVplus_com(i,k)>W_Ct_set(k,1)
                W_CtPV(i,q)=W_PVplus_com(i,k)-W_Ct_set(k,1);
            end
        end
```

Battery voltage definition according to Community size

```
 if k==1
    Cells_Number(k,1)=24;%48V

elseif k==2
    Cells_Number(k,1)=24*2;%96V
elseif k==3
    Cells_Number(k,1)=24*2;%96V
elseif k==4
    Cells_Number(k,1)=24*2;%96V
elseif k==5
    Cells_Number(k,1)=24*2;%96V



else
    Cells_Number(k,1)=24;
 end
Cells_Number_aux=Cells_Number(k,1);
```

Defining battery operation parameters

```
    for j=1:1:var

        Capacity_initial(k,j)=(LaB_Com_REts_2020_var(k,j)/...
            (V_cell*Cells_Number(k,1)))*1000;
        Max_Dis(k,j)=Capacity_initial(k,j)*P_max_dis;
        Max_Char(k,j)=Capacity_initial(k,j)*P_max_char;
        P_inv_var(k,j)=min(P_invLaB_WQ_50_nom(k,1),Cells_Number(k,1)*...
            V_cell*Max_Dis(k,j));
```

Battery cost

```
BoP_cost_var(k,j)=(P_inv_var(k,j)/1000)*LaB_cost_BoP;
```

```
Maintenance_cost_var(k,j)=(P_inv_var(k,j)/1000)*LaB_cost_Maintenance;
Elec_cost_var(k,j)=interp1(Elec_size,Elec_cost,P_inv_var(k,j)/...
    1000,'linear','extrap');
if LaB_Com_REts_2020_var(k,j)>LaB_W_ref
    LaB_cost_var(k,j)=LaB_W_ref*LaB_cost_2020*...
        (LaB_Com_REts_2020_var(k,j)/LaB_W_ref)^p_bat;
else
    LaB_cost_var(k,j)=LaB_cost_2020*LaB_Com_REts_2020_var(k,j);
end
LaB_system_cost_var(k,j)=LaB_cost_var(k,j)+Elec_cost_var(k,j)+...
    BoP_cost_var(k,j)+Maintenance_cost_var(k,j);
```

Energy balances for battery charging and discharging

```
W_daux2(:,q)=W_daux_com(:,k);
W_PVplus_com2(:,q)= W_PVplus_com(:,k);

        for i=1:1:hour*day*year

              if W_daux2(i,q)/eta_conv_aux(22,1)>(1.05*P_inv_var(k,j))
                W_daux2(i,q)=eta_conv_aux(22,1)*(1.05*P_inv_var(k,j));
              end

            if W_PVplus_com2(i,q)>(1.05*P_inv_var(k,j))
                W_PVplus_com2(i,q)=(1.05*P_inv_var(k,j));
            end

        end

             Out_inv=W_daux2(:,q)./P_inv_var(k,j);
             for i=1:1:hour*day*year
                     if  Out_inv(i,1)>=0.9513
                         Out_inv(i,1)=0.9513;
                     end
              end
             In_conv=zeros(hour*day*year,1);
             for i=1:1:hour*day*year
                 if W_PVplus_com2(i,q)>0.05*P_inv_var(k,j)
                     In_conv(i,1)=W_PVplus_com2(i,q)./P_inv_var(k,j);
                 end
             end
```

```
%   SOC at the beginning of the year
SOC_0=0.7;
%   Nominal capacity
Cap_0=Capacity_initial(k,j);


 %  Battery inverter

eta_inv_bat=interp1(Out_aux,eta_conv_aux,Out_inv);
eta_conv_bat=interp1(In_aux,eta_conv_aux,In_conv);
W_batin_aux(:,q,j)=W_PVplus_com2(:,q).*eta_conv_bat;



for i=1:1:hour*day*year
        if W_batin_aux(i,q,j)>Cells_Number(k,1)*V_cell*Max_Char(k,j)
            W_batin_aux(i,q,j)=Cells_Number(k,1)*V_cell*Max_Char(k,j);
            Out_conv(i,1)=W_batin_aux(i,q,j)/P_inv_var(k,j);
           eta_conv_bat(i,1)=interp1(Out_aux,eta_conv_aux,Out_conv(i,1));
        end

        if eta_inv_bat(i,1)>0

           W_batout_aux(i,q,j)=W_daux2(i,q)/eta_inv_bat(i,1);

       end

        if W_batout_aux(i,q,j)>Cells_Number(k,1)*V_cell*Max_Dis(k,j)

            W_batout_aux(i,q,j)=Cells_Number(k,1)*V_cell*Max_Dis(k,j);
            In_inv(i,1)=W_batout_aux(i,q,j)/P_inv_var(k,j);
            eta_inv_bat(i,1)=interp1(In_aux,eta_conv_aux,In_inv(i,1));
        end

end
```

Preparing the data

```
W_bat_aux(:,q,j)=-W_batout_aux(:,q,j)+W_batin_aux(:,q,j);
aux_W_bat_aux=[t_year,W_bat_aux(:,q,j)];
```

Calling the Battery model in Simulink

```
sim('LaB_model_Sim')
```

Loading the results from Simulink

```
V_bat(:,q,j)=V_bat_Sim;
I_bat(:,q,j)=I_bat_Sim;
W_bat(:,q,j)=W_bat_Sim;
SOC(:,q,j)=SOC_Sim;
Capacity(:,q,j)=Capacity_Sim;
```

Managing the results from Simulink

```
aux_min_year=zeros(hour*day*year,1);
for i=1:1:hour*day*year
if W_bat_Sim(i,1)==0
     aux_min_year(i,1)=1;
end
end

CL=sum(aux_min_year)*(1-Life_factor)/CL_factor;
Capacity_fin(k,j)=Capacity_Sim(hour*day*year,1)*(1-CL);

for i=1:1:(hour*day*year)
   if W_bat(i,q,j)>0
       W_bat_char(i,q,j)=W_bat(i,q,j);
       if W_bat_char(i,q,j)>W_batin_aux(i,q,j)
           W_bat_char(i,q,j)=W_batin_aux(i,q,j);
       end
       W_batPV(i,q,j)=W_bat_char(i,q,j);
        eta_inv_bat(i,1)=0;
           if eta_conv_bat(i,1)>0
               W_PVbat_AC(i,q,j)=W_batPV(i,q,j)/eta_conv_bat(i,1);
           end
           if eta_inv_mean(i,k)>0
           W_PVbat_DC(i,q,j)=W_PVbat_AC(i,q,j)/eta_inv_mean(i,k);
           end
   elseif W_bat(i,q,j)<0
       W_bat_dis(i,q,j)=-W_bat(i,q,j);
       eta_conv_bat(i,1)=0;
%
   else
```

```
        eta_inv_bat(i,1)=0;
        eta_conv_bat(i,1)=0;

    end

end
```

Calculating the performance results

```
W_dbat(:,q,j)=W_bat_dis(:,q,j).*eta_inv_bat;

W_dgrid(:,q,j)=W_daux_com(:,k)-W_dbat(:,q,j);
Max_Demand_Com_ES(k,j)=max(W_dgrid(:,q,j));
PS_factor_ES(k,j)=Max_Demand_Com_ES(k,j)/Max_Demand_Com_PV(k,1);


W_gridPV(:,q,j)=W_PVplus_com(:,k)-W_PVbat_AC(:,q,j);
W_gridCt(:,q,j)=W_gridPV(:,q,j);


for i=1:1:(hour*day*year)
    if eta_inv_mean(i,k)>0
        W_PVgrid(i,q,j)=W_gridPV(i,q,j)/eta_inv_mean(i,k);

    end
end



%   Battery efficiency
LaB_eff_AC(k,j)=sum(W_dbat(:,q,j))/(sum(W_PVbat_AC(:,q,j)));
LaB_eff_DC(k,j)=sum(W_bat_dis(:,q,j))/(sum(W_bat_char(:,q,j)));


%   Power curtailment with energy storage
for i=1:1:(hour*day*year)
    if W_gridPV(i,q,j)>W_Ct_set(k,1)
        W_CtES(i,q,j)=W_gridPV(i,q,j)-W_Ct_set(k,1);
    end
end
```

Calculating the daily results

```
for n=1:year

     E_PVbat(n,k,j)=sum(W_PVbat_AC(((n-1)*hour*day+1):...
         ((n-1)*hour*day+hour*day),q,j))/60000;
     E_PVgrid(n,k,j)=sum(W_gridPV(((n-1)*hour*day+1):...
         ((n-1)*hour*day+hour*day),q,j))/60000;

     E_char(n,k,j)=sum(W_bat_char(((n-1)*hour*day+1):...
         ((n-1)*hour*day+hour*day),q,j))/60000;
     E_dis(n,k,j)=sum(W_bat_dis(((n-1)*hour*day+1):...
         ((n-1)*hour*day+hour*day),q,j))/60000;
     E_batPV(n,k,j)=sum(W_batPV(((n-1)*hour*day+1):...
         ((n-1)*hour*day+hour*day),q,j))/60000;

     E_dbat(n,k,j)=sum(W_dbat(((n-1)*hour*day+1):...
         ((n-1)*hour*day+hour*day),q,j))/60000;
     E_dgrid(n,k,j)=sum(W_dgrid(((n-1)*hour*day+1):...
         ((n-1)*hour*day+hour*day),q,j))/60000;
     E_CtPV(n,k)=sum(W_CtPV(((n-1)*hour*day+1):...
         ((n-1)*hour*day+hour*day),q))/60000;
     E_CtES(n,k,j)=sum(W_CtES(((n-1)*hour*day+1):...
         ((n-1)*hour*day+hour*day),q,j))/60000;
%
end
```

Calculating the annual results

```
E_PVbaty(k,j)=sum(E_PVbat(:,k,j));
E_PVgridy(k,j)=sum(E_PVgrid(:,k,j));

E_chary(k,j)=sum(E_char(:,k,j));
E_disy(k,j)=sum(E_dis(:,k,j));
E_batPVy(k,j)=sum(E_batPV(:,k,j));

Discharge_REts(k,j)=sum(E_dbat(:,k,j));
E_dgridy(k,j)=sum(E_dgrid(:,k,j));
E_CtPVy(k,1)=sum(E_CtPV(:,k));
E_CtESy(k,j)=sum(E_CtES(:,k,j));
E_Cty(k,j)=E_CtPVy(k,1)-E_CtESy(k,j);

Demand_ratio(k,j)=Discharge_REts(k,j)/E_dy_com(k,1);
```

```
PV_ratio(k,j)=E_PVbaty(k,j)/E_PVy_com(k,1);

Revenue_REts(k,j)=sum(E_PVbat(:,k,j))*(Price_W*LaB_eff_AC(k,j)...
    -ExportBonus);
Revenue_Ct(k,j)=0*E_Cty(k,j)*(ExportBonus+Generation_bonus);
```

Assessing the durability

```
aux=Capacity_fin(k,j);
aux1=Capacity_initial(k,j);
years=1;
while aux>=Life_factor*Capacity_initial(k,j)
        CapacityLossRatio=aux1/aux;
        aux2=aux1-aux;
        aux1=aux;
        aux=aux-aux2*CapacityLossRatio;
        years=years+1;
end

Life(k,j)=(years-1)+(aux1-Life_factor*Capacity_initial(k,j))/(aux1-aux);
EFC(k,j)=Discharge_REts(k,j)*Life(k,j)/(LaB_Com_REts_2020_var(k,j));
```

Obtaining the economic parameters

```
aux_life=round(Life(k,j));
aux_life2=Life(k,j)-aux_life;
Revenue_y(k,j)=Revenue_REts(k,j)+Revenue_PS_ES(k,j)+Revenue_Ct(k,j);

if aux_life2>0
    %   IRR
    CFy=zeros(1,aux_life+2);
    CFysize=aux_life+2;%    Due to initial investment
    for i=2:1:CFysize-1
        CFy(1,i)=Revenue_y(k,j);
    end
    CFy(1,1)=-LaB_system_cost_var(k,j);
    CFy(1,CFysize)=aux_life2*Revenue_y(k,j);
    %    LCOES REts
    EFREtsy=zeros(1,aux_life+1);
    EFysize=aux_life+1;
    for i=1:1:EFysize-1
        EFREtsy(1,i)=Discharge_REts(k,j);
```

```
    end
    EFREtsy(1,EFysize)=aux_life2*Discharge_REts(k,j);
    %   LCOES Power curtailment
    EFCty=zeros(1,aux_life+1);
    EFysize=aux_life+1;
    for i=1:1:EFysize-1
        EFCty(1,i)=E_Cty(k,j);
    end
    EFCty(1,EFysize)=aux_life2*E_Cty(k,j);

    elseif aux_life2<0
    %   IRR
    CFy=zeros(1,aux_life+1);
    CFysize=aux_life+1;
    for i=2:1:CFysize-1
        CFy(1,i)=Revenue_y(k,j);
    end
    CFy(1,1)=-LaB_system_cost_var(k,j);
    CFy(1,CFysize)=(Life(k,j)-(aux_life-1))*Revenue_y(k,j);
    %    LCOES PVts
    EFREtsy=zeros(1,aux_life);
    EFysize=aux_life;
    for i=1:1:EFysize-1
        EFREtsy(1,i)=Discharge_REts(k,j);
    end
    EFREtsy(1,EFysize)=(Life(k,j)-(aux_life-1))*Discharge_REts(k,j);
    %   LCOES Power curtailment
    EFCty=zeros(1,aux_life);
    EFysize=aux_life;
    for i=1:1:EFysize-1
        EFCty(1,i)=E_Cty(k,j);
    end
    EFCty(1,1)=E_Cty(k,j);
    EFCty(1,EFysize)=(Life(k,j)-(aux_life-1))*E_Cty(k,j);

end
%   IRR
retval = irr(CFy);

IRR(k,j)=retval*100;

for l=0:1:CFysize-1
```

```
    NPV(k,j)=NPV(k,j)+CFy(l+1)/(1+r)^(l);
end

%   LCOES REts
for i=1:1:EFysize
Num_EFREtsy(k,j)=Num_EFREtsy(k,j)+EFREtsy(1,i)/(1+r)^i;
%   LCOES Power curtailment
 Num_EFCty(k,j)=Num_EFCty(k,j)+EFCty(1,i)/(1+r)^i;
end
LCOES_REts(k,j)=LaB_system_cost_var(k,j)/Num_EFREtsy(k,j);
LCOES_Ct(k,j)=LaB_system_cost_var(k,j)/Num_EFCty(k,j);

%   Levelized value of energy storage
LVOES(k,j)=(NPV(k,j)+LaB_system_cost_var(k,j))/Num_EFREtsy(k,j);%

end
```

Searching for the optimum for each community

```
[PV_ratio_max(k,1),I_PV_ratio(k,1)]=max(PV_ratio(k,:));
[Demand_ratio_max(k,1),I_Demand_ratio(k,1)]=max(Demand_ratio(k,:));
[IRR_max(k,1),I_IRR(k,1)]=max(IRR(k,:));
[NPV_max(k,1),I_NPV(k,1)]=max(NPV(k,:));
[Efficiency_max(k,1),I_Efficiency(k,1)]=max(LaB_eff_AC(k,:));
[Life_max(k,1),I_Life(k,1)]=max(Life(k,:));
[EFC_max(k,1),I_EFC(k,1)]=max(EFC(k,:));
[LCOES_PS_min(k,1),I_LCOES_PS(k,1)]=min(LCOES_PS(k,:));
[LCOES_REts_min(k,1),I_LCOES_REts(k,1)]=min(LCOES_REts(k,:));
[LCOES_Ct_min(k,1),I_LCOES_Ct(k,1)]=min(LCOES_Ct(k,:));
[LVOES_max(k,1),I_LVOES(k,1)]=max(LVOES(k,:));

Capacity_PV_ratio(k,1)=LaB_Com_REts_2020_var(k,I_PV_ratio(k,1));
Capacity_Demand_ratio(k,1)=LaB_Com_REts_2020_var(k,I_Demand_ratio(k,1));
Capacity_IRR(k,1)=LaB_Com_REts_2020_var(k,I_IRR(k,1));
Capacity_NPV(k,1)=LaB_Com_REts_2020_var(k,I_NPV(k,1));
Capacity_Life(k,1)=LaB_Com_REts_2020_var(k,I_Life(k,1));
Capacity_EFC(k,1)=LaB_Com_REts_2020_var(k,I_EFC(k,1));
Capacity_Efficiency(k,1)=LaB_Com_REts_2020_var(k,I_Efficiency(k,1));
Capacity_LCOES_REts(k,1)=LaB_Com_REts_2020_var(k,I_LCOES_REts(k,1));
Capacity_LCOES_Ct(k,1)=LaB_Com_REts_2020_var(k,I_LCOES_Ct(k,1));
Capacity_LVOES(k,1)=LaB_Com_REts_2020_var(k,I_LVOES(k,1));

end
```

References

[1] IEA. Key world energy statistics. 2013. IEA Paris, France, 2013.

[2] IEA. Co2 emissions from fuel combustion highlights, 2012.

[3] Adam Brown, SG Müller, and Zuzana Dobrotková. Renewable energy: Markets and prospects by technology. *IEA Information Paper*, 2011.

[4] International Energy Agency. *World Energy Outlook, 2012*. OECD/IEA, 2012.

[5] EDF. Question and answer: Nuclear strike price, 2013.

[6] IEA. Technology roadmap. carbon capture and storage. Technical report, 2013.

[7] National grid. Technical report, July 2012.

[8] DESERTEC FOUNDATION. Desertec foundation [online], Available from http://www.desertec.org/press/pictures/. [Accessed 21/3/2014].

[9] The Guardian. Government gives go-ahead to smart meters [online], Available from http://www.theguardian.com/business/2009/dec/02/smart-meters-go-ahead. [Accessed 21/3/2014].

[10] Jason Makansi and JEFF Abboud. Energy storage. the missing link in the electricity value chain. *Energy Storage Council White Paper*, 2002.

[11] Enea Consulting. Energy storage. facts and figure. issues, technical solutions and development opportunities. Technical report, Enea Consulting, 2013.

[12] IEA. Technology roadmap. concentrated solar power. IEA Paris, France, 2010.

[13] Energy Storage Association. Technology comparisons [online], Available from http://www. electricitystorage. org. [Accessed 21/3/2014].

[14] Elexon. neta - the new electricity trading arrangements, 2014.

[15] Marcelo Carmo, David L Fritz, Jürgen Mergel, and Detlef Stolten. A comprehensive review on pem water electrolysis. *International Journal of Hydrogen Energy*, 38(12):4901–4934, 2013.

[16] Willett Kempton and Jasna Tomić. Vehicle-to-grid power fundamentals: calculating capacity and net revenue. *Journal of Power Sources*, 144(1):268–279, 2005.

[17] Hussein Ibrahim, Adrian Ilinca, and Jean Perron. Energy storage systems. characteristics and comparisons. *Renewable and Sustainable Energy Reviews*, 12(5):1221–1250, 2008.

[18] Ronald M Dell and David AJ Rand. Energy storage, a key technology for global energy sustainability. *Journal of Power Sources*, 100(1):2–17, 2001.

[19] P Taylor, R Bolton, D Stone, Xiao-Ping Zhang, Ch Martin, and P Upham. Pathways for energy storage in the uk. *Report for the Centre for Low Carbon Futures, York*, 2012.

[20] Department of Energy HM Government and Climate Change. 2050 pathways analysis. Technical report, jul 2010.

[21] Leon Freris and David Infield. *Renewable energy in power systems*. John Wiley & Sons, 2008.

[22] Carlo Carraro, Carlo Barbante, Paolo Ruti, and Antonio Navarra. Climate change: everything you need to know about the ipcc 5th assessment report. *Review of Environment, Energy and Economics-Re3*, 2013.

[23] IEA. Deploying renewables. best and future policy practice. Technical report, 2012.

[24] Fraunhofer Institute for Solar Energy ISE. Photovoltaics report, dec 2011.

[25] Carbon Trust. Micro chp (combined heat and power) accelerator - final report. Technical report, Carbon Trust, March 2011.

[26] MC Hidalgo, P Rodríguez Aumente, M Izquierdo Millán, A Lecuona Neumann, and R Salgado Mangual. Energy and carbon emission savings in spanish housing air-conditioning using solar driven absorption system. *Applied Thermal Engineering*, 28(14):1734–1744, 2008.

[27] Ryan P O'Hayre, Suk-Won Cha, Whitney Colella, and Fritz B Prinz. *Fuel cell fundamentals*. John Wiley & Sons New York, 2006.

[28] CE Thomas. Fuel cell and battery electric vehicles compared. *international journal of hydrogen energy*, 34(15):6005–6020, 2009.

[29] Alex MKP Taylor. Science review of internal combustion engines. *Energy Policy*, 36(12):4657–4667, 2008.

[30] Eckard Helmers and Patrick Marx. Electric cars: technical characteristics and environmental impacts. *Environmental Sciences Europe*, 24(1):1–15, 2012.

[31] National grid. Investigation into transmission losses on uk electricity network system. Technical report, June 2008.

[32] JI Utley and LD Shorrock. Domestic energy fact file 2008. *Department of Energy and Climate Change, BRE, Watford*, 2008.

[33] Jens Laustsen. Energy efficiency requirements in building codes, energy efficiency policies for new buildings. *International Energy Agency (IEA)*, 2008.

[34] Great Britain: Department of Energy and Climate Change. *The UK low carbon transition plan: national strategy for climate and energy.* Act on CO2. Stationery Office, 2009.

[35] Michael Dittmar. Nuclear energy: Status and future limitations. *Energy*, 37(1):35–40, 2012.

[36] Michael Marshall. Hinkley point reactors herald new nuclear age for uk. *New Scientist*, 220(2939):6–7, 2013.

[37] EDF Energy. Carbon emissions from nuclear power, 2013.

[38] David Bodansky. *Nuclear energy.* Springer, 2004.

[39] Kamel Bennaceur, Dolf Gielen, Tom Kerr, and Cecilia Tam. *CO2 capture and storage: a key carbon abatement option.* OECD, 2008.

[40] Elke Lorenz, Jan Remund, Stefan C Müller, Wolfgang Traunmüller, Gerald Steinmaurer, David Pozo, José Antonio, Vicente Lara Fanego Ruiz-Arias, Lourdes Ramirez, Martin Gaston Romeo, et al. Benchmarking of different approaches to forecast solar irradiance. In *24th European Photovoltaic Solar Energy Conference*, pages 1–10. Hamburg, Germany, 2009.

[41] Great Britain: Department of Energy and Climate Change. 2010 uk greenhouse gas emissions, final figures, 2012.

[42] European Commission et al. A roadmap for moving to a competitive low carbon economy in 2050. *COM (2011)*, 112(4), 2011.

[43] Bradford P Roberts and Chet Sandberg. The role of energy storage in development of smart grids. *Proceedings of the IEEE*, 99(6):1139–1144, 2011.

[44] Eric Borden and Wolf-Peter Schill. Policy efforts for the development of storage technologies in the us and germany. Technical report, Discussion Papers, DIW Berlin, 2013.

[45] Australian Energy Market Commission. 2013 residential electricity price trends. final report. Technical report, Australian Energy Market Commission, 2014.

[46] PR Thomas, TJ Walker, and CA McCarthy. Demonstration of community energy storage fleet for load leveling, reactive power compensation, and reliability improvement. In *Power and Energy Society General Meeting, 2012 IEEE*, pages 1–4. IEEE, 2012.

[47] Frank Sensfuss, Mario Ragwitz, and Massimo Genoese. The merit-order effect: A detailed analysis of the price effect of renewable electricity generation on spot market prices in germany. *Energy policy*, 36(8):3086–3094, 2008.

[48] Gaynor Hartnell and Lars Landberg. Wind on the system: grid integration of wind power. *Renewable Energy World*, (Mar-Apr 2000 issue):60–62, 2000.

[49] Goran Strbac, Marko Aunedi, Danny Pudjianto, Predrag Djapic, Fei Teng, Alexander Sturt, Dejvises Jackravut, Robert Sansom, Vladimir Yufit, and Nigel Brandon. Strategic assessment of the role and value of energy storage systems in the uk low carbon energy future. Technical report, Carbon Trust, 2012.

[50] European Commission et al. Proposal for a regulation of the european parliament and of the council on guidelines for trans-european energy infrastructure and repealing decision no 1364/2006/ec. *COM (2011)*, 658, 2011.

[51] European Commission. *Interconnecting Europe. New perspectives for transEuropean energy networks*. Office for Official Publications of the European Communities Luxembourg, 2008.

[52] Dirk Van Hertem, Mehrdad Ghandhari, and Marko Delimar. Technical limitations towards a supergrid. a european prospective. In *Energy Conference and Exhibition (EnergyCon), 2010 IEEE International*, pages 302–309. IEEE, 2010.

[53] Goran Strbac. Demand side management: Benefits and challenges. *Energy Policy*, 36(12):4419–4426, 2008.

[54] Peter Palensky and Dietmar Dietrich. Demand side management: Demand response, intelligent energy systems, and smart loads. *Industrial Informatics, IEEE Transactions on*, 7(3):381–388, 2011.

[55] Carlos Batlle and Pablo Rodilla. Electricity demand response tools: current status and outstanding issues. *Special issue on incentives for a low-carbon energy future, European Review of Energy Markets*, 2008.

[56] Jim Eyer and Garth Corey. Energy storage for the electricity grid: Benefits and market potential assessment guide. *Sandia National Laboratories Report, SAND2010-0815, Albuquerque, New Mexico*, 2010.

[57] Energy Research Partnership. The future role of energy storage in the uk. main report. Technical report, Energy Research Partnership, 2013.

[58] Bottling Electricity. Storage as a strategic tool for managing variability and capacity concerns in the modern grid. *A Report of the Electricity Advisory Committee*, 2008.

[59] Didier Mayer, Arthouros Zervos, et al. Fp7 research priorities for the renewable energy sector, eurec. *European Renewable Energy Research Community*, pages 3–10, 2005.

[60] Yves Brunet. *Energy storage*. Wiley. com, 2013.

[61] H Headland. Blaenau ffestiniog and other medium-head pumped storage schemes in great britain. *Proceedings of The Institution of Mechanical Engineers*, 175(1):319–366, 1961.

[62] Chris Le Fevre. *Gas storage in Great Britain*. Oxford Institute for Energy Studies, 2013.

[63] Keith MacLean. Personal conversation with keith maclean from scottish southern energy, 2013.

[64] Peter J Hall and Euan J Bain. Energy-storage technologies and electricity generation. *Energy policy*, 36(12):4352–4355, 2008.

[65] John P Barton and David G Infield. Energy storage and its use with intermittent renewable energy. *Energy Conversion, IEEE Transactions on*, 19(2):441–448, 2004.

[66] Ronald Michael Dell and David Anthony James Rand. *Clean energy*, volume 5. Royal Society of Chemistry, 2004.

[67] Susan M Schoenung. Characteristics and technologies for long-vs. short-term energy storage. *Sandia Report SAND2001-0765*, 2001.

[68] Matthew L Lazarewicz and Alex Rojas. Grid frequency regulation by recycling electrical energy in flywheels. In *Power Engineering Society General Meeting, 2004. IEEE*, pages 2038–2042. IEEE, 2004.

[69] David Connolly, Henrik Lund, P Finn, Brian Vad Mathiesen, and M Leahy. Practical operation strategies for pumped hydroelectric energy storage (phes) utilising electricity price arbitrage. *Energy Policy*, 39(7):4189–4196, 2011.

[70] Lion Hirth. The market value of variable renewables: The effect of solar and wind power variability on their relative price. *Energy Economics*, 2013.

[71] Alaa Mohd, Egon Ortjohann, Andreas Schmelter, Nedzad Hamsic, and Danny Morton. Challenges in integrating distributed energy storage systems into future smart grid. In *Industrial Electronics, 2008. ISIE 2008. IEEE International Symposium on*, pages 1627–1632. IEEE, 2008.

[72] James A McDowall. Status and outlook of the energy storage market. In *Power Engineering Society General Meeting, 2007. IEEE*, pages 1–3. IEEE, 2007.

[73] Nirmal-Kumar C Nair and Niraj Garimella. Battery energy storage systems: Assessment for small-scale renewable energy integration. *Energy and Buildings*, 42(11):2124–2130, 2010.

[74] J Kondoh, I Ishii, H Yamaguchi, A Murata, K Otani, K Sakuta, N Higuchi, S Sekine, and M Kamimoto. Electrical energy storage systems for energy networks. *Energy Conversion and Management*, 41(17):1863–1874, 2000.

[75] Michael J Dolan, Malcolm Barnacle, Simon Gill, Colin Foote, Graham W Ault, and George Bell. Modelling and delivery of an active network management scheme for the northern isles new energy solutions project. In *Electricity Distribution (CIRED 2013), 22nd International Conference and Exhibition on*, pages 1–4. IET.

[76] David Parra, Gavin S Walker, and Mark Gillott. Modeling of pv generation, battery and hydrogen storage to investigate the benefits of energy storage for single dwelling. *Sustainable Cities and Society*, 2013.

[77] Ram B Gupta. *Hydrogen fuel: production, transport, and storage*. CRC Press, 2008.

[78] Haluk Gorgun. Dynamic modelling of a proton exchange membrane (pem) electrolyzer. *International journal of hydrogen energy*, 31(1):29–38, 2006.

[79] Gavin Walker. *Solid-state hydrogen storage: materials and chemistry*. Woodhead Publishing, 2008.

[80] Borislav Bogdanović, Klaus Bohmhammel, Babett Christ, Alexander Reiser, Klaus Schlichte, Ralph Vehlen, and Ulrich Wolf. Thermodynamic investigation of the magnesium–hydrogen system. *Journal of Alloys and compounds*, 282(1):84–92, 1999.

[81] European Commission. Strategic energy technologies information system. technology map chapters. hydrogen and fuel cells, 2013.

[82] Steve Barrett. Fcvs will be a key element in european vehicle powertrains portfolio to achieve 2050 goals. *Fuel Cells Bulletin*, 2011(1):12–15, 2011.

[83] Matthew Little, Murray Thomson, and David Infield. Electrical integration of renewable energy into stand-alone power supplies incorporating hydrogen storage. *International Journal of Hydrogen Energy*, 32(10):1582–1588, 2007.

[84] J Ignacio Ortega, J Ignacio Burgaleta, and Felix M Tellez. Central receiver system solar power plant using molten salt as heat transfer fluid. *Journal of Solar Energy Engineering*, 130(2):24501, 2008.

[85] Ibrahim Dincer and Marc Rosen. *Thermal energy storage: systems and applications*. Wiley. com, 2002.

[86] TR Whiffen and SB Riffat. A review of pcm technology for thermal energy storage in the built environment: Part i. *International Journal of Low-Carbon Technologies*, 2012.

[87] Kari Alanne and Jukka Paatero. Seasonal heat storages and residential micro-cogeneration. In *1st International Conference on Micro-Generation and Application*, 2008.

[88] BRE. Energy use in homes. Technical report, 2007.

[89] Rachael Louise Storry, Graham Ault, and Stuart Galloway. The use of electrical thermal storage to balance the variability and intermittency of renewable energy. In *Universities' Power Engineering Conference (UPEC), Proceedings of 2011 46th International*, pages 1–5. VDE, 2011.

[90] Thomas Nuytten, Bert Claessens, Kristof Paredis, Johan Van Bael, and Daan Six. Flexibility of a combined heat and power system with thermal energy storage for district heating. *Applied Energy*, 104:583–591, 2013.

[91] Larry Hughes. Meeting residential space heating demand with wind-generated electricity. *Renewable Energy*, 35(8):1765–1772, 2010.

[92] Steve Barrett. Ecoislands shown the wight way to go green with smart grid and hydrogen energy. *Fuel Cells Bulletin*, 2012(10):12–15, 2012.

[93] Régine Belhomme, Carolina Tranchita, Anh Vu, Joseph Maire, and Olivier Huet. Overview and goals of the clusters of smart grid demonstration projects in france. In *Power and Energy Society General Meeting, 2011 IEEE*, pages 1–8. IEEE, 2011.

[94] Neal S Wade, PC Taylor, PD Lang, and PR Jones. Evaluating the benefits of an electrical energy storage system in a future smart grid. *Energy Policy*, 38(11):7180–7188, 2010.

[95] Jukka V Paatero and Peter D Lund. Impacts of energy storage in distribution grids with high penetration of photovoltaic power. *International Journal of Distributed Energy Resources*, 3(1):31–45, 2007.

[96] Manuel Castillo-Cagigal, Estefanía Caamaño-Martín, Eduardo Matallanas, Daniel Masa-Bote, A Gutiérrez, F Monasterio-Huelin, and J Jiménez-Leube. Pv self-consumption optimization with storage and active dsm for the residential sector. *Solar Energy*, 85(9):2338–2348, 2011.

[97] Klaus-Henning Ahlert. *Economics of distributed storage systems. An economic analysis of arbitrage-maximizing storage systems at the end consumer level*. KIT Scientific Publishing, 2010.

[98] Eric Hittinger, JF Whitacre, and Jay Apt. What properties of grid energy storage are most valuable? *Journal of Power Sources*, 206:436–449, 2012.

[99] Sandhya Sundararagavan and Erin Baker. Evaluating energy storage technologies for wind power integration. *Solar Energy*, 2012.

[100] Stefan Nykamp, Vincent Bakker, Albert Molderink, Johann L Hurink, and Gerard JM Smit. Break-even analysis for the storage of pv in power distribution grids. *International Journal of Energy Research*, 2013.

[101] James Ayre. Germany´s residential battery storage subsidy a success. 4000 new systems in 1st year., 2014.

[102] Y Riffonneau, S Bacha, F Barruel, and A Delaille. Energy flow management in grid connected pv systems with storage-a deterministic approach. In *Industrial Technology, 2009. ICIT 2009. IEEE International Conference on*, pages 1–6. IEEE, 2009.

[103] Yann Riffonneau, Seddik Bacha, Franck Barruel, and Stephane Ploix. Optimal power flow management for grid connected pv systems with batteries. *Sustainable Energy, IEEE Transactions on*, 2(3):309–320, 2011.

[104] DP Jenkins, J Fletcher, and David Kane. Lifetime prediction and sizing of lead-acid batteries for microgeneration storage applications. *Renewable Power Generation, IET*, 2(3):191–200, 2008.

[105] Martin Braun, Kathrin Büdenbender, Dirk Magnor, and Andreas Jossen. Photovoltaic self-consumption in germany using lithium-ion storage to increase self-consumed photovoltaic energy. *ISET, Kassel*, 2009.

[106] Grietus Mulder, Fjo De Ridder, and Daan Six. Electricity storage for grid-connected household dwellings with pv panels. *Solar energy*, 84(7):1284–1293, 2010.

[107] Grietus Mulder, Daan Six, Bert Claessens, Thijs Broes, Noshin Omar, and Joeri Van Mierlo. The dimensioning of pv-battery systems depending on the incentive and selling price conditions. *Applied Energy*, 111:1126–1135, 2013.

[108] Eoghan McKenna, Marcelle McManus, Sam Cooper, and Murray Thomson. Economic and environmental impact of lead-acid batteries in grid-connected domestic pv systems. *Applied Energy*, 104:239–249, 2013.

[109] Department of Energy and Climate Change. Renewable heat incentive. Technical report, Department of Energy and Climate Change, 2011.

[110] Diana Neves, Carlos A Silva, and Stephen Connors. Design and implementation of hybrid renewable energy systems on micro-communities: A review on case studies. *Renewable and Sustainable Energy Reviews*, 31:935–946, 2014.

[111] Ali Nourai, Ram Sastry, and Thomas Walker. A vision & strategy for deployment of energy storage in electric utilities. In *Power and Energy Society General Meeting, 2010 IEEE*, pages 1–4. IEEE, 2010.

[112] Jürgen Wittlinger. Erneuerbare-energien-gesetz (eeg). In *Photovoltaikanlagen im Steuerrecht*, pages 29–40. Springer, 2012.

[113] Huan-Liang Tsai, Ci-Siang Tu, and Yi-Jie Su. Development of generalized photovoltaic model using matlab/simulink. In *Proceedings of the World Congress on Engineering and Computer Science*, pages 846–851, 2008.

[114] Goverment of the UK. Weekly solar pv installation and capacity based on registration date [online], https://www.gov.uk/government/statistical-data-sets/weekly-solar-pv-installation-and-capacity-based-on-registration-date, [Accessed 14/09/2013].

[115] PAB James, AS Bahaj, Arif A Anwar, and LE Myers. Location, location, location: Domestic small-scale wind field trial report. *Energy Saving Trust*, pages 1–24, 2009.

[116] JF Manwell, JG McGowan, and AL Rogers. Wind energy explained: theory, design and application. 2002. *John Wiley&Sons Ltd, UK*, page 577, 2002.

[117] Neil J Hewitt. Heat pumps and energy storage–the challenges of implementation. *Applied Energy*, 89(1):37–44, 2012.

[118] H Beltran, M Swierczynski, A Luna, G Vazquez, and E Belenguer. Photovoltaic plants generation improvement using li-ion batteries as energy buffer. In *Industrial Electronics (ISIE), 2011 IEEE International Symposium on*, pages 2063–2069. IEEE, 2011.

[119] B Guinot, Y Bultel, F Montignac, D Riu, and I Noirot-Le Borgne. Economic impact of performances degradation on the competitiveness of energy storage technologies–part 2: Application on an example of pv production guarantee. *International Journal of Hydrogen Energy*, 2013.

[120] Energy Saving Trust. Feed-in tariffs scheme (fits) [online], Accessed from http://www.energysavingtrust.org.uk/Generating-energy/Getting-money-back/Feed-In-Tariffs-scheme-FITs, [Accessed 10/01/2013].

[121] FDJ Nieuwenhout, MPF Hommelberg, GJ Schaeffer, JCP Kester, and K Visscher. Feasibility of distributed electricity storage. *International Journal of Distributed Energy Resources*, 2(4):307–323, 2006.

[122] A Oudalov, D Chartouni, C Ohler, and G Linhofer. Value analysis of battery energy storage applications in power systems. In *Power Systems Conference and Exposition, 2006. PSCE'06. 2006 IEEE PES*, pages 2206–2211. IEEE, 2006.

[123] Debra Lew, Lori Bird, Michael Milligan, Bethany Speer, Xi Wang, Enrico Maria Carlini, Ana Estanqueiro, Damian Flynn, Emilio Gomez-Lazaro, Nickie Menemenlis, et al. Wind and solar curtailment. 2013.

[124] UKERC. Milton keynes energy park dwellings [online], Available from http://http://www.ukerc.ac.uk [Accessed 21/03/2014].

[125] Scott Kelly, Doug Crawford-Brown, and Michael G Pollitt. Building performance evaluation and certification in the uk: Is sap fit for purpose? *Renewable and Sustainable Energy Reviews*, 16(9):6861–6878, 2012.

[126] Ian Richardson, Murray Thomson, David Infield, and Conor Clifford. Domestic electricity use: A high-resolution energy demand model. *Energy and Buildings*, 42(10):1878–1887, 2010.

[127] Amir Fazeli, Mark Gillott, Mark Johnson, and Mark Sumner. Investigating the effects of incorporating seasonal variation in a domestic active occupancy model. In *Sustainability in Energy and Buildings*, pages 447–455. Springer, 2012.

[128] Marcelo Gradella Villalva, Jonas Rafael Gazoli, et al. Comprehensive approach to modeling and simulation of photovoltaic arrays. *Power Electronics, IEEE Transactions on*, 24(5):1198–1208, 2009.

[129] Alonso Garcia and JL Balenzategui. Estimation of photovoltaic module yearly temperature and performance based on nominal operation cell temperature calculations. *Renewable Energy*, 29(12):1997–2010, 2004.

[130] John A Duffie and William A Beckman. *Solar engineering of thermal processes*. John Wiley & Sons, 2013.

[131] Sanyo. Hit photovoltaic modulde [online], Available from http://file.ample-energy-services.co.uk/downloads/Sanyo[Accessed 08/01/2013].

[132] Energy Saving Trust. Here comes the sun. a field trial of solar water heating systems. Technical report, Energy Saving Trust, 2013.

[133] AD Peacock and M Newborough. Impact of micro-chp systems on domestic sector co¡ sub¿ 2¡/sub¿ emissions. *Applied Thermal Engineering*, 25(17):2653–2676, 2005.

[134] Iain Staffell. *Fuel cells for domestic heat and power: are they worth it?* PhD thesis, University of Birmingham, 2010.

[135] Pöyry Energy Consulting and Faber Maunsell (AECOM). The potential and cost of district heating networks. Technical report, Department of Energy and Climate Change, London, April 2009.

[136] Adam Hawkes, Iain Staffell, Dan Brett, and Nigel Brandon. Fuel cells for micro-combined heat and power generation. *Energy & Environmental Science*, 2(7):729–744, 2009.

[137] Matthew M Mench. *Fuel cell engines*. Wiley Online Library, 2008.

[138] M Gillott D Parra and G. S. Walker. The role of hydrogen in achieving the decarbonisation targets for the uk domestic sector (in press). *The Intenational Journal of Hydrogen Energy*, 2014.

[139] Dries Haeseldonckx, Leen Peeters, Lieve Helsen, and William D'haeseleer. The impact of thermal storage on the operational behaviour of residential chp facilities and the overall co2 emissions. *Renewable and Sustainable Energy Reviews*, 11(6):1227–1243, 2007.

[140] Energy Saving Trust. Getting warmer: a field trial of heat pumps. *The Energy Saving Trust, London*, 2010.

[141] JD Marcos, M Izquierdo, and D Parra. Solar space heating and cooling for spanish housing: Potential energy savings and emissions reduction. *Solar Energy*, 85(11):2622–2641, 2011.

[142] IN Gale. Ground source heat pumps: development of georeports for potential site characterisation, issue 1.2. british geological survey commissioned report. Technical report, CR/05, 2005.

[143] LA Steijger, Richard A Buswell, V Smedley, Steven K Firth, and Paul Rowley. An air source heat pump model for operation in cold humid environments. 2010.

[144] KC Divya and Jacob Østergaard. Battery energy storage technology for power system. an overview. *Electric Power Systems Research*, 79(4):511–520, 2009.

[145] Abbas A Akhil, Georgianne Huff, Aileen B Currier, Benjamin C Kaun, Dan M Rastler, Stella Bingqing Chen, Andrew L Cotter, Dale T Bradshaw, and William D Gauntlett. Doe/epri 2013 electricity storage handbook in collaboration with nreca. *Report SAND2013-5131, Sandia National Laboratories*, 2013.

[146] Min Chen and Gabriel A Rincon-Mora. Accurate electrical battery model capable of predicting runtime and iv performance. *Energy conversion, ieee transactions on*, 21(2):504–511, 2006.

[147] JB Copetti and F Chenlo. Lead/acid batteries for photovoltaic applications. test results and modeling. *Journal of power sources*, 47(1):109–118, 1994.

[148] Olivier Tremblay and Louis-A Dessaint. Experimental validation of a battery dynamic model for ev applications. *World Electric Vehicle Journal*, 3:13–16, 2009.

[149] Mathworks. Battery block model [online], Accessed from http://www.mathworks.co.uk/help/physmod/powersys/ref/battery.html. [Accessed 06/01/2013].

[150] Lijun Gao, Shengyi Liu, and Roger A Dougal. Dynamic lithium-ion battery model for system simulation. *Components and Packaging Technologies, IEEE Transactions on*, 25(3):495–505, 2002.

[151] O Erdinc, B Vural, and M Uzunoglu. A dynamic lithium-ion battery model considering the effects of temperature and capacity fading. In *Clean Electrical Power, 2009 International Conference on*, pages 383–386. IEEE, 2009.

[152] Stephen Drouilhet, Bertrand L Johnson, et al. A battery life prediction method for hybrid power applications. In *AIAA Aerospace Sciences Meeting and Exhibit*, 1997.

[153] KS Agbli, MC Péra, D Hissel, O Rallières, C Turpin, and I Doumbia. Multiphysics simulation of a pem electrolyser: Energetic macroscopic representation approach. *International Journal of Hydrogen Energy*, 36(2):1382–1398, 2011.

[154] F Marangio, M Santarelli, and M Calì. Theoretical model and experimental analysis of a high pressure pem water electrolyser for hydrogen production. *International Journal of Hydrogen Energy*, 34(3):1143–1158, 2009.

[155] Pyoungho Choi, Dmitri G Bessarabov, and Ravindra Datta. A simple model for solid polymer electrolyte (spe) water electrolysis. *Solid State Ionics*, 175(1):535–539, 2004.

[156] Frano Barbir. Pem electrolysis for production of hydrogen from renewable energy sources. *Solar Energy*, 78(5):661–669, 2005.

[157] A Cherif, M Jraidi, and A Dhouib. A battery ageing model used in stand alone pv systems. *Journal of Power sources*, 112(1):49–53, 2002.

[158] Susan Schoenung. Energy storage systems cost update. *SAND2011-2730*, 2011.

[159] Ömer Faruk Selamet, Fatih Becerikli, Mahmut D Mat, and Yüksel Kaplan. Development and testing of a highly efficient proton exchange membrane (pem) electrolyzer stack. *International Journal of Hydrogen Energy*, 36(17):11480–11487, 2011.

[160] Walter Short, Daniel J Packey, and Thomas Holt. *A manual for the economic evaluation of energy efficiency and renewable energy technologies*. University Press of the Pacific, 2005.

[161] PA Nelson, KG Bloom, and DW I Dees. Modeling the performance and cost of lithium-ion batteries for electric-drive vehicles. Technical report, Argonne National Laboratory (ANL), Argonne, IL (United States), 2011.

[162] Unknown Author. Private communications with hitachi and itm power for battery and h_2 technologies. 2014.

[163] S Eckroad and I Gyuk. Epri-doe handbook of energy storage for transmission & distribution applications. *Electric Power Research Institute, Inc*, 2003.

[164] Paul Bolton. Energy prices. Technical report, House of Commons, 2013.

[165] Goverment of the UK. Energy consumption in the uk. domestic data tables. 2011 update [online], Sep Available from https://www.gov.uk/government/publications/energy-consumption-in-the-uk. [Accessed 01/01/2013].

[166] D Feldman, G Barbose, R Margolis, R Wiser, N Darghouth, and A Goodrich. Photovoltaic (pv) pricing trends: Historical, recent, and near-term projections. Technical report, National Renewable Energy Laboratory (NREL), Golden, CO., 2012.

[167] Joseph C Lam and Sam Hui. Sensitivity analysis of energy performance of office buildings. *Building and Environment*, 31(1):27–39, 1996.

[168] Peter Doubilet, Colin B Begg, Milton C Weinstein, Peter Braun, and Barbara J McNeil. Probabilistic sensitivity analysis using monte carlo simulation. a practical approach. *Medical decision making: an international journal of the Society for Medical Decision Making*, 5(2):157–177, 1984.

[169] Christoph Romaus, Kai Gathmann, and J Bo¨cker. Optimal energy management for a hybrid energy storage system for electric vehicles based on stochastic dynamic programming. In *Vehicle Power and Propulsion Conference (VPPC), 2010 IEEE*, pages 1–6. IEEE, 2010.

[170] Goverment of the UK. Energy price statistics [online], Available from http://www.decc.gov.uk/en/content/cms/statistics/energy$_s tats$/prices/prices.aspx. [Accessed 01/01/2013].

[171] Paul L Joskow and Catherine D Wolfram. Dynamic pricing of electricity. *The American Economic Review*, 102(3):381–385, 2012.

[172] Richard Green and Nicholas Vasilakos. Market behaviour with large amounts of intermittent generation. *Energy Policy*, 38(7):3211–3220, 2010.

[173] Alan Tyldesley. Dsear: The dangerous substances and explosive atmospheres regulations-a new framework to cover old hazards. *Loss Prevention Bulletin*, (173):16–19, 2003.

[174] The Guardian. E.on announces 3.7% price rise, Available from http://www.theguardian.com/money/2013/dec/06/eon-price-rise-gas-electricity. [Accessed 21/3/2014].

[175] Jacques Bernier and J Bernier. *La pompe de chaleur: mode d'emploi*, volume 1. Publications Yves Colombot, 1979.

[176] ASHRAE Handbook. Fundamentals. *American Society of Heating, Refrigerating and Air Conditioning Engineers, Atlanta*, 2001.

[177] Hongxing Yang, Wei Zhou, Lin Lu, and Zhaohong Fang. Optimal sizing method for stand-alone hybrid solar–wind system with lpsp technology by using genetic algorithm. *Solar energy*, 82(4):354–367, 2008.

[178] Ioannis Hadjipaschalis, Andreas Poullikkas, and Venizelos Efthimiou. Overview of current and future energy storage technologies for electric power applications. *Renewable and Sustainable Energy Reviews*, 13(6):1513–1522, 2009.

[179] Carbon Trust. Polymer fuel cells. cost reduction and market potential. Technical report, Carbon Trust, September 2012.

[180] The Department of Energy. The department of energy hydrogen and fuel cells program plan. Technical report, The Department of Energy, September 2011.

[181] European Comission. Fuel cells and hydrogen joint undertaking. multi-annual implementation plan 2008-2013. Technical report, Fuel Cells and Hydrogen Joint Undertaking (FCH JU), 2009.

[182] Jessica Intrator, Ethan Elkind, Steven Weissman, Morgan Sawchuk, Emily Bartlett, Andris R Abele, Bruce S Dunn, Tsu-Chin Tsao, Rita Blaik, Christopher Lim, et al. Final project report 2020 strategic analysis of energy storage technologies. 2011.

[183] NV Dale, MD Mann, and H Salehfar. Semiempirical model based on thermodynamic principles for determining 6kw proton exchange membrane electrolyzer stack characteristics. *Journal of Power Sources*, 185(2):1348–1353, 2008.

[184] Kevin W Harrison, Eduardo Hernández-Pacheco, Hossein Salehfar, and Michael Mann. Semiempirical model for determining pem electrolyzer stack characteristics. *Journal of fuel cell science and technology*, 3(2):220–223, 2006.

[185] Meng Ni, Michael KH Leung, and Dennis YC Leung. Energy and exergy analysis of hydrogen production by a proton exchange membrane (pem) electrolyzer plant. *Energy conversion and management*, 49(10):2748–2756, 2008.

[186] Thomas A Zawodzinski, Charles Derouin, Susan Radzinski, Ruth J Sherman, Van T Smith, Thomas E Springer, and Shimshon Gottesfeld. Water uptake by and transport through nafion® 117 membranes. *Journal of the Electrochemical Society*, 140(4):1041–1047, 1993.

[187] JC Amphlett, RF Mann, BA Peppley, PR Roberge, and A Rodrigues. A model predicting transient responses of proton exchange membrane fuel cells. *Journal of Power Sources*, 61(1):183–188, 1996.

[188] Clarence M Shepherd. Design of primary and secondary cells ii. an equation describing battery discharge. *Journal of the electrochemical society*, 112(7):657–664, 1965.

[189] Michael MD Ross. A simple but comprehensive lead-acid battery model for hybrid system simulation. *cetc-varennes. nrcan. gc. ca/eng/publication/r2002-049e. html*, 2002.

[190] Mamadou Lamine Doumbia, Kodjo Agbossou, and E Granger. Simulink modelling and simulation of a hydrogen based photovoltaic/wind energy system. In *EUROCON, 2007. The International Conference on" Computer as a Tool"*, pages 2067–2072. IEEE, 2007.

[191] G Leng et al. Retscreen: Renewable energy project analysis software [online], Available from http://www.retscreen.net/ang/home.php [Accessed 01/03/2011].

[192] Luis Castaner and Santiago Silvestre. *Modelling photovoltaic systems using PSpice*. John Wiley and Sons, 2002.

[193] University of Wisconsin-Madison. Solar Energy Laboratory and Sanford A Klein. *TRNSYS, a transient system simulation program*. Solar Energy Laborataory, University of Wisconsin–Madison, 1979.

[194] E Hyman, WC Spindler, and JF Fatula. Phenomenological discharge voltage model for lead-acid batteries. 1987.

[195] A Mermoud. Pvsyst version 3.2. user's manual 2002 [online], Available from http://www. pvsyst. com/. [Accessed 01/03/2011].